

Separation of Phenols and Aniline from Water Streams using Poly(ether-block- amide) Membranes

by

Xiaotong Cao

A thesis

presented to the University of Waterloo

in fulfillment of the

thesis requirement for the degree of

Doctor of Philosophy

in

Chemical Engineering

Waterloo, Ontario, Canada, 2021

©Xiaotong Cao 2021

Examining Committee Membership

The following served on the Examining Committee for this thesis. The decision of the Examining Committee is by majority vote.

External Examiner

Dr. Raja Ghosh

Professor

Supervisor

Dr. Xianshe Feng

Professor

Internal Member

Dr. William A. Anderson

Professor

Internal Member

Dr. Yuning Li

Professor

Internal-external Member

Dr. Sigrid Peldszus

Associate Professor

Author's Declaration

This thesis consists of materials all of which I authored or co-authored: see Statement of Contributions included in the thesis. This is a true copy of the thesis, including any required final revisions, as accepted by my examiners.

I understand that my thesis may be made electronically available to the public.

Statement of Contributions

The body of this thesis is based upon a combination of published and unpublished studies. Various chapters are adapted from the followings.

Chapter 3 is based on the work published in Journal of Membrane Science. It was co-authored by myself, my supervisor and one collaborator (Kean Wang). I performed the experiments, data analysis, and manuscript preparation. Citation for Chapter 3 is:

Xiaotong Cao, Kean Wang, Xianshe Feng. “Removal of Phenolic Contaminants from Water by Pervaporation”, Journal of Membrane Science, 623 (2021), 119043.

Chapter 4 is based on the work published in Separation and Purification Technology. It was co-authored by myself, my supervisor and one collaborator (Kean Wang). I performed the experiments, data analysis, and manuscript preparation. Citation for Chapter 4 is:

Xiaotong Cao, Kean Wang, Xianshe Feng. “Perstraction of Phenolic Compounds via Nonporous PEBA Membranes”, Separation and Purification Technology, 257 (2021), 117928.

Chapter 6 is based on the work that has been submitted for publication. It was co-authored by myself, my supervisor and one visiting scholar (Lina Qiu). I performed most of the experiments, data analysis, and manuscript preparation.

Xiaotong Cao, Lina Qiu, Xianshe Feng. “Permeability, Solubility, and Diffusivity of Aniline in Poly(ether-b-amide) Membranes Pertaining to Aniline Removal from Aqueous Solutions by Pervaporation and Sorption”, Journal of Membrane Science, Under Review.

Chapter 7 will be used as the basis of one manuscript which will be submitted for publication after thesis submission. I performed the experiments and data analysis.

Abstract

Phenols and aniline are aromatic compounds in which a hydroxyl group and amine group are attached to the benzene ring, respectively. Both are common organic pollutants in a wide range of effluents from such industries as textile, pharmaceutical, rubber, plastic, wood processing, petrochemical, and coal-tar production. Currently, available technologies to remove these aromatic compounds from water streams includes extraction, sorption, biological treatment, and advanced oxidation. However, none of them is technically viable for all scenarios. Recently, membrane-based processes have drawn attention as a promising way for water treatment due to such advantages as small footprint, no regeneration required, no secondary pollution, and low energy consumption. Compared with the commonly used nanofiltration (NF) and reverse osmosis (RO) for organics/water separation, pervaporation and perstraction are more energy-efficient as the minor component (i.e., organics) are allowed to preferentially permeate through suitable organophilic membranes. For such applications, poly(ether-block-amide) (PEBA) is in general a popular membrane material in view of the easy processing, good mechanical/chemical stability, and high permselectivity towards polar organics. Thus, in this study, the removal of aniline and phenols from water streams using poly(ether-block-amide) (PEBA)-based membranes via pervaporation and perstraction was investigated.

Four representative phenols (including phenol (PhOH), p-cresol (MePhOH), p-chlorophenol (ClPhOH), and p-nitrophenol (O₂NPhOH)) and aniline are selected in the study in view of their wide occurrence in human surroundings. First, nonporous PEBA 2533 membrane was prepared via the solution-casting technique to separate four phenols (PhOH, MePhOH, ClPhOH, and O₂NPhOH) from aqueous solutions by pervaporation. The effects of feed concentration and operating temperature on the separation performance were investigated. While the permeation fluxes of phenolic compounds increased with an increase in feed concentration, the increase in the flux was less than proportional, leading to a decrease in the enrichment factor. It was also shown that both the permeation flux and the enrichment factor increased with increasing temperature. Of particular interest were the coupling effects of co-existing phenolic compounds due to permeant-permeant interactions, which were found to be significant in the permeation of multiple phenolic compounds that were relevant to practical applications. The permeation of PhOH, MePhOH, and ClPhOH was all affected adversely by the presence of other phenolic compounds in the feed solution, while the opposite was true for the permeation of slow-permeating O₂NPhOH.

Given the good permselectivity of PEBA towards phenolic compounds, the nonporous PEBA membrane was applied in perstraction to remove those phenolic compounds. Based on the resistance-in-series model, the mass transfer characteristics of the liquid/membrane/liquid perstraction system were analyzed, and the individual mass transfer resistances from the various steps of the perstraction process were estimated. It was revealed that not only the membrane resistance was significant, the mass transfer resistance at the downstream side of the membrane as a result of sorbate desorption from the membrane and boundary layer effects was also not negligible. It was found that the use of an alkaline stripping agent can effectively enhance the removal of phenolic compounds from water.

To further understand the mass transfer fundamentals of phenols in the membrane, the sorption and diffusion of the four phenols in dense PEBA membranes were investigated. The sorption isotherms for four phenolic compounds fit the Freundlich model most properly. PEBA has high sorption uptake towards phenols, much higher than that of water, and the high solubility selectivity led to the high permselectivity of PEBA. The diffusivity was found to be determined by both the molecular size and the mutual interactions between permeants and membrane.

The mass transfer characteristics (i.e., permeability, solubility, and diffusivity) of aniline in PEBA membrane pertaining to aniline removal by pervaporation and sorption was investigated. The solubility and diffusivity of aniline in PEBA were determined separately by analyzing the sorption isotherm and sorption kinetics. Membrane permeability is affected significantly by the environment in which the membrane equilibrated with, and membrane permeability follows a decreasing order that a “fully wet” membrane (i.e., in liquid permeation) > a “partially wet” membrane (i.e., in pervaporation) > a “dry” membrane (i.e., in vapor permeation).

Finally, zeolite imidazole framework-71 (ZIF-71), a hydrophobic filler with relatively large pore window sizes and cavity sizes, was prepared and incorporated into PEBA membrane to form mixed matrix membranes (MMMs) to inhibit water permeation in order to further improve the membrane permselectivity. The incorporation of ZIF-71 crystals in PEBA membrane significantly inhibited water permeation, while the permeability of two aromatics was largely unaffected (for phenol) or slightly reduced (for aniline), leading to increased enrichment factor. Though the permeability coefficient of aniline was lower than phenol, the permeation flux of aniline was higher because of the higher transmembrane driving force. The ZIF-71/PEBA MMMs showed good stability, demonstrating its applicability in separation of aromatic compounds from their aqueous solutions.

Acknowledgements

First and foremost, I would like to express my deepest gratitude and appreciation to my supervisor, Prof. Xianshe Feng, who gave me such a great opportunity to study at the University of Waterloo. His guidance, inspiration, patience, and encouragement throughout my Ph.D. study are invaluable, and I would never have accomplished this journey without his great support. His conscientiousness, dedication, and meticulous spirit will always inspire me in the future.

Also, I want to thank my Ph.D. thesis examining committee, including Prof. William Anderson, Prof. Yuning Li and Prof. Sigrid Peldszus (all from the University of Waterloo) and Prof. Raja Ghosh (McMaster University) for their valuable time and contributions.

I would like to thank my lab-mates in the Membrane Research Lab and colleagues in University of Waterloo, for all the help and friendship in the last four years.

The research support provided to this project by the Natural Sciences and Engineering Research Council of Canada (NSERC) is gratefully acknowledged. The University of Waterloo Graduate Scholarship, the Chemical Engineering Merit Scholarship, the Jenő Scharer Memorial Award, and the Institute of Polymer Research Scholarship for Academic Excellence in Polymer Science/Engineering awarded to me during the course of my doctoral studies are deeply appreciated.

Last, but not least, I would like to express my gratitude to my husband, my parents, and my sister, for their unconditional support, encouragement, and love.

Table of Contents

Examining Committee Membership	ii
Author's Declaration.....	iii
Statement of Contributions	iv
Abstract.....	v
Acknowledgements.....	vii
List of Figures.....	xiii
List of Tables	xix
List of Symbols.....	xx
Chapter 1 Introduction	1
1.1 Background.....	1
1.2 Research Objectives.....	7
1.3 Thesis Structure	7
Chapter 2 Literature Review	10
2.1 Pervaporation-a Promising Way to Separate Phenols and Aniline from Water Streams.....	10
2.2 Mass Transport Mechanism.....	13
2.3 Performance Characterization.....	16
2.4 Process Variables in Pervaporation.....	17
2.4.1 Feed Concentration	17
2.4.2 Operating Temperature	18
2.4.3 Permeate Pressure	19
2.4.4 Feed Flow Rate	19
2.5 Membrane Materials	20
2.5.1 Organophilic/Hydrophobic Polymeric Membranes	20

2.5.2 Inorganic Membranes	23
2.5.3 Mixed Matrix Membranes (MMMs)	23
2.6 Applications of Organophilic Pervaporation	25
2.6.1 Separation of Organic Contaminates from Water Streams	25
2.6.2 Recovery of Valuable Organic Compounds	26
2.6.3 Process Intensification	27
Chapter 3 Removal of Phenolic Compounds from Water by Pervaporation ¹	32
3.1 Introduction	32
3.2 Experimental	34
3.2.1 Materials	34
3.2.2 Membrane Preparation	36
3.2.3 Pervaporation	36
3.2.4 Sorption Experiments	38
3.3 Results and Discussion	39
3.3.1 Effects of Feed Concentration on Pervaporation Performance	39
3.3.2 Effects of Temperature on Permeation Behavior	55
3.3.3 Coupling Effects among Permeating Components	60
3.4 Summary	64
Chapter 4 Perstraction of Phenolic Compounds via Nonporous PEBA Membrane ¹	65
4.1 Introduction	65
4.2 Experimental	66
4.2.1 Perstraction	66
4.3 Theoretical Analysis	68
4.3.1 Dissociation of Phenolic Compounds	68

4.3.2 Resistance-in-series Model	68
4.4 Results and Discussion	72
4.4.1 Perstraction	72
4.4.2 Resistance Analysis.....	80
4.4.3 Effects of Alkaline in Stripping Liquid on Perstraction.....	83
4.5 Summary	85
Chapter 5 Sorption, Diffusion, and Permeation of Phenolic Compounds in PEBA Membranes	86
5.1 Introduction.....	86
5.2 Theoretical	86
5.3 Experimental	87
5.3.1 Materials	87
5.3.2 Membrane Preparation.....	88
5.3.3 Sorption Experiments.....	88
5.3.4 Permeation Experiments	89
5.4 Results and Discussion	90
5.4.1 Sorption Analysis.....	90
5.4.2 Permeation Analysis	94
5.4.3 Permeability Comparison.....	97
5.5 Summary	98
Chapter 6 Permeability, Solubility, and Diffusivity of Aniline in PEBA Membranes pertaining to Aniline Removal from Aqueous Solutions by Pervaporation and Sorption ¹	99
6.1 Introduction	99
6.2 Experimental.....	101
6.2.1 Materials	101

6.2.2 Membrane Preparation	101
6.2.3 Pervaporation.....	101
6.2.4 Sorption Experiments	101
6.2.5 Liquid Permeation Experiments	102
6.2.6 Sorption-desorption Reversibility	103
6.3 Results and Discussion.....	104
6.3.1 Pervaporation Performance	104
6.3.2 Solubility and Diffusivity from Sorption Measurements	111
6.3.3 Liquid Diffusion/Permeation.....	114
6.3.4 Comparison of Membrane Permeabilities	117
6.3.5 Sorption-desorption Reversibility	119
6.4 Summary	120
Chapter 7 Incorporation of ZIF-71 into PEBA to form Mixed Matrix Membranes (MMMs) for Separation of Phenol (PhOH) and Aniline from Aqueous Solutions by Pervaporation.....	121
7.1 Introduction	121
7.2 Experimental	122
7.2.1 Materials.....	122
7.2.2 Synthesis of ZIF-71 Crystals.....	123
7.2.3 Membrane Preparation	123
7.2.4 Membrane Characterization	123
7.2.5 Pervaporation Experiments	124
7.2.6 Sorption Experiments.....	124
7.3 Results and Discussion.....	124
7.3.1 Membrane Characterization	124

7.4 Pervaporation Performance.....	130
7.4.1 Temperature Dependency of Membrane Performance	139
7.4.2 Membrane Stability.....	141
7.5 Summary	142
Chapter 8 General Conclusions, Original Contributions and Future Prospects.....	143
8.1 General Conclusions and Original Contributions	143
8.2 Recommendations for Future Work.....	144
Bibliography	147
Appendix A Estimation of Individual Resistances	165

List of Figures

Figure 1.1	Thesis structure in terms of chapters and content relevance.	9
Figure 2.1	Schematic diagram of the pervaporation process.	13
Figure 2.2	Illustration of the solution-diffusion model.	15
Figure 2.3	Structure of the commonly used polymers.	21
Figure 2.4	Structures of some representative hydrophobic fillers: silicalite-1, ZIF-8, and COF-300. The structures of silicalite-1 and ZIF-8 is generated from the crystallographic information file obtained from the Cambridge Crystallographic Data Center (CCDC code: GITVIP 1428189 and 864309, respectively); the structure of COF-300 was adapted from ref. [103].	24
Figure 2.5	Schematic process layout for the recovery of phenol from wastewater using the (A) pervaporation-sorption-decanter system and (B) pervaporation-RO system.	31
Figure 3.1	(A) Schematic diagram of the pervaporation setup, and (B) schematic diagram of the membrane cell [163].	37
Figure 3.2	Effects of phenol concentration in the feed on total permeation flux at different temperatures.	40
Figure 3.3	Equilibrium sorption uptake of phenol and water in the membrane as a function of phenol concentration in the liquid at 30°C. A zoomed-in graph showing water sorption uptake in the membrane is also presented.	42
Figure 3.4	Pervaporation performance of different phenolic compounds at various feed concentrations at 30°C.	43
Figure 3.5	Effects of feed phenol concentration on phenol permeation flux at different temperatures.	45
Figure 3.6	Effects of feed phenol concentration on water permeation flux at different temperatures.	46
Figure 3.7	Effects of feed phenol concentration on the overall phenol concentration in the permeate at different temperatures.	48

Figure 3.8	Effects of feed phenol concentration on its enrichment factor at different temperatures.	49
Figure 3.9	Activity coefficients of phenolic compounds in binary phenol/water solutions as calculated via Aspen Plus V8.4 based on the UNIQUAC model.	50
Figure 3.10	Effects of feed concentration on the permeability of different phenol in the membrane at different temperatures.	52
Figure 3.11	Effects of feed concentration on the permeability of water in the membrane in different feed solutions at different temperatures.	54
Figure 3.12	Effects of temperature on the partial permeation fluxes at different feed concentrations.	57
Figure 3.13	Effects of temperature on the permeability coefficients at different feed concentrations.	58
Figure 3.14	A comparison of the total permeation fluxes for binary/ternary/quinary feed solutions that all contain a specific phenolic solute where such a solute is (A) PhOH, (B) MePhOH, (C) ClPhOH, and (D) O ₂ NPhOH. Water flux in absence of phenol solutes is also presented for comparison.....	63
Figure 4.1	Schematic diagram of the apparatus for perstraction experiments.....	67
Figure 4.2	Concentration profile at steady state of perstraction where boundary layer effects at both sides of the membrane are significant. C_F : bulk concentration in feed solution; $C_{F,S}$: liquid solute concentration at the interface between feed solution and the membrane; C_p : bulk concentration in stripping liquid; $C_{p,S}$: liquid solute concentration at the interface between the membrane and the stripping solution.	70
Figure 4.3	Concentration profiles for the four phenolic compounds in the feed compartment with time when receiving compartment was filled with deionized water.	73
Figure 4.4	Effects of membrane thickness on the overall resistance for permeation of phenolic compounds when receiving compartment was filled with deionized water.....	75
Figure 4.5	Percentage of undissociated phenolic compounds as a function of solution pH.....	77

Figure 4.6	Effects of NaOH concentration in the stripping solution on overall mass transfer coefficient for perstraction of phenolic compounds with a membrane thickness of 25.4 μm	78
Figure 4.7	Effects of membrane thickness on overall mass transfer resistance for perstraction of phenolics at various NaOH concentrations in the stripping liquid in mol/L.	79
Figure 4.8	Effects of NaOH concentration in the stripping liquid on the permeability coefficients of the phenolic compounds.	80
Figure 4.9	Distribution of mass transfer resistances for perstraction of phenols using a membrane with a thickness of 25.4 μm when the receiving compartment was filled with deionized water.	82
Figure 4.10	Effects of NaOH concentration in stripping liquid on downstream mass transfer resistance.	83
Figure 4.11	The enhancement factor of membranes with different thicknesses at various NaOH concentrations.....	84
Figure 5.1	The (A) linear, (B) Langmuir, and (C) Freundlich models for sorption of phenolic compounds in PEBA at 30°C.	91
Figure 5.2	The (A) partition coefficient and (B) solubility coefficient of phenolic compounds at various equilibrium concentrations at 30°C.	93
Figure 5.3	Partial vapor pressure of phenolic compounds in equilibrium with the liquid solution at 30°C. Data were estimated using the simulator Aspen Plus based on UNIQUAC model.	94
Figure 5.4	Amounts of phenolic solutes in the receiving compartment as a function of time at various feed concentration at 30°C.....	95
Figure 5.5	The (A) overall mass transfer coefficient, (B) permeability coefficient, and (C) diffusivity coefficient of phenolic compounds at different concentrations at 30°C.	96
Figure 5.6	Comparison of permeabilities obtained from pervaporation (hollow symbols) and obtained from liquid permeation experiments (solid symbols) at 30°C.	98
Figure 6.1	Effects of aniline concentration in feed on permeation flux at different temperatures.	106

Figure 6.2	Effects of feed aniline concentration on (A) the permeate concentration and (B) enrichment factor at different temperatures.	107
Figure 6.3	Permeate concentration as a function of feed concentration for pervaporation as compared to the vapor-liquid equilibrium (VLE) data at 50°C. The VLE data was estimated using Aspen based on the UNIFAC model.....	108
Figure 6.4	Effects of feed concentration on membrane permeability at different temperatures. ...	109
Figure 6.5	Temperature dependency of (A) permeation flux, (B) permeance, and (C) activation energy for permeation at different feed concentrations.	110
Figure 6.6	(A) Aniline sorption isotherms in PEBA, and (B) the solubility coefficient of aniline in PEBA.	112
Figure 6.7	(A) Aniline sorption curves in PEBA membranes with different thicknesses at room temperature, and (B) a comparison of the experimental data of sorption uptake (represented by the symbols) and calculations (solid blue line) using Equation (6.2) with diffusivity value of 8.3×10^{-12} m ² /s.	114
Figure 6.8	(A) The $F(t)$ versus t curve with different feed concentrations at 23°C, (B) Membrane permeability (P' , in units of m ² /s) at different temperatures, and (C) membrane permeability (P , in customary units of Barrer) at different temperatures.	116
Figure 6.9	Comparison of aniline permeability determined via different approaches. Temperature: 23°C.	118
Figure 6.10	Sorption isotherms of aniline in PEBA at room temperature after regeneration with HCl.	119
Figure 7.1	FTIR spectra of ZIF-71 crystals, pure PEBA membrane, and ZIF-71/PEBA MMMs.	125
Figure 7.2	X-ray diffraction pattern of ZIF-71 crystals, pure PEBA membrane, and ZIF-71/PEBA MMMs with a ZIF-71 loading of 9.1 wt% and 23.1 wt%, respectively. The XRD pattern of ZIF-71 reference is generated from the crystallographic information file obtained from the Cambridge Crystallographic Data Center (CCDC code: GITVIP).	126
Figure 7.3	(A) The chemical diagram of the ZIF-71, (B) the 3D structure of ZIF-71 crystals generated from the crystallographic information file obtained from the Cambridge	

	Crystallographic Data Center (CCDC code: GITVIP), and (C) the SEM image of ZIF-71 crystals.....	126
Figure 7.4	(A) Surface SEM images (magnification $\times 1000$) and (B) cross-sectional SEM images (magnification $\times 2000$; a zoomed-in image for 28.6wt% ZIF-71/PEBA MMMs is magnified by 5000) of pure PEBA membrane and MMMs. The numbers in the Figure represent the different ZIF-71 loadings in the MMMs.....	128
Figure 7.5	(A) Surface EDX mapping (magnification $\times 1000$) and (B) cross-sectional EDX mapping (magnification $\times 2000$) for membrane with a ZIF-71 loading of 28.6 wt%...	129
Figure 7.6	Water contact angle of pure PEBA membrane (No ZIF-71 crystals) and MMMs with different ZIF-71 loadings.	129
Figure 7.7	Effects of ZIF-71 loading in MMMs on the total permeation flux for (A) phenol solution and (B) aniline solution at different temperatures. Feed concentration: 6000 ppm.....	131
Figure 7.8	Effects of ZIF-71 loading in MMMs on the permeation flux of (A) phenol, (B) aniline, and (C) water in phenol solution (solid symbols/lines) and in aniline solution (open symbols, dash lines) at various temperatures. Feed concentration: 6000 ppm.....	132
Figure 7.9	Effects of ZIF-71 loading on the permeability coefficient of (A) phenol, (B) aniline, and (C) water in phenol solution and (D) water in aniline solution in the MMMs.....	133
Figure 7.10	Sorption isotherms of (A) phenol and (B) aniline in MMMs at room temperature.....	135
Figure 7.11	The partial vapor pressure of phenol and aniline in equilibrium with their corresponding feed solutions at various temperatures, calculated using Aspen Plus V10 based on UNIQUAC model and UNIFAC model, respectively.....	137
Figure 7.12	Effects of ZIF-71 loading in the MMMs on the enrichment factor of phenol and aniline at 60°C.....	137
Figure 7.13	Temperature dependency of permeation flux for (A) phenol solution and (B) aniline solution, and temperature dependency of permeability coefficients for permeants in (C) phenol solution and (D) aniline solution. ZIF-71 loading (wt%) was shown in the Figure.....	139

Figure 7.14	Effects of ZIF-71 loading in the MMMs on the apparent activation energy for permeation of phenol, aniline, and water.	140
Figure 7.15	Stability of ZIF-71/PEBA MMM with a ZIF-71 loading of 28.6wt% for the separation of phenol solutions with concentration of 6000 ppm at 60°C.....	142

List of Tables

Table 1.1	Phenols and aniline commonly found in wastewater associated with industrial activities [6].	1
Table 1.2	Common technologies for the treatment of water streams containing phenols and aniline.	3
Table 2.1	Pervaporative separation of phenol and aniline using different membranes.	11
Table 3.1	Pervaporation-related research on the separation of phenolic compounds using PEBA membranes.	33
Table 3.2	Physical and chemical properties of phenolic compounds of interest.	35
Table 3.3	Separation performance for binary PhOH/water mixtures with PEBA membranes.	55
Table 3.4	Apparent activation energy for the permeation of phenol (E_{Jp}) and water (E_{Jw}), and the intrinsic activation energy for membrane permeability to phenol (E_{Pp}) and water (E_{Pw}) at various feed concentrations.	59
Table 3.5	Permeation flux ratio with and without the presence of other phenolic solute(s).	62
Table 4.1	Operating parameters used in this study.	67
Table 4.2	Permeability, partition coefficient, and diffusivity coefficients in PEBA at 30°C.	74
Table 4.3	Individual mass transfer resistances for phenolic compounds in the liquid/membrane/liquid perstraction system.	81
Table 5.1	Parameters of the linear, Langmuir, and Freundlich models for the sorption of phenolic compounds in PEBA at 30°C.	92
Table 6.1	Model parameter and coefficient of determination for aniline sorption in PEBA.	113
Table 7.1	Physical and chemical properties of phenol and aniline.	123
Table 7.2	Comparison of the separation of phenol/water mixtures and aniline/water mixtures by pervaporation using different membranes.	138
Table 7.3	Apparent activation energy and intrinsic activation energy for phenol, aniline, and water for MMMs with different ZIF-71 loadings.	141

List of Symbols

A	Effective membrane area, m^2
V	Feed solution volume, L
C_o	Initial feed concentration, mmol/L
C_e	Solute concentration at sorption equilibrium, mmol/L
$C_{i,o(m)}$	Concentration of component i in the membrane at the feed/membrane interface, mol/L
$C_{i,L(m)}$	Concentration of component i in the membrane at the membrane/permeate interface, mol/L
C_t	Instantaneous solute concentration during sorption, mmol/L
C_F	Instantaneous bulk feed concentration in perstraction or liquid permeation, mmol/L
$C_{F,s}$	Liquid solute concentration at the feed/membrane interface, mmol/L
C_p	Bulk solute concentration in stripping liquid, mmol/L
$C_{p,s}$	Solute concentration in stripping solution at the interface between membrane and the stripping solution, mmol/L
C_R	Instantaneous solute concentration in receiving liquid in liquid permeation system, mmol/L
d	Characteristic dimension, m
D_l	Solute diffusivity in liquid, m^2/s
D	Diffusivity or diffusion coefficient in membrane, m^2/s
D_o	Pre-exponential factor for diffusivity, m^2/s
E_D	Activation energy for diffusion, J/mol
E_J	“Apparent” activation energy for permeation, J/mol
E_P	“Intrinsic” activation energy for membrane permeability, J/mol
H	Henry’s sorption constant, $Pa/(mol \cdot m^{-3})$
ΔH	Heat of evaporation, J/mol
J	Permeation flux, $g/(m^2 \cdot h)$
J_o	Pre-exponential factor for permeation flux, $g/(m^2 \cdot h)$
K_a	Acid dissociation constant
K_F	Freundlich sorption constant, $(mmol/L)^{1-1/n}$
K^G, S	Gas/vapor phase sorption coefficient, or called solubility coefficient, $mol/(m^3 \cdot Pa)$
K_H	Henry’s sorption constant

K^L	Liquid phase sorption constant
K_L	Langmuir sorption constant, L/mmol
K_O	Overall mass transfer coefficient under “normal” operating condition in perstraction, m/s
K_O'	Overall mass transfer coefficient with vigorous agitation of stripping solution in perstraction, m/s
K_O''	Overall mass transfer coefficient with vigorous agitation of stripping solution at an alkaline concentration that was sufficiently high in perstraction, m/s
$K_{O,OH}$	Overall mass transfer coefficient with NaOH in stripping liquid, m/s
L	Membrane thickness, m
N	Agitation speed, s ⁻¹
$1/n$	Heterogeneity factor in Freundlich model
M	Molecular weight, g/mol
P'	Permeability coefficient, m ² /s
P, P^G	Permeability coefficient, Barrer
$p_{i,o}$	Partial pressure of component i in equilibrium with the feed solution, Pa
$p_{i,L}$	Partial pressure of component i in the permeate, Pa
p^p	Permeate pressure, Pa
p^{sat}	Saturated vapor pressure, Pa
pK_a	Logarithmic of acid dissociation constant
Q	Total amount of solute permeated through the membrane in liquid permeation experiments, mmol
Q_e	Membrane solute sorption uptake at equilibrium, mmol/L
Q_m	Theoretical maximum sorption capacity in Langmuir model, mmol/L
Q_t	Instantaneous membrane solute sorption uptake, mmol/L
q_p	Equilibrium solute sorption uptake, mg/g
q_t	Total equilibrium sorption uptake (water + solute), mg/g
q_w	Water equilibrium sorption uptake, mg/g
Re	Reynold number
$R_1, 1/K_1$	Mass transfer resistance in boundary layer of feed liquid in perstraction, s/m
R_2	Mass transfer resistance for phenol sorption into membrane in perstraction, s/m
R_3	Mass transfer resistance for phenol desorption from membrane in perstraction, s/m
$R_4, 1/K_4$	Mass transfer resistance in boundary layer of the stripping liquid in perstraction, s/m

R_m	Membrane resistance under “normal” operating condition in perstraction, s/m
R_m''	Membrane resistance when the alkaline concentration of the stripping solution was high enough in perstraction, s/m
R_{total}	Overall mass transfer resistance of perstraction, s/m
S_o	Pre-exponential factor for solubility, mol/(m ³ ·Pa)
Sc	Schmidt number
Sh	Sherwood number
T	Temperature, K
t	Time, s
V	Feed solution volume, L
V_R	Volume of receiving liquid in liquid permeation system, L
V_s	Molar volume of the phenolic solute as liquid at its normal boiling point, cm ³ /mol
W_o	Weight of dry PEBA membrane, g
W_e	Weight of PEBA membrane at sorption equilibrium, g
X	Molar fraction of permeant in the feed
Y	Molar fraction of permeant in the permeate

Greek symbols

α	Separation factor
β	Enrichment factor
γ	Activity coefficient
λ_{max}	Maximum absorption wavelength, nm
θ	Time lag
μ	Liquid viscosity, Pa·s
ν	Agitator tip speed, m/s
ρ	Density of liquid, kg/m ³
ρ_m	Density of membrane, g/L
ψ	Association parameter
ω	Degree of phenol dissociation

Note: all concentrations measured in this research were in units of ppm based on mass, which were converted to mmol/L as necessary.

Chapter 1

Introduction

1.1 Background

Phenols and aniline are important organic intermediates, extensively used in the production of pesticides, pharmaceuticals, petrochemicals, and dyestuffs. Phenols and aniline are therefore usually present in the effluents from relevant industries, with typical concentrations from a few ppm to several grams per liter [1]. Table 1.1 shows some of the phenolic compounds and aniline that are commonly found in the effluents from different industries. These compounds can impose both chronic effects (e.g., irritation in the nerve system/liver/kidney, weight loss, and vertigo) and acute effects (e.g., tremor, coma, and respiratory arrest at lethal doses) on human health [2]. In addition, they tend to persist in the environment over a long period of time, and some can be transformed into other forms that are even more toxic than the original compounds [3]. Because of their wide existence, high toxicities and carcinogenicities, phenols and aniline are classified as pollutants of priority concerns by a number of environmental protection agencies [4, 5]. As such, to minimize the adverse effects of these chemicals on human and animals, effective methods must be developed to remove phenols and aniline from water streams before discharge.

Table 1.1 Phenols and aniline commonly found in wastewater associated with industrial activities [6].

Compounds	Industries
Phenol	Coal-tar production, pesticides, explosives, dyes, textile, pharmaceuticals
Methylphenols	Coal-tar, petrochemical, cosmetics, disinfectant, pesticide, explosives, plastics, dyes
Chlorophenols	Pharmaceutical, metallurgic, textile, wood processing
Nitrophenols	Dyes, plastics, explosives, pharmaceuticals
Aniline	Dyes, pesticides, resin production, pharmaceuticals

Traditionally, techniques to remove phenols and aniline include extraction [7, 8], sorption [9, 10], advanced oxidation processes [11, 12] and biological treatment [13, 14]. Extraction is an efficient method widely used for treating wastewater with high pollutants concentrations (over 3000 ppm) [15, 16]. Jiang et al. [16] used octanol as an extractant to separate phenol from wastewater (6000 ppm), and

over 99% phenol was recovered. The main drawback of liquid extraction is the regeneration of the exhausted extractants for reuse, especially for extractants with a high boiling point [15]. In addition, when the concentration of the organic contaminants in the wastewater is quite low, the removal rate by extraction will be low. Sorption is a versatile method to remove pollutants from wastewater. It can effectively remove various types of pollutants [17-20]. Activated carbon is the most extensively used sorbent material due to its high sorption capacity, fast sorption rate, and mechanical stability. Phenol removal rate can be as high as over 99% at optimal conditions [19]. However, the regeneration of activated carbon is time-consuming and expensive to perform [21]. Advanced oxidation (including photocatalysis, ozonation, Fenton process) is considered to be promising for the removal of recalcitrant organic pollutants from wastewater [12]. These processes are based on the generation of the highly reactive hydroxyl radical, which can react with organic substances present in the wastewater [22]. For ozonation, the high cost of ozone generation and low ozone solubility in water limit its application. While hydrogen peroxide is more cost-effective than ozone, but the oxidizability of hydrogen peroxide is relatively low. Fenton reagent can effectively degrade majority of pollutants unselectively, including some recalcitrant pollutants (cyanide, coking wastewater, etc.). However, these methods often have high operating costs. In addition, such destructive methods do not allow the recovery of the organics (including phenols and aniline) as valuable chemicals, which is a potential economic loss. Phenols can also be degraded by microorganisms or enzymes under mild conditions [23-25]. However, wastewater with a high phenol concentration could inhibit the growth of the microorganisms, and a long treatment time is typically needed for biodegradation to degrade phenol [16]. Table 1.2 shows a brief comparison of the currently used techniques to separate phenols and aniline from water streams, and none of them is viable under all scenarios.

Table 1.2 Common technologies for the treatment of water streams containing phenols and aniline.

Technique	Pros.	Cons.	Ref.
Extraction	<ul style="list-style-type: none"> (1) Simple and easy operation. (2) Efficient for wastewater with high phenol concentrations. (3) Recovery of phenols and aniline. 	<ul style="list-style-type: none"> (1) Produce secondary pollution. (2) Energy consumption could be high when recovering some extractant with a higher boiling point. (3) Low efficiency with low concentration pollutants. 	[15, 16]
Sorption	<ul style="list-style-type: none"> (1) Widely used. (2) High efficiency. (3) Phenols can be potentially recovered when resins are used as sorbent. 	<ul style="list-style-type: none"> (1) Produce secondary pollution when disposing or burning the exhausted sorbent, or during sorbent regeneration. (2) Regeneration of activated carbon is time-consuming and expensive. 	[21]
Biological treatment	<ul style="list-style-type: none"> (1) Phenols can be degraded to harmless compounds by microorganisms or enzymes. (2) Low operational cost. (3) Modest reaction conditions. 	<ul style="list-style-type: none"> (1) Cannot treat with a high phenol concentration as microorganisms cannot survive by high concentrations of phenol. (2) Treatment time is long. 	[3, 13, 16, 21]
Advanced oxidation processes	<ul style="list-style-type: none"> (1) Degrade a wide range of pollutants including recalcitrant pollutants. (2) High efficiency. 	<ul style="list-style-type: none"> (1) Organics were destructed and cannot be recycled. (2) Catalysts are expensive, and subsequent catalyst/water separation is required. 	[3, 21]

On the other hand, membrane-based processes are playing an important role for water treatment because of such advantages as small footprint, ease of operation, and low-operating costs. Technically, the separation of organic compounds from water can be achieved by nanofiltration (NF) and reverse osmosis (RO), in which processes the small water molecules permeate through the membrane while the organic compounds are rejected by the membrane. However, the organic compounds can adsorb on/into the polymeric membranes, and then diffuse through the membrane via “solution-diffusion” mechanism, deteriorating separation performance. Nowadays, pervaporation has drawn attention as an energy-efficient technology to separate organics from water, especially when the concentration of organics in the feed is low. Compared with NF or RO, pervaporation requires less energy as the minor components (i.e., organic pollutants) can preferentially permeate through the membrane. In pervaporation, the energy required is mainly to evaporate the permeating molecules, and this portion of energy can in principle be recovered, at least, by the condensation of the permeant [26]. Therefore, in this project, pervaporation was used to separate phenols and aniline from their aqueous solutions.

Perstraction (sometimes also called pertraction) is another membrane-based process combining selective permeation of a solute component through nonporous polymeric membranes and extraction into an extracting solution [27, 28]. It appears to be particularly suitable for removing phenols and aniline from water. In a perstraction system, the feed solution and the stripping agent are separated by a nonporous membrane, and the target solute molecules in the feed (i.e., phenols and aniline in wastewater for this study) are selectively transferred into the stripping liquid across the membrane. The mass transport is driven by the difference in the chemical potential of the feed liquid and the stripping liquid. Nonporous polymeric membranes with suitable solubilities and/or diffusivities to the target molecules can be used to selectively extract these molecules from a feed mixture via perstraction. For example, Han et al. [29] reported a PhOH recovery system using a tubular PDMS membrane for membrane separation combined with reactive extraction using a basic solution. Ferreira et al. [30] scaled up a PhOH recovery system to pilot trials where a silicone rubber tube containing 30 wt% fumed silica was used as the membrane phase to demonstrate the feasibility of perstraction for industrial applications. Sawai et al. [31, 32] used a flat PDMS membrane to recover phenol derivatives by perstraction and pervaporation, and the results showed that perstraction was more effective to remove phenol than standalone pervaporation. In view of these advantages, perstraction was also employed to separate phenols and aniline from water streams in this doctoral project.

In this work, four representative phenols (i.e., phenol, p-cresol, p-chlorophenol, and p-nitrophenol) and aniline, which are widely occurring in environments and human surroundings, were selected as representatives to investigate their separation performance by pervaporation and perstraction. All aromatic contaminants have functional groups connected to the benzene ring, making it easier to compare how the physicochemical characteristics of the aromatic contaminants affect their separation performance. In addition, all of them are partially ionizable organic compounds, with a slight acidity (for phenols) or basic property (for aniline) in aqueous solutions. By choosing aniline and phenols as model pollutants, we could know whether our strategies would be able to handle both types of aromatic compounds.

In pervaporation, the feed liquid contacts with one side of the membrane, where the molecules selectively permeate through the membrane and are removed as a low-pressure vapor from the downstream side of the membrane. While in perstraction, the permeating molecules permeate through the membrane and then are extracted into an extracting solution. In both membrane-based processes, the selection of suitable membrane material is crucial for the separation performance. For such applications, nonporous polymer membranes with high solubility and diffusivity towards target permeating components are required, so that the target components (i.e., phenols and aniline) can preferentially permeate through the membrane. The permselectivity of the membrane material towards phenols and aniline is an important parameter in membrane material screening.

Currently, poly(dimethylsiloxane) (PDMS) membranes are the most commonly used membrane to separate organic compounds from water by pervaporation [33-36] and perstraction [29-32] due to its good permselectivity, ease of fabrication, and favorable chemical/mechanical stability. Nowadays, poly(ether-block-amide) (PEBA) has drawn interest for separation of low concentrations of polar aromatic compounds from water in view of its higher separation factor than PDMS because of the relatively higher polarity [37-39]. PEBA is a group of copolymers with micro-biphasic structures composed of soft polyether segments and hard polyamide segments. By adjusting the composition of the two segments, membranes with different properties could be obtained. Actually, PEBA from GKSS was initially patented for the treatment of phenol-containing water streams [40]. Among the various grades of PEBA, PEBA 2533, which has the highest content of the soft poly(tetramethylene oxide) segment (~80 wt%), showed excellent permselectivity towards some phenols due to its high solubility. Our previous work showed that PEBA 2533 can be used successfully for the sorptive removal of

phenolic compounds as well [41]. Therefore, PEBA 2533 was selected as the membrane material to separate phenolic compounds and aniline from aqueous solutions in this study.

In practical wastewater streams, multiple contaminants are generally present, where coupling effects among different permeants are expected to occur. However, essentially all the studies to date are focused on the separation of a single phenolic compound from water, which is apparently inadequate for real wastewater treatment. Therefore, the separation performance for feed solutions containing a single phenolic component and multiple phenolics can fill in such a knowledge gap. On the other hand, in pervaporation and perstraction, the separation performance was predominantly determined by the sorption and diffusion of permeating components within the membrane. The solubility determines the concentration of the permeating molecules accommodated in the membrane, and the diffusivity determines the migration rate of the penetrant through the polymer matrix. The evaluation of the solubility and diffusivity of penetrants in the membrane allows for a better understanding of permeation mass transfer.

In membrane separation, permeability is an attribute of the membrane used to understand the permeation behavior of the membrane. It is therefore important to evaluate membrane permeability. However, the membrane permeability determined via different approaches can result in different values, presumably due to the different membrane properties affected by the different contacting fluids. Therefore, caution should be exercised in using the membrane permeability as an intrinsic property. To fill in the knowledge gap as how the membrane permeability determined via different approaches would differ, membrane permeabilities were evaluated and compared with different approaches, thereby providing an insight into the mass transfer in the membrane. For such purposes, the permeability, solubility, and diffusivity of aniline in PEBA membranes pertaining to aniline removal from aqueous solutions by pervaporation and sorption were investigated.

To further improve the separation performance, appropriate hydrophobic fillers can be incorporated into PEBA membrane to form the mixed matrix membranes (MMMs). The development of MMMs is considered to be a promising and cost-effective way to push up the trade-off between permeability and selectivity of polymeric membranes and achieve long-term operation stability [42, 43]. The incorporation of hydrophobic fillers is expected to increase membrane hydrophobicity, thus inhibiting water permeation, thereby increase selectivity. The properties of the fillers influence the mutual interactions between the penetrates and MMMs, and are crucial for the performance of MMMs.

Attempts were made in this study to prepare MMMs to improve the selectivity of PEBA for the separation of phenol and aniline.

1.2 Research Objectives

This research aimed to investigate the separation performance of PEBA 2533 as a suitable membrane material to remove phenolic compounds and aniline from aqueous solutions. The specific objectives of this project are presented below:

- (1) To investigate the separation performance of phenols and aniline from water streams by pervaporation using PEBA 2533 membrane, and to identify the coupling effects between multiple permeating components.
- (2) To investigate the perstraction performance using PEBA membrane for the separation of phenols from water streams.
- (3) To study the fundamentals (i.e., solubility, diffusivity and permeability) of related to mass transport within PEBA membrane.
- (4) To improve the membrane performance for pervaporative separation of phenol and aniline from water by incorporating ZIF fillers into the membrane to form MMMs.

1.3 Thesis Structure

The overall thesis structure is illustrated in Figure 1.1 for an overview of the research. The thesis consists of eight chapters, and they are organized as follows:

Chapter 1 presents the background and the objectives of this study.

Chapter 2 is the literature review. As a promising technique to treat wastewater containing phenols and aniline, pervaporation for removing such aromatic compounds was reviewed in detail. The mass transport mechanism, membrane materials commonly used for separation of organic compounds from aqueous solutions, operating parameters that influence the separation performance, and the main applications of organophilic pervaporation separation have been introduced. Some of the prior work reported in the literature relevant to the subject matter was further reviewed in respective chapters.

Chapter 3 presents the experimental results of pervaporation with binary feed solutions containing a single phenolic compound (one phenolic compound + water) and multi-component feed solutions containing two or more phenolic compound (multiple phenolic compounds + water) using PEBA 2533

membrane. The effects of feed concentration and operating temperature on the separation characteristics were investigated, and the coupling effects among the permeants due to permeant-permeant interactions were evaluated.

Chapter 4 presents the perstraction performance using PEBA membrane to separate phenolic compounds from aqueous solutions. The mass transfer characteristics of phenolic solutes during perstraction processes were discussed, and the influence of the alkaline stripping solution on perstraction performance was evaluated.

Chapter 5 provides a detailed study on the solubility, diffusivity, and permeability of phenolic compounds in PEBA membrane. The effects of the physicochemical properties of the molecules on their permeation behavior were analyzed.

Chapter 6 presents a comprehensive study on the permeation of aniline in PEBA membrane. The separation of aniline from aqueous solutions by pervaporation was investigated. The solubility and diffusivity of aniline in PEBA were evaluated. The influence of the contacting fluids (liquid, or vapor) on membrane permeability was discussed.

Chapter 7 presents the preparation of ZIF-71/PEBA mixed matrix membranes (MMMs) and their application to remove phenol and aniline from aqueous solutions by pervaporation. The effects of filler loading and operating conditions on the membrane performance were investigated.

Chapter 8 is a summary of the general conclusions drawn from the research and the original contributions of the work, and recommendations for future research are also presented.

Chapter 2

Literature Review

2.1 Pervaporation-a Promising Way to Separate Phenols and Aniline from Water Streams

As mentioned in Chapter 1, among the various techniques to treat wastewater containing phenols and aniline, pervaporation has demonstrated itself as a promising method, especially when the concentration of the organics is low. Table 2.1 summarizes some recent studies on the separation of phenols and aniline using different membranes by pervaporation. As shown in Table 2.1, the majority of the studies to date focus on the separation of a single phenolic compound (primarily phenol, the simplest phenolic compound), while research on separation of other phenolic compounds by pervaporation is rare, not to mention the separation of multiple phenolic compounds (though multiple phenolic compounds are commonly present in practical wastewater). This project thus serves to fill in such knowledge gap.

Furthermore, as shown in Table 2.1, for the pervaporative separation of phenols and aniline, the majority of membranes are made from PDMS, polyurethane (PU), and PEBA. Though the operating conditions are not totally the same, PEBA tends to outperform other membranes considering both the permeation flux and separation factor. Generally, PDMS-based membranes show a high permeation flux due to the flexibility of the -Si-O- backbone, but the separation factor is not always satisfactory, especially for the removal of polar organics. PU-based membranes show a high selectivity; however, the low flux limits their applications. In addition, PDMS polymers modified with a proper amount of ethylether or dimethylamino groups show good selectivity and permeation flux. Compared with chemically modified PDMS, which involves a complicated and time-consuming process, PEBA films can be prepared readily by a solution-casting technique. In view of the good separation performance and the simple membrane preparation process, PEBA polymer was selected as the membrane material to separate phenols and aniline from water in the current research.

Table 2.1 Pervaporative separation of phenol and aniline using different membranes.

Membranes ^a	Temperature (°C)	Feed conc. ^b (wt.%)	Effective thickness (μm)	Permeate pressure (mbar)	Organic flux ^b (g/(m ² ·h))	Separation factor ^b	Ref.
Phenol (PhOH)							
PDMS	65	1	8	8-10	91.5	4.4	[44]
PERVAP-1060	60	1.1	8	< 1	32	4.7	[35, 37]
PERVAP-1070	60	1	10	< 1	25	15.5	[35, 37]
PDMS	70	2	50	≤ 2	70.8	11.6	[33]
PDMS-AEE	70	2	50	≤ 2	108.3	19	[33]
PDMS-AMI	70	2	50	≤ 2	100	20.8	[33]
PDMS-PY	70	2	50	≤ 2	108.3	17.9	[33]
PU	60	1	19	3.33	80	15	[45]
PU	60	3	150	6.67	4.4	240	[46]
ZSM-5/PU	60	0.3	80~130	< 2	1.19~1.94	7	[47]
ZSM-5-EPI- CD/PU	60	0.3	80~130	< 2	9.9~16.1	5.8	[47]
PEBA 3533	50	0.01	30	Unknown	1.6	31.4	[48]
PEBA 4033	50	0.1	46	1.94	12.7	67.0	[48]
PEBA 2533	70	0.6~0.8	30	4	160	23	[38]
ZIF-8/PEBA 2533	70	0.8	50	2.8	390	53	[49]

Continued next page

Membrane ^a	Temperature (°C)	Feed conc. ^b (wt.%)	Effective thickness (μm)	Permeate pressure (mbar)	Organic flux ^b (g/(m ² ·h))	Separation factor ^b	Ref.
p-cresol (MePhOH)							
PDMS	70	2	50	≤ 2	154.2	28.1	[33]
PDMS-AEE	70	2	50	≤ 2	295.8	28.2	[33]
PDMS-AMI	70	2	50	≤ 2	325	68.4	[33]
PDMS-PY	70	2	50	≤ 2	279.2	67	[33]
p-chlorophenol (ClPhOH)							
PUU-PMMA	60	0.7	250	5	23.8	713	[50]
Aniline							
PDMS	80	1.86	1	30	500	3.6	[51]
PU	70	0.612	Unknown	5	29	10.1	[52]
PB	80	1.1	Unknown	30	125	45	[51]
PEBA	80	1	70	30	185	75	[51]

^aThe material of a dense membrane or the top layer of a composite membrane.

^bCalculated from the data given in literature or obtained from the figure.

PERVAP-1060: commercial membrane with PDMS as selective layer (Sulzer Chemtech); PERVAP-1070: commercial membrane with zeolite filled PDMS as selective layer (Sulzer Chemtech); PDMS-AEE: PDMS modified with 10% ethylether; PDMS-AMI: PDMS modified with 10% dimethylamino; PDMS-PY: PDMS modified with pyridyl; ZSM-5-EPI-CD/PU: MMMs incorporated with epichlorohydrin modified ZSM-5 with PU; PUU-PMMA: polyurethane urea-poly(methyl methacrylate); PB: polybutadiene.

Given the advantageous characteristics of pervaporation, numerous efforts have been made to expand the applications of pervaporation, mainly focused on azeotrope separation[53], recovery of valuable compounds from water [54], and separation of low concentrations of organic contaminants from water for pollution control [55]. Currently, the solvent dehydration using pervaporation, such as the production of anhydrous ethanol, has achieved industrialization, while the application of organophilic pervaporation membranes for selective permeation of organic compounds from aqueous solutions is less developed, mainly due to the lack of suitable membranes [56]. This is because for organophilic pervaporation, the membranes are usually case-specific. As the separation of phenolic compounds and aniline by pervaporation falls into the category of organophilic pervaporation, the recent development on organophilic membranes relevant to pervaporation separation will be introduced in detail later, covering the principles of pervaporation, mass transport mechanism, commonly used membrane materials and the primary applications.

2.2 Mass Transport Mechanism

Figure 2.1 is a schematic illustration of a pervaporation process. The feed liquid to be separated contacts with one side of the membrane and the permeate vapor is removed from the other side. The mass transfer driving force is the vapor pressure difference between the feed and the permeate vapor. The low permeate pressure can be induced by applying a vacuum pump or inert purge on the permeate side, or the permeate vacuum can be simply generated by cooling the permeate vapor, as the condensation of the vapor can create a partial vacuum.

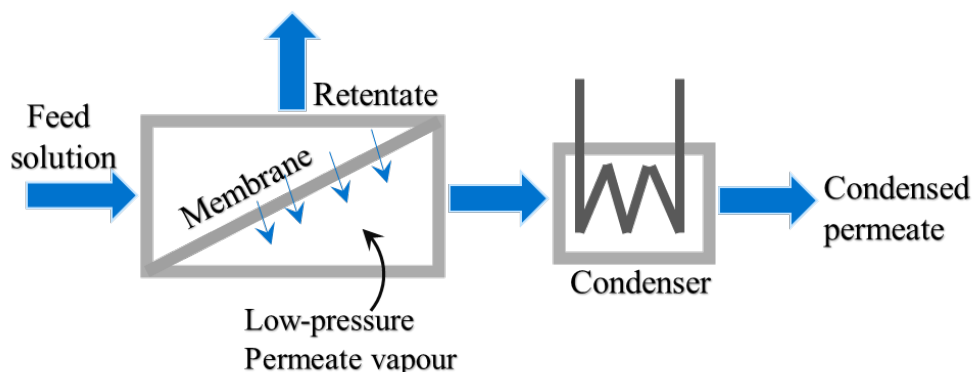


Figure 2.1 Schematic diagram of the pervaporation process.

Based on the solution-diffusion mechanism [55, 57, 58] (Figure 2.2), pervaporation process generally involves three sequential steps: (1) the sorption of the penetrates onto the membrane surface, (2)

molecular transport through the membrane, and (3) desorption of the permeate vapor. Both the sorption and desorption steps are thought to occur very fast and equilibria are built instantaneously on both sides of the membrane, and pervaporation can be treated as a diffusion-controlled process. To describe the pervaporation process, Fick's law can be used

$$J_i = -D_i \frac{dC_i}{dL} \quad (2.1)$$

where J_i is the permeation flux of component i (mol/(m²·h)); D_i is the diffusion coefficient (m²/s); L represents membrane thickness (m), and dC_i/dL is the concentration gradient across the membrane (mol/m⁴). It should be noted that C_i is the solute concentration (mol/m³) in the membrane, not the concentration of the liquids on either side of the membrane. Assuming the diffusion coefficient D_i is independent of local solute concentration or membrane thickness, Equation (2.1) can be integrated over the membrane thickness to the form

$$J_i = \frac{D_i (C_{i,o(m)} - C_{i,L(m)})}{L} \quad (2.2)$$

the subscripts o and L represent the position of the feed and permeate interfaces of the membrane, respectively, and the subscript m represents "in the membrane". On the permeate side, the concentration of component i in the membrane at the membrane/permeate vapor interface, $C_{i,L(m)}$, can be written as

$$C_{i,L(m)} = K_i^G p_{i,L} \quad (2.3)$$

where K_i^G is the gas/vapor phase sorption coefficient, and $p_{i,L}$ is the partial pressure of component i in the permeate. The concentration of component i in the membrane at the feed/membrane interface, $C_{i,o(m)}$, can be represented by

$$C_{i,o(m)} = K_i^L C_{i,o} \quad (2.4)$$

where K_i^L is the liquid phase sorption coefficient, which is essentially a partition coefficient. According to Henry's law, the concentration of component i in the liquid phase, $C_{i,o}$ can be given in the form of

$$C_{i,o} H_i = p_{i,o} \quad (2.5)$$

where H_i is Henry's sorption constant, and $p_{i,o}$ is the partial pressure of component i in equilibrium with the solution ($\text{Pa}/(\text{mol}\cdot\text{m}^{-3})$). Considering the membrane was in direct contact with the hypothetical vapor of component i , the vapor-membrane phase equilibrium can be written as

$$C_{i,o(m)} = K_i^G \cdot p_{i,o} \quad (2.6)$$

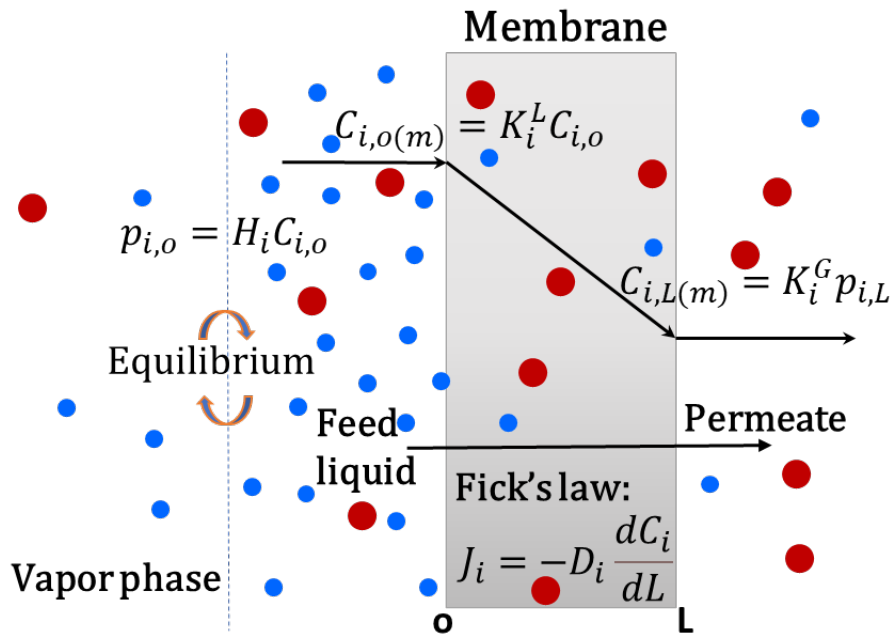


Figure 2.2 Illustration of the solution-diffusion model.

Based on Equations (2.4) to (2.6), we have

$$K_i^G = \frac{K_i^L}{H_i} \quad (2.7)$$

Combining Equations (2.2) to (2.7) gives

$$J_i = \frac{D_i (K_i^G \cdot p_{i,o} - K_i^G \cdot p_{i,L})}{L} = \frac{P_i^G}{L} (p_{i,o} - p_{i,L}) \quad (2.8)$$

where P_i^G is known as the permeability coefficient of component i in the membrane (for simplification, it was denoted as P_i in the following). It is a product of $(D_i \cdot K_i^G)$, the diffusivity multiplying solubility (K_i^G is also denoted as S , the solubility coefficient). More specifically, Equation (2.8) can be further expressed as

$$J_i = P_i \frac{X_i \gamma_i p_i^{sat} - Y_i p^p}{L} \quad (2.9)$$

where p_i^{sat} and γ_i represent the saturated vapor pressure and activity coefficient of the permeating component i in the feed, respectively, and X_i and Y_i are the molar fractions of the permeating component i in the feed and permeate, respectively, and p^p is permeate pressure.

2.3 Performance Characterization

In general, the membrane performance is expressed in terms of permeation flux (J_i), and separation factor (α) or enrichment factor (β). The permeation flux, J_i , which is the permeation rate per unit membrane area, can be expressed as

$$J_i = \frac{m_i}{A \cdot t} \quad (2.10)$$

where m_i is the amount of species i collected in the permeate during a period of time t , and A is the effective membrane area.

The membrane selectivity, defined as the ratio of the permeability coefficients of different permeating species, is given by

$$\alpha_{ij} = \frac{P_i}{P_j} = \frac{D_i S_i}{D_j S_j} \quad (2.11)$$

Practically, the separation factor may also be used to characterize membrane permselectivity, and it is defined as

$$\alpha = \frac{Y_i/Y_j}{X_i/X_j} \quad (2.12)$$

where X and Y are the concentrations of the permeant in the feed and permeate, respectively, and it can be any convenient but consistent concentration unit. The subscripts i and j denote different permeation components.

In addition, the enrichment factor can also be used to characterize membrane permselectivity. It is expressed as the permeant concentration ratio in permeate to feed

$$\beta = Y_i / X_i \quad (2.13)$$

For convenience, weight fractions were used to calculate the enrichment factor in this research.

When the permeate pressure is quite low and can be neglected, by combining Equations (2.9) and (2.12), the separation factor can be expressed as

$$\alpha = \frac{P_i}{P_j} \cdot \frac{\gamma_i}{\gamma_j} \cdot \frac{P_i^{sat}}{P_j^{sat}} \quad (2.14)$$

As can be seen from Equation (2.14), the membrane selectivity is determined by (1) membrane intrinsic property (i.e., permeability coefficient to permeating species), (2) the activity coefficients of permeating species in the feed, which are determined by the feed composition and temperature, and (3) the saturated vapor pressure of the permeating species. All these factors influence pervaporation performance, and this will be discussed further later.

The permeability coefficient of the membrane to a specific component can be calculated from the permeation flux according to Equation (2.9), where the saturated vapor pressure and the activity coefficient in the feed can be determined using a process simulator, (e.g., Aspen). In practice, permeance, which is defined as the permeability coefficient normalized by membrane thickness, P_i/L , is also commonly used especially for composite membranes and asymmetric membranes where it is difficult to determine the effective membrane thickness accurately. The permeance is given by

$$\frac{P_i}{L} = \frac{J_i}{X_i \gamma_i P_i^{sat} - Y_i P^p} \quad (2.15)$$

2.4 Process Variables in Pervaporation

2.4.1 Feed Concentration

Feed concentration can influence the pervaporation performance in three aspects: mass transfer driving force, the sorption process, and the diffusion process. Feed concentration directly affects the partial vapor pressure of the permeating components, and thus influences the transmembrane driving force. In addition, the sorption uptake of permeant in the membrane increases with an increase in feed concentration. The diffusivity is also affected by the local permeant concentration, as the permeant

sorbed by the membrane can affect the polymer structure. As a result, the feed concentration affects both the solubility and diffusivity of the permeant in the membrane, and thus influences the permeability of the membrane. In addition, when multi-components are present in the feed, the interactions among the multiple compounds will also affect the permeation behavior of the individual component, and this phenomenon is usually termed as “coupling effect”.

2.4.2 Operating Temperature

Temperature can affect the pervaporation performance significantly because both the solubility and diffusivity coefficients are temperature dependent. Besides, the saturated vapor pressure is also temperature dependent. The temperature dependence of permeation flux follows the Arrhenius type of relationship:

$$J_i = J_{oi} \exp(-E_{Ji} / RT) \quad (2.16)$$

where E_{Ji} is the “apparent” activation energy for permeation of component i (J/mol). J_{oi} is a pre-exponential factor, R and T are the universal gas constant (8.314 J/(mol·K)) and the temperature (K), respectively. As a matter of fact, E_{Ji} characterizes the overall effect of temperature on both membrane permeability and driving force. The permeability coefficient can be related to the diffusivity coefficient and solubility coefficient, i.e.,

$$P_i = D_i \cdot S_i \quad (2.17)$$

and the temperature dependence of D_i and S_i can be generally expressed by

$$D_i = D_{oi} \exp(-E_{Di} / RT) \quad (2.18)$$

$$S_i = S_{oi} \exp(-\Delta H_i / RT) \quad (2.19)$$

and thus

$$P_i = P_{oi} \exp(-E_{Pi} / RT) \quad (2.20)$$

where $E_P = E_D + \Delta H$, and E_P is the ‘true’ activation energy of permeability, which is a combination of the activation energy of diffusion (E_D) and the enthalpy of dissolution (ΔH) of the permeant in the membrane. D_{oi} , S_{oi} , and P_{oi} are the pre-exponential factors and $P_{oi} = D_{oi} \cdot S_{oi}$. Combining Equations (2.15) and (2.20) yields

$$\frac{P_i}{L} = \frac{J_i}{\Delta p} = \frac{P_{oi}}{L} \exp(-E_{Pi} / RT) \quad (2.21)$$

where Δp is the partial pressure difference across the membrane. Thus, the activation energy for permeation E_P can be obtained from the slope of $\ln(J_i/\Delta p)$ vs. $1/T$ plot. A rule of thumb to estimate E_P is to subtract the molar heat of vaporization ΔH_V from the ‘apparent’ activation energy of permeation E_J ,

$$E_{Pi} = E_{Ji} - \Delta H_{Vi} \quad (2.22)$$

Equation (2.22) is useful to estimate E_P from corresponding E_J data since plotting $\ln J$ vs. $1/T$ is much easier. Caution should be exercised because Equation (2.22) applies only when (1) the permeate pressure is sufficiently low, and (2) the activity coefficient and the heat of evaporation of the permeants are not significantly influenced by temperature. Feng et al. [59] summarized the numerical values of E_J , which are usually in the range of 4 to 92 kJ/mol. They may be smaller than the heat of vaporization of many organic compounds, indicating a negative E_P value. This is understandable because $E_P = E_D + \Delta H$, and E_D is positive while the heat of dissolution ΔH is negative for exothermic sorption processes. When the dissolution process dominates over the diffusion process, a negative E_P value will be obtained, suggesting that membrane permeability decreases with increasing temperature.

2.4.3 Permeate Pressure

To maximize the transmembrane driving force for mass transfer, a low pressure on the permeate side is required. It has been proved that an increase in the permeate pressure will decrease the permeation flux significantly [60, 61]. In addition, the permeate pressure also affects the selectivity, and the selectivity may increase or decrease with an increase in permeate pressure, depending on the relative volatility of the permeating components. In general, the effects of permeate pressure on pervaporative recovery of components with a low saturated vapor pressure is much more significant than that of components with a high saturated vapor pressure.

2.4.4 Feed Flow Rate

The hydrodynamic conditions of the feed solution can also affect pervaporation performance. The selective permeation leads to accumulation of the slow permeating component on the membrane surface on feed side, which is referred to as “concentration polarization”. Because organic compounds are to permeate through the membrane preferentially, and their concentrations at the membrane surface are

depleted compared to bulk feed concentration, imposing an extra mass transfer resistance to permeation, i.e., the additional resistance to mass transfer from the bulk of the feed to the membrane upstream surface. Generally, concentration polarization is not significant for a majority of membranes used for pervaporation due to their limited permselectivity [61]. Besides, in dilute solutions, concentration polarization does not affect water permeation significantly because water concentration on the membrane surface is very similar to its bulk concentration. However, for membranes with high permselectivity, concentration polarization can be significant, thus the hydrodynamic conditions of the feed solution should be carefully controlled to minimize concentration polarization. Usually, a high turbulence on the feed side is recommended, providing the energy consumption is not too high.

2.5 Membrane Materials

For the separation of organic compounds from aqueous streams by pervaporation, organic compounds should preferentially permeate through the membranes. The membrane materials are thus required to be organophilic or hydrophobic to increase the affinity towards the organic compounds.

Among the current existed membrane materials, polymeric membranes are the most versatile and extensively used both in lab-scale and in industry due to the low production cost and easy processibility. Although molecularly sieving inorganic membranes usually have a higher separation factor and good chemical/mechanical/thermal stability, it is difficult or expensive to fabricate into large-area membranes without defects. The mixed matrix membranes (MMMs) combine both the advantages of polymeric membranes and inorganic membranes by incorporating the inorganic fillers into the polymer matrix. In the following, the common membrane materials used for the separation of organic compounds from aqueous solutions will be introduced as polymeric, inorganic, and MMMs, and emphasis will be placed on polymeric membranes and MMMs.

2.5.1 Organophilic/Hydrophobic Polymeric Membranes

Figure 2.3 shows the structures of the polymeric membranes that are commonly used in pervaporation. For the separation of organic compounds from water streams, membranes made from PDMS (also called silicone rubber) are widely used. PDMS is a state-of-the-art membrane material. It has an alternating -O-Si-O- structure with high flexibility. It is chemically/mechanically stable, easy fabricate into dense tubes or the selective layer of composite membranes, with good permselectivity for the separation of both some volatile organic compounds (VOCs) such as benzene, toluene, methanol, etc. and some organics with high boiling points in practice [35, 36, 55, 62-65]. Silicone rubber membranes

have been applied into industrial applications successfully, with separation factors up to 1000 for the removal of VOCs from water. Though some other rubbery materials with higher selectivity have been developed, PDMS is still prevailing for VOCs separation, because once the separation factor is high enough, the ease of membrane fabrication and membrane stability, etc. become important [39]. In addition to PDMS, other rubbery polymers such as polybutadiene [66], nitrile butadiene rubber, styrene butadiene rubber [67, 68], polyurethane [69, 70], etc. have also shown to be excellent materials for the separation of organic compounds from water.

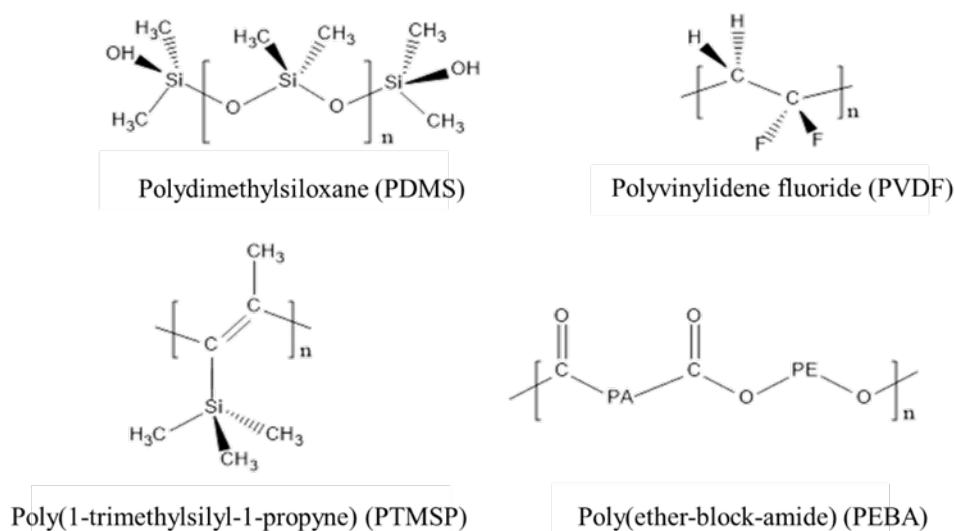


Figure 2.3 Structure of the commonly used polymers.

To improve the permeation flux of the rubbery polymers, which is generally low, some other materials with a high free volume such as poly(1-trimethylsilyl-1-propyne) (PTMSP), poly-4-methyl-2-pentyne (PMP), and other polymers of intrinsic microporosity (PIMs) are explored to give a high permeation flux [39, 71]. PTMSP, which has a very rigid backbone and an exceptional high fractional free volume (0.34), is the most permeable glassy polymer known up to today. It has gained much attention in a large number of studies for gas separation and separation of organics from water due to the extremely high permeabilities and high separation factors [39, 72]. However, PIM membranes have not found industrial applications yet because of the drastically reduced permeability over time. The performance of these membranes is quite unstable because of film densification and reduction of the free volume as a result of the relaxation of the polymer chains over time [39, 73]. Though it is difficult

to preserve the initial high free volume state over time, their separation characteristics and stability can be enhanced via chemical modification (crosslinking, functionalization, graft-polymerization, etc.) or physical modification (incorporation of inorganic or organic fillers) [74-76], and this may improve the prospects of this material.

Fluorine-containing polymers, including poly(vinylidene fluoride) (PVDF) and polytetrafluoroethylene (PTFE), are another commonly used glassy polymers in pervaporation because of their excellent thermal/mechanical stability, resistance to plasticization by organic compounds, ease of fabrication, and highly hydrophobic nature [77, 78]. In view of their strong mechanical strength and high hydrophobicity, PVDF and PTFE are usually fabricated into microporous membranes or integral asymmetric membranes which contain a relatively thin dense layer and a microporous support layer, or to yield a high flux. Previous investigation revealed that PVDF membrane had excellent pervaporation performance with both polar and non-polar organics [79], for example, ethanol [77], butanol [78], and benzene [80].

In addition to the aforementioned polymers, block copolymers with tunable properties have drawn attention as a promising material to fabricate membranes used in pervaporation. A block copolymer comprises two or more polymers with different properties, and by adjusting the composition of the copolymer and changing the molecular weight/chemical structure of the block, polymers with desirable properties can be obtained [81]. Among the various copolymers, poly(ether-block-amide) (PEBA) copolymers are most widely used, where the soft polyether segment favors the permeation of the desired species, and the hard polyamide segment increases the mechanical stability of the polymer. PEBA copolymers have been used for the pervaporation of some polar organics, exhibiting high permselectivity due to the excellent affinity between the polyether segment and the target organics [35, 38, 48, 82]. PDMS has also been assembled into copolymers with other mechanically strong polymer blocks [81, 83, 84], to improve the membrane rigidity to withstand harsh operating conditions. Polystyrene, an extremely stiff glassy polymer, can be introduced to form a copolymer with PDMS or polybutadiene, to change the polarity of the membrane, thus the sorption, diffusion, and pervaporation behavior [85-88].

Membrane material is the most important factor in membrane separation process, and future work should focus on the molecular design and exploring of new membrane materials using polymer chemistry [89], or proper post treatment of membranes to improve the hydrophobicity and/or free volume size [90].

2.5.2 Inorganic Membranes

Inorganic membranes made from silica, alumina or zeolite are of high mechanical, thermal and chemical stabilities, and free of swelling in solvents. They can be operated at higher temperatures with higher fluxes, thereby reducing the required membrane area. Zeolites (aluminasilicates) membranes are most extensively studied inorganic membranes due to their highly ordered well-defined structures. Zeolites with a high silicon to aluminum ratio tends to be more hydrophobic with a preferential sorption of organic compounds [42]. For example, Korelskiy et al. [91] prepared a ZSM-5 membrane with a thickness of 0.5 μm (silica to aluminum ratio of 139) on an α -alumina support for separation of ethanol/water and n-butanol/water, and the results showed that the flux was 100 times higher than that previously reported for n-butanol/water separation and 5 times higher than that for ethanol/water separation because of the thinner zeolite film. Inorganic membranes should be fabricated into large area without defect with a thin thickness to widen the practical applications [43].

2.5.3 Mixed Matrix Membranes (MMMs)

Organophilic/hydrophobic membranes usually suffer from low flux and low separation factor. To improve the separation performance, proper fillers can be incorporated into the polymer matrix by physical blending. The so-prepared membranes are called mixed matrix membranes (MMMs). The MMMs combining both the advantages of polymeric membranes (low cost, easy fabrication) and inorganic fillers (high mechanical/thermal stability), is a promising and cost-effective way to break the trade-off between permeability and selectivity of polymeric membranes, also can achieve long-term operation stability [42, 43]. With the development of advanced material and nanotechnology, numerous hydrophobic inorganic fillers such as zeolites [92-95], metal organic frameworks (MOFs) [49, 96, 97], covalent organic frameworks (COFs) [98-101], and many others (as shown in Figure 2.4) have been incorporated into the polymeric matrix to prepare MMMs for the separation of organic compounds from water. The properties of the fillers, including the hydrophobicity/hydrophilicity, surface chemistry and particle size, are crucial for the performance of the MMMs [102]. Appropriate fillers should be selected carefully based on the above criteria to prepare the MMMs with the desired properties. For organophilic pervaporation, hydrophobic fillers are preferred. The large surface area and high hydrophobicity can increase the sorption uptake of organic compounds in the MMMs, and the nanochannels within the fillers favor the permeation of the large organic molecules, leading to an increased flux and selectivity. For example, Li et al. [98] prepared a COF-300 and incorporated it into a PDMS membrane to form a MMM. They found the MMM promoted the permeation of furfural,

aniline, phenol, and butanol due to the ultrahigh affinity towards those organic compounds and simultaneously inhibited water transport. Zeolite imidazolate frameworks (ZIFs), a subset of MOFs, are also widely used to prepare MMMs. Ding et al. [49] prepared ZIF-8/PEBA MMMs to separate phenol from water streams, and they found the permeation flux and separation factor increased significantly with a 10wt% ZIF-8 loading in the MMMs because ZIF-8 increased both the sorption uptake of phenol and the diffusivity. Nonetheless, the compatibility between the inorganic filler and the polymer in the MMMs might not be so good, and the inorganic fillers can agglomerate, forming defects and decreasing membrane selectivity. In addition, the introduction of the fillers into the polymer might alter the polymer chain packing thus the free volume, leading to a decreased permeation flux. The compatibility of the polymer phase and the inorganic phase can be improved by modifying the inorganic fillers with coupling agents or coating the fillers with a polymeric layer prior to physical blending [42].

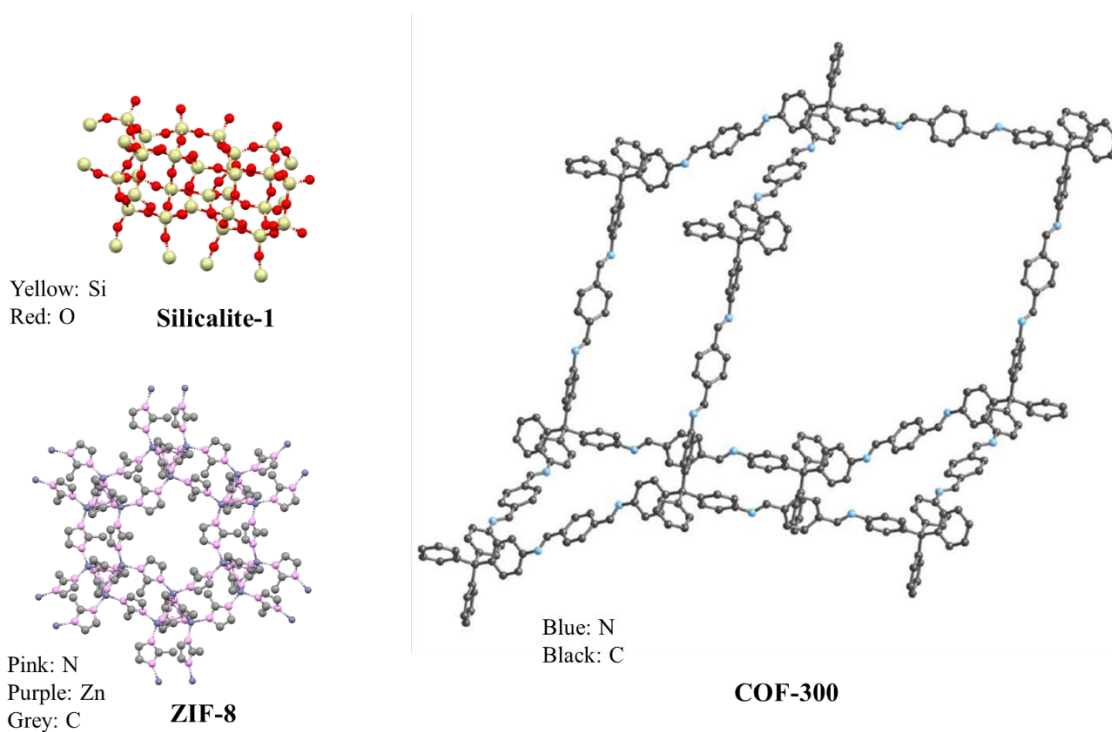


Figure 2.4 Structures of some representative hydrophobic fillers: silicalite-1, ZIF-8, and COF-300. The structures of silicalite-1 and ZIF-8 is generated from the crystallographic information file obtained from the Cambridge Crystallographic Data Center (CCDC code: GITVIP 1428189 and 864309, respectively); the structure of COF-300 was adapted from ref. [103].

2.6 Applications of Organophilic Pervaporation

The current applications of organophilic pervaporation mainly focus on: (1) removal/recovery of organic compounds from water, (2) recovery of valuable organic compounds, and (3) integration with other processes for process intensification. Nonetheless, the commercial development on organophilic pervaporation to treat aqueous mixtures is limited [56, 104], primarily due to the lack of specialized membranes (the membranes are designed to have high affinity towards the specific target compounds, thus case-sensitive), the high cost of the membranes, and the low treatment capacities [56, 105].

2.6.1 Separation of Organic Contaminates from Water Streams

The removal of organic contaminants from water streams by pervaporation is an economic method for wastewater treatment, groundwater purification, and other aqueous stream processing. When the concentration of the organic compounds in the feed stream is low, the concentration of the contaminants can be further lowered by pervaporation to reach the environmental regulation standard; and when the organic concentration is high, the concentrated organic compound in permeate can be readily recycled. Membranes used for the separation of organic contaminants are generally composite membranes with a thin layer of dense hydrophobic polymer as the selective layer on the top of a highly porous support. As mentioned before, PDMS, PEBA, and polybutadiene-based membranes are effective to remove the VOCs from water, and they have been reported extensively in the literature [66, 87, 106]. The commercial membranes of PERVAP 1060 and 1070 (Sulzer Chemtech) made from PDMS are recommended for the removal of hydrophilic organics, which usually have a separation factor of lower than 10, while a series of GKSS PEBA is patented to separate polar phenol with a high boiling point [40]. Wijmans et al. [106] used an organophilic MTR-200 PDMS membrane with a permselective layer of approx. 2.0- μm -thick on the top of a microporous support to remove and then concentrate some organic solvents from aqueous streams. It was found the membranes are effective to remove hydrophobic volatile solvents such as 1,1,2-trichloroethane, some halocarbons or hydrocarbons such as benzene, toluene, naphtha, and some other sparingly soluble solvents such as butanol, methyl ethyl ketone, ethyl acetate, etc. Economic analysis showed that pervaporation process using MRT-200 membrane for the removal of the dissolved organics outperformed other waste treatment methods. However, it was found that the membrane is not selective enough for very hydrophilic polar solvents such as ethanol, methanol, and isopropanol.

To improve the permeation flux of the organic compounds and the selectivity in pervaporation, various hydrophobic fillers such as ZSM-5 [107-109], silicate-1 [110, 111], carbon nanotubes [112,

113], ZIFs [96, 114], and COFs [98, 115] could be incorporated into the polymeric matrix to form MMMs. Compared with the pure polymeric membranes, all reported MMMs display an increased separation factor, and the permeation flux may increase or decrease depending on the different properties of the MMMs. For example, some studies showed that both the permeation flux and the selectivity increased with an increase in the filler loading in the MMMs provided that the filler loading was not too high to affect the formation of defect-free membranes [109-111, 114, 116-118]. They ascribed this phenomenon to the hydrophobic property of the fillers, where the hydrophobic filler increased the sorption and diffusion of organic compounds more pronounced than that of water. However, Liu et al. [107] observed a decreased permeation flux/permeability for water and ethanol and an increased selectivity with an increase in zeolite loading when incorporating ZSM-5 into PDMS membranes. They speculated that the reduced flux was caused by the increased transport resistance and the alteration of the polymer chain property in MMMs. Similar phenomena were also observed by Han et al. [108], who incorporated ZSM-5 into PDMS to separate ethanol/water mixture by pervaporation. The addition of crystallization fillers can change the chain packing of PDMS [119], thus the polymer free volume for permeation would be changed. In addition, membrane swelling would be restricted with an increase in the filler content in the MMMs. In an improved case, not only the higher separation factor, but a higher organic flux and lower water flux could be achieved for the separation of organic contaminants from water streams. Li et al. [98] found the PDMS membrane incorporated with COF-300 enhanced the permeability of butanol, phenol, furfural, and ethanol, simultaneously decreasing the permeability of water. Nevertheless, it cannot be generalized that COFs will be versatile fillers to prepare such MMMs with an increased organic flux and an inhibited water flux for pervaporation of various organic compounds, as organophilic pervaporation is generally case-specific. For example, Wu et al. [115] prepared a COF-LZU1/PEBA MMMs for pervaporative separation of n-butanol/water mixture, and they found the permeance of both water and butanol was decreased with increasing COF loading in the MMMs, but the decrease in butanol was much less than that of water, leading to an increased selectivity.

2.6.2 Recovery of Valuable Organic Compounds

Pervaporation has advantages in the recovery of many valuable organic compounds because it operates at low or moderate temperatures, avoiding the degradation of thermally sensitive but highly valued compounds. For example, it has been widely used to recover some aroma compounds [120], in which cases PDMS [121-126], poly(octyl-methylsiloxane) (POMS) [122, 123, 126-129] and PEBA [130-133]

are most commonly used membrane material, and all three polymers show good recovery performance. Bengtsson et al. [121] used a composite membrane with PDMS as the active layer to recover three types of aroma compounds (including alcohols, aldehydes, and esters) from an apple juice model solution by pervaporation. The results showed that the recovery performance differs a lot for different types of aroma compounds, where the alcohols with high hydrophilicity are least enriched (with an enrichment factor of approx. 5-13), and the esters are most concentrated (up to 100-fold) by pervaporation. This is indeed the case as the organophilic pervaporative membranes are more effective to recover the compounds with higher hydrophobicity [134]. Among the most commonly investigated aroma compounds, lactones and esters are most hydrophobic, usually displaying a high enrichment factor. Though aldehydes and alcohols are generally considered as hydrophilic compounds, organophilic pervaporation is still effective to recover these compounds, especially for molecules with a benzene ring [134]. In addition, organophilic pervaporation can efficiently recover ketones with more than 6 carbon atoms (i.e., high hydrophobicity), though a low selectivity was displayed for ketones with high hydrophilicity. It should be noted that the recovery of such species from practical natural sources where complex multiple components (e.g., proteins, lipids, carbohydrates, even microorganisms) co-exist need pretreatment prior to pervaporation to remove the possible components that would lead to membrane fouling, especially when MMMs are used, as the cages of the hydrophobic fillers are very vulnerable to be blockage by the molecules with a high molecular weight. Prior work concerning the recovery of aroma compounds by pervaporation using PEBA membranes has been well documented [135], and thus this aspect will not be further introduced.

2.6.3 Process Intensification

In addition to performing as a standalone separation process, organophilic pervaporation can be integrated with other processes to form a hybrid system to achieve process intensification, and this will further expand the application of organophilic pervaporation [136]. Particularly, organophilic pervaporation can be integrated with some reactive systems to remove the products and/or by-products to break the thermodynamic limit (or to alleviate product inhibition). On the other hand, as pervaporation alone might not supply waste disposal in accordance with the environmental regulation standard or might not produce permeate products suitable for further processing, it can be coupled with other separation processes to overcome such limitations. The integration of pervaporation with other chemical processes has huge potential in practical applications, and it will be introduced follows, which

is sub-categorized into: (1) integration with a reactor for product removal, and (2) integration with other separation processes.

Integration with a chemical or biochemical reactor

Many reactions are equilibrium limited, and the product/by-product can limit the conversion rate. The removal of the product/by-product species from the reactor can thus shift the reaction equilibrium, leading to higher product yield and throughput. As an energy-efficient process, organophilic pervaporation can be integrated with such reactions to remove the organic products. In most cases, the reactor and pervaporation unit are configured in separate unit, where the reaction mixture from the reactor is passed to the pervaporation unit for separation, and the retentate from the membrane unit is continuously returned to the reactor. Such configuration allows both the reaction and separation units to be operated under optimal conditions.

Pervaporation can be integrated with fermenters to remove the products, and of particular interest is the recovery of biofuel such as ethanol and butanol from fermentation. Acetone-butanol-ethanol (ABE) fermentation is a potential process to produce ethanol and butanol. Nonetheless, it suffers from strong product inhibition, leading to low solvent productivity. Products removal from the fermentation system can thus increase productivity [26, 137]. A great of work has been done to enhance solvent productivity by coupling pervaporation with fermentation [112, 138-140]. For example, Yen et al. [138] integrated pervaporation with a fermenter using PEBA membrane, and both the ABE productivity and the glucose yield were enhanced when compared with the batch fermentation system without pervaporation. Hecke et al. [140] found that in-situ product removal during fermentation by pervaporation with PDMS membrane can efficiently alleviate product inhibition and significantly enhance productivity. Compared with the standalone fermentation, an increase in productivity of 300-500% and 80-100% can be achieved when pervaporation was integrated with a batch fermentation process and a continuous process, respectively [141]. In addition to the alcohols, the productivity of other organic products such as aroma compounds from fermentation can also be enhanced significantly by integrating pervaporation with fermenters using suitable hydrophobic membranes [142, 143]. Nonetheless, some non-alcohol inhibitors such as organic acid can hardly be removed by organophilic pervaporation, and this can deteriorate fermentation performance. To overcome this, the culture medium can be partially replaced with fresh medium after the process proceeded for some time (fed-batch operation mode). In addition, when dealing with practical fermentation broth, the performance of these hydrophobic membranes

might not be stable due to membrane fouling because some big molecules or colloidal components could deposit on the membrane surface [144, 145].

In addition to integration with bioreactor (fermenter), pervaporation can also be coupled with chemical reactors to increase productivity. Camera-Roda et al. did lots of work on the integration of pervaporation with photocatalytic reaction, where the reaction kinetics, parameters pertinent to the integrated processes, optimization of the process were investigated experimentally and theoretically [133, 146-149]. Camera-Roda et al. [147] integrated the photocatalytic degradation of p-chlorophenol with pervaporation using two commercial organophilic membranes (GFT 1060, and GFT 1070, Sulzer Chemtech), and the reaction rate was improved significantly by continuous removal of the intermediates of hydroquinone and benzoquinone which hindered the photocatalytic reaction. However, not only the two intermediates, but p-chlorophenol can also permeate through the membranes. In another case where vanillin was produced by photocatalytic of ferulic acid, Camera-Roda et al. [149] integrated it with pervaporation to continuously recover vanillin from the reacting solution. With the integration of pervaporation, the undesired oxidative degradation of vanillin was largely avoided, and vanillin production was highly improved. PEBA membrane with a good affinity towards vanillin was used in this setup, and the permeance of the ferulic acid as well as the by-product was very low due to the low volatility. In another work, they found the whole process can be intensified by optimizing the pervaporation rate and the reaction rate [133]. Nonetheless, such investigations do not exceed the lab-scale level.

Integration with other separation processes

As mentioned before, due to the limited membrane permselectivity, in many cases, pervaporation alone is either insufficient to provide a complete solution for waste disposal in accordance with the environmental standards or permeate products are unsuitable for further processing economically. The integration of pervaporation with other separation processes can overcome these limitations. For example, pervaporation can be integrated with a decanter to improve the quality of the permeate, where the purity of the organic phase can be improved as long as phase separation occurs in the permeate, and the aqueous phase from the decanter can be recycled to the feed to maximize the overall efficiency [150, 151]. Lipnizki et al. [152] analyzed the feasibility of a pervaporation-adsorption-decanter hybrid system for the treatment of phenolic wastewater, where the retentate of pervaporation was fed into a sorption unit for further purification, and the permeate of pervaporation was introduced to a decanter (as shown in Figure 2.5A). The results showed that the hybrid process can produce a water stream for

direct discharge met the environmental regulations, and this system is economically superior to the stand-alone pervaporation units. In another case, Lipnizki et al. [150] investigated the pervaporation-decanter system for methyl-isobutylketone (MIBK) recovery and the pervaporation-adsorption-decanter system for chloroform recovery from wastewaters. It was found both systems are effective to treat such wastewaters taking the environmental and economic aspects into account. Nonetheless, it should be noted that the stand-alone adsorption (with heat regeneration) is the most economic process compared with pervaporation or pervaporation-based processes if the reuse of the solvent is not critical. In addition, pervaporation was also integrated with reverse osmosis (RO) to treat phenol-contaminated water [153]. In such a system, the retentate of pervaporation was polished by a RO membrane and the permeate stream from RO can be discharged directly (Figure 2.5B). It was shown that the overall cost of such a combination is lower than that of pervaporation alone.

Above all, the general function of pervaporation in a hybrid process is either to overcome the reaction limitations or as a concentration step prior to the final polishing step. The pervaporation-based hybrid process is economically advantageous over other conventional technologies as well as the stand-alone pervaporation. Nonetheless, though the coupling of pervaporation with other processes has immense value, only the pervaporation-esterification process to remove by-product water and the pervaporation-distillation process to split azeotropes have been realized on an industrial scale [154]. The great value of such integrations with organophilic pervaporation has not been fully exploited. The main reason lies in the high capital investment due to the complexity of the hybrid systems and the high price of the membrane unit. The development of highly efficient and economic membranes is therefore of great significance for the widespread implementation of hybrid processes.

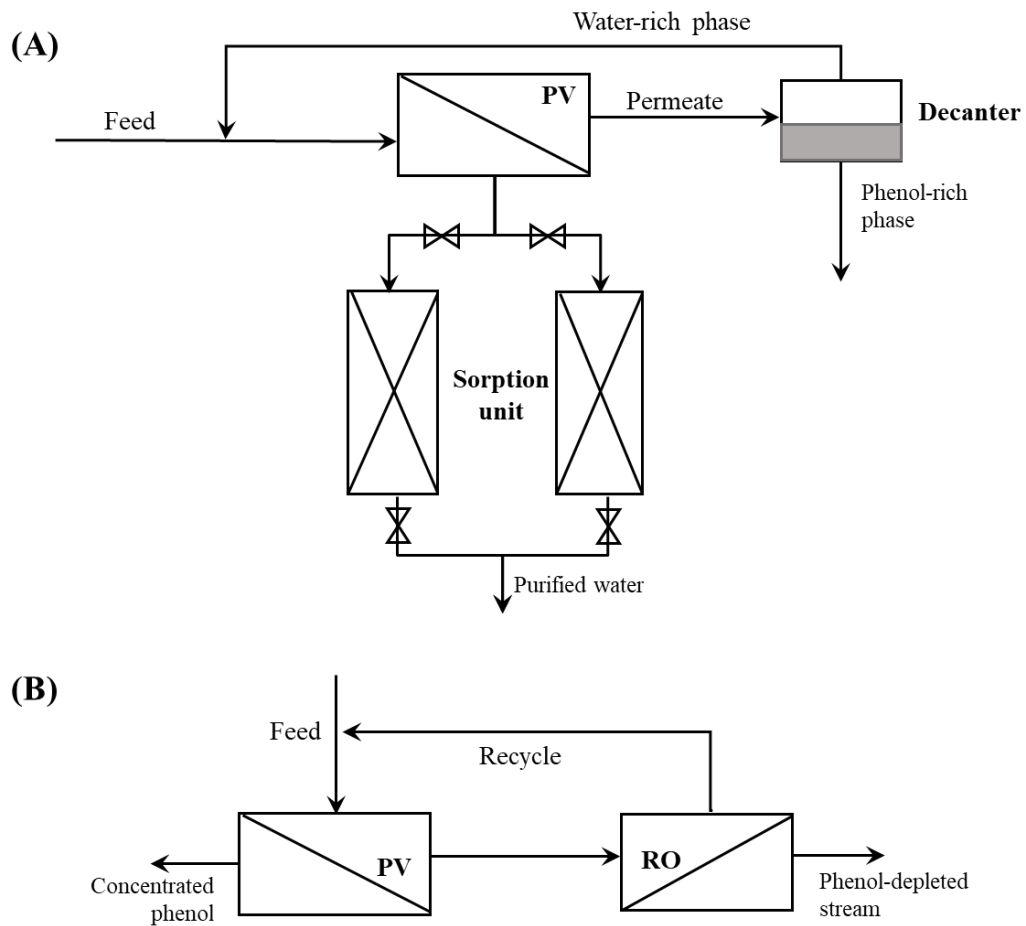


Figure 2.5 Schematic process layout for the recovery of phenol from wastewater using the (A) pervaporation-sorption-decanter system and (B) pervaporation-RO system.

Chapter 3

Removal of Phenolic Compounds from Water by Pervaporation¹

3.1 Introduction

As shown in Table 2.1, poly(ether-block-amide) (PEBA) membrane outperformed other materials for the separation of phenolic compounds by pervaporation. PEBA is a group of copolymers with micro-biphasic structures composed of soft polyether segments and hard polyamide segments. By adjusting the composition of the two segments, membranes with different properties could be obtained. A series of the copolymers from Arkema Inc. consisting of poly(tetramethylene oxide) (PTMO) and polyamide 12, is designated as PEBA xx33, with xx representing the shore D hardness that is determined by the PTMO content in the copolymer. A higher PTMO content corresponds to a lower hardness. The first report on PEBA membrane for pervaporative separation of phenol from aqueous solutions may be attributed to Bøddeker of GKSS [40] who disclosed in 1989 that PEBA 5533 outperformed other elastomeric polymers. Then PEBA 4033 membranes were produced at GKSS and investigated extensively for phenol separation [48, 155]. Kujawski et al. [35, 37] showed that the PEBA 4033 membrane from GKSS had a higher phenol flux and enrichment factor than two other PDMS-based commercial membranes. Kondo et al. [156] of Mitsui E&S also prepared a PEBA 4033 membrane on a nonwoven fabric substrate for phenol separation. Later, we [38] showed that PEBA 2533, which has the highest content of the soft PTMO segment in the thermoplastic elastomer copolymer series (80 wt%), had excellent permselectivity to phenol due to its good affinity. A chronological account of pervaporation studies on phenol separation using PEBA membranes is presented in Table 3.1. All the research focused on separation of single phenol solute, and no other coexisting phenolic compounds were involved despite that multiple phenolic compounds are generally present in actual wastewater from various sources [6, 21], where coupling effects among the different permeants are expected to occur.

¹ Portions of this chapter have been published in *J. Membr. Sci.*, **623**, 119043 (2021).

Table 3.1 Pervaporation-related research on the separation of phenolic compounds using PEBA membranes.

PEBA polymer	Phenolic solute	Co-existing solute in feed	Operating mode	References
5533	Phenol	-	Pervaporation (PV)	[40]
4033	Phenol	-	PV	[48]
4033	Phenol	-	PV	[155]
- ^a	Phenol	Methanol, formaldehyde	PV	[157]
4033	Phenol	-	PV	[156]
4033 (incorporated with palladium catalyst)	p-Chlorophenol	-	Catalytic PV	[158]
4033	Phenol	-	PV	[35]
4033	Phenol	Acetone	PV	[37]
2533	Phenol	-	PV	[38]
2533	Phenol	-	PV-crystallization	[82]

^a Not specified; presumably PEBA 4033, based on work presented at 6th Intl Conf Pervaporation Pro in Chem Ind [159].

Compared with other PEBA polymers, PEBA 2533 (~80 wt% organophilic polyether and ~20 wt% polyamide) is expected to yield a high permselectivity for the removal of hydrophobic phenolic contaminants in view of the high polyether content and the high free volume [160]. Thus, in this work, PEBA 2533 was selected as the membrane material to separate phenolic contaminants from their aqueous solutions. Although the pervaporation performance of PEBA 2533 for the simplest phenolic compounds (i.e., phenol) has been reported [38], comparative studies on pervaporative separation of other phenolic compounds are lacking, making it difficult to gain an insight into how the physicochemical properties of the phenolic compounds affect their permeation characteristics. In addition, as far as we know, all current studies focus on feed water containing a single phenolic solute, despite that multiple phenolic compounds are generally present in practical wastewater where complicated interactions among different permeants and the membrane exist. It is thus necessary to

study the pervaporation behavior of feed solutions containing multiple phenolic solutes. Furthermore, permeation flux and enrichment factor are used customarily to characterize the pervaporation performance. However, permeation flux is a quantity dependent on the membrane thickness and driving force for permeation, and therefore it is difficult to compare the permeabilities that are the attribute of the membranes based on the data sets from various sources where the operating conditions are not identical [161]. In this work, the membrane permeability, a quantity that is equal to flux normalized by the membrane thickness and the transmembrane driving force, was evaluated to provide an insight into the intrinsic property of the PEBA membrane as related to specific penetrants.

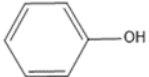
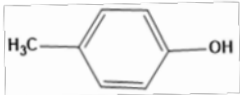

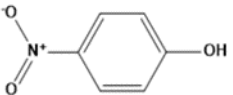
In this work, four representative phenolic compounds, including the simplest phenol (PhOH), p-cresol (MePhOH), p-nitrophenol (O₂NPhOH) and p-chlorophenol (ClPhOH) were selected to investigate their pervaporative removal from aqueous solutions. The influence of operating conditions (feed concentration and temperature) on the pervaporation performance of feed solutions containing a single phenolic component was investigated first. Then feed solutions containing multiple phenolic compounds were studied to quantify the coupling effects among the different phenolic compounds. For convenience, unless specified otherwise, the word “phenol” was used to represent a phenolic compound in the feed solution, and the specific phenolic compounds were denoted by their abbreviations (as described above). To the best of our knowledge, this is the first work investigating the separation of multiple phenolics by membrane pervaporation, which can provide valuable guidance in practical phenolic wastewater treatment.

3.2 Experimental

3.2.1 Materials

PEBA pellets (grade 2533) (comprised of ~80 wt% ether segment of poly(tetramethylene oxide) and ~20 wt% amide segment of nylon 12) were kindly provided by Arkema Inc. N,N-dimethylacetamide (DMAc), purchased from Sigma Aldrich, was used to dissolve PEBA for membrane casting. PhOH, MePhOH, ClPhOH and O₂NPhOH were all purchased from Acros Organics Inc, and their properties were shown in Table 3.2. The feed solutions used in all experiments were freshly prepared by dissolving predetermined amounts of phenolic compounds in de-ionized water. The pH of the four phenols in the feed was approximately 4.2-5.2, and the four phenols primarily existed in un-ionized state.

Table 3.2 Physical and chemical properties of phenolic compounds of interest.

Compound	Abbreviation	Molecular structure	Molar mass (g/mol)	Molar volume (cm ³ /mol) ^a	λ_{\max} , (nm)	Solubility in water (g/L) at 20°C	pK_a^b at 25°C	Boiling point under atmospheric pressure (°C)
Phenol	PhOH		94.11	85.5	269	83	9.99	181.7
p-cresol	MePhOH		108.13	101.1	276	20	10.26	202
p-chlorophenol	ClPhOH		128.6	99	279	27	9.41	219.7
p-nitrophenol	O ₂ NPhOH		139.11	111.5	317	11.6	7.15	279

λ_{\max} : wavelength of the maximum sorption of light in a solution.

^a From ref. [29]

^b From ref. [162]

3.2.2 Membrane Preparation

Membranes were prepared by the solution-casting technique. Briefly, a predetermined amount of PEBA was dissolved in DMAc to form a 15 wt% solution, which was heated at 80°C under vigorous stirring for 24 h to ensure a homogenous solution was formed. The solution was then allowed to stand still at 70°C overnight to release any entrapped gas bubbles before being cast onto a hot glass plate (70°C), followed by heating in an oven at 70°C for at least 48 h to evaporate the solvent. Finally, the membrane was detached from the glass plate. The thickness of the so obtained PEBA membrane was measured using a Starrett micrometer to be ca. 25 μm .

3.2.3 Pervaporation

Pervaporation experiments were conducted in a lab-scale setup, as shown in Figure 3.1A. The feed tank was thermostated by a Dyna-Sense® Thermoregulator Control System to control the operating temperature. The feed solution (1.2 L) was continuously circulated through the permeation cell, and the effective area of the membrane was 22.1 cm^2 . The membrane cell is composed of two detachable stainless-steel parts with inlet/outlet for feed flow and an outlet for the withdrawal of the permeate vapor (Figure 3.1B). A porous stainless-steel plate was embedded in the membrane cell to support the membrane. The two parts of the cell were clamped and sealed tightly using a rubber O-ring. Vacuum was provided using a vacuum pump on the permeate side to induce permeation, and the permeate pressure was maintained at ca. 40 Pa absolute. The permeate vapor was condensed and collected in a cold trap immersed in liquid nitrogen, and the permeation rate was measured gravimetrically. The concentrations of the feed and permeate mixtures were determined using a Shimadzu UV-vis spectrophotometer for binary phenol/water mixtures; an Agilent high performance liquid chromatography (HPLC) was used for solutions with multiple phenolic solutes. If necessary, the samples were diluted using deionized water before composition analysis. When testing the membrane for a given phenol solute at a new operating condition, i.e., new feed concentration or temperature, the system was conditioned by circulating the feed solution through the membrane cell at the predetermined operating conditions for at least 2 h to reach steady state. During this process, the permeation flux was measured periodically until it no longer changed with time, indicating steady state of permeation was reached. It required approx. 2 h before the system temperature was stabilized since the feed was circulated from the feed tank to the membrane cell continuously. When tested at different phenol solute compositions, the system was flushed with deionized water until no organic compound from previous runs was detected in the flushing solution before the target feed solution was admitted.

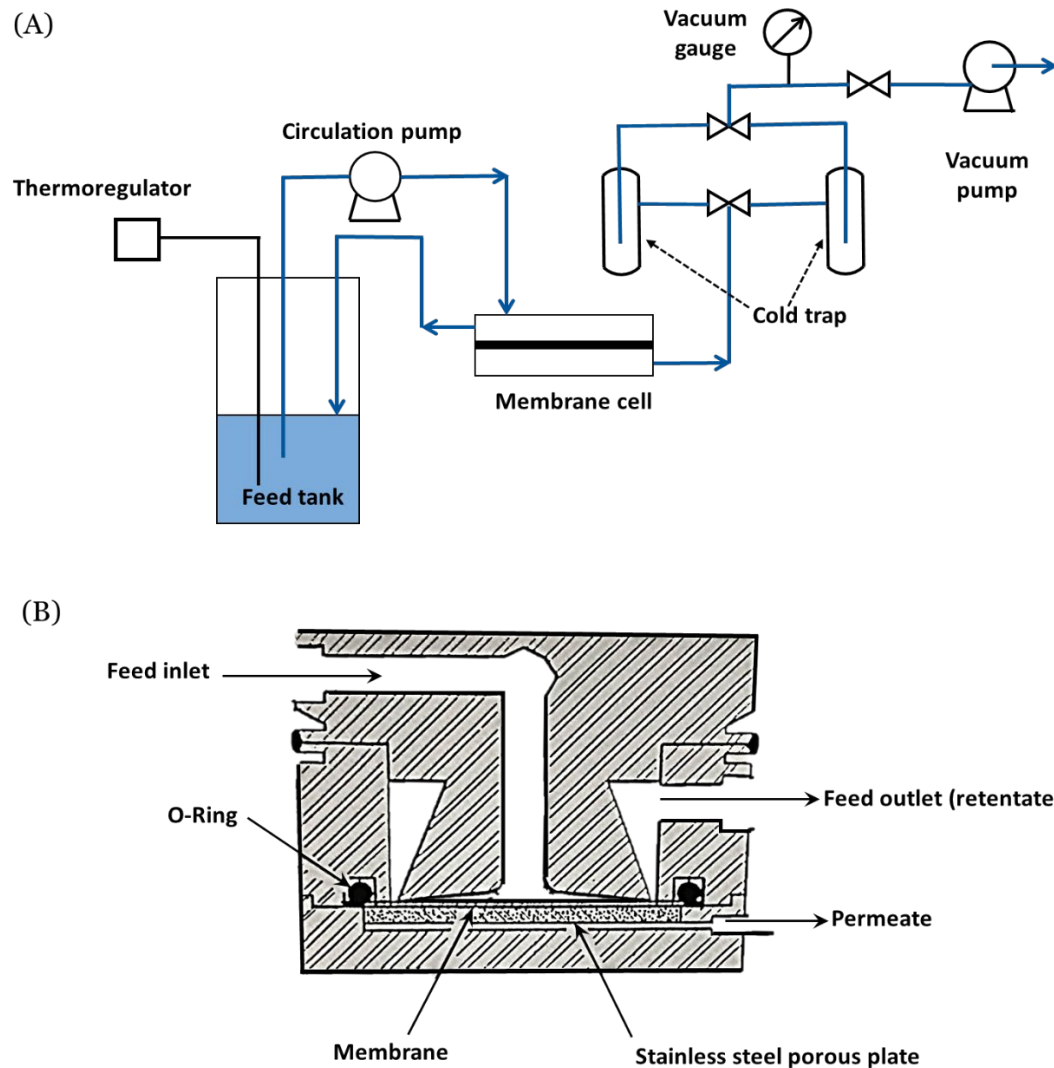


Figure 3.1 (A) Schematic diagram of the pervaporation setup, and (B) schematic diagram of the membrane cell [163].

For easy comparison, feed solutions with multiple phenolic compounds were prepared such that each phenolic solute has a concentration of 100 ppm (based on mass), and the pervaporation tests were carried out at 30°C. The permeate concentration was determined chromatographically using an Agilent 1100 HPLC equipped with a UV-vis detector and a C18 column (Zorbax SB-C18; 250 mm × 4.6 mm i.d., particle size 5 μm) at the following operating conditions: isocratic elution with 60% HPLC-grade water, 30% acetonitrile and 10% 0.2M ammonium dihydrogen phosphate buffer (V/V/V); flowrate 1.0 mL/min; injection volume 10 μL; the column oven temperature 30°C, and detection wavelength 225

nm. All the measurements were repeated at least three times and the average experimental error was found to be less than 10%.

The permeation flux (J) and enrichment factor (β) were calculated according to Equation (2.10) and Equation (2.13), respectively. The permeability coefficient (P), in analogue to gas permeation, was evaluated with

$$P_i = \frac{J_i \cdot L}{X_i \gamma_i p_i^{sat} - Y_i p^p} \quad (3.1)$$

The activity coefficient and saturated vapor pressure of permeant i in the feed were determined using Aspen Plus V8.4 based on the UNIQUAC model (Note that the activity coefficient of O₂NPhOH were unavailable as the relevant thermodynamic data were lacking in the data base [164]).

3.2.4 Sorption Experiments

Dry PEBA membranes were immersed in aqueous phenol solutions with various concentrations at 30°C for 3 days to reach sorption equilibrium, and the weights of the membrane samples before and after the sorption experiments were determined (denoted as W_o and W_e , respectively). The total sorption for phenol and water (q_t , mg/g), relative to the mass of the membrane, was calculated by

$$q_t = 1000 \times \frac{W_e - W_o}{W_o} \quad (3.2)$$

The reduction on the concentration of the phenolic compounds due to sorption was measured using a spectrophotometer to determine the sorption uptake of phenol (q_p):

$$q_p = \frac{V(C_o - C_e)M}{W_o} \quad (3.3)$$

where C_o and C_e are phenol concentrations (mmol/L) in the solution before and after sorption, respectively, and V is the volume of the feed solution that is largely constant, M is the molar mass of the solute. The water sorption uptake (q_w) was given by

$$q_w = q_t - q_p \quad (3.4)$$

3.3 Results and Discussion

3.3.1 Effects of Feed Concentration on Pervaporation Performance

The effects of feed phenol concentration on the total permeation flux at different temperatures (30 to 70°C) are shown in Figure 3.2. As expected, different molecules of the phenolic compounds have different behavior in pervaporation transport. At a given temperature, the total permeation fluxes for the PhOH solution and MePhOH solution increased only slightly as the feed solute concentration increased, while the opposite was observed for the ClPhOH solution. This can be explained from two opposite effects as discussed below. On the one hand, when the phenolic compounds are dissolved in the membrane, membrane swelling will occur as the structure of the polymer matrix is loosened by the sorbate, making it easier for the diffusion of the permeating molecules in the membrane. The extent of membrane swelling increases with an increase in the feed solute concentration. On the other hand, it has been proved that such aromatic molecules as phenol could interact with each other forming intermolecular clusters via hydrogen bonding [165-167]. Because of the considerably high phenol content in the membrane due to good phenol/PEBA affinity, the phenolic molecules in the membrane could interact with each other to form “phenol-phenol” clusters. The clustering of phenol molecules within membrane will become more significant as the concentration of the phenolic compounds in the membrane rises. While the phenol-phenol clusters in the membrane will diffuse more slowly than diffusion of non-clustered individual phenol molecules, the clusters are also going to block the free volume elements in the membrane to some extent, slowing down the movement of all the permeating molecules.

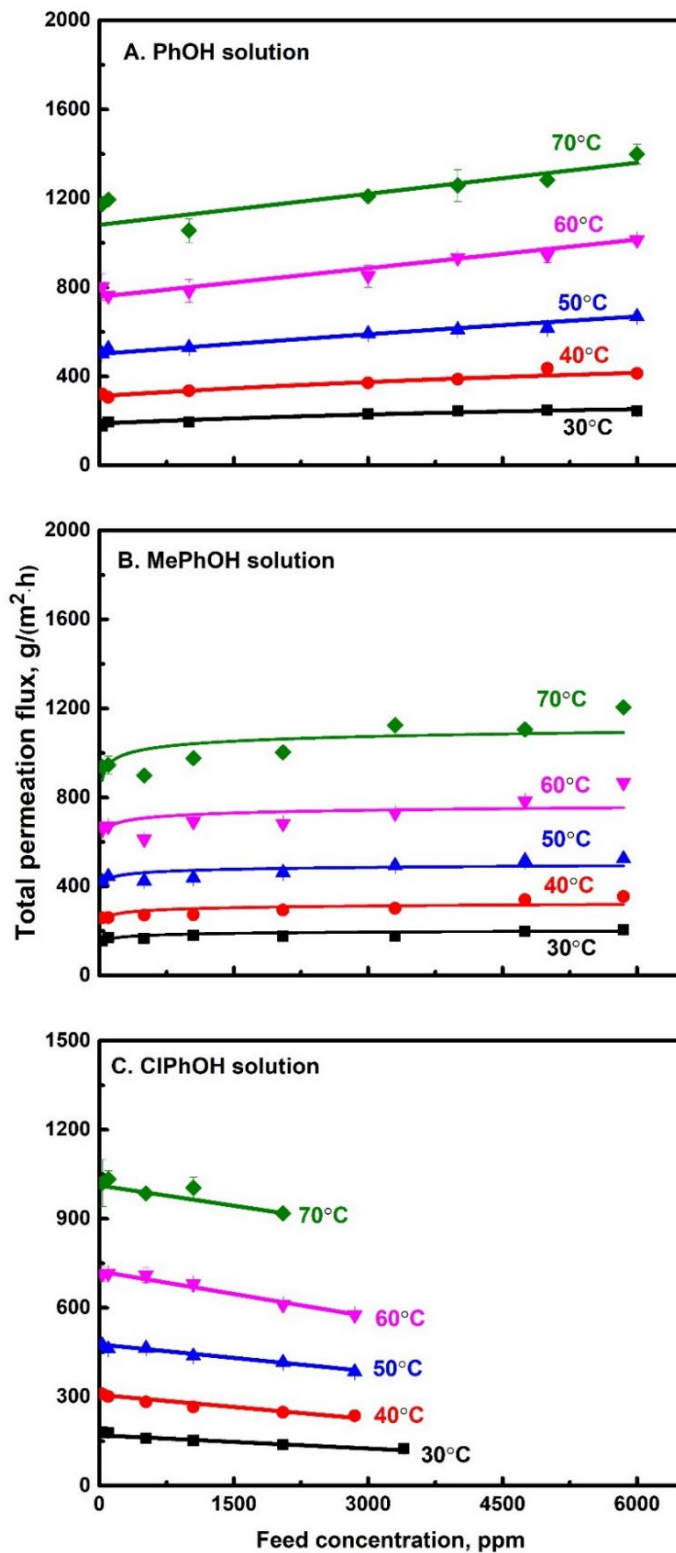


Figure 3.2 Effects of phenol concentration in the feed on total permeation flux at different temperatures.

The mass transport in pervaporation is determined by sorption and diffusion of the permeant in the membrane. Figure 3.3 shows the sorption uptake of phenol and water in the membrane at 30°C. Clearly, the sorption uptake of phenol is much higher than that of water, demonstrating the good solubility selectivity of PEBA toward the phenolics. Within the concentration range studied, the sorption uptake of phenol in PEBA follows the order of ClPhOH > O₂NPhOH > MePhOH > PhOH, which is consistent with the observation that phenolic compounds with electron-withdrawing groups (e.g., -NO₂ and -Cl) are more easily sorbed in various sorbents than phenolic compounds with electron-donating groups (e.g., -CH₃) [17, 168]. For PhOH and MePhOH, which have a relatively low sorption uptake in the membrane, the phenol-phenol clustering in the membrane was expected to be insignificant, and thus the effects of membrane swelling were dominant. As a result, the total permeation flux increased with an increase in feed phenol concentration. Among the four model phenols, ClPhOH displayed the highest sorption uptake in the membrane and thus ClPhOH clustering was more significant, and the blockage of transport passageways in the membrane and decreased mobilities of clustered molecules became noteworthy enough to cause a decrease in the permeation flux. This phenomenon was expected to be more pronounced at high feed ClPhOH concentrations.

It should be pointed out that if the phenol solubility in the membrane is sufficiently high, membrane stability will be compromised. Preliminary experiments showed that when the concentration of ClPhOH (which has the highest sorption uptake in PEBA) in the feed was greater than 3000 ppm, the mechanical strength of the membrane was significantly reduced. This is because the large quantity of sorbed solutes swelled the polymer matrix and compromised the mechanical strength of the membrane significantly (in fact, the membrane became “sticky” when the solute concentration in the membrane was high). This was why the membrane was not used to separate ClPhOH from solutions at high concentrations in this study, especially at high temperatures. In addition, it should be noted that O₂NPhOH permeation flux was very low, which may limit its application in practice, because of the low driving force for O₂NPhOH to penetrate the membrane due to its low volatility (saturated vapor pressure ca. 0.62 Pa at 65.5°C [169]). The permselectivity of the PEBA 2533 membrane to O₂NPhOH was thus only determined at 30°C at low concentrations for the purpose of comparing pervaporation behavior of the different phenolic compounds. The permeation flux, enrichment factor and permeate concentration for the four phenolic solutes at 30°C are shown in Figure 3.4.

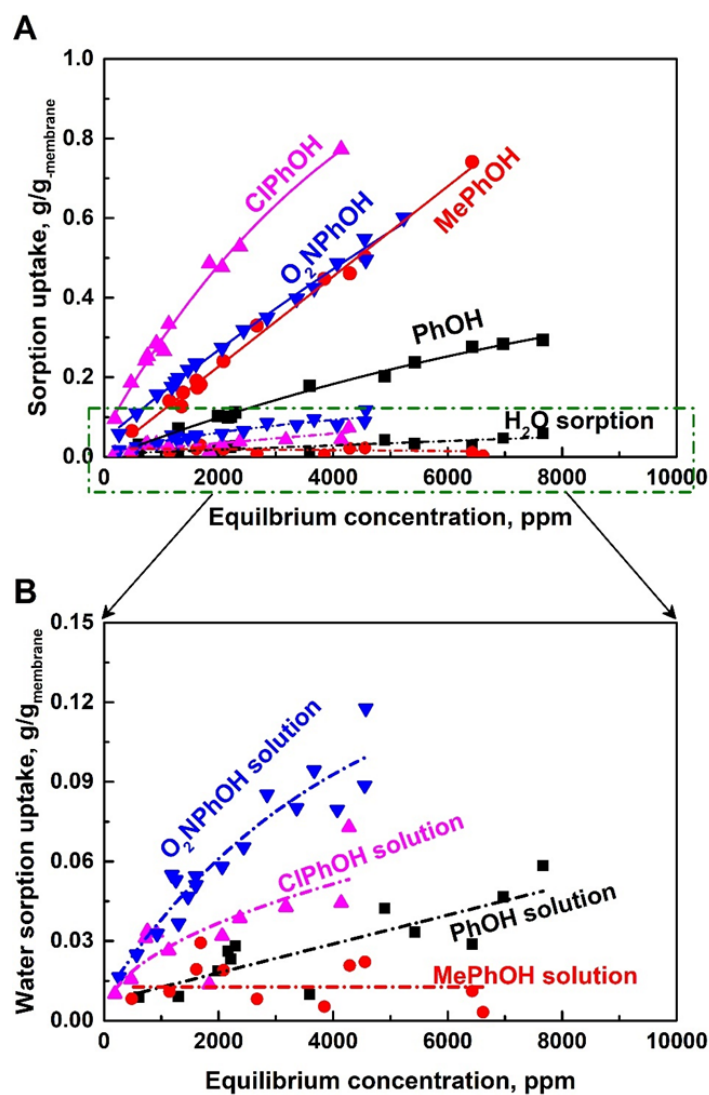


Figure 3.3 Equilibrium sorption uptake of phenol and water in the membrane as a function of phenol concentration in the liquid at 30°C. A zoomed-in graph showing water sorption uptake in the membrane is also presented.

Figure 3.4A shows the total permeation fluxes for the four phenol/water solutions. With an increase in the feed phenol concentration, the total permeation fluxes of the CIPhOH and O₂NPhOH solutions decreased, while the total fluxes of the PhOH and MePhOH solutions continued to increase. The difference in the permeation performance has been explained earlier based on membrane swelling and clustering of phenol molecules within the membrane when the sorption uptake became high. In addition, it was observed that the total permeation flux of PhOH solution was higher than MePhOH

solution within the concentration range studied. This is not surprising in view of the lower hydrophilicity of MePhOH, and it is expected that the permeation of a hydrophilic solute will be accompanied with a higher water permeation rate.

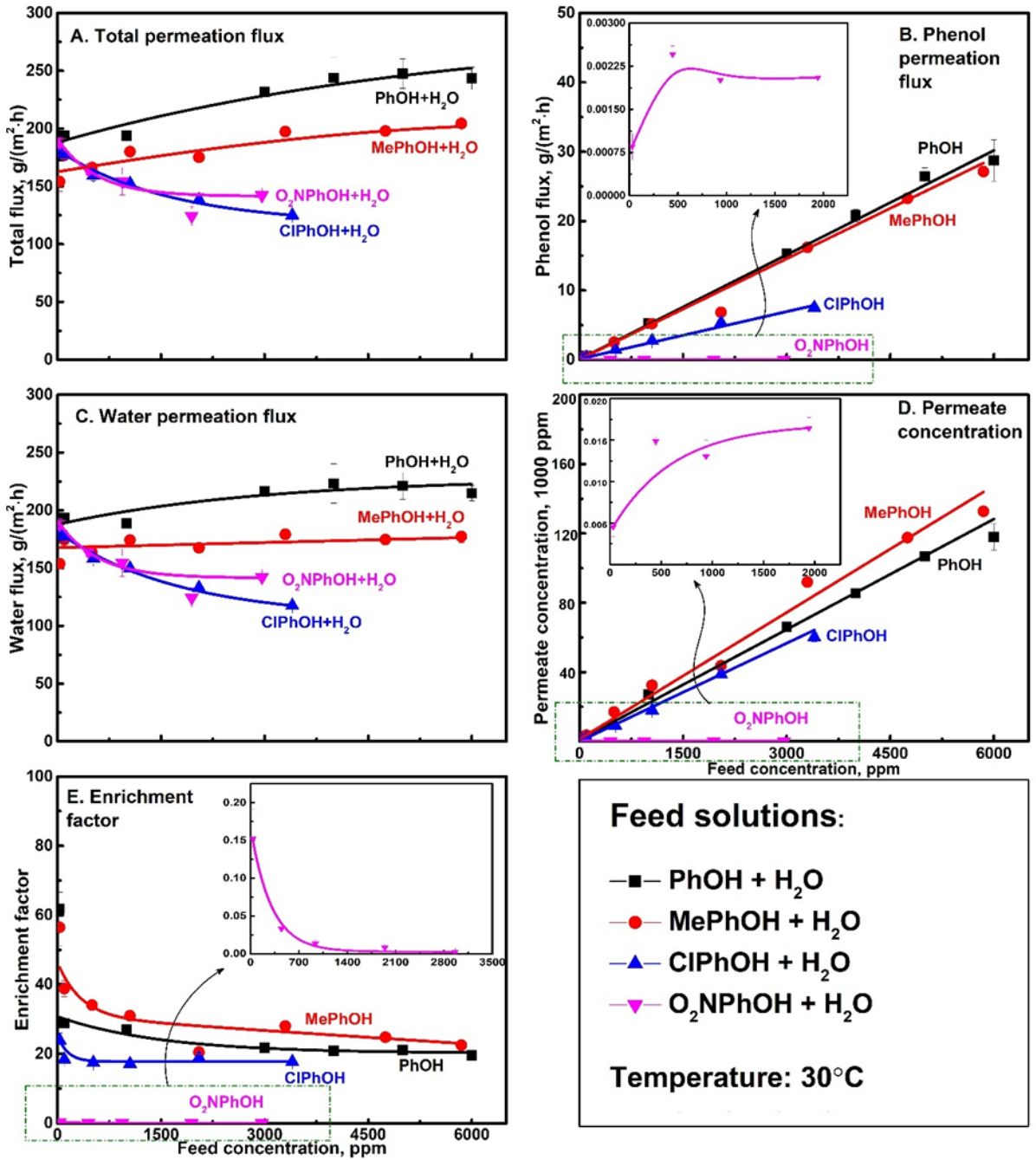


Figure 3.4 Pervaporation performance of different phenolic compounds at various feed concentrations at 30°C.

Figure 3.5 shows the effects of feed concentration on phenol permeation flux at different temperatures. At a given temperature, the permeation fluxes of PhOH, MePhOH and ClPhOH all increased with an increase in the feed phenol concentration. This is easy to understand as an increase in their feed concentration increased the transmembrane driving force for permeation. However, this trend was not particularly apparent for permeation of O₂NPhOH which displayed a much lower permeation flux (Figure 3.4B). In general, at a given phenol concentration in the feed, the phenol permeation flux was in the order of PhOH \approx MePhOH > ClPhOH > O₂NPhOH, which appeared to be negatively correlated to their molecular sizes (Table 3.2). This is not difficult to perceive because the movement of the large molecules in the polymer matrix is restricted, leading to a low diffusivity. On the other hand, while an increase in phenol concentration in a binary phenol/water solution would mean a decreased driving force for water permeation, such a decrease was negligibly small over the range of low phenol concentrations (<6000 ppm) investigated here. As shown in Figure 3.6, increasing the phenol solute concentration in the feed solution tended to slightly increase water flux for PhOH/water and MePhOH/water solutions, and the opposite was observed for ClPhOH/water and O₂NPhOH/water solutions. Due to hydrophilic properties of the phenolics, phenol sorption in the membrane is expected to increase the uptake of water in the membrane. As shown in Figure 3.3, within the concentration range investigated, the solubility of water in the membrane increased with an increase in phenol concentration in the liquid, while this trend was less pronounced for the MePhOH/water solution due to the lower hydrophilicity of MePhOH. Bøddeker et al. [48] and Kondo et al. [157] also observed a slow increase in water sorption with an increase in PhOH sorption in PEBA 4033 membrane. When the polymer softens as a result of the sorption uptake in the membrane, the diffusivity of the permeant in the membrane is enhanced as well. Consequently, both the solubility and diffusivity of water molecules were increased with an increase in phenol concentration, leading to a slightly increased water flux for PhOH/water and MePhOH/water solutions. For ClPhOH/water and O₂NPhOH/water solutions, however, water permeation flux was reduced due to blockage of the mass transport passageways by the large quantity of sorbed solutes in the membrane matrix.

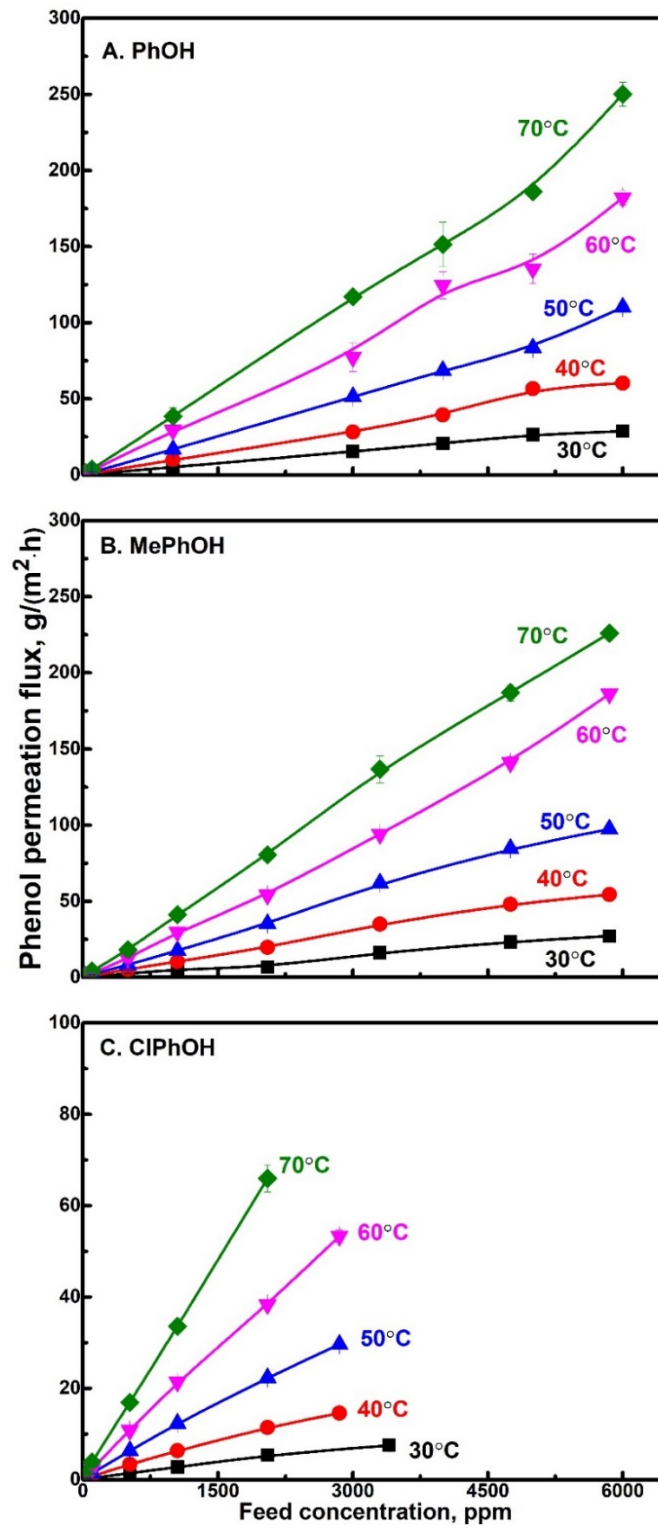


Figure 3.5 Effects of feed phenol concentration on phenol permeation flux at different temperatures.

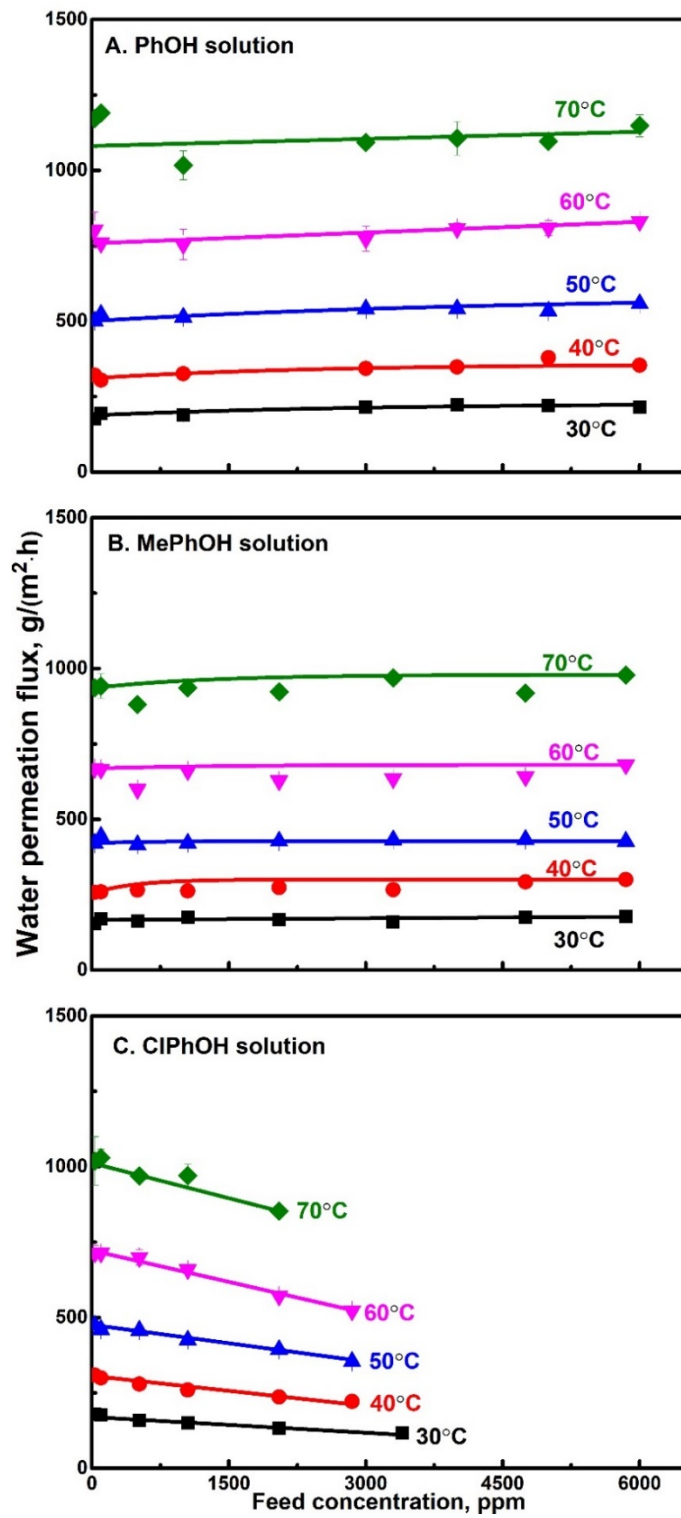


Figure 3.6 Effects of feed phenol concentration on water permeation flux at different temperatures.

Depending on operating temperature and phenol concentration in the feed, the phenol-enriched permeate could reach a concentration well above their solubility limit to induce phase separation at room temperature. This is shown in Figure 3.7 where the overall phenol concentration in the permeate is plotted against phenol concentration in the feed. Clearly, all the PhOH, MePhOH and ClPhOH were highly concentrated by pervaporation because of their excellent affinities with PEBA. Taking MePhOH as an example (Figure 3.7B), at a MePhOH concentration of 0.6 wt% in the feed, the MePhOH can be enriched in the permeate to a concentration of as high as 15 wt% at 40°C, much higher than its solubility in water (2.4 wt% at 40°C). This can readily be exploited for further purification (i.e., in conjugation with a decantation). It was of particular interest that some crystals of the phenolic compounds were precipitated on the wall of the cold traps because of de-sublimation of the vaporous phenols at the sub-atmospheric pressures during the pervaporation experiments, and as such de-sublimation may also be used to separate and recover phenolic solutes (at least partly) from aqueous solutions as high purity phenol crystals [82, 170]. In depth research in this regard, which is beyond the scope of the present work, will be carried out in separate studies.

Figure 3.8 shows the enrichment factor of the phenolic solutes based on the overall phenol concentration in the permeate relative to feed concentration. At a given temperature, the enrichment factor decreased quickly with increasing feed phenol concentration, and a largely constant enrichment factor was obtained when the feed phenol concentration was high enough. Similar trends can be seen for separation of PhOH from dilute aqueous solutions by pervaporation using different organophilic membranes [38, 157]. To gain a better understanding about the concentration dependency of phenol enrichment, we looked into the activity coefficients (γ) of phenols in water, which were shown to decrease with an increase in feed phenol concentration (Figure 3.9). That is, the vapor pressure of the phenol permeant in equilibrium with the liquid feed increases less than proportionally with an increase in the feed phenol concentration, resulting in a reduction in the enrichment factor. In addition, the aforementioned clustering of phenol molecules and membrane swelling also affected the permeation of phenol and water differently, resulting in variations in the extent of phenol enrichment.

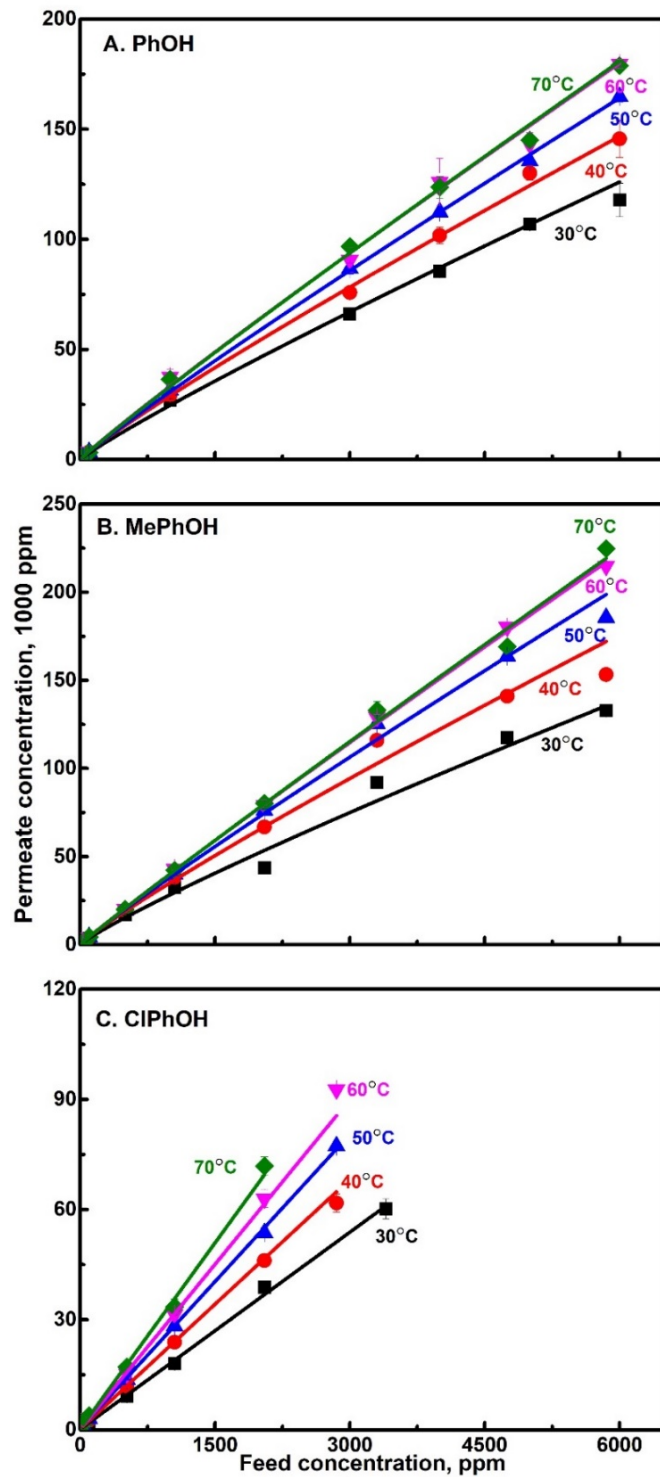


Figure 3.7 Effects of feed phenol concentration on the overall phenol concentration in the permeate at different temperatures.

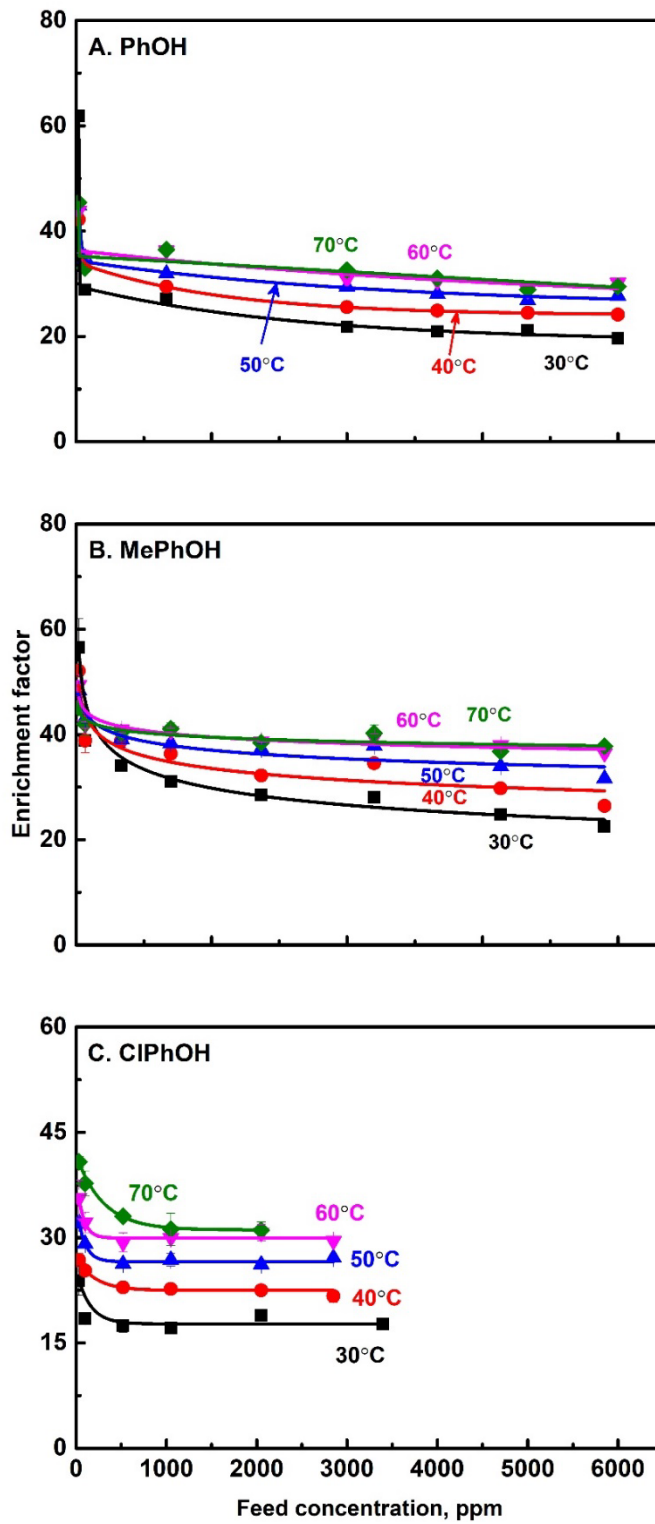


Figure 3.8 Effects of feed phenol concentration on its enrichment factor at different temperatures.

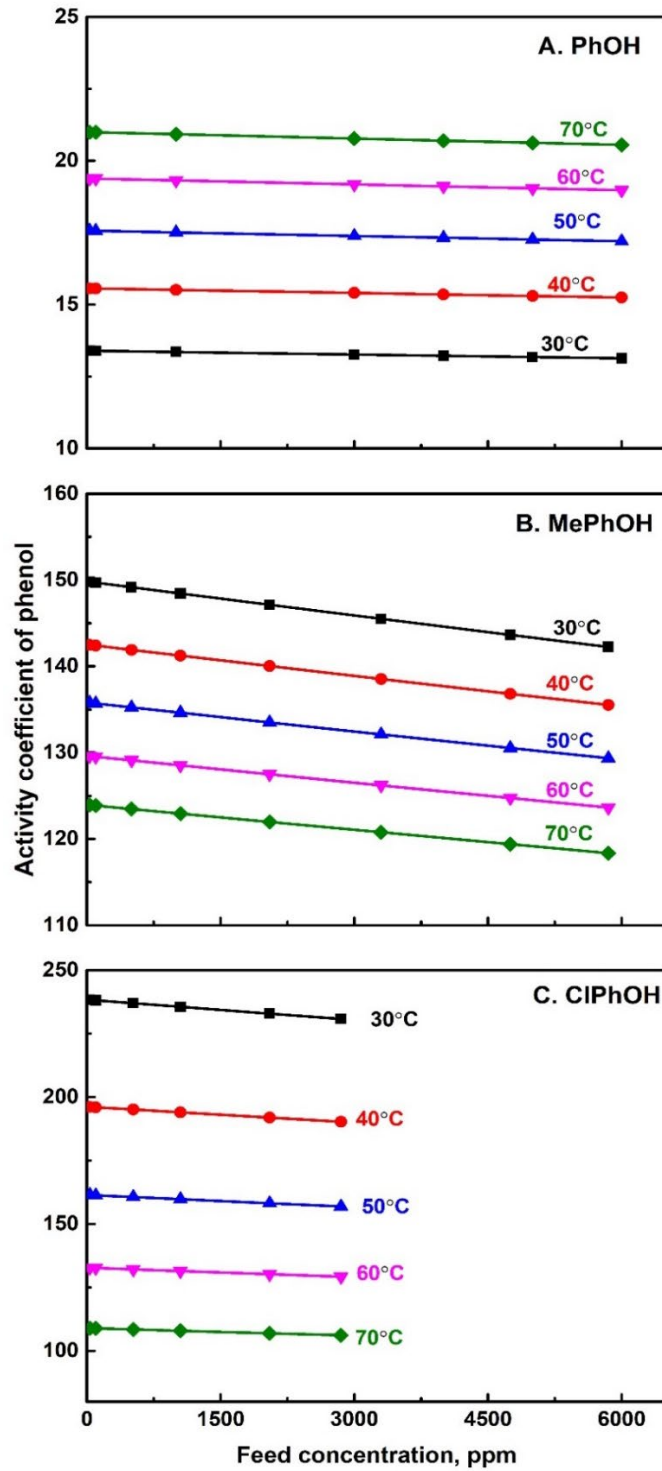


Figure 3.9 Activity coefficients of phenolic compounds in binary phenol/water solutions as calculated via Aspen Plus V8.4 based on the UNIQUAC model.

As the permeation flux is determined by both the membrane permeability and the driving force for permeation, it is of interest to distinguish these two effects in order to get an insight into pervaporation transport. The permeability coefficients of PhOH, MePhOH, and ClPhOH in the PEBA membrane were calculated using Equation (3), and the results are shown in Figure 3.10. Note that the permeability of PhOH at 30°C was not determined because of the very low partial vapour pressure differentials across the membrane $(X_i \gamma_i p_i^{sat} - Y_i p^p)$ that could not be evaluated accurately under such conditions. In general, the permeability coefficients of the phenolic solutes decreased with feed concentration, and they become largely constant for PhOH and MePhOH at high feed concentrations, whereas the membrane integrity would be an issue when exposed to high concentrations of ClPhOH. In addition to phenol-phenol clusters, phenolic compounds could also form phenol-water clusters with water molecules in dilute solutions [167, 171]. The clustering effects restrained phenol movement in the membrane. On the other hand, increasing the phenol concentration in feed led to increased sorption uptake in membrane, and membrane swelling was favorable to the membrane permeability. The concentration dependency of membrane permeability appeared to suggest that at low phenol concentrations, the effect of membrane swelling was insufficient to compensate the reduced phenol diffusivity due to molecular clustering, whereas the two opposite effects were largely balanced to yield a relatively constant permeability when the feed phenol concentration was high.

It is shown that the permeability coefficients of PhOH and MePhOH decreased with an increase in temperature, while the opposite was observed for ClPhOH. This is understandable in view of the temperature dependencies of solubility and diffusivity. An increase in temperature will not only enhance the local segment motion of the polymer chains, the permeating molecules also become more energetic, resulting in a faster diffusivity. However, because of the exothermic characteristics of phenol sorption in the membrane, a higher temperature is less favorable for phenol sorption. Therefore, the overall temperature dependency of permeability will be determined by the two opposing effects. As shown in Figure 3.3, PEBA has a low/moderate solubility for PhOH and MePhOH. Thus, the solubility reduction at higher temperatures had a more significant impact on the overall solubility for these two solutes, and such a reduction in solubility could not be compensated by the enhancement in diffusivity, leading to a lowered permeability. On the other hand, the effects of solubility reduction at higher temperatures would be less remarkable for ClPhOH, and the increased diffusivity with temperature would dominate over the reduced solubility, resulting in an increase in its permeability in the membrane.

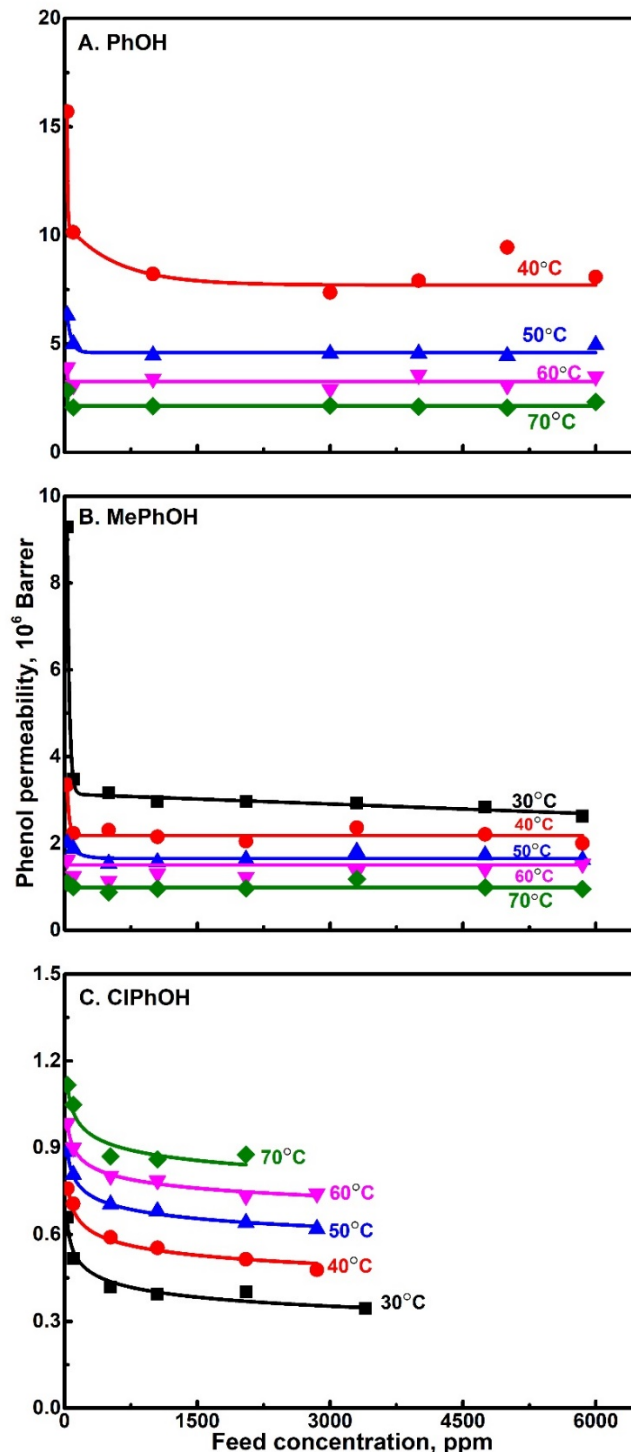


Figure 3.10 Effects of feed concentration on the permeability of different phenol in the membrane at different temperatures.

The permeability of water in PEBA was in the range of $(3 \text{ to } 7) \times 10^4$ Barrer, as shown in Figure 3.11, which was much lower than the phenol permeabilities. These results demonstrate the excellent permselectivity of phenol in PEBA. As one may expect, different phenol-membrane interactions will affect water permeability. With an increase in feed phenol concentration, the increased membrane swelling by PhOH and MePhOH in the feed solutions will facilitate water permeability in the membrane, as the small water molecules can readily permeate through the swollen polymer matrix. However, a reverse trend was observed for ClPhOH/water system, presumably due to predominating effect of ClPhOH-ClPhOH and ClPhOH-water clustering in membrane as a result of the high sorption amount that slowed down water permeation.

The comparison of phenol separation performance by pervaporation with commonly used membranes shown in Table 2.1 revealed that PEBA generally outperforms other membranes in terms of permselectivity. Similar conclusion was also obtained by other researchers [38, 47]. Attempt was made here to compare the membrane performance of different grades of PEBA copolymers for PhOH separation, and the results are presented in Table 3.3. Under similar operating conditions, PEBA 2533 generally has both PhOH flux and enrichment factor higher than other PEBA grades because of the high content of the soft ether block segment in PEBA 2533, demonstrating the potential of this grade of PEBA as a membrane material for pervaporative removal of phenolic compounds from water.

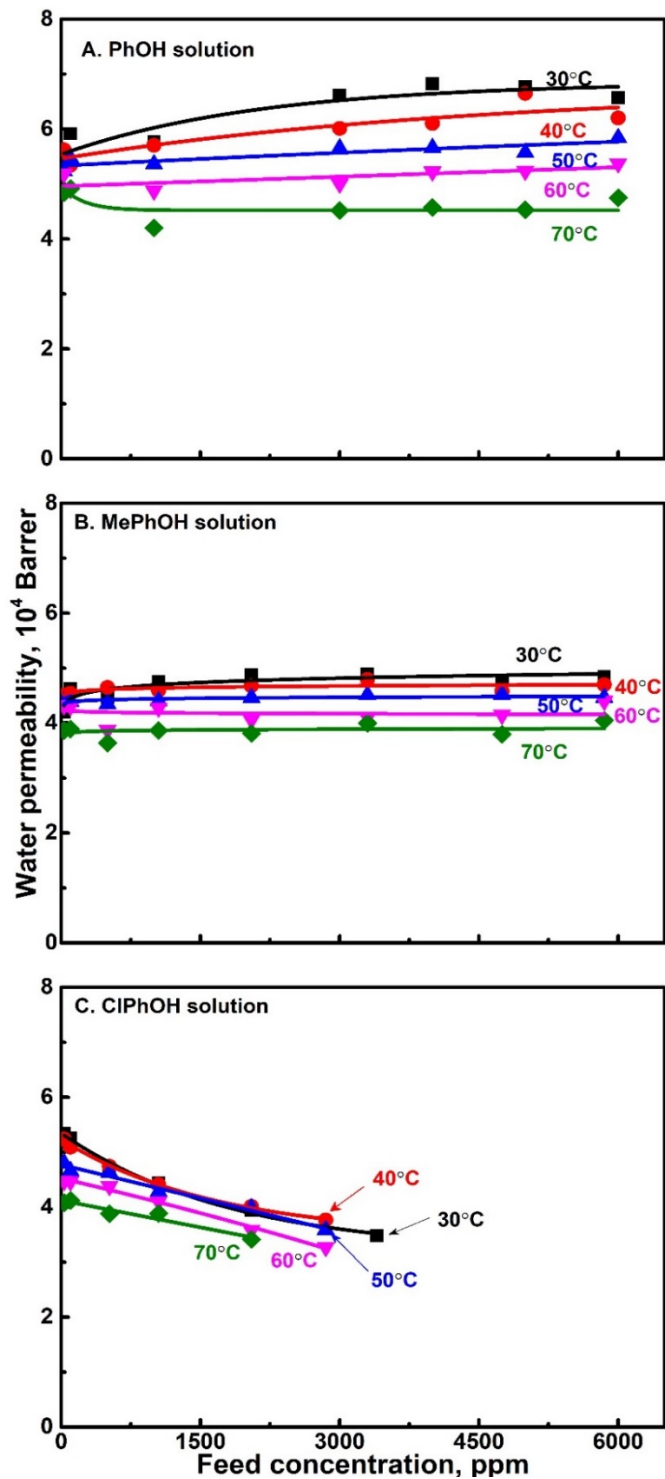


Figure 3.11 Effects of feed concentration on the permeability of water in the membrane in different feed solutions at different temperatures.

Table 3.3 Separation performance for binary PhOH/water mixtures with PEBA membranes.

PEBA grade	Temp. (°C)	Feed conc. (wt%)	Membrane thickness (μm)	PhOH flux (g/(m ² ·h))	Enrichment factor	Reference
5533	50	0.35	25.4-50.8	24	47	[40]
2533	50	0.4	25	68.5	28	This work
3533	50	0.01	25	1.35	27	[48]
4033	50	0.01	5	1.8	20	[48]
2533	50	0.01	25	1.8	34	This work
4033	60	1	80	75	32	[35, 37]
2533	60	0.6	25	182	30	This work

3.3.2 Effects of Temperature on Permeation Behavior

The temperature dependency of the permeation flux follows an Arrhenius type of relation (Equation (2.16)). Figure 3.12 shows the partial permeation fluxes of phenol and water as a function of reciprocal temperature on a semi-log scale, where we can see that both the phenol and water fluxes increased significantly with temperature. For example, there was a seven-fold increase in the phenol flux when temperature increased from 30 to 70°C. This is understandable in view of the following: (1) an increase in temperature increased the saturated vapor pressure of the penetrant in the liquid feed, thereby increasing transmembrane driving force for permeation; (2) at higher temperatures, the permeating molecules were more energetic, and the thermal motion of the polymer chains was enhanced, which favor penetrant diffusion in the membrane. In spite of the unfavorable impact of temperature on permeant solubility in the membrane, the permeation flux was shown to be affected positively by temperature. It appears phenol flux was more sensitive to a change in temperature than water flux within the concentration range studied. The apparent activation energy for permeation (E_J), which was obtained from the slope of the straight lines in Figure 3.12, was in the order of ClPhOH > MePhOH > PhOH > H₂O, the same order as their molecular sizes. This also explains the data displayed in Figure 3.8 that the phenol enrichment factor increased with an increase in temperature.

The apparent activation energy for permeation, E_J , obtained from Figure 3.12, characterizes the overall temperature dependency of permeation flux that has accounted for both the driving force and membrane permeability. According to Equation (2.20), the temperature dependency of membrane permeability also follows an Arrhenius type of relation (as shown in Figure 3.13). The activation

energies E_p for PhOH and MePhOH were negative (Table 3.4), suggesting that temperature had an adverse effect on membrane permeability. E_p may be considered to be a sum of the activation energy for diffusion (a kinetic parameter) and the enthalpy change of sorption (a thermodynamic parameter) of the membrane/penetrant system. The activation energy for molecular diffusion in a polymer is generally positive, and the enthalpy change of phenol sorption is negative. When the negative enthalpy change of sorption was dominant over the positive activation energy for diffusion as far as the membrane permeability was concerned, a negative value of E_p would be observed. The negative E_p for PhOH and MePhOH also suggests that their increased permeation fluxes at a higher temperature was mainly attributed to their increased driving force for permeation, as their permeabilities in the membrane were actually lowered at higher temperatures. The E_p value for ClPhOH was positive, suggesting that temperature has a positive influence on the permeability of ClPhOH. For water permeation, E_p was also negative, indicating that temperature influenced water solubility more significantly than diffusivity. Furthermore, as shown in Table 3.4, neither the apparent activation energy for permeation nor the intrinsic activation energy for membrane permeability showed an infinite trend with phenol concentration in the feed. The activation energy, which represents an energy barrier to be overcome by the permeating molecules for permeation to occur, is an intensive property depends largely on the nature of the permeant and the polymer. In view of the accuracy in calculating the activation energy and the relatively low feed concentrations studied, it is not unexpected that the feed solute concentration showed little impact on the activation energy. In an ideal case where the solubility and diffusivity in a membrane are constant, the activation energy will be independent of the feed composition.

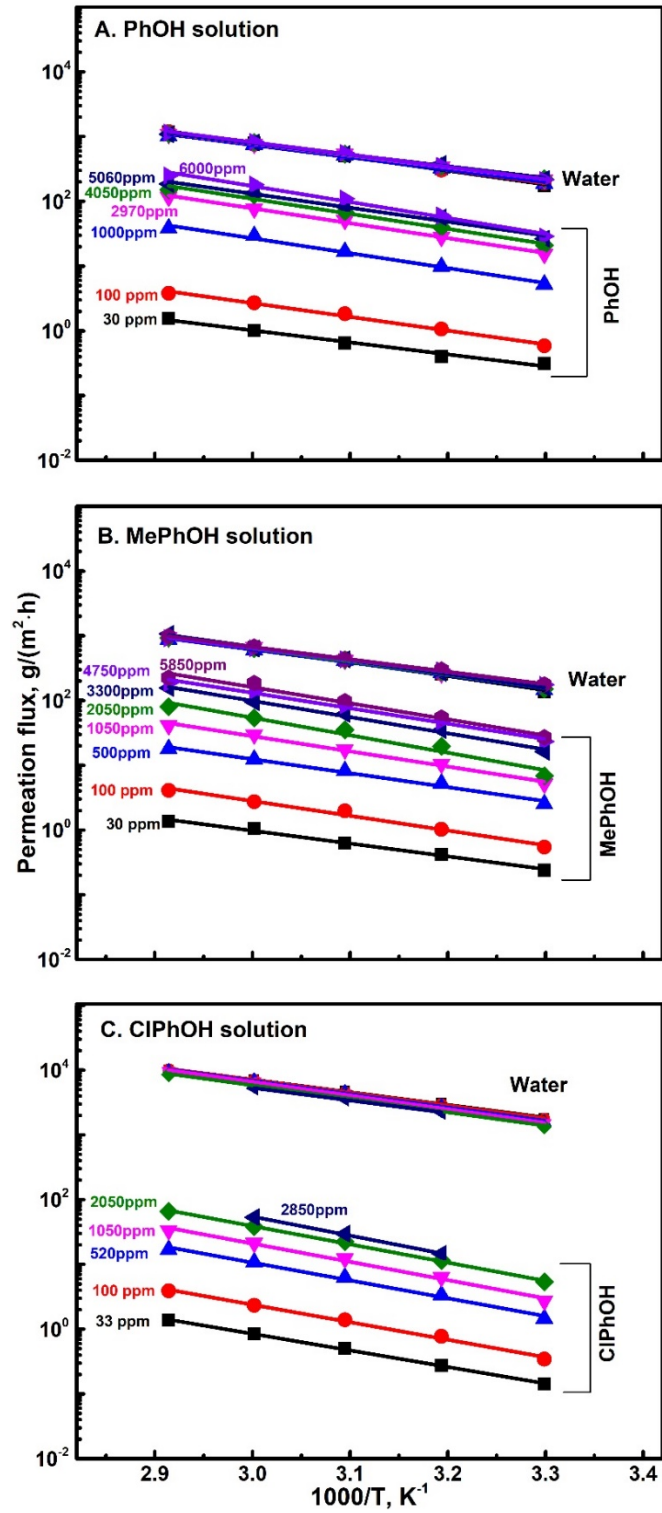


Figure 3.12 Effects of temperature on the partial permeation fluxes at different feed concentrations.

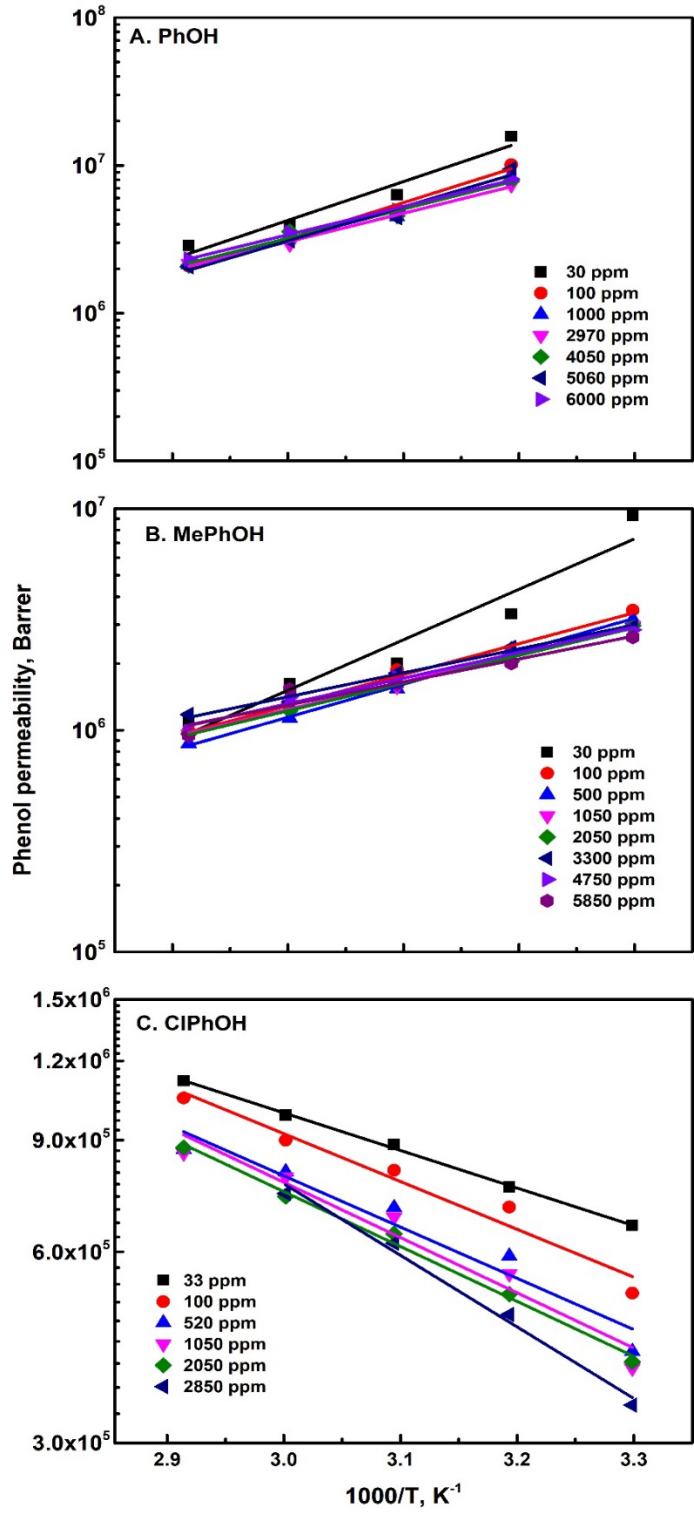


Figure 3.13 Effects of temperature on the permeability coefficients at different feed concentrations.

Table 3.4 Apparent activation energy for the permeation of phenol (E_{Jp}) and water (E_{Jw}), and the intrinsic activation energy for membrane permeability to phenol (E_{Pp}) and water (E_{Pw}) at various feed concentrations.

Feed conc., ppm	E_{Jp} , kJ/mol	E_{Pp} , kJ/mol	E_{Jw} , kJ/mol	E_{Pw} , kJ/mol
PhOH				
30	35.5	-50.2	40.8	-4.1
100	40.6	-47.0	39.3	-3.9
1000	44.1	-38.8	36.5	-6.7
2970	44.0	-36.9	35.1	-8.2
4050	44.4	-37.8	35.0	-8.2
5060	41.4	-44.2	34.1	-8.9
6000	47.2	-36.5	36.5	-6.8
MePhOH				
30	38.0	-43.6	41.6	-4.2
100	43.6	-26.7	39.9	-3.4
500	41.4	-28.5	38.2	-7.6
1050	45.0	-23.9	39.1	-4.2
2050	51.8	-23.9	38.7	-5.5
3300	48.0	-20.7	40.3	-4.8
4750	45.6	-22.1	35.6	-7.7
5850	47.5	-19.9	36.7	-6.6
ClPhOH				
33	49.0	11.3	37.3	-6.0
100	51.8	14.4	38.0	-5.3
520	52.7	15.5	39.4	-3.9
1050	54.0	16.7	40.4	-2.9
2050	54.0	16.6	39.8	-5.3
2850	56.3	21.6	37.2	-6.0

In pervaporation, because of the similar mathematical forms of temperature dependencies of permeation flux and membrane permeability followed, the intrinsic activation energy (E_p) is often related to the apparent activation energy (E_J), by an approximation $E_{p_i} = E_{J_i} - \Delta H_{V_i}$ (Equation (2.22)), when (1) the downstream side pressure is much lower than the vapor pressure in equilibrium with the feed; (2) the heat of evaporation and the activity coefficient of permeating molecules are not significantly influenced by temperature. The E_p and E_J relation was found to apply for the permeation of water, as shown in Table 3.4, where the $(E_J - E_p)$ values (43.8 ± 0.9 kJ/mol) were comparable with the ΔH_V value (42.9 kJ/mol over the temperature range of interest) for all the water/phenol feed mixtures. However, this semi-empirical $(E_J - E_p)$ relation did not apply for the phenolic permeants. While the average $(E_J - E_p)$ values were 84.1, 71.3 and 37.0 kJ/mol for PhOH, MePhOH and ClPhOH, respectively, their corresponding ΔH_V values were 58.0, 61.1 and 54.0 kJ/mol as estimated with the modified Watson equation using parameters from Yaws' Chemical Properties Handbook [172]. This was not unexpected because of the significant departure from solvent behavior as a result of the high boiling points of the phenol compounds and the low phenol concentrations as reflected by the strong temperature effect on the activity coefficients of the phenolic compounds (see Figure 3.9). Thus caution should be taken when using the approximation relation $E_p = E_J - \Delta H_V$, which is sometimes used for convenience to estimate the intrinsic activation energy for permeation (E_p) from the more readily available E_J and ΔH_V , as it does not work well for permeants with low volatilities.

3.3.3 Coupling Effects among Permeating Components

As mentioned before, almost all studies on pervaporative separation of phenol from water have focused so far only on feed water containing a single phenol. However, in practice, multiple phenolic compounds often coexist in the effluent, where interactions among the different phenolic compounds cannot be neglected. Such interactions are expected to influence the sorption and diffusion (and thus pervaporation) of individual phenol compounds. To quantify the coupling effect on permeation of individual phenol permeant, a relative permeation flux with and without the presence of other phenolic compound(s) was used to characterize the interactions between different phenolic solutes. Thus a permeation flux ratio (η_{ji}) was defined as the ratio of the permeation flux of solute i in the presence of solute(s) j (where $j \neq i$) in the feed solution (i.e., water + solute i + solute(s) j) to the permeation flux of solute i in the feed solution without other phenolic solute(s) (i.e., binary solution of water + solute i). For a given phenol component i in the feed, if the presence of a second phenol has no impact on the permeation of component i , then the flux ratio will be equal to 1; a flux ratio (η_{ji}) greater than 1 means

the permeation of phenol component i was enhanced by the presence of the additional phenol component. The results are shown in Table 3.5. For the permeation of PhOH, MePhOH, and ClPhOH, the permeation flux ratios were all less than 1, indicating the permeation of these individual phenol components was slowed down by the presence of other phenol components. Such inhibitive coupling effect can be attributed to two aspects: reductions in solubility and diffusivity in the membrane. Because of competitive sorption, the sorption uptake of a given phenol solute will be reduced by the presence of other phenols present in the feed solution. This is supported by the study of Raisi et al. [122], who found that the preferential sorption of n-hexanol in a PDMS membrane reduced the sorption of isopentyl acetate and adding n-hexanol to an aqueous isopentyl acetate solution caused a negative coupling effect on the permeation flux of the ester molecules. In addition, clustering of different phenol compounds tends to slow down the movement of all phenol permeants in the membrane, resulting in a lower diffusivity. Although the presence of additional phenol solutes in the feed will increase the extent of membrane swelling, the inhibitive coupling effect of coexisting phenolic compounds seems to indicate that the reduced diffusivity and solubility due to molecular clustering and sorption competition were not sufficiently compensated by the membrane swelling as far as the phenol permeation flux was concerned.

On the other hand, the permeation flux of O₂NPhOH was increased significantly by the addition of other phenols. In general, O₂NPhOH permeation through the membrane was quite slow due to its small driving force in spite of its high sorption uptake in the membrane. However, it may be hypothesized that the presence of other fast permeating phenol compounds would facilitate O₂NPhOH permeation because O₂NPhOH molecules would be carried over by the fast-permeating phenol molecules as a result of O₂NPhOH clustering with other phenol molecules. Trifunovic et al. [173] also suggested that the effects of clustering are likely to be evident in diffusion through polymer membranes in separation of multiple organic solutes from water. It is expected that the almost-impermeable O₂NPhOH will be “dragged” by the fast-permeating species across the membrane due to the formation of phenol clusters. When PhOH (which has the highest permeability among the phenols studied here) was added to the O₂NPhOH solution, O₂NPhOH experienced the most significant enhancement in its permeation flux. As expected, O₂NPhOH permeation was less enhanced when MePhOH and/or ClPhOH co-existed in the feed because of their relatively large molecular size and thus low diffusivity. As the four phenols primarily existed in un-ionized state in the feed, the ionic interactions were unlikely to cause such coupling effect. It should be noted that in spite of the permeation enhancement by other co-existing phenols, O₂NPhOH permeation rate was in general rather low.

Table 3.5 Permeation flux ratio with and without the presence of other phenolic solute(s).

Phenol solute <i>i</i>				Coexisting phenol solute(s) <i>j</i>
PhOH	MePhOH	ClPhOH	O ₂ NPhOH	
-	0.70	0.68	98.7	PhOH
0.64	-	0.66	35.7	MePhOH
0.59	0.60	-	43.7	ClPhOH
0.68	0.74	0.68	-	O ₂ NPhOH
-	-	0.67	40.4	PhOH/ MePhOH
-	0.60	-	39.3	PhOH/ ClPhOH
-	0.66	0.80	-	PhOH/ O ₂ NPhOH
0.67	-	-	46.0	MePhOH/ ClPhOH
0.69	-	0.83	-	MePhOH/ O ₂ NPhOH
0.66	0.63	-	-	ClPhOH/ O ₂ NPhOH
-	-	-	40.9	PhOH/ MePhOH/ ClPhOH
-	-	0.82	-	PhOH/ MePhOH/ O ₂ NPhOH
-	0.67	-	-	PhOH/ ClPhOH/ O ₂ NPhOH
0.70	-	-	-	MePhOH/ ClPhOH/ O ₂ NPhOH

The permeation flux ratio is defined as the ratio of permeation flux of phenol component *i* with and without other coexisting phenolic solute(s) *j* in the feed solution, i.e., $\eta_{ji} = \frac{J_i \text{ in solution comprising of } i, j \text{ and } H_2O}{J_i \text{ in binary } i/H_2O \text{ solution}}$, where *j* represents 1, 2 or 3 other phenol components in addition to a given phenol component *i* in the feed.

To further illustrate the coupling effects, the total permeation fluxes of binary, ternary and quinary feed solutions that all contained a specific phenol were determined, as shown in Figure 3.14, where the permeation flux of pure water was also presented for comparison. As mentioned before, membrane swelling due to the dissolution of phenolic compounds in the membrane favors permeation, and the data in Figure 3.14A show that the addition of 100 ppm PhOH into pure water increased the total permeation flux slightly due to membrane swelling. Nonetheless, the data in Figure 3.14B,C,D show that the total permeation flux varied only slightly when 100 ppm MePhOH, ClPhOH, or O₂NPhOH was added into pure water, which is not unexpected as phenol clustering is significant for phenols with a high sorption uptake in the membrane. When MePhOH, ClPhOH or O₂NPhOH was added to the

PhOH/water solution respectively (i.e., ternary solutions containing water and two phenolic compounds), the total permeation flux decreased suggesting that clustering of PhOH with other co-existing phenolic solutes became increasingly important that resulted in a reduction in the permeation flux. As shown in Figure 3.14A, the total permeation flux for the ternary solutions containing two co-existing phenol solutes followed the order of CIPhOH/PhOH < O₂NPhOH/PhOH < MePhOH/PhOH. It was evident that the reduction in total permeation flux was more pronounced when a second phenol of high sorption uptake was added to the PhOH/water solution. This is understandable because a high phenol sorption uptake in the membrane favors clustering of phenol molecules. Following the same line of thought, a further reduction in the total permeation flux was expected when all the four phenolic solutes were present in the feed solution. This was indeed the case, as shown in Figure 3.14.

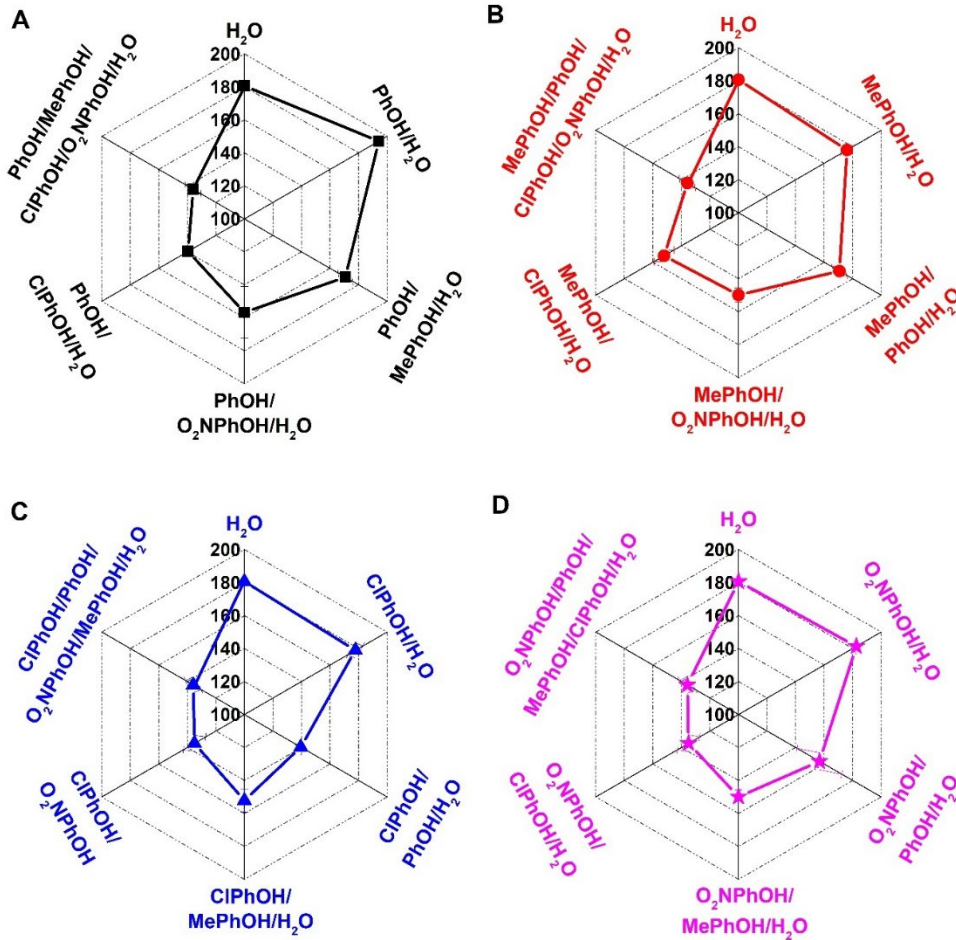


Figure 3.14 A comparison of the total permeation fluxes for binary/ternary/quinary feed solutions that all contain a specific phenolic solute where such a solute is (A) PhOH, (B) MePhOH, (C) CIPhOH, and (D) O₂NPhOH. Water flux in absence of phenol solutes is also presented for comparison.

3.4 Summary

The separation of phenolic compounds from aqueous solutions by pervaporation was investigated. PEBA 2533 displayed excellent performance as an organophilic material for pervaporative removal of PhOH, MePhOH and ClPhOH from aqueous solutions, but it was not particularly effective for O₂NPhOH separation. Depending on the specific phenol solute, high-purity phenol crystals could be produced from the phenol-enriched permeate via de-sublimation in the cold trap. Due to the increased driving force for permeation, the permeation fluxes of PhOH, MePhOH and ClPhOH all increased with an increase in feed concentration. The membrane permeability to phenols and water was found to follow an order of PhOH > MePhOH > ClPhOH >>H₂O. Both the permeation flux and enrichment factor increase with an increase in temperature, and the temperature dependencies of permeation flux and permeability follow an Arrhenius type of relation. However, the permeability coefficients of PhOH and MePhOH in the membrane were affected by temperature negatively, while the opposite was true for ClPhOH permeability. Furthermore, the coupling effects in permeation of multiple phenolic compounds were investigated. The permeation of PhOH, MePhOH, and ClPhOH was generally slowed down by the presence of other co-existing phenolic solutes in the feed solution, while the permeation of slow-permeating O₂NPhOH through the membrane was enhanced by co-existing fast-permeating phenolic solutes. This study confirmed the potential of using PEBA 2533 membranes for pervaporative separation of phenolic compounds from aqueous solutions, providing an insight into wastewater treatment involving feed solutions containing multiple phenolic compounds.

Chapter 4

Perstraction of Phenolic Compounds via Nonporous PEBA Membrane¹

4.1 Introduction

As mentioned in section 1.1, perstraction can effectively remove phenolic compounds from water. In view of the good permselectivity of PEBA 2533 to phenolic compounds as demonstrated in Chapter 3, PEBA 2533 was also selected to separate phenols via perstraction.

To accomplish perstraction, the stripping liquid should have a stronger affinity towards target components than the membrane phase so that the phenolic molecules will be removed from the membrane upon reaching the downstream side. The latter is often achieved via a chemical reaction. Phenolic compounds are mildly acidic and will dissociate under alkaline conditions to form phenolate salts. As organophilic membranes have little or no affinity to the salt compounds, the desorption of the phenolic permeant from the membrane surface is thus enhanced by the chemical reaction, thereby facilitating the permeation rate. Therefore, in this chapter, sodium hydroxide solution was used as stripping liquid to perstract phenolic compounds from aqueous solutions.

Most studies on organics separation using membrane perstraction look into the overall mass transfer, and little work is reported on the mechanism of mass transport in such liquid/membrane/liquid systems. Same as in pervaporation, the mass transfer through a dense membrane generally involves three sequential steps: the sorption of the permeating components onto the membrane surface at the upstream feed side, molecular transport through the membrane via diffusion, and desorption of the permeant from the membrane surface at the downstream side. An additional step is involved in perstraction when the stripping phase reacts with the permeant. The permeant desorption step is often not explicitly considered to be rate-limiting for the overall mass transfer process since the desorption is usually considered to happen very quickly [174]. However, this may not be appropriate for membranes with strong affinities towards the target permeant molecules. In addition, the boundary layer effects near the surfaces of the membrane can lower the mass transfer rates significantly. Schlosser et al. [175] found the mass transfer resistance in the feed boundary layer represented 10-40% of the overall mass transfer resistance for perstraction of dimethylcyclopropanecarboxylic acid in a hollow-fiber contactor. Cao et

¹ Portions of this chapter have been published in *Sep. Purif. Technol.*, **257**, 117928 (2021).

al. [176] showed that the membrane performance was drastically deteriorated by the boundary layer effect during the membrane-based extraction of methane dissolved in water. Xiao et al. [177] found the flow conditions (i.e., boundary layer) of the feed solution had a significant impact on the overall mass transfer coefficient of a phenol (PhOH) perstraction system.

The resistance-in-series approach has been widely used to describe the mass transfer in membrane separation processes [63, 178, 179], where the overall resistance for mass transfer is considered as the sum of individual resistances originated from every steps involved in the mass transport from the feed liquid to the permeate side, including the resistances of the liquid boundary layers. Looking into the individual resistances and analyzing how the operating parameters affect perstraction will help provide an insight into solute transfer in the liquid/membrane/liquid perstraction system, thereby guiding proper design of perstraction systems for effective removal of organic compounds.

The objective of this work was to extract phenolic compounds from aqueous solutions via perstraction using PEBA 2533 membrane. The mass transfer mechanism in the perstraction system for removing phenolic compounds from water was investigated, and the individual resistances involved in the various mass transport steps were evaluated.

4.2 Experimental

Sodium hydroxide was purchased from Sigma Aldrich. All other materials used were the same as used in Chapter 3, and the basic information of the four phenolics were shown in Table 3.2. The membranes with different thicknesses used here were prepared by the solution casting technique as described in Section 3.2.2.

4.2.1 Perstraction

The experimental apparatus used for perstraction studies was shown in Figure 4.1. It was comprised of a feed compartment and a receiving compartment to be filled with a stripping liquid. Membranes with different thicknesses (14 - 62 μm) were mounted horizontally at the bottom of the feed compartment. The receiving compartment was filled with 2 L of pure water or NaOH solutions of known concentrations, and then the feed compartment was positioned to be partially immersed in the stripping liquid. At time zero, the feed compartment was filled with 100 mL of a phenolic solution at a given concentration, and agitations were provided in both the feed solution and stripping solution to reduce the boundary layer effects. During perstraction process, the stripping solution was sampled (~3 mL) periodically for concentration measurement, and all the samples were returned to the receiving

compartment immediately once the spectrophotometric analysis was completed. The effective membrane area for perstraction was 11.34 cm², and the experiments were carried out at 30°C. Other operating parameters were shown in Table 4.1.

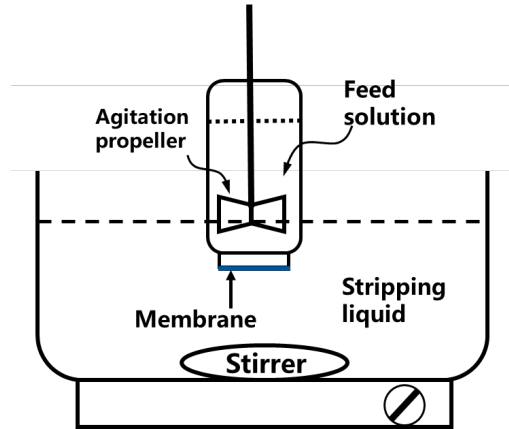


Figure 4.1 Schematic diagram of the apparatus for perstraction experiments.

Table 4.1 Operating parameters used in this study.

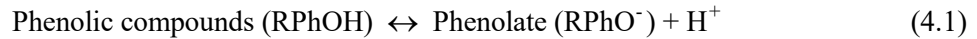
Temperature	30 °C
Volume of feed solution	0.1 L
Initial phenol concentration in feed	3000 ppm
Volume of stripping solution	2 L
Effective membrane area	11.34 cm ²
Diameter of agitation propeller in feed compartment	2.8 cm
Agitation speed of propeller in feed compartment	360 rpm
<i>Re</i> in feed compartment	5800
Stirrer size in receiving compartment	3.8 cm
Stirring speed in receiving compartment	100 rpm
<i>Re</i> in receiving compartment	3000

Note: *Re* in agitation system is defined as $Re = \rho N d^2 / \mu$, where ρ is the liquid density (kg/m³), d is the diameter of the agitation propeller (m), N is the rotation speed (s⁻¹), and μ is the viscosity of the liquid (Pa·s) [180].

4.3 Theoretical Analysis

4.3.1 Dissociation of Phenolic Compounds

Phenolic compounds are mildly acidic, and therefore they can dissociate under alkaline conditions. Thus, the use of an alkaline solution as the stripping phase at the downstream side of the membrane will help their desorption from the membrane phase and increase the driving force for perstraction. The dissociation of phenolic compounds may be expressed as



where R represents hydrogen or a functional group (i.e., methyl-, chloro-, nitro-) on the benzene ring. The dissociation equilibrium constant, K_a , can be written as

$$K_a = \frac{[\text{RPhO}^-][\text{H}^+]}{[\text{RPhOH}]} \quad (4.2)$$

From Equation (4.2), the degree of dissociation (ω) is related to solution pH by

$$\omega = \frac{[\text{RPhO}^-]}{[\text{RPhOH}] + [\text{RPhO}^-]} = \frac{K_a}{K_a + 10^{-\text{pH}}} \quad (4.3)$$

4.3.2 Resistance-in-series Model

The permeation rate of a phenolic compound in the liquid/membrane/liquid perstraction system can be characterized by the overall mass transfer coefficient that is based on the concentration difference between the two liquid phases. Assuming negligible accumulation of the phenolic permeant in the membrane in view of the very small amount of sorption uptake in the membrane as compared to the total amount of solute in the system and negligible amount of un-ionized phenol in the stripping liquid as compared to the amount of phenol in the feed solution, the following equation applies based on mass balance:

$$-VdC_F = K_O A C_F dt \quad (4.4)$$

where V and A are the volume of the feed solution and the effective membrane area, respectively; C_F is the instantaneous concentration of phenol in the feed solution, and K_O is the overall mass transfer coefficient. With an initial condition that $C_F = C_o$ at $t = 0$, Equation (4.4) can be integrated to give

$$\ln \frac{C_F}{C_o} = -\frac{A}{V} K_O t \quad (4.5)$$

The overall mass transfer coefficient K_O of the perstraction system can be evaluated from phenol concentration change with time using Equation (4.5).

The mass transfer through a membrane with liquid films on both sides can be described by the resistance-in-series model. In a liquid/membrane/liquid perstraction system, the liquid boundary layers are established on both sides of the membrane at the feed/membrane and membrane/extractant interfaces. Figure 4.2 illustrates the concentration profile in the membrane and the two liquid boundary layers. The mass transport can be considered to involve five successive steps: (1) mass transport from the bulk feed solution to the feed/membrane interface, (2) partition and dissolution of the permeant into the membrane surface, (3) diffusion through the membrane, (4) desorption of the permeant from the membrane surface to reach the stripping liquid phase, and (5) transport of the permeant from the membrane/extractant interface to the bulk of the stripping extractant. Assuming solubility and diffusivity of phenol permeant in the membrane are concentration independent, the overall mass transfer resistance ($1/K_O$) under steady state of perstraction can be expressed as

$$\frac{1}{K_O} = R_1 + R_2 + R_m + R_3 + R_4 \quad (4.6)$$

where R_1 and R_4 are the mass transfer resistances in the liquid boundary layers on the feed and extractant sides of the membrane, respectively (which are equal to the reciprocal of the mass transfer coefficients, i.e., $R_1 = 1/K_1$, $R_4 = 1/K_4$), R_2 and R_3 represent the resistances for partition/sorption into the membrane and desorption from the membrane, respectively. $R_m (= L/(D \cdot K^L))$ is the mass transfer resistance of the membrane, where D and K^L are the diffusivity and partition coefficient (or liquid phase sorption constant) of the phenol permeant in the membrane, and L is the membrane thickness. For solution-diffusion membranes, R_2 and R_3 are often considered to be negligibly small, but this cannot be taken for granted unless equilibria are established instantly.

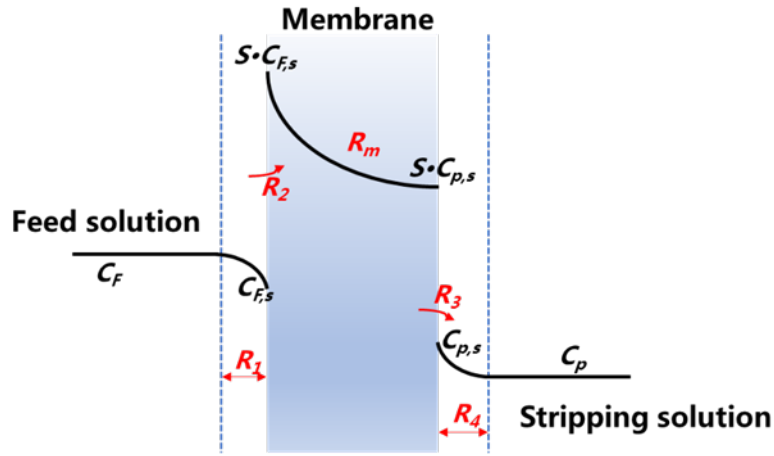


Figure 4.2 Concentration profile at steady state of perstraction where boundary layer effects at both sides of the membrane are significant. C_F : bulk concentration in feed solution; $C_{F,s}$: liquid solute concentration at the interface between feed solution and the membrane; C_p : bulk concentration in stripping liquid; $C_{p,s}$: liquid solute concentration at the interface between the membrane and the stripping solution.

Equation (4.6) indicates that under given hydrodynamic conditions on the feed and stripping sides, plotting the overall mass transfer resistance versus membrane thickness will yield a straight line, with a slope that is equal to the reciprocal of the permeability coefficient ($P' = D \cdot K^L$) and an intercept that is equal to the sum of $(R_1 + R_2 + R_3 + R_4)$.

The mass transfer coefficient in a liquid boundary layer is primarily determined by the hydrodynamic conditions, and the steady state mass transfer coefficient in the feed liquid phase, K_L , can be estimated from the semi-empirical Sherwood correlation [181]

$$Sh = 1.128(Re Sc)^{1/2} \quad (4.7)$$

where the Sherwood, Reynolds, and Schmidt numbers are defined as $Sh = \frac{K_L d}{D_l}$, $Re = \frac{\rho v d}{\mu}$, and

$Sc = \frac{\mu}{\rho D_l}$, respectively, with Re being defined in terms of the maximum velocity (i.e., v is the agitator

tip speed (m/s)). Here the characteristic dimension d is the diameter of the agitation propeller (m), ρ the density of the solution (kg/m^3), μ the viscosity of the solution (Pa.s), and D_l the diffusivity of the solute in the solution (m^2/s). The agitation propeller in the feed was located approx. 1 cm above the membrane

surface to provide sufficient turbulence. The diffusion coefficient of phenolic solutes in water can be estimated from the Wilke-Chang equation [182]

$$D_l = 7.4 \times 10^{-8} \frac{T \sqrt{\psi M}}{1000 \mu V_s^{0.6}} \quad (4.8)$$

where V_s is the molar volume of the phenolic solute as liquid at its normal boiling point, ψ is an association parameter for the solvent (recommended value for water is 2.6), M is the molar mass of the solvent, and T is the absolute temperature.

Equation (4.4) applies when phenol concentration in the stripping solution is at a sufficiently low level. Thus, the volume of the stripping solution used in the perstraction experiments was much greater (20 times) than the volume of the feed solution. This, however, may result in insufficient turbulence in the receiving compartment. Consequently, an alternative approach was used to determine the boundary layer resistance on the stripping side of the perstraction system experimentally. After K_O was evaluated from phenol concentration change with time using Equation (4.5), the experiment was conducted again under the same conditions except that the stripping solution was vigorously agitated using two additional agitation propellers (See Appendix A). In view of the low phenol concentration in the stripping solution and its vigorous agitation, the boundary layer mass transfer resistance in stripping

liquid phase would be negligible (i.e., $\frac{1}{K_O'} = R_1 + R_2 + R_m + R_3$). This was also justified by

experimental results that a further increase in mixing of the stripping solution did not change the overall mass transfer rate anymore. Thus, the boundary layer resistance R_4 in the stripping liquid phase under normal perstraction condition can be estimated from the change in the overall mass transfer resistance

$$\text{(i.e., } R_4 = \frac{1}{K_O} - \frac{1}{K_O'} \text{)}.$$

Furthermore, as mentioned before, phenolic compounds will dissociate in alkaline solutions. When the alkaline concentration was high enough and the stripping liquid was agitated sufficiently, the phenolic molecules could be considered to dissociate in the stripping liquid as soon as they reached the membrane/stripping liquid interface. As the hydrophobic membrane had little affinity towards the ionic species, both the desorption resistance (R_3) and the boundary layer resistance in stripping liquid (R_4)

became negligible (i.e., $\frac{1}{K_O''} = R_1 + R_2 + R_m''$). As an approximation, the mass transfer resistances

related to the boundary layer and phenol sorption to the membrane on the upstream feed side were considered to be unaffected by the presence of NaOH in the stripping solution in view of the fact that PEBA is essentially impermeable to NaOH. This allows the estimation of the resistance component (R_3) from the difference between the overall resistances ($\frac{1}{K_O''}$) and ($\frac{1}{K_O'}$), that is,

$$R_3 = \frac{1}{K_O'} - \frac{1}{K_O''} - (R_m - R_m'').$$

With the resistance components R_1 , R_m , R_3 and R_4 evacuated, the

resistance component R_2 was determined from the difference between the overall resistance $\frac{1}{K_O}$ and

the sum of R_1 , R_m , R_3 , and R_4 using Equation (4.6), that is, $R_2 = \frac{1}{K_O} - (R_1 + R_m + R_3 + R_4)$. The detailed

information on estimating the individual resistances can be found in Appendix A.

4.4 Results and Discussion

4.4.1 Perstraction

Figure 4.3 shows phenol concentration in the feed compartment for the four model phenolic compounds as perstraction proceeded with time when the stripping liquid in receiving compartment was deionized water. $\ln(C_F/C_0)$ decreased with time linearly, and thus the value of K_O was obtained from the slope of the straight line. The mass transfer rates of the phenolic compounds are in the order of ClPhOH > MePhOH > O₂NPhOH > PhOH, which may be attributed to their different affinities with the membrane and different sizes of the molecules. Their partition coefficients in the membrane determined from the sorption experiments were presented in Table 4.2, and they were in the order of ClPhOH > O₂NPhOH > MePhOH > PhOH, consistent with the reports that phenolic compounds with electron withdrawing groups (e.g., -NO₂ and -Cl) are more easily sorbed into various sorbents than phenolic compounds with electron donating groups (e.g., -CH₃) [17, 168]. In rubbery polymer membranes, the solute transport is usually solubility controlled. It was therefore no surprise to notice that PhOH had the lowest permeation rate through the membrane among the four phenolic solutes, in spite of its smallest molecular size, due to its lowest partition coefficient, while ClPhOH which had the highest sorption uptake in the membrane, displayed the highest permeation rate. O₂NPhOH has good sorption in the membrane, and its relatively low mass transfer rate may be attributed to its large molecular size. In addition, polarity among the four phenol solutes, O₂NPhOH has the strongest due to its nitril groups, which tends to strengthen hydrogen

bonding with the relatively polar PEBA polymer, resulting in a low permeation rate of O_2NPhOH in the membrane.

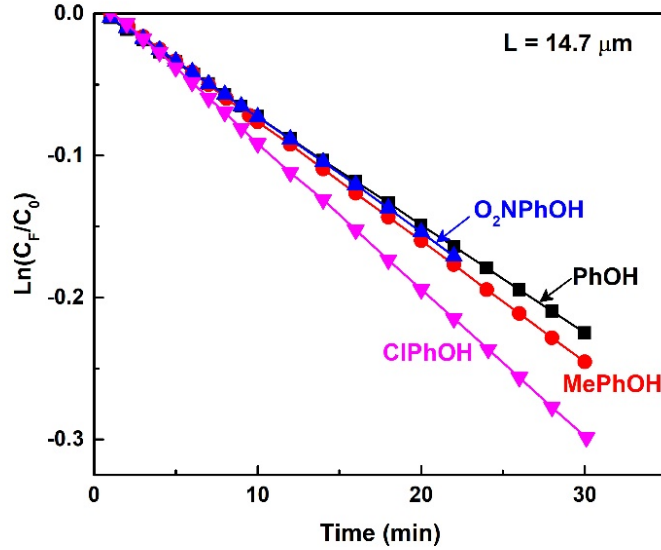


Figure 4.3 Concentration profiles for the four phenolic compounds in the feed compartment with time when receiving compartment was filled with deionized water.

For nonporous membranes, the spaces between polymer chains are typically less than 5-10 Å. The solute molecules penetrate the membrane through the free volume elements between polymer chains which are transient on the time scale of the diffusion process [39]. As it is difficult to quantify how the transient state of the nonporous membrane affects mass transport on a molecular scale, the interactions between the polymer chains and the permeating molecules, which are vital to the overall perstraction performance, are assessed customarily in terms of such macroscopic quantities as sorption constant, diffusivity, and mass transfer coefficient. Therefore, in what follows, an in dept analysis of the mass transfer characteristics of the perstraction system in relation to liquid sorption constant and diffusivity will be carried out.

Table 4.2 Permeability, partition coefficient, and diffusivity coefficients in PEBA at 30°C.

	Permeability, P' , (10^{-10} m ² /s)	Partition Coefficient, K^L	Diffusivity, D , (10^{-12} m ² /s)
PhOH	5.0	40	12.5
MePhOH	7.9	90	8.8
O ₂ NPhOH	5.9	119	5.0
ClPhOH	9.5	240	4.0

Note: The partition coefficient was measured with an equilibrium concentration of approx. 3000 ppm.

Figure 4.4 shows the overall mass transfer resistance ($1/K_O$) versus membrane thickness (L) when the receiving compartment was filled with deionized water. As expected, an increase in membrane thickness would increase the mass transfer resistance, and a linear relationship between $1/K_O$ and L was obtained. From the intercepts of the straight lines, the total resistance to mass transfer due to liquid boundary layers and the phenol sorption/desorption at the liquid/membrane interfaces were found to be in the range of $(4.5 \text{ to } 6.0) \times 10^4$ s/m for four phenolic compounds, which obviously cannot be neglected. For example, even for a relatively thick membrane (61.45 μm), the resistances other than membrane itself accounted for 30 - 45% of the overall resistance, indicating that the mass transfer resistances resulting from the liquid boundary layers and the sorption/desorption were significant to the overall mass transfer. Prior work has also shown that the liquid boundary layer resistance cannot be neglected in perstraction processes. Schlosser et al. [175, 183] found the mass transfer resistance of the boundary layer in a liquid membrane for perstraction of phenol (PhOH) with a hollow fiber pertractor was 42% of the overall resistance. Another study of Schlosser et al. [184] showed the boundary layer resistance was 20 - 30% of the overall resistance for the perstraction of butyric acid in a three phase hollow fiber contactor. Similar results were also observed in many pervaporation processes. For example, She et al. [185] found that the magnitudes of the mass transfer coefficients in the boundary layer were comparable with the mass transfer coefficients of the membrane in pervaporation separation of flavor compounds from dilute aqueous solutions using a PDMS/PVDF composite membrane. Li et al. [63] also reported a considerable concentration polarization in the boundary layer in pervaporative removal of organic compounds from water using a PDMS membrane, and the mass transfer of acetone was found to be determined by both the membrane resistance and the boundary layer resistance. The above results

suggest that it is inappropriate to assume membrane as the rate controlling step while ignoring the resistances from the liquid boundary layer and sorption/desorption at the membrane/liquid interfaces for perstraction of phenolics through the PEBA membrane.

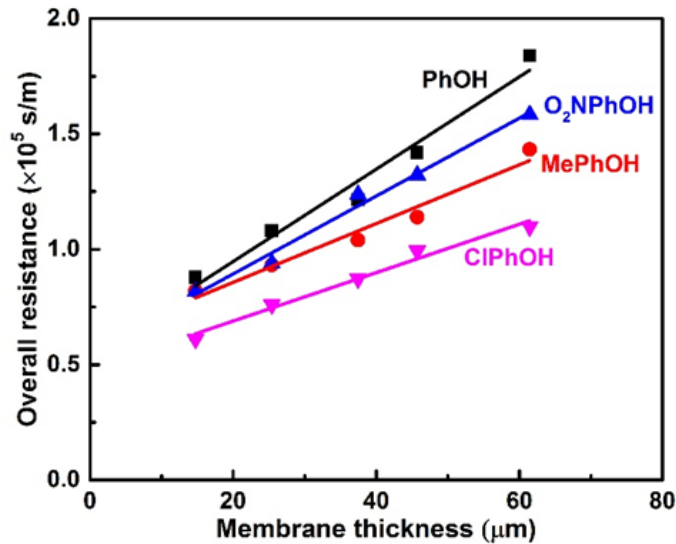


Figure 4.4 Effects of membrane thickness on the overall resistance for permeation of phenolic compounds when receiving compartment was filled with deionized water.

The permeability coefficients of the four phenolic compounds in the membrane were obtained from the slopes of the straight lines in Figure 4.4. As an approximation, the diffusivity of the phenolics in the membrane can be estimated from the ratio of their permeability coefficients (P') to the partition coefficients (K^L), as shown in Table 4.2. The diffusivity of the phenolic solutes in the membrane was affected by their molecular sizes and interactions with the membrane, and the larger phenolic molecules would diffuse in the polymer matrix more slowly. PhOH, which has no additional functional groups adjacent to the phenol ring, showed a diffusivity much greater than the other three phenolic compounds, while O₂NPhOH and ClPhOH had a low diffusivity because of the relatively large size and strong affinity with PEBA. At 30°C, the diffusivity of PhOH in silicon rubber was estimated using the correlation developed by Lapack to be 2.5×10^{-11} m²/s [186], which was greater than the PhOH diffusivity in PEBA determined in the present study (1.25×10^{-11} m²/s). This was understandable as silicone rubber has a better phenol permeability than almost all other polymers due to excellent flexibility of the -Si-O- backbone. Doig et al. reported a higher PhOH diffusivity of 4.6×10^{-11} m²/s at

37°C in silicone rubber when the membrane was swollen with decanol [187]. This is obviously expectable because an increase in temperature will not only facilitate the thermal motion of the polymer chains, but the permeating molecules will be more energetic, making the permeant molecules to diffuse through the membrane faster. In addition, when the membrane was swollen by decanol, the polymer matrix became less compact and more flexible, resulting in enhanced diffusivity of permeating molecules. The above analysis shows that the phenol diffusivity so estimated in the current work was reasonable in comparison to the results reported in the literature. In addition, temperature showed a significant effect on the phenol diffusivity in the membrane. Preliminary experiments also showed that phenol sorption uptake in PEBA decreased with an increase in temperature, and a higher temperature would favor the desorption of phenol solutes. An appropriate operating temperature for perstraction should be determined based on the overall mass transfer coefficients and other process considerations (e.g., energy consumption and heat sources). Nonetheless, for the purpose of demonstrating the effects of alkaline solution on phenol stripping from the membrane, a temperature of 30°C was used in the study.

The phenolic compounds have acidic characteristics and can react with sodium hydroxide to form soluble sodium phenolates. Because of the hydrophobic nature of PEBA polymer, only the undissociated phenolic molecules can sorb into the membrane phase. It was thus believed that the desorption of phenolic compounds from a polymeric membrane could be facilitated by using an alkaline stripping liquid, which is the basis of the perstraction. Obviously, the pH of the stripping liquid will have a significant impact on the mass transfer rate of phenolic compounds in a perstraction system, primarily on the desorption rate. Due to different substituent groups on the phenol ring, the four phenolic compounds studied here have different dissociation constants. The percentage of undissociated phenol as a function of pH can be calculated from the degree of dissociation using Equation (4.3). As shown in Figure 4.5, the percentage of undissociated phenolics decreases sharply with an increase in the solution pH beyond a certain threshold (a pH value of ~6 for O₂NPhOH, ~8 for ClPhOH, and ~9 for PhOH and MePhOH), and they are almost completely dissociated when the solution pH is above 10, 12 and 13, respectively. Therefore, it can be anticipated that an increase in the pH of the stripping solution will increase the phenol concentration gradient across the membrane which serves as the driving force for phenol mass transfer through the membrane, and a maximum enhancement in mass transfer will be reached when pH is sufficiently high.

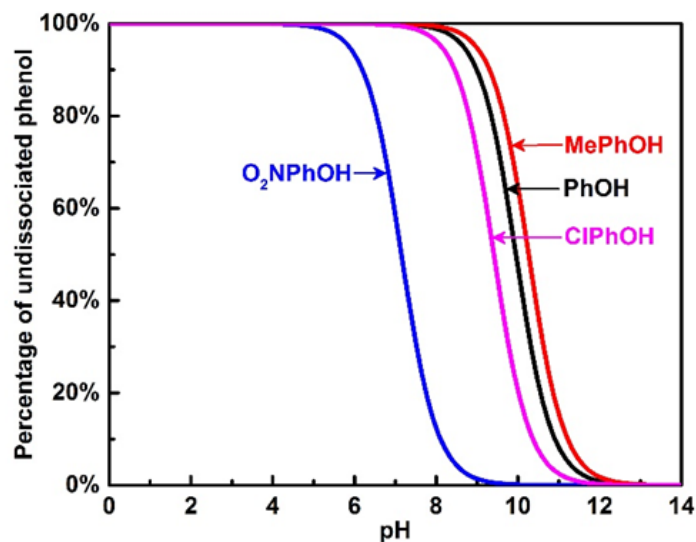


Figure 4.5 Percentage of undissociated phenolic compounds as a function of solution pH.

The pH of the four phenolics in the feed is approximately 4.2 - 5.2, and thus they primarily exist in an un-ionized state. In view of the chemical structures of the phenol compounds and PEBA, it is believed that the sorption of the phenols in PEBA is mainly driven by hydrophobic interaction, π - π interaction and hydrogen bonding, while electrostatic interaction is unlikely [188].

In the membrane perstraction process, phenolics penetrate the PEBA membrane and then react with the OH^- in the stripping liquid. The effects of the NaOH concentration in the stripping solution on the phenol perstraction were examined experimentally, where a phenol concentration of 3000 ppm in the feed solution was used, whereas the NaOH concentration in the stripping solution was varied in the range of 0 - 100 mmol/L. The results were shown in Figure 4.6, where the overall mass transfer coefficient, K_O , was plotted as a function of the NaOH concentration. With an increase in the NaOH concentration of the stripping liquid, the mass transfer coefficient increased and then levelled off when the NaOH concentration was high enough. It is expected that all the phenolic compounds will dissociate as soon as they reach the stripping liquid from the membrane surface when the concentration of OH^- is high enough. Under such circumstances, the concentration of un-ionized phenolics on the membrane surface at the downstream side would therefore be zero, and the mass transfer driving force was maximized and a further increase in the NaOH concentration could not enhance the mass transfer anymore.

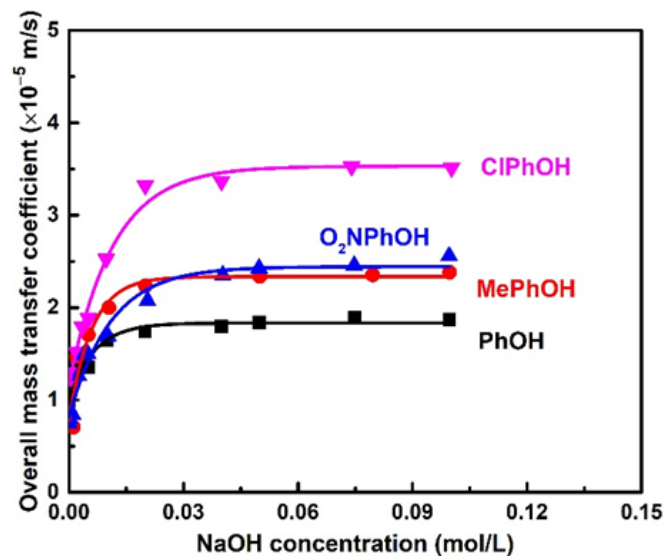


Figure 4.6 Effects of NaOH concentration in the stripping solution on overall mass transfer coefficient for perstraction of phenolic compounds with a membrane thickness of 25.4 μm .

To have a closer look into the effects of NaOH concentration on mass transfer resistance, the perstraction characteristics of the four phenolic compounds through PEBA membranes with different thicknesses at different amounts of NaOH in the stripping liquid were determined, as shown in Figure 4.7; the data with zero NaOH concentration in the stripping liquid were plotted as well for comparisons. As expected, there was a linear relationship between the overall mass transfer resistance and the membrane thickness. With an increase in NaOH concentration in the stripping liquid, the intercepts of the straight lines in Figure 4.7 decreased, indicating a reduction in the mass transfer resistance related to the boundary layer and phenol desorption from the membrane on the downstream side. This will be discussed in more details later.

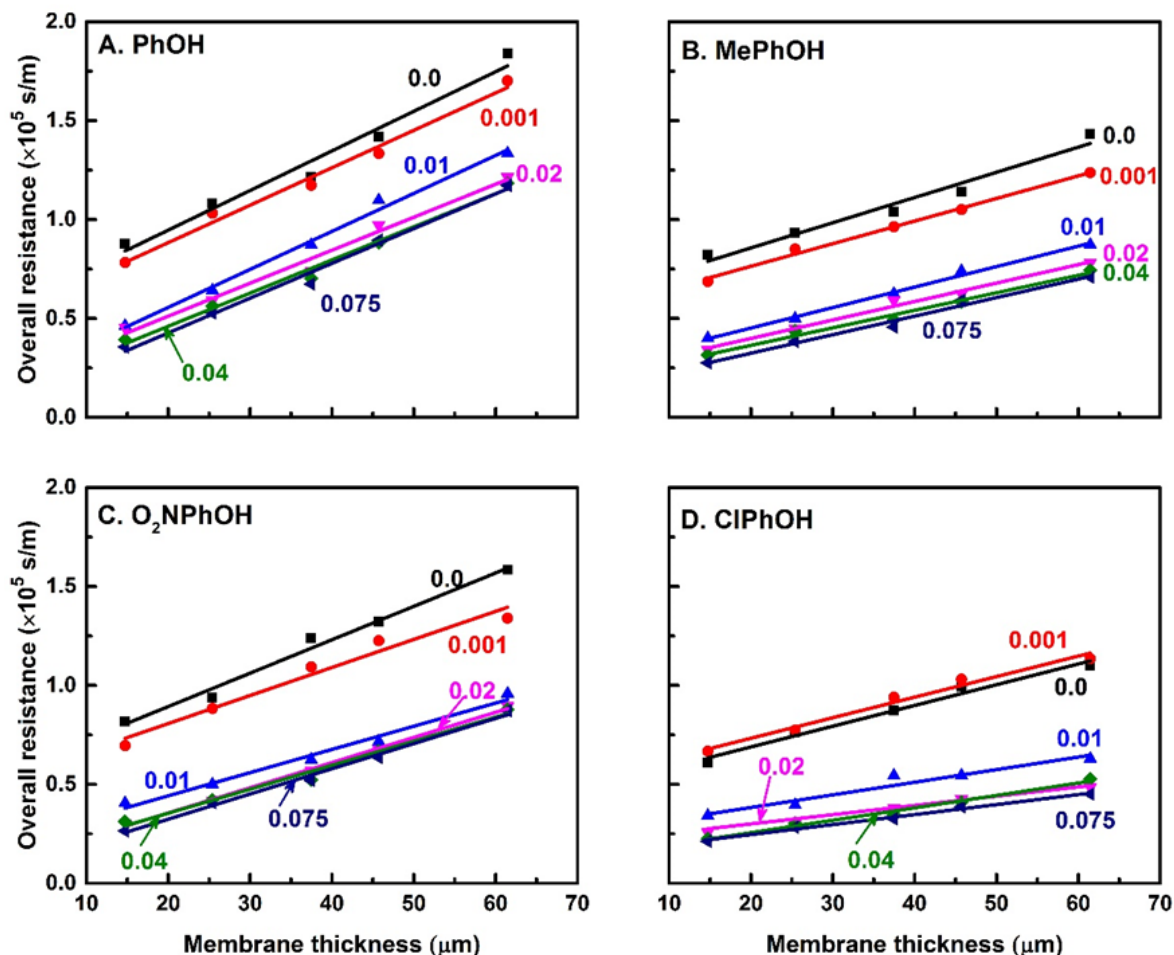


Figure 4.7 Effects of membrane thickness on overall mass transfer resistance for perstraction of phenolics at various NaOH concentrations in the stripping liquid in mol/L.

The permeability of the membrane to the phenolic compounds can be determined from the slopes of the straight lines in Figure 4.7. As shown in Figure 4.8, the permeability coefficient of the four phenolic compounds generally increased and then levelled off when increasing the NaOH concentration in the stripping solution from 0 to 0.075 mol/L, and this trend is more obvious for phenolics with larger molecular sizes. The phenol permeability was not expected to be affected significantly by the presence of NaOH in the stripping solution since ionic species in the stripping solution could hardly permeate through the nonporous hydrophobic PEBA membrane to the upstream side. This was justified by the experimental results that there was only a slight change in the pH of the phenol solution in the feed after the perstraction experiment (for example, the pH of the MePhOH solution in the feed changed from 5.2 to 5.9 after perstraction with a membrane of 14.7 μm using 0.075 mol/L NaOH solution), and

this pH change was also partly due to phenol depletion in the feed as a result of permeation. In view of the very small amounts of ions permeating into the feed solution, the sodium hydroxide in the stripping liquid would have little impact on the dissociation state of the phenolics in the feed solution on the upstream side of the membrane and thus the sorption of the phenolics in the membrane. However, PEBA is a copolymer having 80% polyether (i.e., poly(tetramethylene oxide)) segments and 20% polyamide (i.e., polyamide 12) segments. Though the PEBA copolymer is chemically stable at a high pH, it has been reported that polyamides (e.g., polyamide 6 and 12) could be dissociated moderately to become negatively charged and that the dissociation occurred mainly on the surface in contact with the alkaline solutions but scarcely within the membrane [189, 190]. This appeared to have influenced phenol permeation in PEBA membrane, though information about the polymer property change at molecular scale was still lacking.

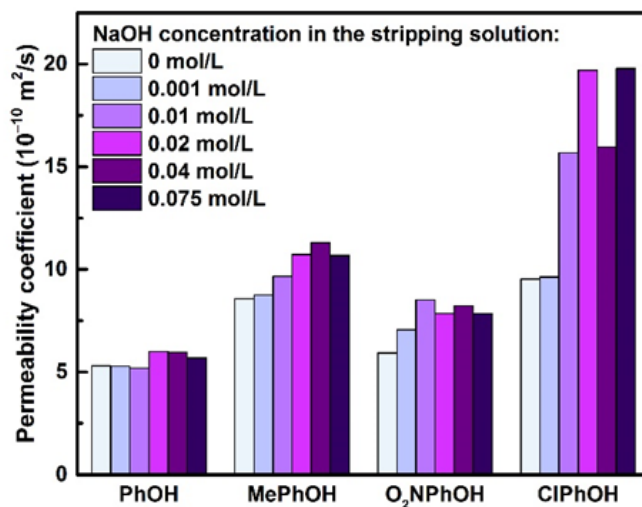


Figure 4.8 Effects of NaOH concentration in the stripping liquid on the permeability coefficients of the phenolic compounds.

4.4.2 Resistance Analysis

As discussed previously, the overall mass transfer resistance in a liquid/membrane/liquid perstraction system is the sum of individual resistances from the liquid boundary layers, the membrane, and the membrane/liquid interfaces. Table 4.3 shows the individual resistances from the different steps

involved in the perstraction process. The liquid phase mass transfer coefficient on the feed side (K_1) was on the order of 10^{-4} m/s. In addition, it can be seen that the boundary layer resistance in the stripping liquid phase was much higher due to the less vigorous hydrodynamic conditions (i.e., stirring speed, volumetric power input). It was clear that the boundary layer resistances will deteriorate the mass transfer significantly unless vigorous agitation is provided to minimize the boundary layer effects.

Table 4.3 also shows the mass transfer resistances for phenol sorption to and desorption from the membrane. In general, the sorption resistances ($1/K_2$) for the four phenolic compounds are relatively low, demonstrating quick sorption of phenolics in the membrane due to excellent affinities of PEBA towards the phenolic compounds. However, the desorption resistances ($1/K_3$) are higher. The sorption/desorption kinetics were determined by the properties of the sorbent (membrane) and sorbates. Generally speaking, it is the good affinity of the membrane material to the target organic molecules that results in the sorptive, extractive, and pervaporative removal of organic pollutants from water. However, the good retainability of phenolics in the membrane due to the polymer-phenol affinity makes it difficult for the phenolic molecules to desorb from the membrane, resulting in a high desorption resistance.

Table 4.3 Individual mass transfer resistances for phenolic compounds in the liquid/membrane/liquid perstraction system.

Compound	$K_1, 10^{-4}$ m/s	$1/K_1, s/m$	$1/K_2, s/m$	$1/K_3, s/m$	$1/K_4, s/m$
PhOH	1.79	5600	200	16600	32300
MePhOH	1.70	5900	7700	10800	35900
O ₂ NPhOH	1.71	5900	700	17800	31100
ClPhOH	1.65	5800	6600	5400	30100

Figure 4.9 shows the relative contribution of the individual resistances to the overall mass transfer resistance for perstraction with the membrane having a thickness of 25.4 μm . Clearly, membrane exerted a significant resistance to phenol perstraction, accounting for 30 - 50% of the overall mass transfer resistance. Of the four phenolic compounds, the membrane resistance to ClPhOH permeation was the lowest due to its highest partition coefficient in the membrane, whereas the opposite was true for PhOH. Both resistances resulting from sorption ($1/K_2$) and feed boundary layer ($1/K_1$) were insignificant, and their influences would be more trivial when thicker membranes were used. On the

other hand, the mass transfer resistance for desorption ($1/K_3$) was significant due to strong interactions between the penetrant molecules and the membrane. The resistance of the boundary layer ($1/K_4$) in the stripping liquid (at $Re = 3000$) was also rather high. The results shown in Figure 4.9 demonstrate that not only highly permeable membranes are desired in perstraction, facilitation of permeant desorption from the membrane at the downstream side is also important to the overall separation performance. In addition, the fluid hydrodynamic conditions of the perstraction system should be controlled properly to enhance the mass transfer in the liquid boundary layers in order to work out at its full potential.

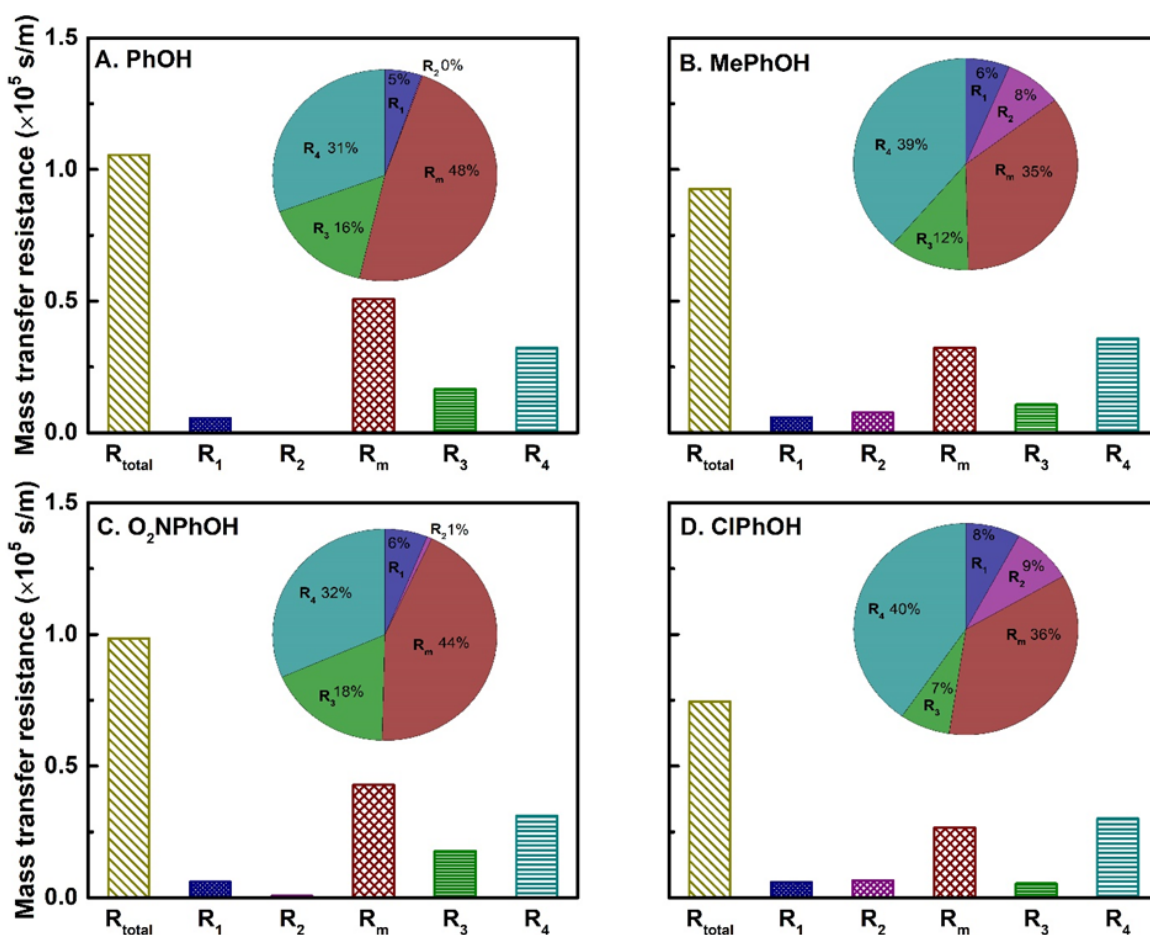


Figure 4.9 Distribution of mass transfer resistances for perstraction of phenols using a membrane with a thickness of $25.4 \mu\text{m}$ when the receiving compartment was filled with deionized water.

4.4.3 Effects of Alkaline in Stripping Liquid on Perstraction

Though the addition of NaOH in the stripping solution can reduce the mass transfer resistance of the membrane to some extent (Figure 4.8), a more notable impact on perstraction was the facilitation in mass transfer at the downstream side of the membrane as a result of the reaction between phenol and OH⁻. The downstream mass transfer resistance (i.e., resistance due to phenol desorption plus boundary layer resistance in the stripping liquid, $1/K_3+1/K_4$) as a function of alkaline concentration of the stripping solution was shown in Figure 4.10. As mentioned before, phenol desorption from PEBA membrane was difficult because of the strong affinity between the membrane and the phenolic compounds. However, the downstream mass transfer resistance was reduced drastically by even a small amount of NaOH in the stripping solution, indicating that the chemical reaction was effective to facilitate phenol removal from the membrane surface. As expected, the reduction in the downstream mass transfer resistance was more drastic at higher NaOH concentrations. The results demonstrate the effectiveness of liquid/membrane/liquid perstraction to remove phenolic compounds from aqueous solutions.

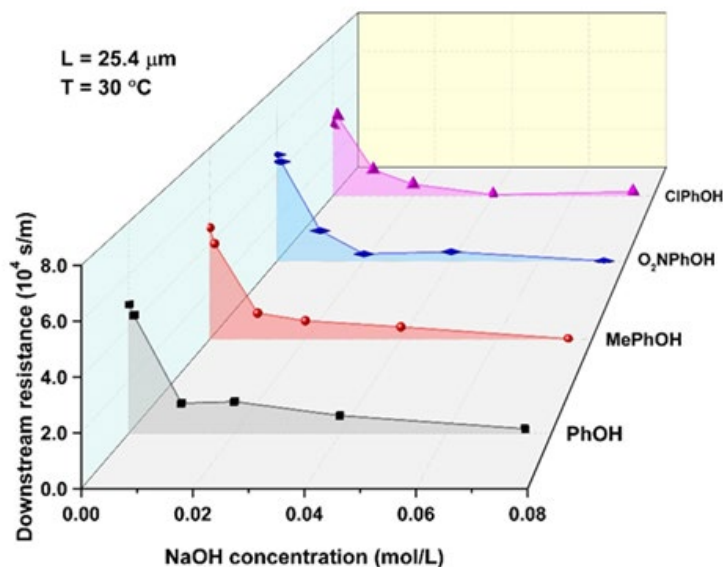


Figure 4.10 Effects of NaOH concentration in stripping liquid on downstream mass transfer resistance.

Figure 4.11 shows the effects of alkaline concentration in the stripping liquid on perstraction as measured in terms of enhancement factor defined as $\frac{K_{O,OH}-K_O}{K_O} \times 100\%$, where $K_{O,OH}$ is the mass transfer coefficient when NaOH was present in the stripping liquid. Obviously, the enhancement factor

was zero when the stripping liquid contained no NaOH. As shown in Figure 4.11, the enhancement factor increased with an increase in the NaOH concentration in stripping liquid, and then levelled off when the NaOH concentration was sufficiently high. At a given NaOH concentration, the enhancement factor was higher when thinner membranes were used. This was easy to understand because the effect of NaOH on membrane resistance was much less pronounced than the effect on the mass transfer resistance on the downstream side, and the membrane resistance was directly influenced by the membrane thickness. For practical applications, thin membranes are preferred to increase the throughput, and in such cases the enhancement in mass transfer as a result of using alkaline stripping liquids will be increasingly significant.

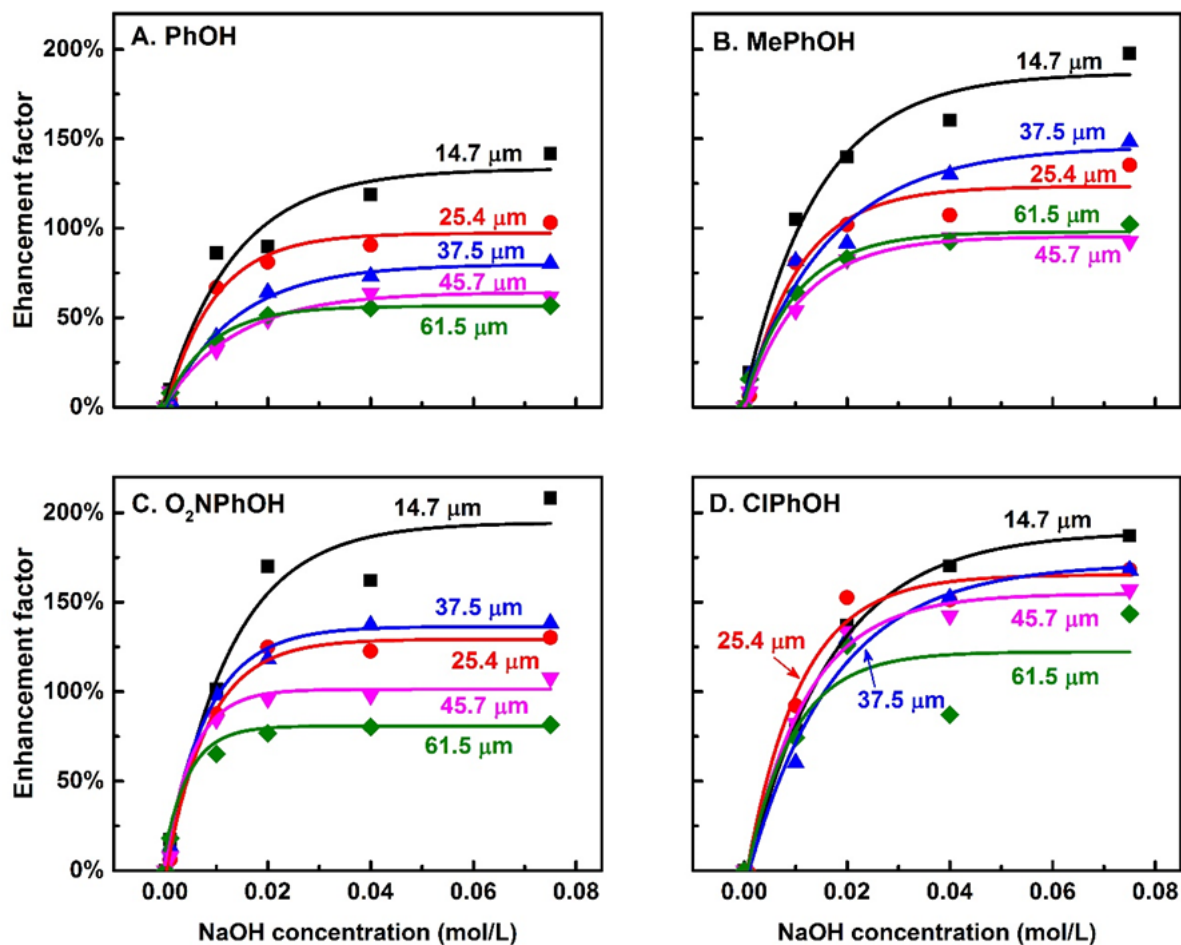


Figure 4.11 The enhancement factor of membranes with different thicknesses at various NaOH concentrations.

4.5 Summary

Removal of phenolic compounds from dilute solutions by perstraction using a PEBA membrane was studied. The partition coefficient, diffusivity coefficient, and permeability coefficient (in unit of m^2/s) of phenolics pertinent to membrane perstraction were investigated. A resistance-in-series model was used to look into the mass transfer in perstraction of phenolic compounds, and individual resistances from the different steps of the perstractive mass transport were evaluated. While the membrane resistance to phenol transport was significant, the mass transfer resistance at the downstream side of the membrane due to phenol desorption from the membrane and liquid boundary layer effect was not negligible. It was shown that the phenol perstraction rate was significantly enhanced by using an alkaline stripping solution, and the degree of enhancement was affected by the alkaline concentration and the membrane thickness.

Chapter 5

Sorption, Diffusion, and Permeation of Phenolic Compounds in PEBA Membranes

5.1 Introduction

The results in Chapter 3 and Chapter 4 showed that PEBA membrane has good permselectivity towards phenolic compounds. For the separation of phenolic compounds from water streams, the good phenol/water permselectivity primarily comes from the solubility selectivity, while the diffusivity selectivity is unfavorable for phenol permeation because of smaller size of water molecule. Studies on sorption and diffusion will help understand the permeation behavior and mass transfer mechanism of phenolic compounds within the membrane. Nonetheless, despite that various grades of PEBA has been under extensive investigations for the separation of phenolic compounds from water streams by pervaporation, the sorption and diffusion fundamentals are rarely reported.

This chapter deals with the sorption, diffusion, and permeation of four phenolic compounds in nonporous PEBA membrane. The solubility and permeability were determined experimentally from sorption experiments and liquid permeation experiments, respectively, and the diffusivity was evaluated as a ratio of the permeability and sorption constant. The permeability obtained from liquid permeation experiments will be compared with the permeability obtained from pervaporation, which will shed light on the nature of membrane permeability.

5.2 Theoretical

There are three stages during permeation through a membrane: (1) transient permeation at the beginning when permeation is initiated as it takes time to establish the concentration profile within the membrane, (2) pseudo-steady state permeation when the concentration difference across the membrane is largely constant, and (3) unsteady state permeation when the solute concentration at the downstream of the membrane is significantly high and the solute concentration in the feed becomes depleted considerably. The pseudo-steady state solute permeation can be described by [191, 192]

$$Q = \frac{P' \cdot A \cdot C_o}{L} \left(t - \frac{L^2}{6D} \right) \quad (5.1)$$

where Q is the total amount of solute that had passed through the membrane (area A and thickness L) at time t , C_o is the initial solute concentration in the feed solution. P' and D represents the permeability

(m²/s) and diffusivity coefficients (m²/s), respectively. Equation (5.1) can be used customarily to determine the permeability coefficient, and this method is called the “time lag method”. The term $\theta = L^2/6D$ is the so-called “time lag”. It is a time-like quantity extrapolated from the pseudo-steady state permeation data. Several assumptions should be made concerning the above “time lag” method: (1) the solute concentration in feed liquid (C_o) is constant, (2) the solute concentration at the receiving side is negligible in comparison to the feed concentration, and (3) concentration-independent diffusivity and solubility coefficients. Another important assumption when using Equation (5.1) is that the overall mass transport is controlled by permeant diffusion across the membrane, whereas the equilibria for sorption to and desorption from the membrane at both membrane interfaces are established instantaneously and the effects of boundary layer are negligible. A large volume of the receiving liquid may be used to maintain a sufficiently low level of concentration of phenolic compounds in the permeate side. This, however, may result in insufficient turbulence in the receiving liquid, as demonstrated in Chapter 4. Nonetheless, in such cases where other mass transfer resistances are not negligible, the pseudo-steady state permeation process can be expressed as

$$Q = K_o A C_o (t - \varphi) \quad (5.2)$$

where K_o is the overall mass transfer coefficient in the liquid permeation process, φ is a time-like quantity extrapolated from pseudo-steady state permeation data. Plotting Q versus t will yield a straight line after an initial transient period, and the mass transfer coefficient could be determined from the slopes of the straight line. Based on the results in Chapter 4, the relative contribution of the membrane resistance to the overall mass transfer resistance, ξ , can be determined, then

$$\frac{L}{P'} = \frac{1}{K_o} \xi \quad (5.3)$$

where L/P' is membrane resistance, and $1/K_o$ is the total mass transfer resistance. The membrane permeability, P' , thus can be obtained based on Equations (5.2) and (5.3).

5.3 Experimental

5.3.1 Materials

All materials were the same as used in Chapter 3, and the detailed properties were presented in Table 3.2.

5.3.2 Membrane Preparation

The membranes used in liquid permeation experiments were prepared via the solution-casting technique as described in Chapter 3. Thick membranes used in sorption experiments were prepared by pouring the homogenous polymer solution after degassing into a Petri dish. After solvent evaporation, dry membranes were detached from the Petri dish.

5.3.3 Sorption Experiments

The sorption of phenolic compounds in PEBA 2533 was investigated as follows. Feed solutions of phenolic compounds with various initial concentrations were prepared and poured into 125 mL plastic bottles. Dry PEBA membranes were weighted and immersed into the liquid solutions for 3 days at 30°C to reach sorption equilibrium. The concentrations of phenolic compounds in feed solutions before and after sorption were measured using a spectrophotometer. The equilibrium sorption uptake Q_e (mmol/L) was calculated by

$$Q_e = \frac{V(C_o - C_e)}{W_o/\rho_m} \quad (5.4)$$

where C_o and C_e are the concentrations of the phenolic solutions at the beginning and equilibrium (mmol/L), V is the volume of the feed solution (L), W_o is the weight of PEBA sorbent (g), and ρ_m is the density of PEBA sorbent (g/L). The partition coefficient, or liquid phase sorption constant, K^L , was calculated by

$$K^L = \frac{Q_e}{C_e} \quad (5.5)$$

For a dilute liquid solution, the partial vapor pressure of the solute can be linked with the solute concentration in the liquid phase using the Henry's law equation

$$H \cdot C_e = p_o \quad (5.6)$$

where H is Henry's law constant in units of Pa/(mol·m⁻³), and p_o is the partial vapor pressure of the solute in equilibrium with the liquid solution, which can be obtained using Aspen Plus based on an appropriate model. Considering the membrane was in direct contact with the hypothetical vapor of the solute, the solubility coefficient can be written as $S=Q_e/p_o$. Based on Equations (5.5) and (5.6), the solubility coefficient was given

$$S = \frac{Q_e}{p_o} = \frac{K^L}{H} \quad (5.7)$$

To have a better understanding of the sorption mechanism, the sorption isotherms were studied. In this chapter, three models were used to analyze the sorption isotherm:

$$\text{Linear model: } Q_e = K_H \cdot C_e \quad (5.8)$$

$$\text{Linearized Langmuir model: } \frac{1}{Q_e} = \frac{1}{Q_m} + \frac{1}{Q_m K_L} \cdot \frac{1}{C_e} \quad (5.9)$$

$$\text{Linearized Freundlich model: } \ln Q_e = \ln K_F + \frac{1}{n} \ln C_e \quad (5.10)$$

where K_H , K_L and K_F represent Henry's sorption constant, the Langmuir sorption constant (L/mmol) and Freundlich constant ((mmol/L)^{1-1/n}) respectively, Q_m refers to the theoretical maximum sorption capacity (mmol/L), and 1/n is the heterogeneity factor.

5.3.4 Permeation Experiments

The experimental apparatus used for permeation was the same as used in Chapter 4 (Figure 4.1) except that the receiving compartment was filled with deionized water. Membranes with a thickness of approx. 25 μm were used in permeation experiments, and all the experiments were carried out at 30°C.

From Equations (5.2) and (5.3), the permeability coefficient P' in units of m²/s could be obtained from the liquid permeation tests. The diffusivity coefficient could be obtained as a ratio of the permeability coefficient and partition coefficient, giving

$$D = \frac{P'}{K^L} \quad (5.11)$$

Combining Equations (2.17), (5.7) and (5.11), the above permeability coefficient (P' , m²/s) can be converted into the permeability coefficient in customary units of Barrer:

$$P = D \cdot S = \frac{P'}{K^L} \cdot \frac{K^L}{H} = \frac{P'}{H} \quad (5.12)$$

5.4 Results and Discussion

5.4.1 Sorption Analysis

The equilibrium sorption uptake of four phenolic compounds in PEBA at various concentrations is shown in Figure 5.1, where the sorption data were fitted into the Linear, Langmuir, and Freundlich models, respectively. The parameters for the Linear, Langmuir, and Freundlich models are shown in Table 5.1. It seems that the Freundlich isotherm, a widely used empirical relation, is most appropriate to describe the sorption of the four representative phenolic compounds in PEBA as it has the highest R^2 value. The Linear model is suitable to describe the sorption isotherms when the solute concentration in the solution is rather low. As shown in Figure 5.1A, the sorption uptake increases with an increase in the equilibrium solute concentration, however, such an increase was less than proportional with liquid concentration, and the Linear model was unable to describe the sorption isotherm. On the other hand, the Langmuir model assumes that adsorption takes place at well-defined localized states, and the sorbate/sorbate interactions were neglected in the Langmuir model. However, the dissolution of phenolic compounds in PEBA polymer can loosen the polymer matrix, enlarging the free volume available to accommodate the sorbate. This could result in significant deviations from the Langmuir model. In addition, the clustering of phenolic compounds also leads to deviations from the Langmuir model.

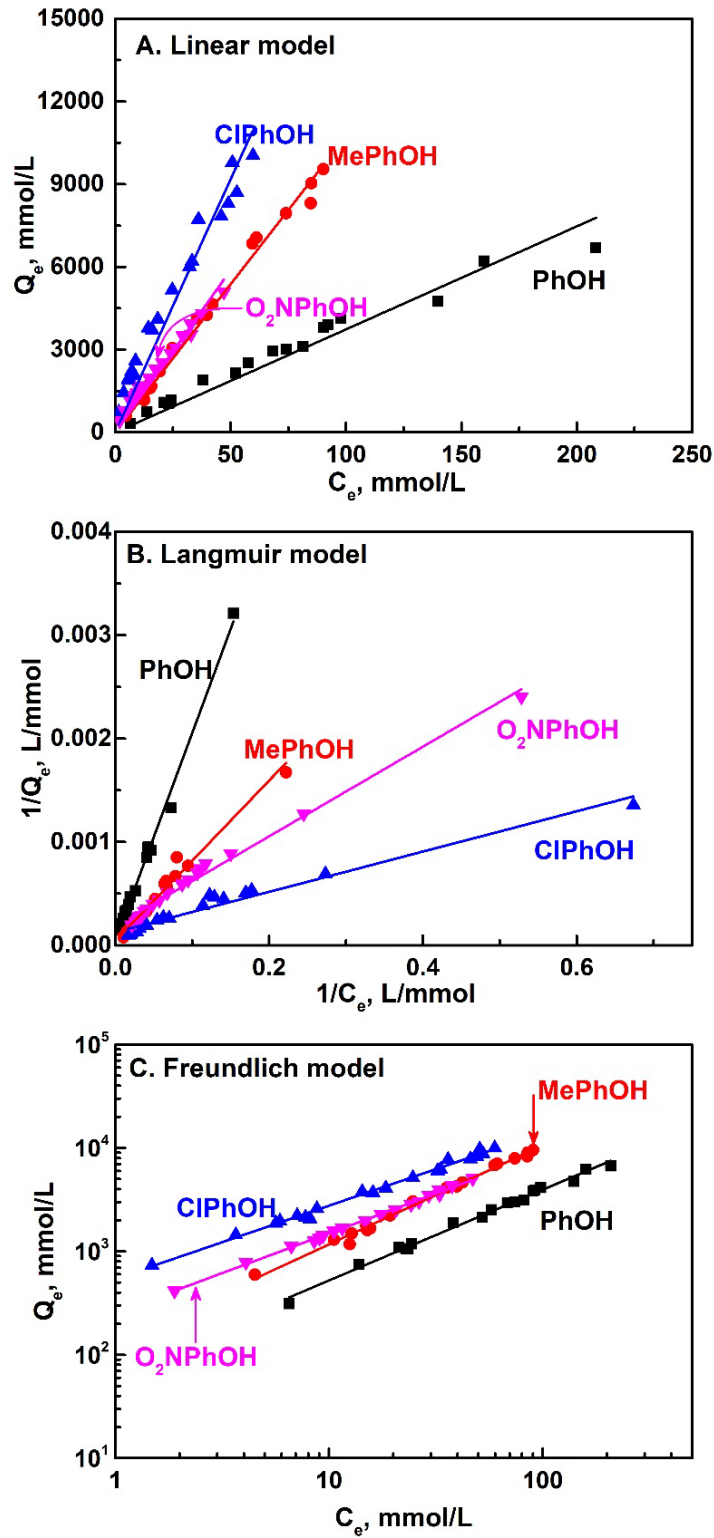


Figure 5.1 The (A) linear, (B) Langmuir, and (C) Freundlich models for sorption of phenolic compounds in PEBA at 30°C.

Table 5.1 Parameters of the linear, Langmuir, and Freundlich models for the sorption of phenolic compounds in PEBA at 30°C.

	Linear model		Langmuir model			Freundlich model		
	K_H	R^2	Q_m , mmol/L	K_L , L/mmol	R^2	K_F , (mmol/L) ^{1-1/n}	1/n	R^2
PhOH	33.2	0.984	24868	0.002	0.994	69.5	0.878	0.991
MePhOH	104.2	0.997	23572	0.005	0.978	129.4	0.956	0.992
ClPhOH	156.0	0.980	7830	0.065	0.963	544.1	0.707	0.992
O ₂ NPhOH	101.5	0.990	5342	0.043	0.989	254.9	0.769	0.997

Using Equations (5.5) and (5.7), the partition coefficient and solubility coefficient of the phenolic compounds in PEBA can be obtained, and they are shown in Figure 5.2. The partition coefficient follows the order of ClPhOH > O₂NPhOH > MePhOH > PhOH, the same order as the sorption capacity. The solubility coefficient of the phenolic compounds generally follows the reverse order, i.e., PhOH > MePhOH > ClPhOH (unfortunately, the solubility of O₂NPhOH could not be determined accurately due to difficulty in estimating the vapor pressure of O₂NPhOH in its binary aqueous solutions via Aspen Plus using the UNIQUAC or UNIFAC models. The saturated vapor pressure of pure O₂NPhOH can be estimated using the NRTL model, and it is found to be quite low). In analogue with gas sorption, the solubility coefficient is defined as the sorption uptake divided by vapor pressure. As shown in Figure 5.3, the vapor pressure of the phenolic compounds in equilibrium with the feed liquid solution follows the order of PhOH < MePhOH < ClPhOH. Thus, though the partition coefficient (or sorption uptake) of PhOH is lowest, the solubility of PhOH in the membrane is highest due to the lowest vapor pressure in equilibrium with the feed solution, while ClPhOH with the highest sorption uptake in the membrane has a low solubility coefficient. Nonetheless, the solubility coefficients of the three phenolic compounds are all high, with values in the range of 1000-3000 mol/(m³·Pa). At room temperature, the sorption uptake of water in PEBA membrane is approx. 7.8 mg/g-membrane, corresponding to a solubility coefficient of 0.15 mol/(m³·Pa). Above results demonstrate that PEBA has a very high solubility selectivity towards phenolic compounds, and the overall permselectivity of PEBA comes exclusively from the high solubility selectivity.

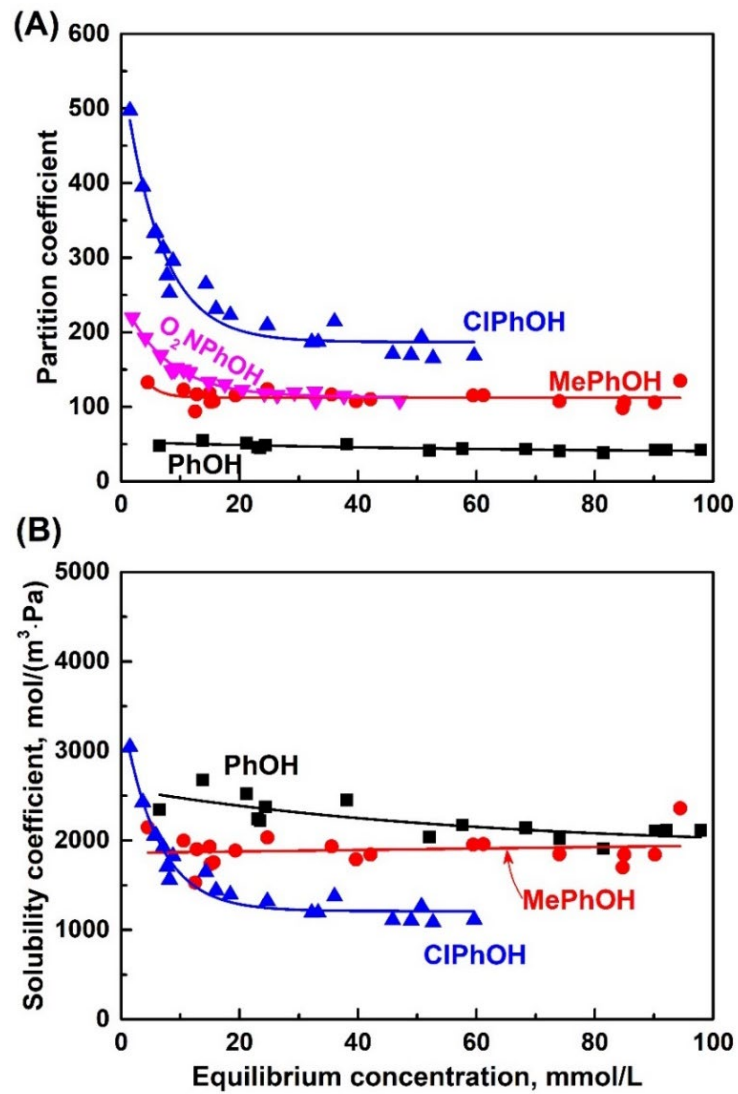


Figure 5.2 The (A) partition coefficient and (B) solubility coefficient of phenolic compounds at various equilibrium concentrations at 30°C.

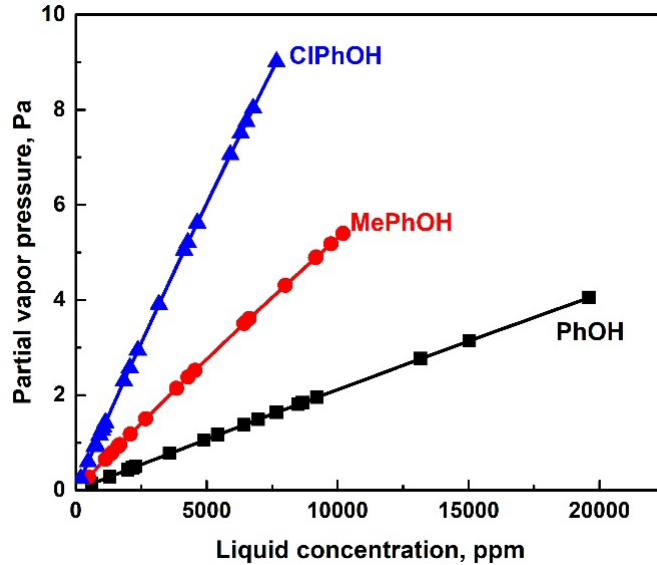


Figure 5.3 Partial vapor pressure of phenolic compounds in equilibrium with the liquid solution at 30°C. Data were estimated using the simulator Aspen Plus based on UNIQUAC model.

Furthermore, though the sorption uptake of phenolic compounds in the membrane increases with an increase in liquid concentration, both the partition coefficient and solubility coefficient decrease with an increase in the liquid concentration. Obviously, PEBA sorbent cannot sorb phenolic compounds infinitely because of the finite sorption sites, and sorption saturation will be reached gradually with an increase in liquid feed concentration. As a result, in the later stage of the sorption isotherms when the solute concentration in the solution is high, the increment in the sorption uptake with increasing liquid concentration will be less than proportionally due to the limited sorption sites, leading to a reduction in partition coefficient as well as solubility coefficient. Such a reduction is more significant for phenolic compounds with a high sorption uptake in the membrane, for example, CIPhOH and O₂NPhOH, as they are ready to reach sorption saturation.

5.4.2 Permeation Analysis

Figure 5.4 shows the experimental data for the permeation of different phenolic compounds through PEBA membrane at various initial feed concentrations. Apparently, the quantity of phenolic compounds in the receiving liquid increases gradually with time. After a period of the transient permeation, a linear relationship (pseudo-steady state) between the amount of the permeated solutes and permeation time was observed, and the overall mass transfer coefficient can be evaluated from the slopes of the straight lines.

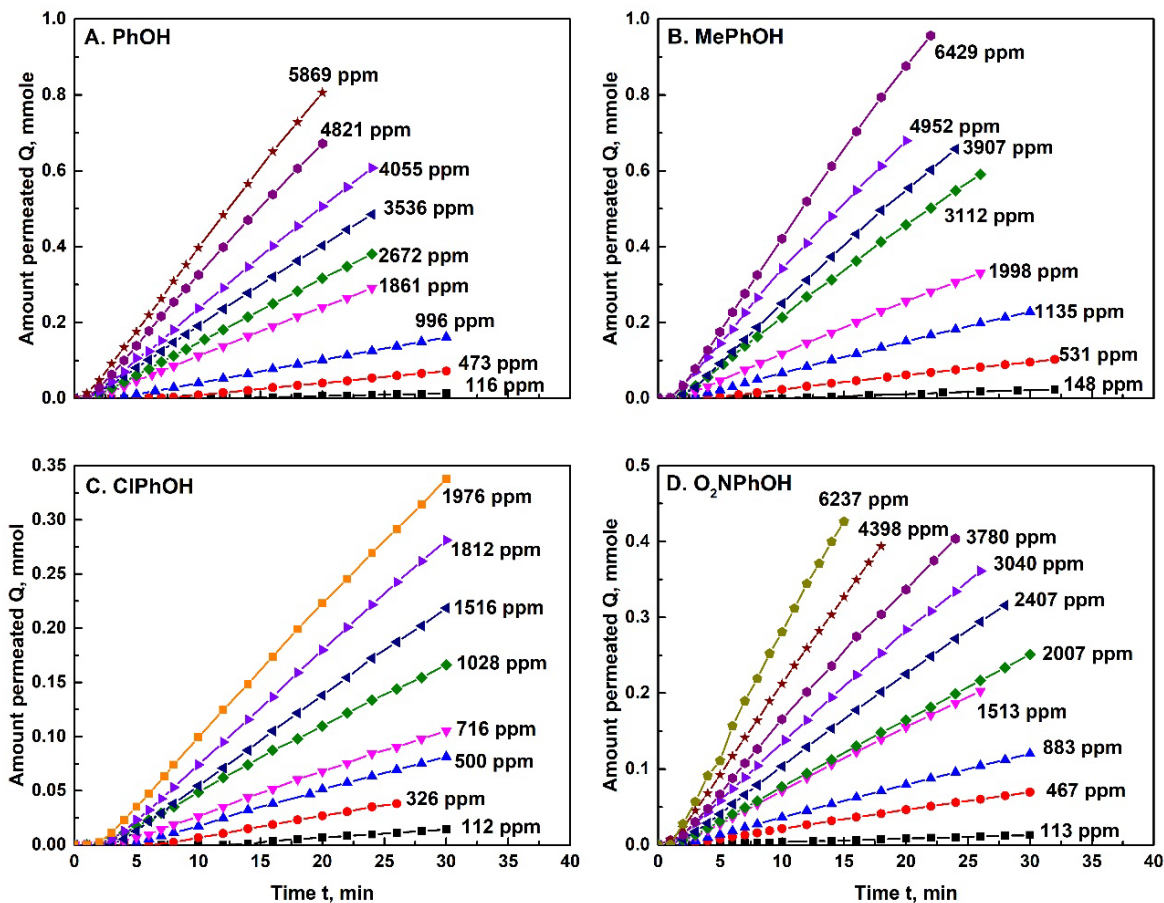


Figure 5.4 Amounts of phenolic solutes in the receiving compartment as a function of time at various feed concentration at 30°C.

The overall mass transfer coefficient for four phenolic compounds at different feed concentrations can be obtained from the slopes of the pseudo-steady state permeation period shown in Figure 5.4, and the results are shown in Figure 5.5A. To determine the membrane permeability, the relative contribution of the membrane resistance to the overall mass transfer resistance, ξ , is required, and these values can be found in Chapter 4. According to Equation (5.3), the membrane permeability in units of m^2/s can be obtained, and the results are shown in Figure 5.5B. The permeability coefficient (P' , m^2/s), was in the order of $\text{ClPhOH} \approx \text{MePhOH} > \text{O}_2\text{NPhOH} > \text{PhOH}$, generally following the same order as the sorption uptake. In rubbery polymers, solute permeation is usually sorption governed, and therefore it makes sense that the permeability of phenolic compounds follows the same order with the sorption uptake.

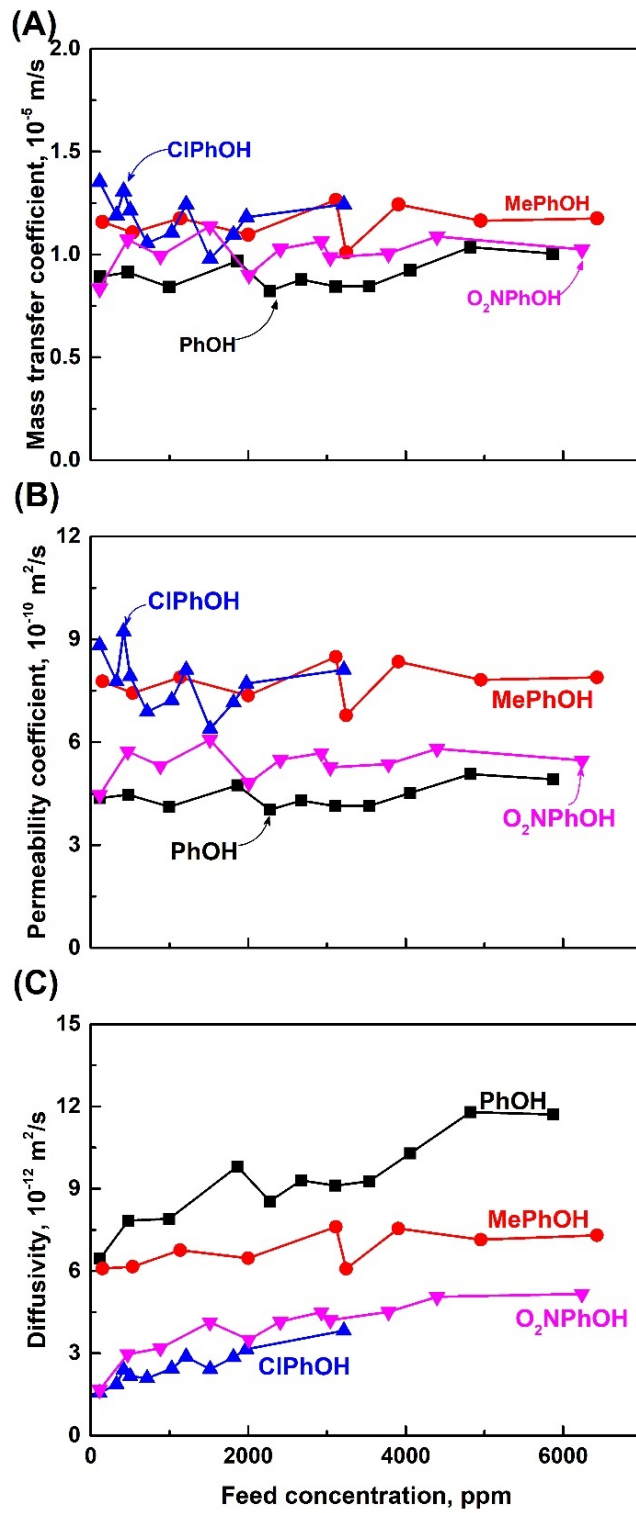


Figure 5.5 The (A) overall mass transfer coefficient, (B) permeability coefficient, and (C) diffusivity coefficient of phenolic compounds at different concentrations at 30°C.

With the permeability coefficient and the partition coefficient known, the diffusivity coefficient was obtained, and the results were displayed in Figure 5.5C. The diffusivity coefficient increases with an increase in feed concentration due to membrane swelling. With an increase in liquid concentration, the extent of membrane swelling caused by the dissolution of phenolic solutes in the membrane increases, and the membrane swelling enhances the diffusion of permeating molecules through the membrane. Mujiburohman et al. [130] found the diffusivity of propyl propionate through PEBA membrane increased exponentially with increasing concentration, suggesting that the effect of membrane swelling caused by the dissolution of propyl propionate was very significant. Furthermore, it can be seen that the diffusivity coefficient follows the order of ClPhOH < O₂NPhOH < MePhOH < PhOH. In addition to the well-known molecular size effect on diffusivity, the mutual interactions among phenolic solutes and membrane also affect the diffusion processes.

5.4.3 Permeability Comparison

Considering the vapor-liquid equilibrium, the permeability in units of m²/s can be converted into Barrer using Equation (5.12), and the results are shown in Figure 5.6, where the permeability obtained from pervaporation was also presented for comparisons. The permeability obtained from liquid permeation experiments follows the order of PhOH > MePhOH > ClPhOH, in the same sequence with those obtained from pervaporation. Nonetheless, the permeability data obtained from liquid permeation is higher than those obtained from pervaporation experiments. This is because the permeation characteristics of the membrane depend strongly on the environment in which the membrane is equilibrated. During the liquid permeation process, both sides of the PEBA membrane were in direct contact with the liquid solution, where the membrane was in a well swollen condition [193]. In such cases, the penetrates would permeate through the membrane at a rate to their fully potential. While in pervaporation, the feed liquid contacts the upstream side of the membrane, and the downstream side of the membrane is subjected to vacuum to remove the vapor. Thus, the “wetness” of the membrane was decreased across the membrane from the feed side to the permeate side, and the membrane was less swollen overall. As a result, compared with in liquid permeation where the polymer matrix is well swollen, the mass transfer rate in pervaporation is slower.

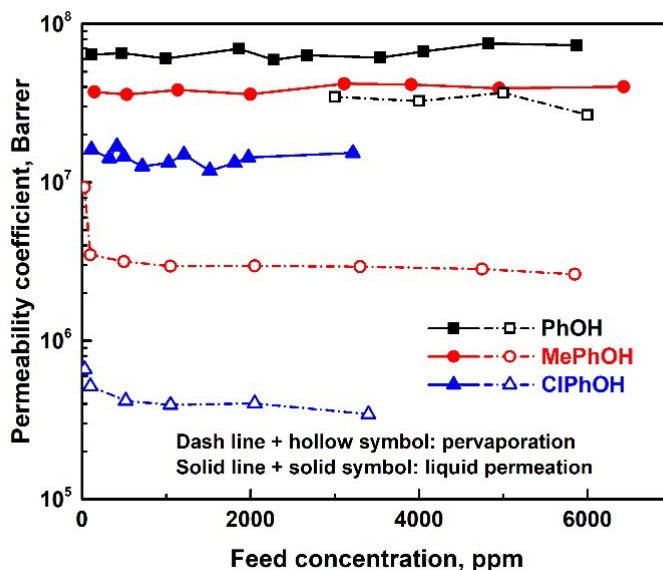


Figure 5.6 Comparison of permeabilities obtained from pervaporation (hollow symbols) and obtained from liquid permeation experiments (solid symbols) at 30°C.

5.5 Summary

The sorption and diffusion of phenolic compounds in PEBA membrane were evaluated separately. The sorption isotherm of phenolic compounds in PEBA can be fitted into the Freundlich model properly. The solubility coefficient of phenolic compounds in PEBA is on the order of $10^3 \text{ mol}/(\text{m}^3 \cdot \text{Pa})$ at 30°C, much higher than that of water, indicating that the good permselectivity of PEBA towards phenolic compounds predominantly comes from the excellent solubility selectivity. Contrary to the sorption uptakes, the solubility coefficient was found to follow the order of $\text{PhOH} > \text{MePhOH} > \text{ClPhOH}$ taking the vapor pressure into account. As a result of the molecular size effect and different mutual interactions between the polymer and phenolic solutes, their diffusivity coefficients follow the order of $\text{PhOH} > \text{MePhOH} > \text{ClPhOH}$. The diffusivity coefficients of the phenolic compounds in the membrane during liquid permeation increases with an increase in feed concentration due to membrane swelling. Furthermore, it was found the permeability coefficient obtained by liquid permeation experiments was higher than pervaporation experiments, presumably due to the different membrane “wetness” under different experiments conditions.

Chapter 6

Permeability, Solubility, and Diffusivity of Aniline in PEBA Membranes pertaining to Aniline Removal from Aqueous Solutions by Pervaporation and Sorption¹

6.1 Introduction

As mentioned before, membrane permeability is an attribute of the membrane, and it is an important parameter to understand the permeation behavior of the membrane. The permeability coefficient can be obtained experimentally based on the permeation flux obtained in pervaporation according to Equation (3.1). Nonetheless, the membrane permeability determined via different approaches can result in different values, and sometimes they can differ significantly (Chapter 5). This is the case even for permeabilities determined with a process variant (e.g., pervaporation and evaporation (sometimes also referred to as vapor permeation)) based on the same working equation for mass transfer. In evaporation, the vapor in equilibrium with the liquid feed contacts with and permeates through the membrane under a driving force induced by a vapor pressure difference across the membrane. That is, in principle, largely the same permeation fluxes in both pervaporation and evaporation with the same membrane under same operating conditions (i.e., feed composition, temperature, permeate pressure) would be expected. However, a close look at the permeability/permeation flux for pervaporation and evaporation in prior work shows a different situation [193-195]. There are different views on the root cause. A hypothesis is that the activities of the permeating components in evaporation are less than the activities of the penetrants in pervaporation unless the vapor is replenished fast enough to maintain the concentration of the fast-permeating component at the membrane surface. Otherwise, the vapor in contact with the membrane is not completely saturated [57]. An alternate explanation is that the fluids in contact with the membrane at different physical states (i.e., liquid, vapor) affect the property of the membrane [193, 195], leading to different permeabilities. Therefore, caution should be exercised in using the membrane permeability as an intrinsic property. To fill in the knowledge gap as how the membrane permeability determined via different approaches would differ, an attempt was made in this work to evaluate and compare the membrane permeabilities obtained with different approaches, thereby providing an insight into the mass transfer in the membrane. For such purposes, the permeability, solubility, and diffusivity of aniline, another commonly present chemical

¹ Portions of this chapter have been submitted to *J. Membr. Sci.*, Under Review.

contaminants in water streams, in PEBA membrane pertaining to aniline removal from aqueous solution by pervaporation and sorption were investigated. Both phenols and aniline are the simplest aromatics with slightly acidic (for phenols) and basic (for aniline) properties, and the investigation on the separation of aniline allows us to see whether PEBA is able to separate both aromatics from water.

Aniline, the simplest aromatic amine with a phenyl group attached to an amino group, is an important organic intermediate used extensively in the production of a broad range of chemicals (e.g., dyes, pesticides, resins, and pharmaceuticals) [196, 197]. As a result, aniline is often found in various industrial wastewaters at high concentrations, imposing various adverse effects on human health, and it is classified as a principal organic contaminant by the US Environmental Protection Agency [4]. It is therefore of great importance to scavenge aniline effectively from the wastewater before discharge. In 1996, Meckl and Lichtenthaler [51] showed that PEBA membrane was suitable for removal of aniline from water because of its high solubility towards aniline, and almost two decades later Li et al. [198] reported a pervaporation process using PEBA membrane with partial permeate condensation to enhance the purity of aniline recovered from aqueous solutions. Given the good permselectivity of PEBA 2533 towards phenolic compounds and aniline, PEBA 2533 membrane was used as well here to separate aniline from its aqueous solution, and the mass transfer fundamentals of aniline in PEBA were investigated.

Based on the solution-diffusion model, membrane permeability is related to the solubility (S , mol/(m³·Pa)) and diffusivity (D , m²/s) under the assumption that both S and D are constant, i.e., $P_i = S_i \cdot D_i$. The solubility determines the concentration of the permeating molecules accommodated in the membrane, and the diffusivity determines the migration rate of the penetrant through the polymer matrix. Thus, evaluating the solubility and diffusivity independently allows not only an alternative estimate of the permeability; it also helps with a better understanding of the permeation behavior. On the other hand, the membrane permeability can also be evaluated using a method proposed by Chen et al. [199] that uses both the mass balance and time lag methods based on the transient and (pseudo-) steady state permeation rates. Preliminary experiments showed that such a measurement technique was also applicable to aniline permeation, and as such aniline permeability in the PEBA membrane was determined as well via the concentration-driven liquid diffusion/permeation process.

In the present work, the permselectivity of PEBA 2533 membrane for the separation of aniline from dilute solutions by pervaporation was evaluated, and the impacts of feed concentration and operating temperature on the pervaporation performance were investigated, with an emphasis placed on the fundamental understanding of membrane permeability in light of the knowledge gap mentioned above.

Thus, the membrane permeability was determined via three different approaches: (1) by normalizing the permeation flux in pervaporation with membrane thickness and mass transfer driving force, (2) by multiplying the solubility coefficient and the diffusivity coefficient determined independently from liquid sorption experiments, and (3) by direct measurements from liquid permeation experiments over the period of pseudo steady state permeation. It was demonstrated that the permeabilities so determined needed to be converted properly in order to reconcile the permeability data with a unified dimension. In addition, the sorption-desorption reversibility was investigated to demonstrate the reusability of PEBA as a sorbent for aniline removal from water by sorption. The reversible sorption-desorption is also an underlying requirement for pervaporative separation of aniline as aniline molecules sorbed into the membrane are continuously removed from the membrane via desorption at the downstream side of the membrane.

6.2 Experimental

6.2.1 Materials

Aniline (≥ 99.5 wt%) was purchased from Sigma Aldrich. All aqueous aniline solutions used in the experiments were freshly prepared by dissolving a given amount of aniline in de-ionized water. All other materials were identical as described in Chapter 3.

6.2.2 Membrane Preparation

Membranes used in pervaporation and liquid permeation experiments were prepared by the solution casting technique, which has been described in Chapter 3. Thicker membranes with different thicknesses (ca. 250 – 800 μm) used in the sorption experiments were prepared as described in Chapter 5.

6.2.3 Pervaporation

Pervaporation tests were carried out as described in Chapter 3. To calculate the permeability coefficient, the saturated vapor pressure and activity coefficient of aniline in the feed were estimated using Aspen Plus based the UNIFAC model [200, 201].

6.2.4 Sorption Experiments

Sorption isotherms were determined as described in Chapter 5 (section 5.3.3). All experiments were conducted at room temperature (23°C). The solubility coefficients were evaluated according to Equations (5.4) to (5.7).

To evaluate the diffusivity coefficient, the kinetics of aniline sorption in PEBA films were determined. Dry PEBA films with known masses and thicknesses were immersed into aniline solutions at given concentrations at room temperature (23°C). As sorption proceeded, the concentration of aniline in the liquid solution decreased, and the variation in aniline concentration was monitored using a spectrophotometer. The sorption uptake Q_t at a given instant time t was given by

$$Q_t = \frac{V \cdot (C_o - C_t)}{W_o / \rho_m} \quad (6.1)$$

where C_t is the instantaneous aniline concentration (mol/m³) at time t . The diffusivity (D) was calculated from the time-dependent sorption uptake data according to [191, 192]

$$\frac{Q_t}{Q_e} = 1 - \frac{8}{\pi^2} \sum_{n=0}^{\infty} \frac{1}{(2n+1)^2} \exp\left[-\frac{D(2n+1)^2 \pi^2 t}{L^2}\right] \quad (6.2)$$

where Q_e is the equilibrium sorption uptake.

6.2.5 Liquid Permeation Experiments

The permeability coefficient of aniline in the membrane was also measured in a liquid diffusion/permeation system, as described by Chen et al [199]. The detailed experimental procedures were described in Chapter 5 (5.3.4). In brief, the membrane was mounted at the bottom of the feed (donor) compartment horizontally, and the receiving compartment (receptor) was filled with 2 L of deionized water. The membrane was submerged into deionized water in the receiving compartment. At time zero, 100 mL aniline solution at a given concentration was filled into the feed compartment, and permeation began to occur under the driving force of a concentration difference across the membrane. To eliminate the boundary layer effect, vigorous agitations were provided at both the donor and receptor sides. As aniline permeation proceeded with time, aniline concentration in the receptor was measured periodically, for a period of 30 min. Aniline permeability in the membrane was calculated using the following [199]

$$-\ln\left(\frac{C_o V - (V + V_R) C_R}{C_o V - (V + V_R) a}\right) = \frac{P' A}{L} \left(\frac{1}{V} + \frac{1}{V_R}\right) (t - t_0) \quad (6.3)$$

where V and V_R are the volumes (m³) of the feed liquid and the receiving liquid, respectively; C_o is the initial aniline concentration (mol/m³) in the feed compartment, a is aniline concentration (mol/m³) in the receiving compartment when the elapsed time is at least three times of the time lag, C_R is the aniline

concentration in receiving compartment. Defining the left-hand side of Equation (6.3) as $F(t)$, plotting $F(t)$ vs t will yield a straight line, and the membrane permeability (P') can be obtained from the slope.

It should be mentioned that the permeability coefficient obtained in such a liquid permeation measurements was in units of m^2/s , different with the customarily used units of Barrer [equivalent to SI units of $\text{mol}\cdot\text{m}/(\text{m}^2\cdot\text{s}\cdot\text{Pa})$] in pervaporation. This is caused by the different expressions of the transmembrane driving force in liquid permeation and in pervaporation and vapor (gas) permeation. In liquid permeation where both sides of the membrane are in contact with the liquid directly, the solute concentration in the membrane was correlated to the liquid concentration using a dimensionless partition coefficient (Equation (2.4)). Assuming the partition coefficient is independent of solute concentration, the permeability coefficient in liquid permeation (P') equals the partition coefficient (K) multiplying the diffusivity coefficient (D) (that is, $P'=K\cdot D$) in SI units of m^2/s . This is the permeability based on the liquid concentration difference across the membrane as the driving force for mass transport. On the other hand, in vapor permeation or pervaporation, the driving force for mass transport is conveniently represented using the vapor pressure difference across the membrane (or equivalent vapor pressure difference in the case of pervaporation). Thus, it is difficult to compare membrane permeabilities measured using different techniques and in different units. To fill the gaps, an attempt was made in this work to reconcile the membrane permeabilities. Similar to pervaporation, the sorption equilibrium between the liquid and membrane phases at both the upstream and downstream liquid/membrane interfaces in liquid permeation can be considered in conjunction with vapor-liquid equilibrium correlating the liquid phase composition and the vapor pressure. The vapor-liquid equilibrium can be regarded as an equilibrium state of vapor sorption into the liquid and can be described by the Henry's law. This way, the permeability coefficient as measured in liquid permeation (P' , m^2/s) can be easily converted to the permeability (P) in units of Barrer using Equation (5.12).

6.2.6 Sorption-desorption Reversibility

An important underlying assumption in the mass transfer considerations in sorption and permeation is that the solubility and diffusivity of the membrane are a response of the membrane to the permeant at a given feed concentration, unaffected by prior exposure to feed solutions at other concentration. That is, the sorption-desorption is considered to be reversible, and there is no permanent trapping of aniline within PEBA. This was confirmed by experiments where the aniline sorption isotherms were measured several times using the same films after regeneration of aniline-loaded PEBA films to evaluate the sorption-desorption reversibility. This is also highly relevant to the reusability of PEBA as a sorbent to aniline. After reaching sorption equilibrium at room temperature, the exhausted films were submerged

in a 0.2 M HCl solution for 2 h, followed by rinsing with deionized water. After drying in air, the regenerated films were subjected to sorption measurement with aniline solutions. The sorption isotherms for the regenerated films were determined. The above sorption-regeneration steps were repeated for 6 times, verifying the sorption-desorption reversibility and constant sorption capacity.

6.3 Results and Discussion

6.3.1 Pervaporation Performance

Figure 6.1 shows the effects of aniline concentration in the feed on permeation flux at different temperatures. At a given temperature, with an increase in feed aniline concentration, aniline flux increased almost linearly, while water flux also increased but at a much lesser extent. The results for aniline permeation are easy to understand as a higher aniline concentration in the feed means a higher transmembrane driving force aniline permeation. While the driving force for water permeation is reduced, such a reduction is insignificant because of the low aniline concentration levels investigated (from 90 to 6000 ppm). On the other hand, the dissolution of aniline into the membrane tends to swell the membrane and loosen the structure of the polymer matrix, resulting in enhanced diffusivity of the permeating molecules in the membrane [130, 202-205]. The extent of membrane swelling increases with an increase in aniline concentration, and so does the diffusivity of water in the membrane. In addition, the dissolution of aniline in membrane is expected to have a positive impact on water sorption as well in light of the increased space in swollen membrane to accommodate additional water molecules and clustering of aniline with water molecules due to their strong affinity [206]. This consideration is also supported by the sorption data of PhOH/water in PEBA where water uptake in PEBA was shown to have increased with an increase in PhOH concentration [48]. The slightly enhanced water permeation observed at a higher aniline concentration in the feed can be attributed to the enhanced solubility and diffusivity of water in the PEBA membrane. Furthermore, the increased aniline flux with an increase in aniline concentration in the feed may also help facilitate water permeation due to the formation of aniline-water clusters.

Figure 6.2 shows the effects of feed concentration on the concentration of aniline in the permeate and the corresponding enrichment factor. Due to the strong affinity between aniline and PEBA, aniline was enriched substantially by pervaporation. For example, at a feed aniline concentration of 0.6 wt%, a permeate concentration of 25 wt% was achieved at 23°C, which is much higher than the solubility limit (the solubility of aniline in water is 3.66 wt% at 22.7°C and 3.69 wt% at 27°C [207]). Therefore, the permeate undergoes a phase separation, where the organic phase contains substantially pure aniline

(94.87 wt% at 20°C [207]). The phase separation can be easily exploited to augment pervaporation for further aniline purification [198]. The enrichment factor tended to decrease with an increase in feed concentration. Please note that the enrichment factor shown in Fig. 4 is based on the overall permeate concentration, and a much higher enrichment will be achieved should the phase separation of the permeate stream be considered.

To better illustrate the contribution of the membrane to pervaporative separation of aniline from water, the concentrations of aniline in the permeate at different feed concentrations are compared to the concentrations of aniline in the vapor phase that is in equilibrium with the feed liquid, as shown in Figure 6.3. The much higher aniline concentration in the permeate than that of the saturated vapor indicates that the membrane permselectivity contributes more significantly than the solution thermodynamics toward aniline enrichment. Over the feed concentrations investigated, the aniline enrichment caused by the membrane (β_{mem}), which may be defined as the ratio of aniline concentration in the permeate to aniline concentration in the vapor phase, was in the range of 10-13, whereas the enrichment caused by evaporation (β_{evp} , which is defined as the ratio of aniline concentration in the vapor phase to aniline concentration in the liquid feed) was about 4-5. These results clearly show that pervaporation is more efficient than evaporation-based processes (e.g., gas stripping) for aniline enrichment from dilute solutions as far as the degree of separation is concerned.

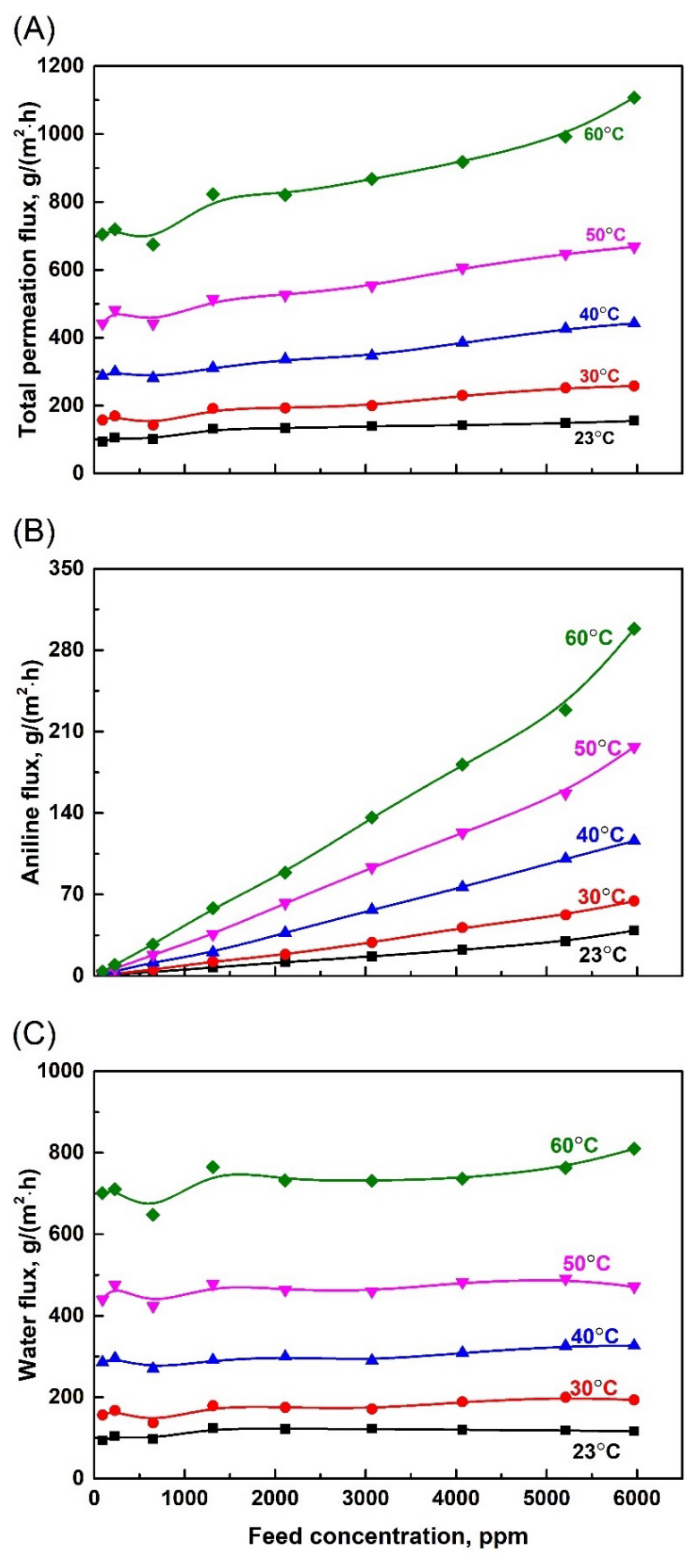


Figure 6.1 Effects of aniline concentration in feed on permeation flux at different temperatures.

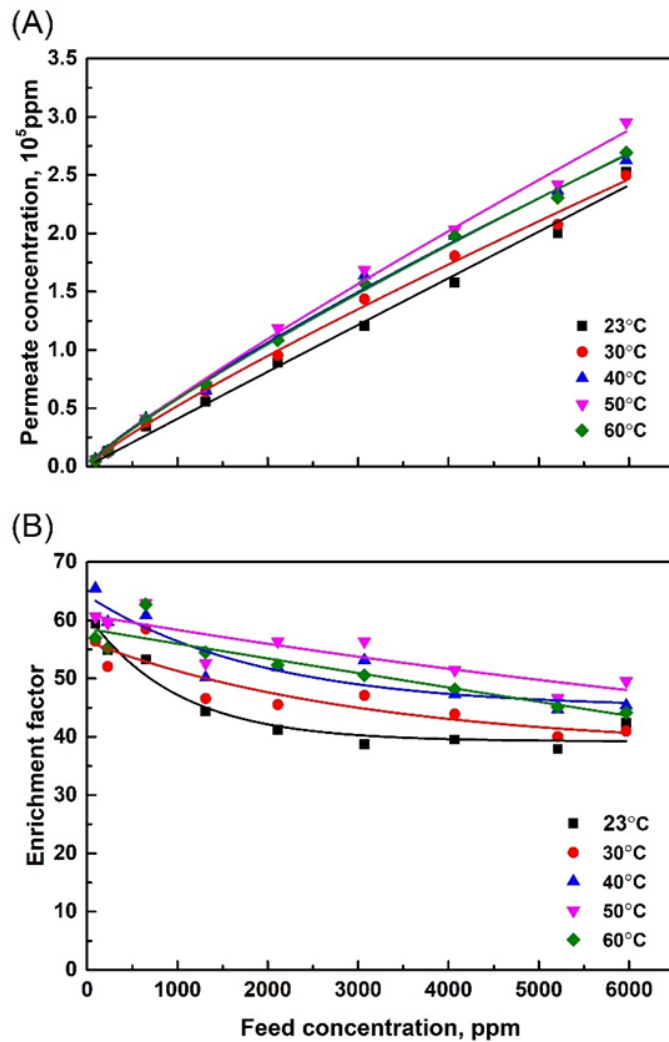


Figure 6.2 Effects of feed aniline concentration on (A) the permeate concentration and (B) enrichment factor at different temperatures.

The permeability coefficients of aniline and water in the membrane for pervaporation mass transfer were calculated according to Equation (3.1), and the results are shown in Figure 6.4. The permeability of aniline is on the order of 10^5 Barrer, much higher than water permeability, demonstrating the good permselectivity of PEBA towards aniline. It appeared that aniline permeability was largely constant within the concentration range investigated, while water permeability increased slightly with an increase in feed concentration. Aniline molecules can interact with each other to form intermolecular clusters [208], and the clusters are expected to diffuse through the membrane via the solution-diffusion mechanism at a lower diffusivity than the non-clustered molecules as the clustering restrains the

movement of aniline in the membrane. On the other hand, the membrane is increasingly swollen at a high aniline concentration, which favors the diffusion of the penetrants in the membrane. The concentration dependency of aniline permeability appears to suggest that the effects of membrane swelling is counterbalanced by the lowered aniline diffusivity due to molecular clustering. The increased membrane swelling by aniline with an increase in aniline concentration in the feed favored water permeation, leading to an increased membrane permeability to water.

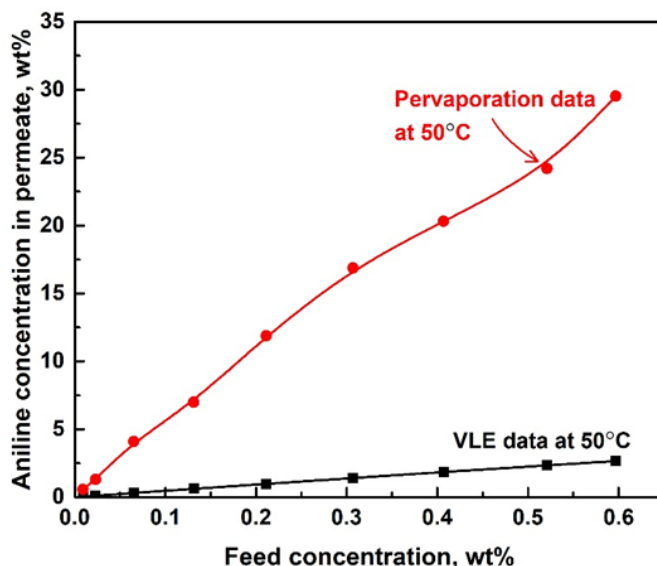


Figure 6.3 Permeate concentration as a function of feed concentration for pervaporation as compared to the vapor-liquid equilibrium (VLE) data at 50°C. The VLE data was estimated using Aspen based on the UNIFAC model.

The temperature dependencies of both the permeation flux (J) and permeability were quantified with an Arrhenius type of relation, that is, $J_i = J_{oi} \exp\left(-\frac{E_{Ji}}{RT}\right)$ and $P_i = P_{oi} \exp\left(-\frac{E_{Pi}}{RT}\right)$. The partial permeation fluxes of aniline and water and their permeability are plotted as a function of reciprocal temperature on a semi-log scale, as shown in Figure 6.5A and Figure 6.5B, respectively. As expected, both aniline and water fluxes increased with an increase in temperature. A high temperature favors both the diffusivity and the driving force for permeation, though the sorption aspect of the permeation is negatively affected. However, increasing temperature resulted in a decrease in the membrane permeance (or permeability) to both aniline and water. The permeability is mainly determined by the

solubility and diffusivity. Though an increase in temperature will increase the diffusivity, the solubility will decrease because of exothermic dissolution of aniline/water in the membrane. The work in Chapter 3 showed that for compounds having low or moderate sorption uptakes in PEBA (e.g., PhOH, MePhOH), there was a significant reduction in the solubility at higher temperatures, and the reduced solubility could not be made up by the increased diffusivity as far as the permeability was concerned, resulting in a decrease in the permeability. The sorption uptake of aniline in PEBA is much lower than that of PhOH or MePhOH. The negative temperature dependence of the membrane permeability to aniline and water appeared to come from the exothermic sorption.

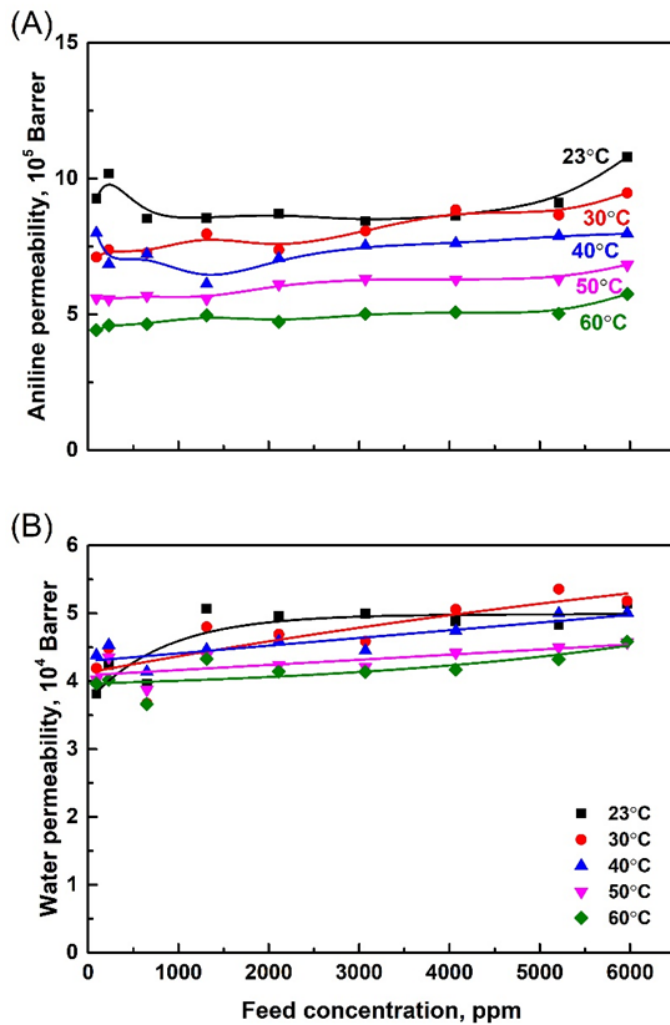


Figure 6.4 Effects of feed concentration on membrane permeability at different temperatures.

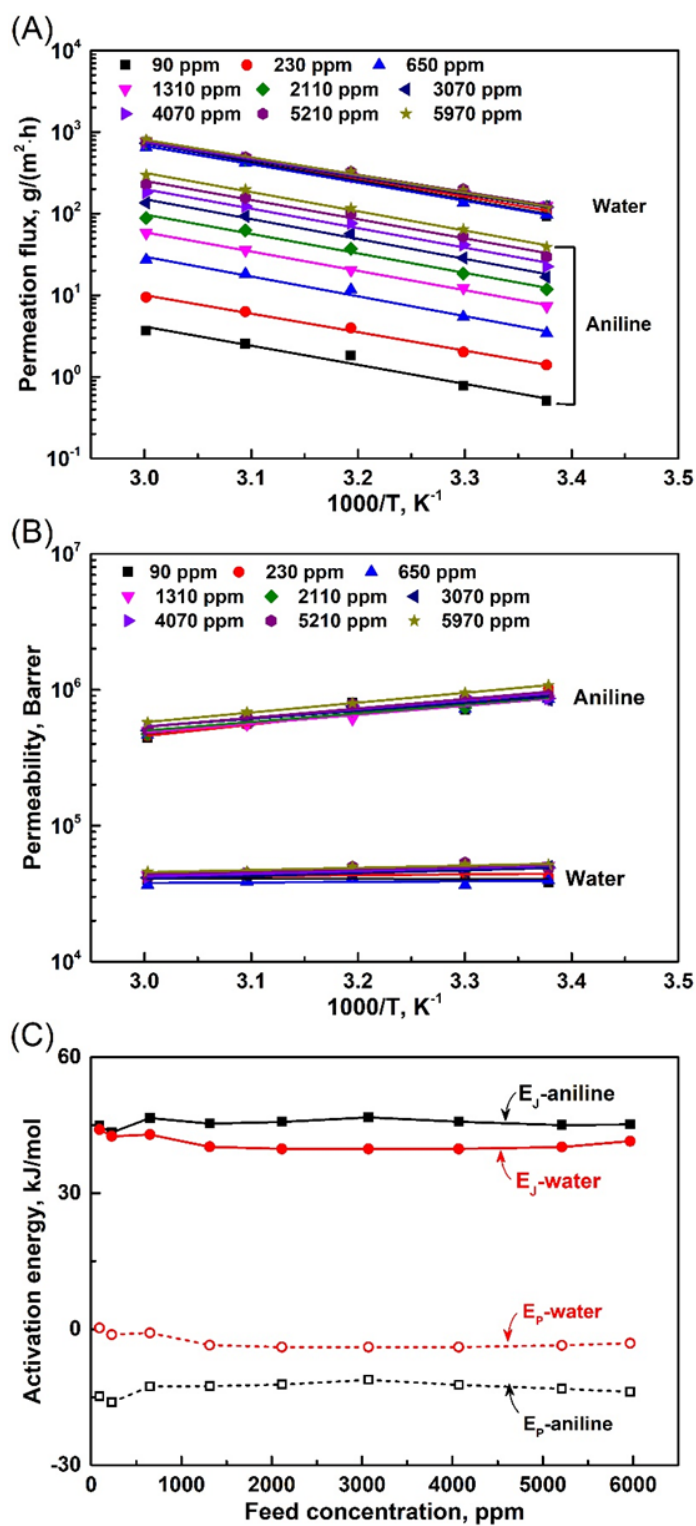


Figure 6.5 Temperature dependency of (A) permeation flux, (B) permeance, and (C) activation energy for permeation at different feed concentrations.

From the slopes of the straight lines in Figure 6.5A and B, the apparent activation energy (E_J) and the intrinsic activation energy (E_P) for aniline and water permeation were evaluated, and they are presented in Figure 6.5C. E_J for aniline was slightly higher than for water, suggesting that for a given feed composition, the permeation rates of aniline were affected by temperature more significantly than water. In principle, energy cannot be negative. However, since E_P is essentially a composite parameter equal to the activation energy for diffusion (a positive quantity) plus the enthalpy change of sorption (negative for exothermic sorption), negative E_P values will result when the heat effect of sorption outweighs the energy barrier for activated diffusion [59]. This has also been explained in Chapter 3. A negative E_P means increasing temperature will lower the membrane permeability. This is the case for permeation of aniline and water in the membrane. The positive E_J and negative E_P suggest that with an increase in temperature, in spite of the decreased membrane permeability, the permeation fluxes increased primarily due to increased transmembrane driving force. In addition, it was found the E_J - E_P relation ($E_P = E_J - \Delta H_V$) was applicable for aniline permeation in PEBA membrane. Within the temperature range investigated, the ($E_J - E_P$) values for aniline (58 - 60) kJ/mol and 43.7 kJ/mol for water are comparable with the ΔH_V values of (54 - 56) kJ/mol for aniline and 42.9 kJ/mol for water (the ΔH_V values of aniline were estimated based on the Yaws' Chemical Properties Handbook [172]).

6.3.2 Solubility and Diffusivity from Sorption Measurements

The above results showed that PEBA membrane was effective to separate aniline from aqueous solutions by pervaporation. To have a close look into the permselectivity, the solubility and diffusivity of aniline in PEBA were evaluated separately. Figure 6.6A shows the sorption isotherms of aniline in PEBA membrane at different temperatures. The Linear sorption model was found to be adequate to describe the sorption isotherm, and the sorption constant as well as the coefficient of determination was shown in Table 6.1. The sorption constant decreased with an increase in temperature, suggesting that aniline sorption in PEBA is indeed exothermic. Figure 6.6B shows the solubility coefficient of aniline in PEBA as calculated using Equations (5.4) to (5.7), where the vapor pressure of aniline in equilibrium with the aniline solution was estimated using Aspen Plus. The data in Figure 6.6B shows that within the concentration range investigated, the solubility coefficient of aniline is largely constant. At room temperature (23°C), the solubility of aniline in PEBA is approx. 105 mol/(m³·Pa), much higher than the solubility of water. As a comparison, water solubility in PEBA is 0.15 mol/(m³·Pa), as determined from pure water sorption data. Clearly, there is a very high solubility selectivity (as measured with aniline to water solubility ratio) for sorptive aniline/water separation. In view of their molecular sizes, water

diffusivity should be greater than aniline diffusivity, but PEBA still exhibited a high permselectivity to aniline in pervaporation, thanks to the high solubility selectivity.

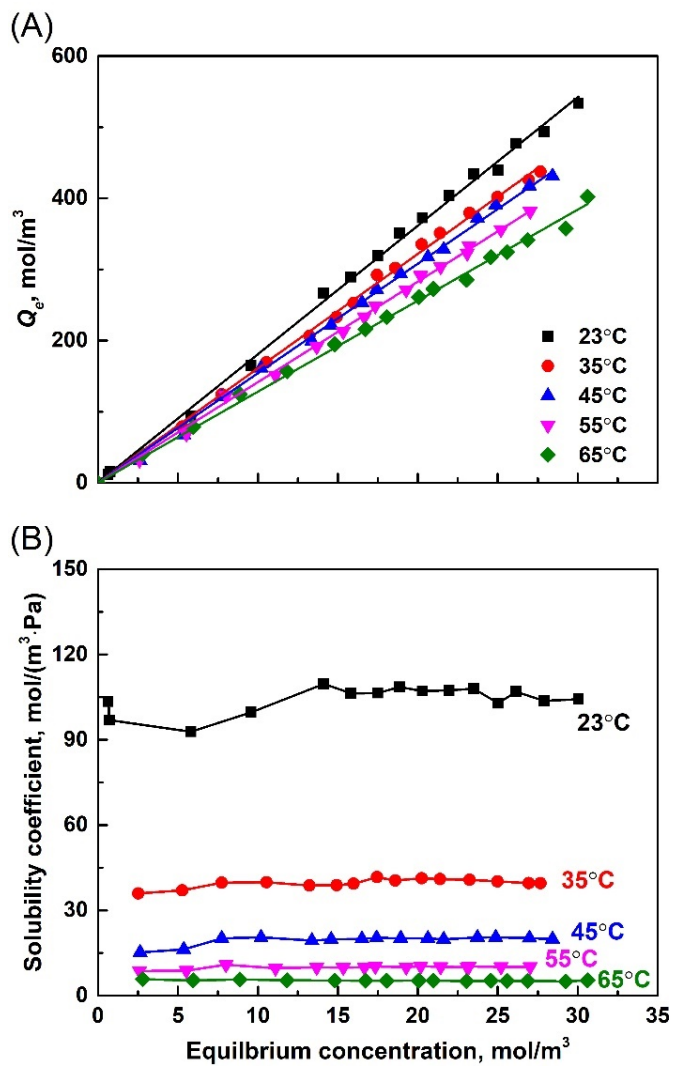


Figure 6.6 (A) Aniline sorption isotherms in PEBA, and (B) the solubility coefficient of aniline in PEBA.

Table 6.1 Model parameter and coefficient of determination for aniline sorption in PEBA.

Temperature (°C)	K_H	R ²
23	18.1	0.9994
35	16.1	0.9995
45	15.4	0.9995
55	14.1	0.9996
65	12.8	0.9992

The diffusivity of aniline in PEBA membrane was determined from the sorption kinetics data. Figure 6.7A shows the instantaneous sorption uptake of aniline in PEBA films with different thicknesses at room temperature. Obviously, it takes a longer period of time to reach sorption equilibrium for a thicker film. The diffusivity of aniline in PEBA film was calculated by fitting the sorption data to Equation (6.2), which yielded an average diffusivity value of 8.3×10^{-12} m²/s at 23°C. Note that an underlying assumption in Equation (6.2) is that the diffusivity is constant, independent of aniline concentration in the feed. This approximation is believed to be reasonable for aniline sorption in view of the low concentration levels investigated, which is also supported by the largely constant permeability observed in pervaporation. To confirm that the diffusivity so obtained was overall adequate to describe the sorption behavior, the experimental data was compared with the calculated data, as shown in Figure 6.7B, where the sorption uptake was plotted against \sqrt{t}/L . The good agreement between measured sorption uptake and the calculations (based on Equation (6.2)) indicates that the so-obtained diffusivity is applicable to describe the sorption behavior here. It is worth mentioning that the diffusivities of aniline in natural rubber and nitrile butadiene rubber at 25°C were 1.04×10^{-11} m²/s and 8.4×10^{-12} m²/s [68], respectively, and the aniline diffusivity in PEBA determined here was on the same magnitude. The work in Chapter 4 showed a PhOH diffusivity of 1.25×10^{-11} m²/s in PEBA (at 30°C), which is slightly higher than the aniline diffusivity (23°C). The phenol and aniline diffusivity data are comparable in view of the lower operating temperature in this study (i.e., 23°C) and the slightly larger molecular size of aniline than phenol [209].

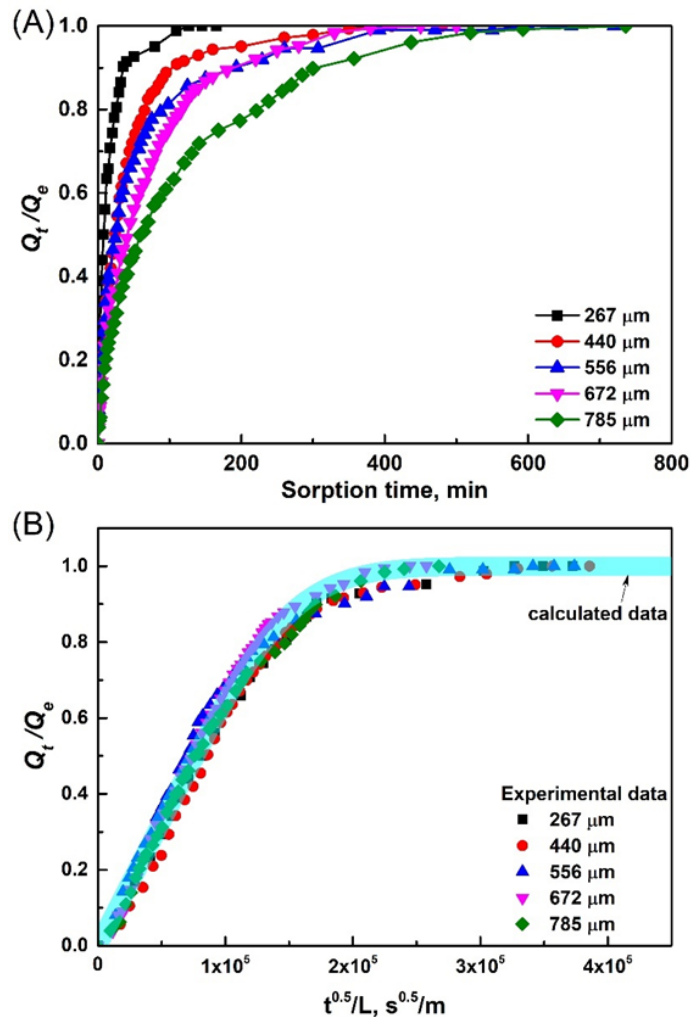


Figure 6.7 (A) Aniline sorption curves in PEBA membranes with different thicknesses at room temperature, and (B) a comparison of the experimental data of sorption uptake (represented by the symbols) and calculations (solid blue line) using Equation (6.2) with diffusivity value of $8.3 \times 10^{-12} \text{ m}^2/\text{s}$.

6.3.3 Liquid Diffusion/Permeation

Aniline permeability in PEBA was also determined using the permeation experiments (Figure 4.1), where an improved method combining the time lag and mass balance method was used [199]. In light of Equation (6.3), $F(t)$ versus t was plotted, as illustrated in Figure 6.8A for different aniline concentrations at 23°C. The membrane permeability to aniline (P' , in unit of m^2/s) was obtained from the slopes of the straight lines. The permeability is largely unaffected by aniline concentration under

the experimental conditions conducted, with an experimental error in the permeability measurements of within 6%. Figure 6.8B shows the measured permeability at different temperatures. Now that within the concentration range investigated, both the permeability and solubility (Figure 6.6B) of aniline in PEBA membrane are shown to be independent of concentration, it can thus be deduced that the diffusivity of aniline is also concentration independent. That is, the overall effect of membrane swelling and aniline clustering is not strong enough to cause considerable changes in aniline solubility, diffusivity and permeability within the accuracies of the experimental approaches. This is not unexpected in view of the following. At a molecular level, membrane swelling by the sorbate tends to increase the diffusivity and permeability in a swollen polymer matrix. However, at low concentration levels, significant membrane swelling is unlikely due to the low aniline sorption uptake in PEBA (Figure 6.6A). In addition, the effect of membrane swelling on aniline diffusion will be counterbalanced by aniline clustering. Consequently, a concentration independency of aniline diffusivity is observed.

The data presented in Figure 6.8B show that aniline permeability expressed in terms of P' (in units of m^2/s) increases with an increase in temperature. There is seemingly a contradiction to the permeability data (in customary units of Barrer) for pervaporative mass transfer shown in Figure 6.4A, where temperature showed a negative impact on membrane permeability. This is understandable in view of the physical meaning of the permeabilities presented in different units. As illustrated before, the permeability coefficient in pervaporation has accounted for the vapor-liquid equilibrium so that the transmembrane driving force can be represented conveniently using an equivalent vapor pressure difference, though pervaporation is not a sequential process of liquid evaporation and vapor permeation. The vapor-liquid equilibrium can be described by Henry's law, and the Henry's law constant [H , in units of $\text{Pa}/(\text{mol}\cdot\text{m}^{-3})$] increases with increasing temperature. In liquid permeation, the transmembrane driving force was represented by the liquid concentration difference across the membrane, and the resulting membrane permeability (P' , m^2/s) did not involve the vapor-liquid sorption equilibrium. Actually, the two permeabilities P' and P are consistent if the driving force would be expressed on an equivalent basis. As shown in Figure 6.8, though there was an increase in P' (in m^2/s) with an increase in temperature, once converted to the units of Barrer, a negative temperature dependency of permeability P was displayed (Figure 6.8C). It is clear that caution should be exercised when determining or characterizing membrane permeability based on different measurement approaches, and this is especially the case since membrane permeabilities expressed in units of m^2/s and Barrer are widely used in the literature without distinctions. It is shown in the present study that they can be reconciled by proper conversions.

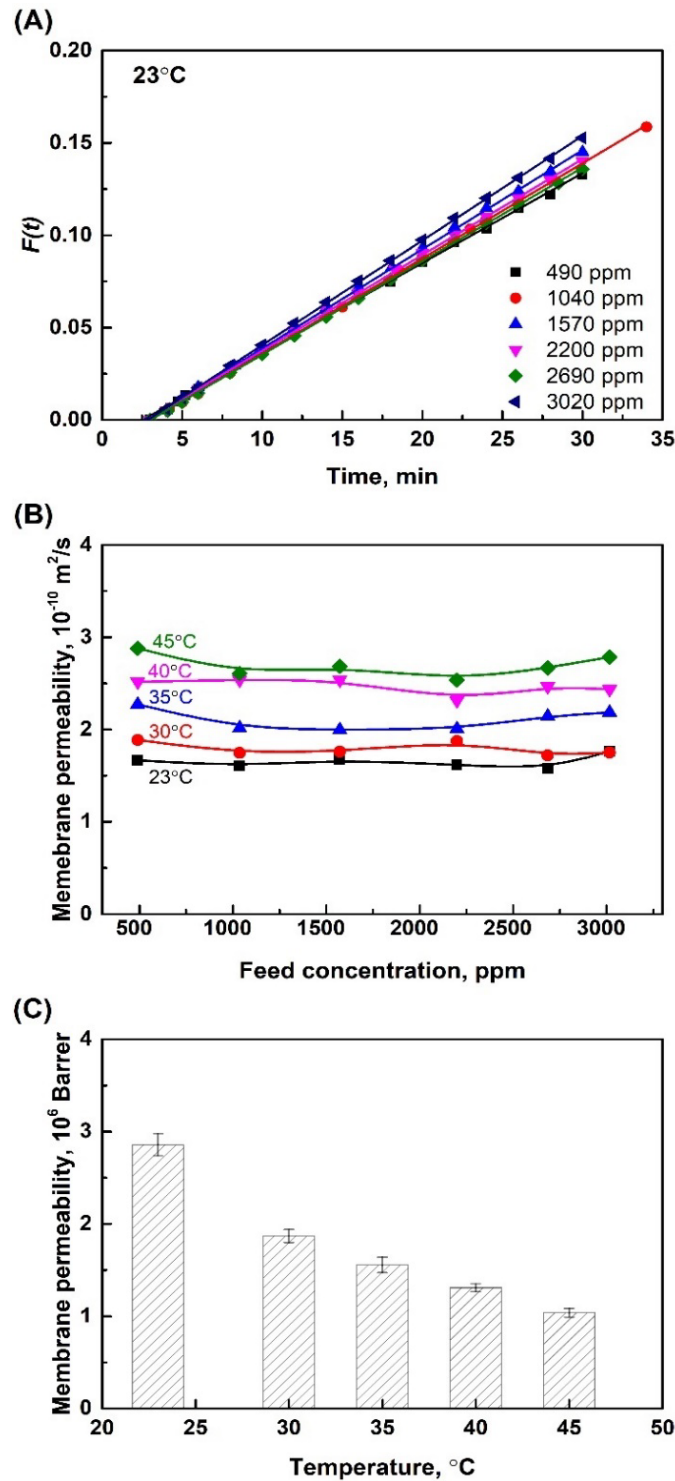


Figure 6.8 (A) The $F(t)$ versus t curve with different feed concentrations at 23°C , (B) Membrane permeability (P' , in units of m^2/s) at different temperatures, and (C) membrane permeability (P , in customary units of Barrer) at different temperatures.

6.3.4 Comparison of Membrane Permeabilities

As mentioned before, membrane permeabilities measured via different approaches may give different values, and it is thus helpful to compare these values in order to have a closer look into the essence of membrane permeability. Figure 6.9 shows the aniline permeabilities in PEBA membrane determined via three different methods: (1) the permeability measured from pervaporation experiments, (2) the permeability estimated as a product of solubility and diffusivity measured from sorption experiments, and (3) the permeability evaluated from the modified pseudo steady state liquid permeation. It was shown that the permeabilities obtained from the latter two methods [i.e., (2) and (3)] were comparable, and both were higher than that obtained from pervaporation. This is not surprising in consideration of the membrane states in determining the membrane permeability with these measurement techniques. When evaluating the solubility and diffusivity via sorption experiments, both sides of the membrane were in direct contact with the aqueous aniline solution, and thus the membrane is fully wet and swollen by the liquid. Under such circumstances, the permeating molecules will travel in the membrane at a rate to their full potential. Similar situation is also true in the liquid permeation experiments, except that the liquid boundary layer effect on the downstream side should be negligibly small so that the permeant will leave the membrane and enter the receptor chamber once reaching the downstream side of the membrane. Otherwise, the permeability will be underestimated because the concentration difference between the donor and receptor chambers is used as the driving force in the calculation. In pervaporation, however, the feed liquid solution was in direct contact with the upstream side of the membrane, while vacuum was applied to the other side to induce permeation. Thus, there was a decreasing “wetness” across the membrane from the feed side to the permeate side. As a result, in comparison to fully wet membranes, the membrane in pervaporation was less swollen overall, leading to a lower membrane permeability. The results in Chapter 5 also showed that the permeability of three phenolic compounds obtained from liquid permeation is much higher than obtained from pervaporation, consistent with the results here.

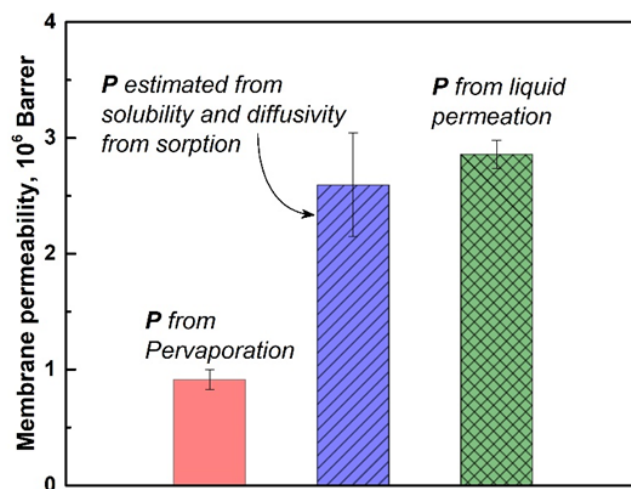


Figure 6.9 Comparison of aniline permeability determined via different approaches. Temperature: 23°C.

Following the same line of analysis, it is reasonable to suspect that the membrane would have even a lower permeability in vapor permeation than in pervaporation, and this is found indeed the case in prior studies reported in the literature [193-195, 210]. In vapor permeation, both sides of the membrane are in direct contact with the vapor phase, and the entire membrane is “drier” than in pervaporation, and thus a lower permeability is displayed. In a study to separate methanol/benzene azeotrope using plastic films, Binning et al. [193] observed that the permeation rate with liquid contacting the films was almost two-fold higher than that obtained when the feed charge is in the vapor phase at identical operating conditions. Using polyimide membranes to separate water-ethanol mixtures, Okamoto et al. [194] also reported a higher permeability of water and ethanol in pervaporation than in vapor permeation. In addition, the difference in the permeability between pervaporation and vapor permeation was found to be more significant for membranes having a higher sorption uptake in the liquid phase [194]. Similar observations were made by Teng et al. [195] in alcohol/water separation using a series of fluorine-containing polyamide membranes. As the membrane permeability to a certain compound depends on the state of the membrane, it can be conceived that the membrane permeability will follow a decreasing order that a “fully wet” membrane (i.e., in liquid permeation) > a “partially wet” membrane (i.e., in pervaporation) > a “dry” membrane (i.e., in vapor permeation). It is clear from the above

analysis that the membrane permeabilities measured under different operating modes cannot be compared directly without distinguishing the driving force for permeation and the state of the membrane.

6.3.5 Sorption-desorption Reversibility

The isotherms of aniline sorption in pristine and regenerated PEBA films over six sorption-desorption cycles are shown in Figure 6.10. All the data points fell in a single line, indicating that the sorption-desorption was reversible and that the sorption capacity remained the same. Aniline is a weak base and can react with HCl to form anilinium chloride, a salt soluble in aqueous solutions. This was the basis of using HCl to facilitate the desorption of aniline from PEBA in the experiments. The data in Figure 6.10 also serve as a confirmation of the good reusability of PEBA as a sorbent for aniline removal from water via sorption, followed by desorption to regenerate the sorbent for reuse. In addition, the sorption-desorption reversibility indicates that the sorption characteristics was not affected by prior sorption history that PBEA experienced in contacting the feed solutions, which is also important for removal of aniline from water by pervaporation operated under steady state to extract aniline continuously.

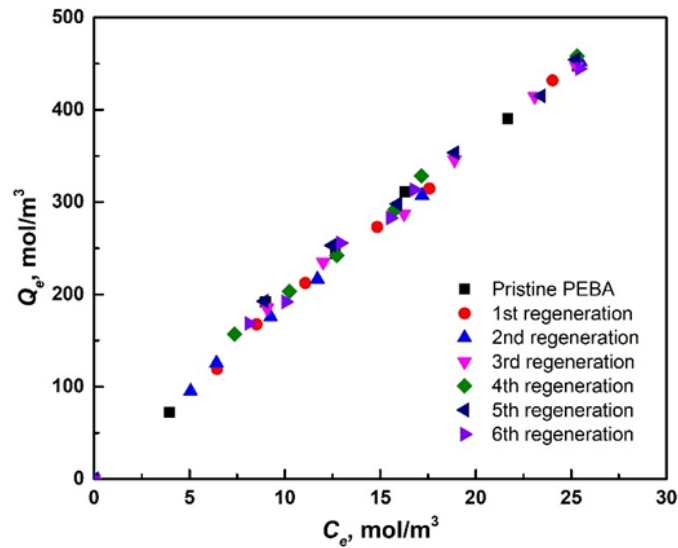


Figure 6.10 Sorption isotherms of aniline in PEBA at room temperature after regeneration with HCl.

6.4 Summary

The solubility, diffusivity, and permeability of aniline in PEBA pertaining to aniline removal from water via pervaporation and sorption were investigated, with an emphasis on the fundamental understanding of membrane permeability determined via three different approaches: (1) pervaporation experiments, (2) sorption experiments, and (3) direct measurements from pseudo steady state liquid permeation experiments. The following conclusions may be drawn:

- (1) The membrane exhibited excellent permselectivity for aniline extraction via pervaporation due to the high solubility selectivity to aniline.
- (2) Over a wide range of operating conditions, aniline was enriched in the permeate to an extent way beyond its solubility limit, and the overall separation was significantly augmented by phase separation.
- (3) Based on sorption kinetics data, the diffusivity of aniline in the membrane was determined to be $8.3 \times 10^{-12} \text{ m}^2/\text{s}$ at 23°C ; the permeability of aniline in pervaporation from 23°C to 60°C was on the order of 10^5 Barrer.
- (4) It was demonstrated that caution should be exercised when determining or characterizing the membrane permeability based on different measurement techniques, which was largely overlooked in prior studies, and proper unit conversions were needed for reconciliation.
- (5) PEBA showed good reusability as a sorbent for aniline removal from water by sorption, and the sorption-desorption reversibility was also relevant to pervaporative separation of aniline operated under steady state.

Chapter 7

Incorporation of ZIF-71 into PEBA to form Mixed Matrix Membranes (MMMs) for Separation of Phenol (PhOH) and Aniline from Aqueous Solutions by Pervaporation

7.1 Introduction

As demonstrated in previous chapters, PEBA can effectively separate phenols and aniline from aqueous solutions by pervaporation. Nonetheless, the water content in the permeate is still significant because of the large driving force for water permeation and the small size of water molecules, which represents another opportunity for improvement in membrane permselectivity. To further improve the membrane performance, mixed matrix membranes (MMMs) can be exploited by incorporating certain hydrophobic fillers into the polymer matrix to increase the hydrophobicity of the membrane to inhibit water permeation. It was reported that the incorporation of COF-300 [98], ZIF-8 [49], and ZIF-71 [118] into polymer membranes can significantly push up the trade-off between permeability and selectivity, thereby improving the separation performance of the membrane.

Among the numerous fillers, zeolite imidazole frameworks (ZIFs) with three-dimensional structures connected by metal centers and organic imidazolate linkers have received enormous attention as a promising material for separation and sorption due to their porosity, high thermal and chemical stability, and inherent hydrophobicity if the imidazolate linkers do not contain hydrophilic functionalities [211, 212]. The flexible nature of the ligands within the ZIFs allows for the sorption of sorbates much larger than the crystallographic diameter in the framework [213]. Moreover, the organic nature of the ZIFs framework could achieve good interfacial interaction between ZIFs and the polymer matrix, avoiding incompatibility problems.

Zeolitic imidazolate framework-71 (ZIF-71), which has a pore window size of 0.48 nm and a large cavity size of 1.68 nm, is very hydrophobic [214, 215], and it has been widely used in adsorption and membrane separation applications. Dong et al. [96] synthesized an organophilic ZIF-71 membrane and it shows good performance for methanol/water and ethanol/water separations, as well as dimethyl carbonate/methanol separation due to the preferential sorption of dimethyl carbonate. Li et al. [114] prepared a ZIF-71 incorporated PDMS membrane for the separation of methanol, ethanol, isopropanol, and sec-butanol from aqueous solutions, and the separation factor was almost doubled compared with the unfilled PDMS membrane. Yin et al. [116] also found enhanced 1-butanol/water and ethanol/water

separation performance when a PDMS membrane was incorporated with ZIF-71. All these motivated us to look into ZIF-71 as an excellent candidate to enhance the separation performance of the PEBA-based membrane for extracting phenols and aniline from aqueous solutions. However, to date, the majority of current ZIF-incorporated MMMs are mainly used for the recovery of alcohols via pervaporation, and there are few studies on the separation of phenols and aniline.

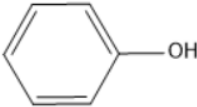
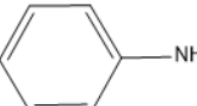
Previous chapters dealt with the separation of phenols and aniline independently, and no direct comparison between phenols and aniline was made. It is necessary to investigate how the amino group and the hydroxyl group would affect the mass transfer of the permeating molecules within the membrane directly. Therefore, in this chapter, the separation of phenol (PhOH) and aniline from their aqueous solutions by pervaporation was investigated using MMMs fabricated by incorporating ZIF-71 particles into PEBA membranes. Both compounds are the simplest aromatic compounds with a single functional group (-OH and -NH₂) on the benzene ring, and this allows for easy comparisons of the effects of the physicochemical properties on pervaporation behavior. The detailed information of these two aromatics were shown in Table 7.1. The membrane morphology, contact angle, permeation flux, and enrichment factors were investigated to understand the effects of ZIF-71 on the membrane performance. For convenience, in this chapter, the word “phenol” is used to represent the specific phenolic compound, PhOH.

7.2 Experimental

7.2.1 Materials

Zinc acetate dihydrate ($\geq 99.9\%$) was purchased from Fisher Chemical. 4,5-dichloroimidazole (dcIm) (98%) was purchased from Alfa Aesar. Methanol ($\geq 99.9\%$) and chloroform ($\geq 99.8\%$, amylene stabilized) were purchased from Sigma Aldrich. All reagents were used as received. All other chemicals and materials were the same as those described previously.

Table 7.1 Physical and chemical properties of phenol and aniline.

Compound	Chemical structure	Molar mass, g/mol	Molar Volume, cm ³ /mol [209]	λ_{\max} , nm	Solubility in water at 20°C	Boiling point under atmospheric pressure, °C
Phenol		94.11	87.8	269	8.3 g/100 mL	181.7
Aniline		93.13	91.7	280	3.6 g/100 mL	184.1

7.2.2 Synthesis of ZIF-71 Crystals

The ZIF-71 crystals were prepared via the method proposed by Lively et al. [215]. A solution of zinc acetate (0.879 g, 4 mmol) in 150 ml of methanol was rapidly poured into a solution of dcIm (2.198 g, 16 mmol) in 150 ml of methanol under stirring. The mixture turned turbid immediately. After stirring at room temperature for 24 h, the mixture was separated. The crystals were washed with methanol for three times, then soaked in chloroform for two days (2×100 ml). The crystals were finally recovered and dried under vacuum at 80°C for 36 h to remove any of the remaining solvents.

7.2.3 Membrane Preparation

Pre-determined amounts of ZIF-71 crystals were dispersed in DMAc, and the mixtures were sonicated for 1 h for even dispersion. Then certain amounts of PEBA pellets were dissolved in the above DMAc/ZIF-71 mixtures (PEBA:DMAc = 15:85). The mixture was placed in water bath at 80°C with stirring for 24 h to form a well-mixed PEBA/ZIF-71/DMAc mixture. Thereafter, the mixture was cast onto a hot glass plate (70°C), followed by solvent evaporation in an oven at 70°C for 2 days. The membranes were finally detached from the glass plate. A PEBA membrane containing no ZIF-71 was also prepared for comparison.

7.2.4 Membrane Characterization

The surface hydrophobicity of the pure PEBA membrane and the MMMs with different ZIF-71 loadings was evaluated with the static contact angle measurements using a contact angle meter (Camplus Micro, Tantec Inc.). An average value of at least ten measurements taken at different spots of the

membrane surface was reported for each membrane. The crystal structure of ZIF-71 and the membranes were characterized by X-ray diffraction (XRD, Rigaku MiniFlex II) in the range of 5-50° with an increment of 0.05° at room temperature. Fourier Transform Infrared spectrometry (FTIR) of ZIF-71 powder and the membranes was recorded via an FTIR spectrometer (Nicolet Nexus™) to analyze the chemical structures of ZIF-71 (KBr test: compacted powder tablet with 1% ZIF-71 and 99% KBr) and the membranes (ATR mode, Attenuated Total Reflectance, ZnSe 45°). All samples were dried at 60°C for 2 days prior to XRD and FTIR tests. The surface and cross-sectional morphologies of pure PEBA membrane and ZIF-71/PEBA MMMs were characterized using a scanning electron microscopy (SEM, Zeiss Ultra). The associated energy dispersive X-ray spectroscopy (EDX) was used to analyze the distribution of the ZIF-71 crystals in the PEBA matrix. The morphology of ZIF-71 crystals was characterized using Quanta FEG 250 SEM.

7.2.5 Pervaporation Experiments

Pervaporation experiments were conducted as described in Chapter 3. The saturated vapor pressure and activity coefficient of phenol and aniline in the feed were estimated using Aspen Plus based the UNIQUAC model and UNIFAC model, respectively.

7.2.6 Sorption Experiments

Sorption experiments were performed as described in section 5.3.3. In brief, certain weights of dry membranes with different ZIF loadings were immersed into aqueous phenol solutions or aniline solutions over a given range of concentrations at room temperature for 3 days to reach sorption equilibrium (preliminary experiments had shown that 3 days were more than enough to reach sorption equilibrium, thereafter the feed concentrations did not change with time anymore). The concentrations in the solution at time zero and at sorption equilibrium were measured, and the sorption uptake was calculated using Equation (5.4). Sorption of pure PEBA membrane was also evaluated for comparison.

7.3 Results and Discussion

7.3.1 Membrane Characterization

The FTIR-ATR spectra of PEBA, ZIF-71, and ZIF-71/PEBA MMMs are shown in Figure 7.1. For ZIF-71, the peak at 665 cm⁻¹ is assigned to the 4,5-dichloroimidazole; the peak at 1053 cm⁻¹ is attributed to the N=C-N stretching vibrations in the imidazole ring [118, 216]. For PEBA membrane, the strong peak at 1110 cm⁻¹ is attributed to the C-O-C stretching in the polyether segment, the band at 2920 cm⁻¹ is assigned to the acyclic CH₂ stretching in both the polyether and polyamide segment [216]. The band

at 1637 cm^{-1} is attributed to the O=C-N-H group in the PEBA backbone [118]. For the ZIF-71/PEBA MMMs, the FTIR spectrum for both PEBA and ZIF-71 can be observed, indicating successful incorporation of ZIF-71 into PEBA matrix. In addition, the intensity of the bands at 665 cm^{-1} and 1053 cm^{-1} increases with an increase in the ZIF-71 loading. There were no noticeable shifts in the bands nor new bands observed for the ZIF-71 filled MMMs.

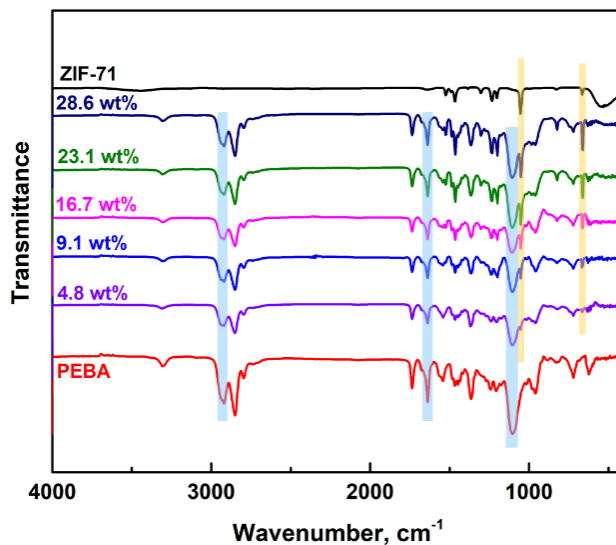


Figure 7.1 FTIR spectra of ZIF-71 crystals, pure PEBA membrane, and ZIF-71/PEBA MMMs.

The X-ray diffraction patterns of ZIF-71, pure PEBA membrane, and ZIF-71/PEBA MMMs are presented in Figure 7.2. The XRD pattern of the ZIF-71 prepared in this work is crystalline, and it matches well with the reference XRD pattern of ZIF-71. The characteristic peak at about $2\theta = 7.6^\circ$ is observed for both the reference ZIF-71 and the ZIF-71 prepared in the present work [96]. The broad peak of the pure PEBA membrane indicates that PEBA is amorphous at room temperature. The XRD patterns of the ZIF-71/PEBA MMMs confirmed successful incorporation of ZIF-71 into PEBA. No apparent shifts of the peaks in the XRD pattern of the ZIF-71/PEBA MMMs were observed, suggesting that there were no chemical interactions between ZIF-71 and PEBA, and the structure of ZIF-71 crystals was well-preserved in the polymer matrix.

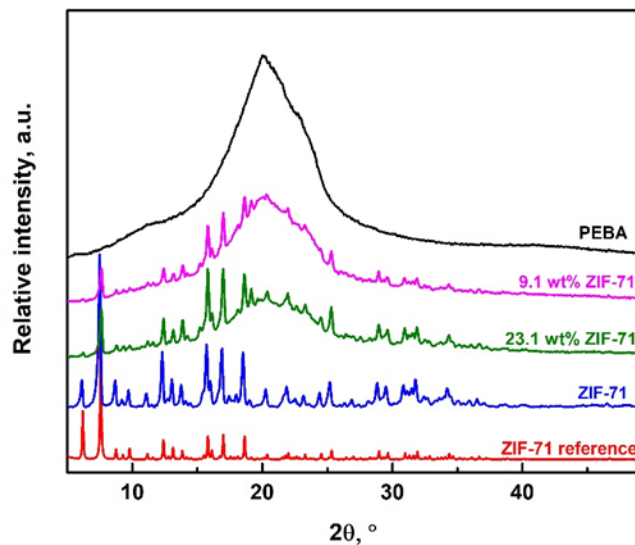


Figure 7.2 X-ray diffraction pattern of ZIF-71 crystals, pure PEBA membrane, and ZIF-71/PEBA MMMs with a ZIF-71 loading of 9.1 wt% and 23.1 wt%, respectively. The XRD pattern of ZIF-71 reference is generated from the crystallographic information file obtained from the Cambridge Crystallographic Data Center (CCDC code: GITVIP).

Figure 7.3 shows the chemical diagram of ZIF-71, the 3D model of ZIF-71, and the SEM morphology of the ZIF-71 crystals. As shown in Figure 7.3A and B, ZIF-71 is constructed by linking four-coordinated zinc through imidazolate units to form an extended framework. The ZIF-71 crystals are cubic-shaped, with a particle size of approx. 1 μm , as shown in Figure 7.3C.

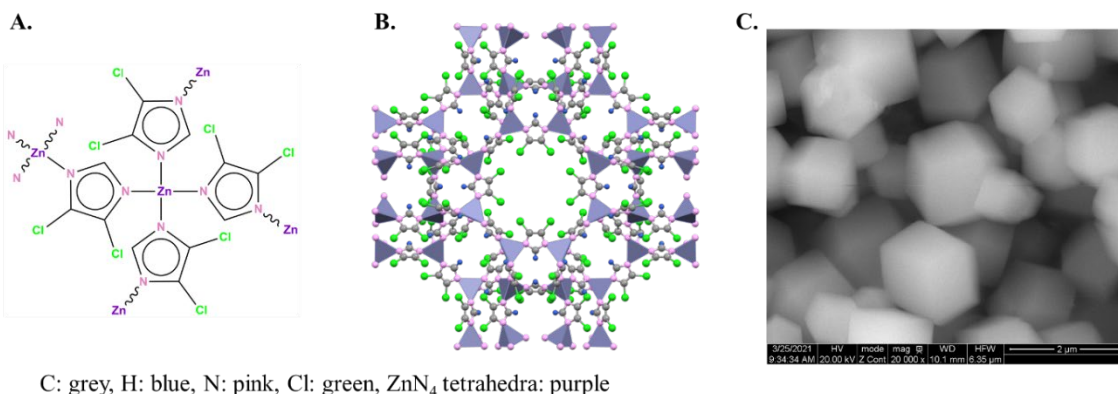


Figure 7.3 (A) The chemical diagram of the ZIF-71, (B) the 3D structure of ZIF-71 crystals generated from the crystallographic information file obtained from the Cambridge Crystallographic Data Center (CCDC code: GITVIP), and (C) the SEM image of ZIF-71 crystals.

Figure 7.4 shows the morphology of the pure PEBA membrane and the MMMs with different ZIF-71 loadings. For pure PEBA membrane, both the surface and cross-sectional images show that the dense polymeric membrane is uniform and defect-free. For ZIF-71 incorporated MMMs, with an increase in ZIF-71 loading from 0 to 28.6wt%, more and more cubic ZIF-71 crystals can be found clearly within the membrane matrix, and no interfacial voids or defects were observed. It should be mentioned that a further increase in ZIF-71 loading over 28.6wt% will make it difficult to form defect-free membranes. To further evaluate the distribution of the ZIF-71 crystals in the membrane, an EDX analysis was conducted, and the results are shown in Figure 7.5. The signals of zinc and chloride come exclusively from ZIF-71 crystals, suggesting successful incorporation of ZIF-71 crystals into the PEBA membrane. The well-distributed zinc and chloride signals in the EDX map confirm the even dispersion of ZIF-71 crystals in the membrane, which can also be verified by the SEM images of the MMMs.

For the separation of organic compounds from water streams by pervaporation, the preferential sorption of the organics is crucial as water molecules with a small molecular size will have a large diffusivity in the membrane. The water contact angle measurements for pure PEBA membrane and MMMs with different ZIF-71 loadings were therefore conducted to quantify the hydrophobicity of the mixed matrix membranes, as shown in Figure 7.6. As expected, the water contact angle increased with an increase in ZIF-71 loading, suggesting that the MMMs incorporated with ZIF-71 were more hydrophobic than the pure PEBA membrane due to the hydrophobic nature of ZIF-71. It should be mentioned that it is difficult to measure the contact angle with pure ZIF-71 crystals in the form of powders; however, the variations in the contact angle of the MMMs with different ZIF-71 loadings suggest that ZIF-71 is very hydrophobic, consistent with the reported results [214, 217]. In addition, as can be seen from Figure 7.4A, the membrane surface roughness increased with an increase in the ZIF-71 loading in the MMMs, and this also leads to an increased water contact angle. It should be mentioned that the water contact angle of pure PEBA membrane is approx. 83°, indicating PEBA itself is hydrophobic and has a good affinity towards some hydrophobic organic compounds.

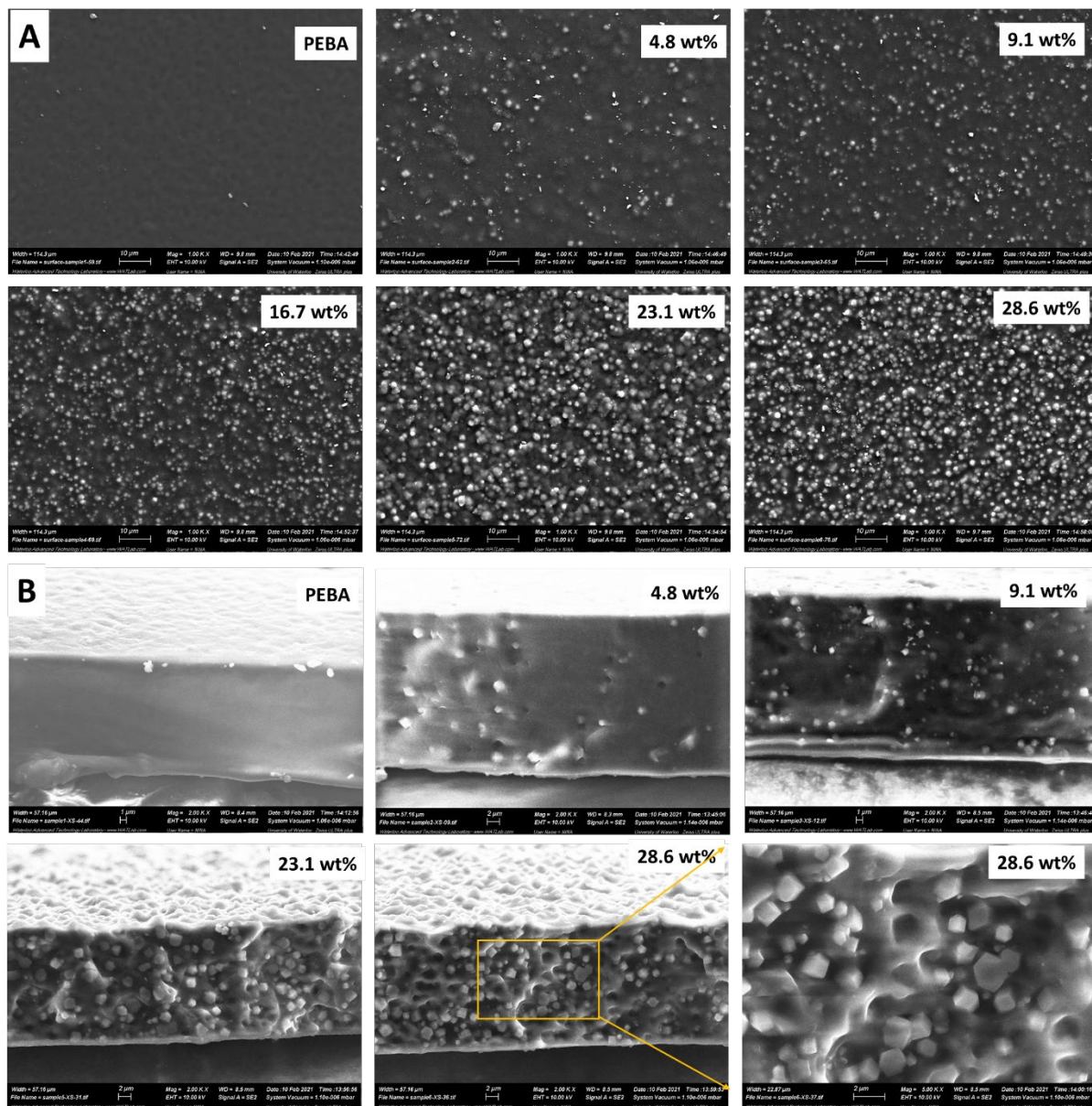


Figure 7.4 (A) Surface SEM images (magnification $\times 1000$) and (B) cross-sectional SEM images (magnification $\times 2000$; a zoomed-in image for 28.6wt% ZIF-71/PEBA MMMs is magnified by 5000) of pure PEBA membrane and MMMs. The numbers in the Figure represent the different ZIF-71 loadings in the MMMs.

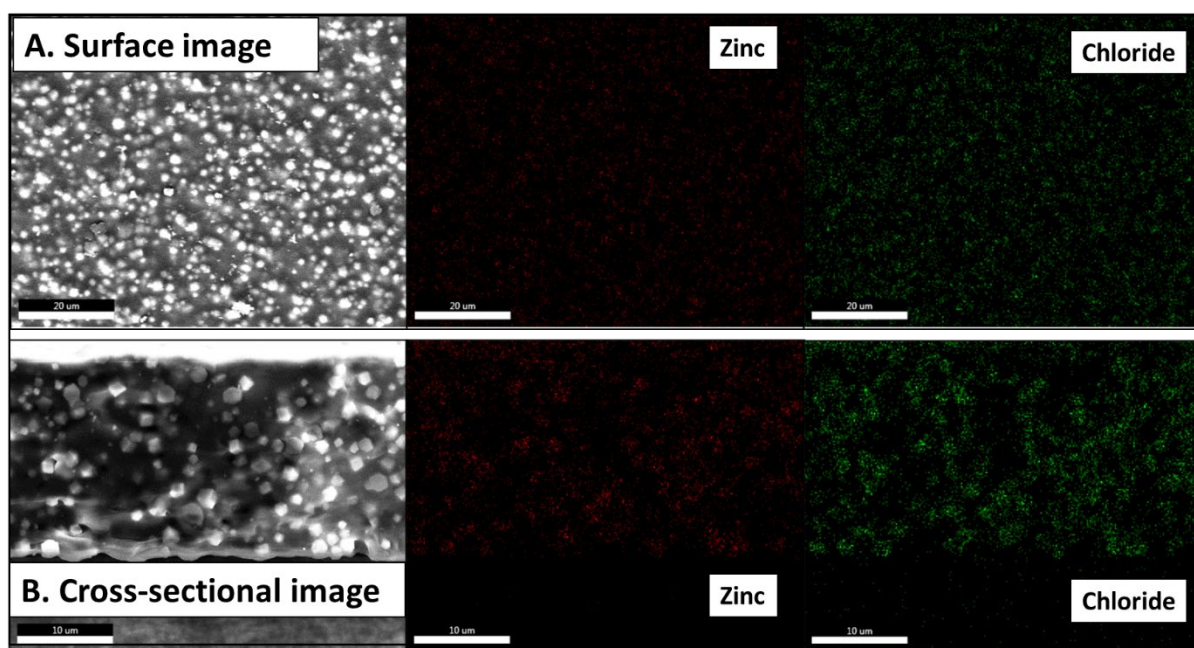


Figure 7.5 (A) Surface EDX mapping (magnification $\times 1000$) and (B) cross-sectional EDX mapping (magnification $\times 2000$) for membrane with a ZIF-71 loading of 28.6 wt%.

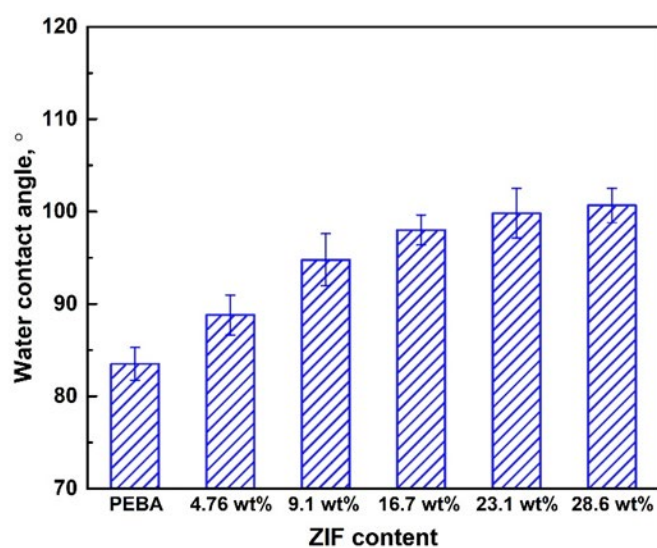


Figure 7.6 Water contact angle of pure PEBA membrane (No ZIF-71 crystals) and MMMs with different ZIF-71 loadings.

7.4 Pervaporation Performance

Figure 7.7 shows the effects of ZIF-71 content in the MMMs on the total permeation flux for the pervaporative separation of phenol and aniline from their aqueous solutions. The total permeation fluxes of phenol solution and aniline solution decreased with an increase in ZIF-71 loading in the membrane, and such a decrease comes predominantly from the decreased water flux (Figure 7.8). The significantly reduced water flux can be explained as follows. First, the solubility of water in the MMMs was decreased significantly. Due to the hydrophobic nature of ZIF-71, the hydrophobicity of the MMMs increased as ZIF-71 loading increased (Figure 7.6), thus the sorption uptake of water in the membrane was decreased. The experimental results showed that water sorption uptake at room temperature decreased from approx. 7.8 mg per gram membrane to 1 mg per gram membrane when increasing the ZIF-71 loading in the MMMs from 0 to 28.6wt%. On the other hand, the diffusivity of water in the MMMs was also inhibited. The incorporation of the crystals in the polymer membrane can alter the chain packing of the polymer and thus the free volume of the membrane. Liu et al. [119] found the fractional free volume of a PDMS membrane filled with crystalline calixarene and calixarene derivative (filler contents varying from 1wt% to 10wt%) is lower than the pure PDMS membrane, and the permeation flux showed the same trend with the variations of the free volume. In addition, the presence of ZIF-71 crystals could hinder the torsional motions of the polymer chain segments and constrain the mobility of the chain segments, leading to a reduced diffusivity within the polymer matrix. This is supported by the fact that the diffusion coefficient of a permeant in nanoscale polymer layers supported on a substrate is smaller than the diffusion coefficient in thicker films as the polymer chains are hindered to access all conformational states in the presence of a substrate [218]. As a result, both the solubility and diffusivity of water were reduced by the incorporation of ZIF-71 crystals, leading to a decreased water flux with an increase in the ZIF-71 loading. Similar phenomena were also observed in other studies [107, 108, 115]. For example, Liu et al. [107] found that for the separation of ethanol/water mixtures, the total flux declined with an increase in the zeolite loading of the surface-modified ZSM-5 filled PDMS membranes, and they thought this might be attributed to the increased transport resistance or the alteration of the PDMS network due to incorporation of ZSM-5. Wu et al. [115] found the permeation flux of COF-LZU1/PEBA MMMs was lower than pure PEBA membrane. In addition, it should be noted that the continuous decrease in water flux with increasing ZIF-71 loading up to 28.6wt% indicates that there are no defects/interfacial voids between the crystals and the polymer. Though there are no chemical interactions between the ZIF-71 crystals and the polymer matrix, the

hydrogen bonding between the -NH groups on the surface of the ZIF-71 crystal and the polyamide segment in PEBA is considered to contribute to such good compatibility.

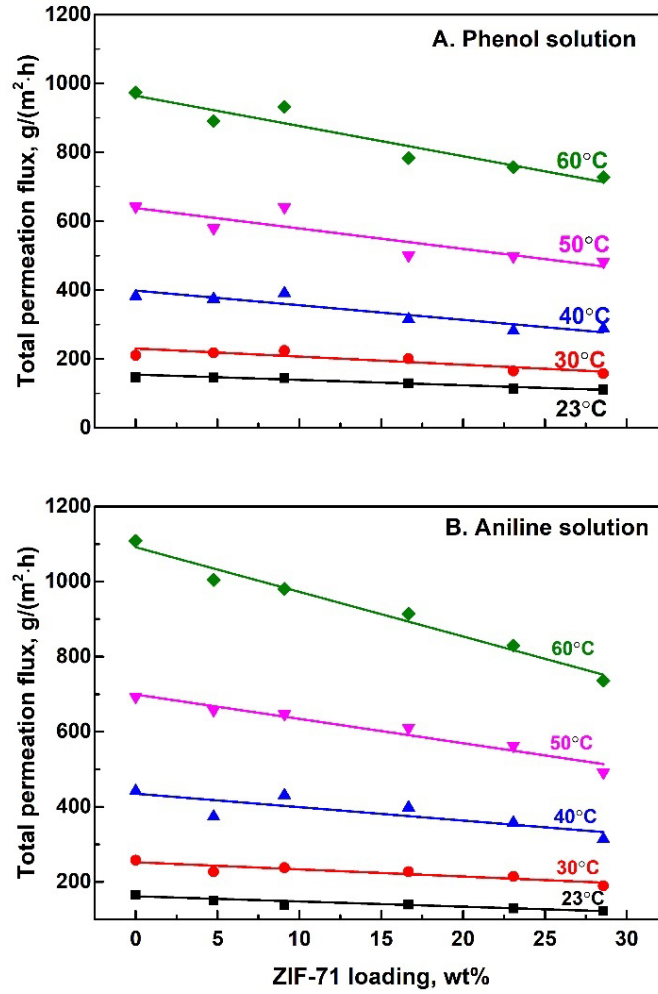


Figure 7.7 Effects of ZIF-71 loading in MMMs on the total permeation flux for (A) phenol solution and (B) aniline solution at different temperatures. Feed concentration: 6000 ppm.

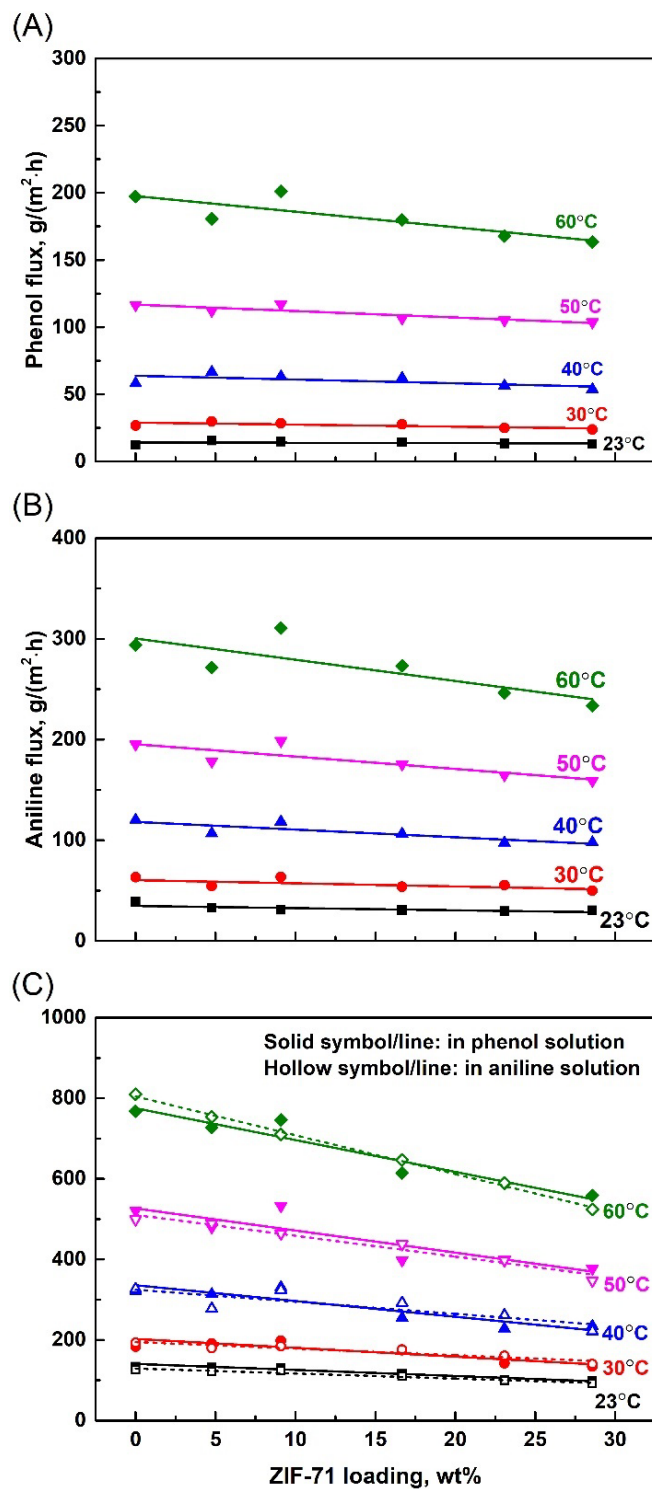


Figure 7.8 Effects of ZIF-71 loading in MMMs on the permeation flux of (A) phenol, (B) aniline, and (C) water in phenol solution (solid symbols/lines) and in aniline solution (open symbols, dash lines) at various temperatures. Feed concentration: 6000 ppm.

As shown in Figure 7.8, the permeation fluxes of phenol and aniline decreased slightly with an increase in ZIF-71 loading in the membrane, while water flux decreased much more significantly. To further understand the effects of ZIF-71 on the intrinsic membrane property, the permeation fluxes were normalized by the driving force and membrane thickness, and the resulting membrane permeabilities are shown in Figure 7.9. The permeabilities of phenol were largely unaffected by the presence of ZIF-71 in the membrane, while aniline permeability decreased slightly with an increase in ZIF-71 loading in the MMMs. Nonetheless, water permeability decreased much more significantly with an increase in the ZIF-71 loading in the MMMs. As mentioned before, both the solubility and diffusivity of water in MMMs were decreased by the presence of ZIF-71 particles in the membrane due to increased membrane hydrophobicity and decreased free volume and flexibility of the polymer. However, for the two aromatics, ZIF-71 shows different effects on their permeability, and this will be explained in detail in the following.

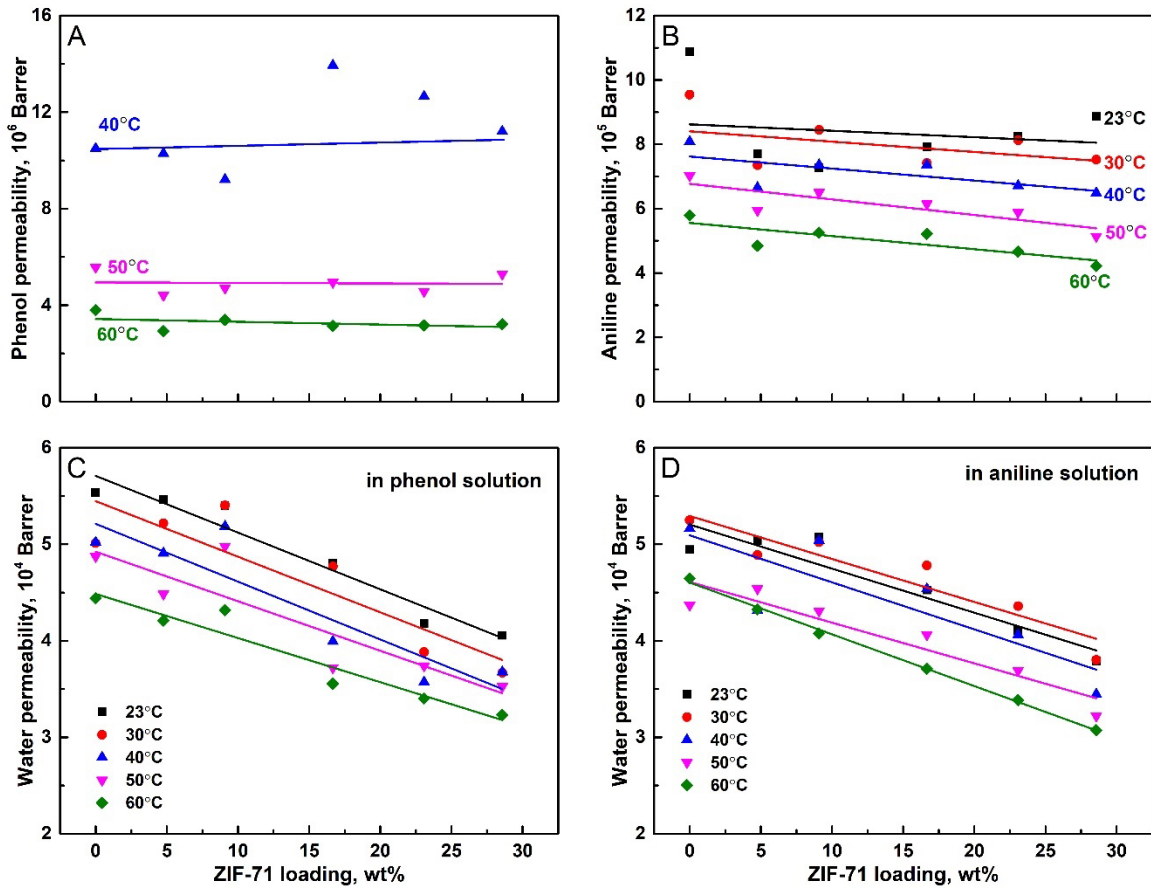


Figure 7.9 Effects of ZIF-71 loading on the permeability coefficient of (A) phenol, (B) aniline, and (C) water in phenol solution and (D) water in aniline solution in the MMMs.

As shown in Figure 7.10, the sorption uptake of phenol and aniline in MMMs decreased with an increase in the ZIF-71 content in the MMMs, and this trend was more obvious for phenol sorption. The sorption in the MMMs is a sum of the sorption in the ZIF crystals (crystal region) and the sorption in the polymer matrix. Due to the hydrophobic nature of ZIF-71 and the flexible nature of the ligands within the ZIF-71, ZIF-71 has a high sorption uptake towards phenol and aniline, and it is expected the ZIF-71 crystals within the MMMs will serve as a reservoir for hydrophobic solute sorption. However, the solute sorption in the polymer phase of the MMMs is decreased when ZIF-71 crystals are incorporated into PEBA. As mentioned before, the incorporation of the ZIF crystals in polymer membranes can alter the free volume of the membrane and decrease polymer chain flexibility, and such a change in polymer property will decrease solute sorption uptake in the polymer matrix. As a result, though ZIF-71 crystals have high sorption capacity towards phenol, the overall sorption uptake in the MMMs decreases with increasing ZIF-71 content due to the significantly lowered sorption uptake in the polymer phase. Similar results have also been reported previously. For example, Basu et al. [219] measured the sorption of toluene and isopropanol in several MOF-filled PDMS membranes, and it was shown that the sorption of toluene and isopropanol decreased with increasing the filler loading. Li et al. [114] studied the sorption of alcohols in PDMS membranes filled with ZIF-71, and they found that introducing ZIF-71 into PDMS membrane would increase the sorption uptake of methanol and ethanol, which had a low sorption uptake in pure PDMS membrane. On the other hand, PDMS has a high sorption capacity for isopropanol and sec-butanol, and their sorption uptake in the MMMs had no considerable change with an increase in ZIF-71 loading in the MMMs. For components with a high sorption uptake within the polymer, the reduction in the polymer free volume and polymer chain flexibility in the MMMs would lead to a significant solubility loss in the polymer matrix, and the decrease in the solubility cannot be compensated by the sorption increment due to the hydrophobic fillers, and this is indeed the case here for phenol sorption, where the overall sorption uptake of phenol in the MMMs decreased with an increase in ZIF-71 loadings. For aniline, the sorption uptake in PEBA was less than phenol, and thus the sorption reduction in polymer phase caused by the incorporation of ZIF crystals was less significant than that of phenol. As a result, aniline sorption uptake did not show a clear trend with the ZIF-71 loadings in the MMMs.

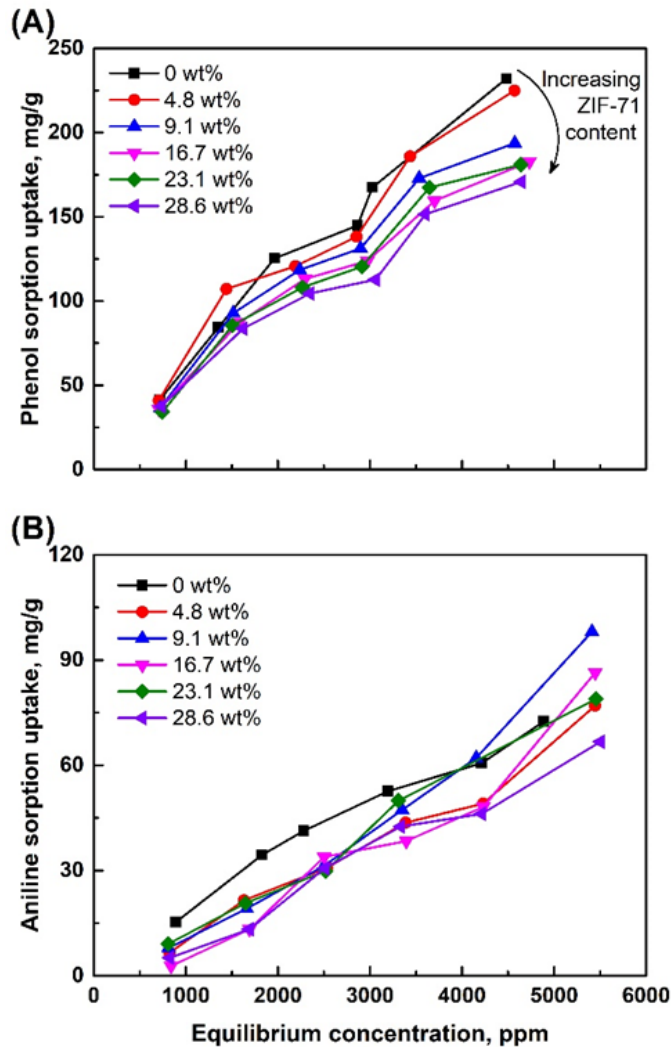


Figure 7.10 Sorption isotherms of (A) phenol and (B) aniline in MMMs at room temperature.

Similar to the solubility, the incorporation of ZIF-71 crystals also shows opposing effects on the membrane diffusivity. In the MMMs, the permeating molecules can penetrate the membrane through the dense polymer matrix and through the ZIF-71 channels. Compared with the dimensions of the free volume elements (typically less than 5-10 Å) of the typically “solution-diffusion” manipulated mass transport processes in dense polymer membranes, the mass transfer passageway within the ZIF-71 crystals is larger (cage size of 1.68 nm and window size of 0.48 nm). Though the molecular dimension of phenol and aniline is larger than the window size of ZIF-71, the “gate opening” effect due to the swing effect of the imidazolate linker allows the diffusion of phenol and aniline within ZIF-71 crystals [220, 221]. Thus, ZIF-71 can act as a highly permeable region to the permeant. However, for the dense

polymeric region, where the mass transports of the permeants are governed by the “solution-diffusion” mechanism, the incorporation of ZIF-71 crystals constrains the polymer chain flexibility and thus decreases the diffusivity of the permeants within the polymeric phase. In addition, the presence of the ZIF-71 particles makes the solution-diffusion passageway in the polymer region more tortuous. Therefore, the diffusivity increment in ZIF-71 regions is compromised by the diffusivity reduction in the polymer phase. In view of the largely constant phenol permeability (Figure 7.9A) and the decreased solubility (Figure 7.10A), it can be speculated that the overall diffusivity of phenol in the MMMs is enhanced. The diffusivity of aniline within the ZIF-71 channels is expected to be lower than that of phenol based on their molecular sizes, and the incorporation of ZIF-71 thus showed less significant improvement on aniline diffusivity. In view of the decreased solubility (Figure 7.10B) and less enhanced diffusivity of aniline in the MMMs, it is not unexpected that aniline permeability decreased slightly with an increase in the ZIF-71 loading in the membranes (Figure 7.9B).

As shown in Figure 7.9, the permeability of phenol was higher than that of aniline, however, the permeation flux of phenol was lower than aniline under the same operating conditions (Figure 7.8). This is because the transmembrane driving force for aniline permeation was much higher than that for phenol. As shown in Figure 7.11, the partial vapor pressure of aniline in equilibrium with the feed liquid is several-times higher than that of phenol, leading to a larger driving force and a higher permeation flux for aniline permeation. These results also demonstrate that pervaporation is more efficient to remove high volatility components.

Figure 7.12 shows the effects of ZIF-71 loading in the MMMs on the enrichment factor at 60°C. As expected, due to the significantly reduced water permeation flux, the enrichment factor for both phenol and aniline increased with an increase in ZIF-71 loading. From an energy consumption point of view, the incorporation of ZIF-71 crystals reduces the permeate throughput significantly due to reduced water flux, and thus reduces the heat required for the vaporization of the permeants in pervaporation. Furthermore, the use of the ZIF-71 filled MMMs resulted in a much higher solute concentration in the permeate, making it easier for subsequent further purification of the permeate stream, i.e., purification of phenol or aniline for solute recycling.

The pervaporation performance of the ZIF-71 incorporated MMMs was compared with other membranes reported in the literature, as shown in Table 7.2. It is difficult to make direct comparison as the operating conditions are not always identical. For phenol separation, the 28.6wt% ZIF-71/PEBA2533 MMMs outperformed other membranes previously reported in terms of both the separation factor and phenol flux except for the 10wt% ZIF-8/PEBA 2533 MMM reported by Ding et

al. [49]. Similar conclusion can also be found for the separation of aniline from water solutions using the 28.6wt% ZIF-71/PEBA2533 MMMs.

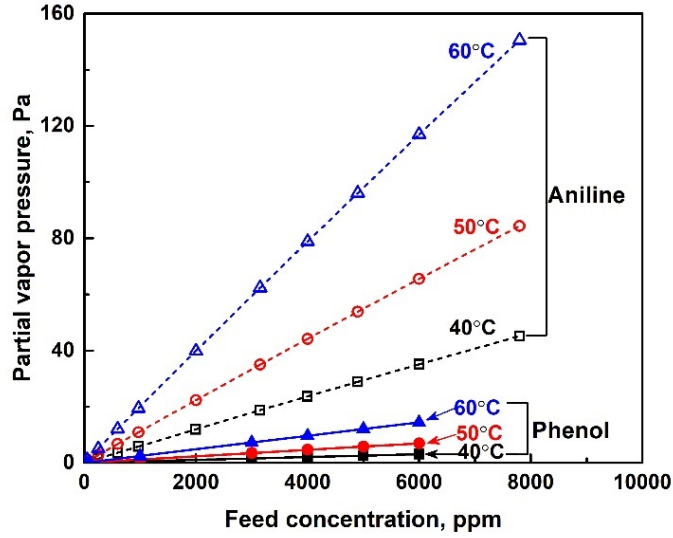


Figure 7.11 The partial vapor pressure of phenol and aniline in equilibrium with their corresponding feed solutions at various temperatures, calculated using Aspen Plus V10 based on UNIQUAC model and UNIFAC model, respectively.

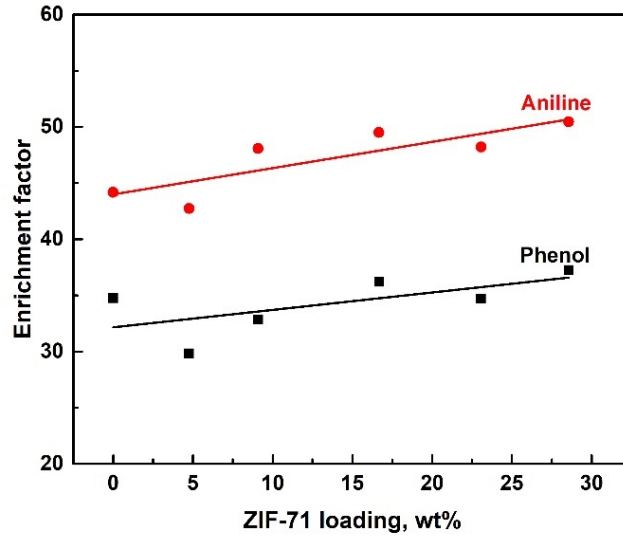


Figure 7.12 Effects of ZIF-71 loading in the MMMs on the enrichment factor of phenol and aniline at 60°C.

Table 7.2 Comparison of the separation of phenol/water mixtures and aniline/water mixtures by pervaporation using different membranes.

Membrane	Feed conc., wt. %	Temp., °C	Permeate pressure, mbar	Effective thickness, μm	Total flux, $\text{g}/(\text{m}^2 \cdot \text{h})$	Solute flux, $\text{g}/(\text{m}^2 \cdot \text{h})$	Separation factor	Ref.
<i>Phenol</i>								
Polydimethylsiloxane (PDMS)	2	70	≤ 2	50	371	70.8	11.6	[33]
PERVAP-1070 (ZSM-5 filled PDMS)	0.65	60	≤ 1	10	258	18	11.5	[37]
Polyurethane (PU)	1	60	3.3	19	550	73	15	[45]
Polyurethaneurea (PUU)	3	60	6.7	150	6.7	4.6	71	[222]
PEBA (GKSS, unknown grade)	0.7	60	≤ 1	80	188	38	36	[37]
10wt% ZIF-8/PEBA 2533	0.8	70	2.8	50	1310	390	53	[49]
PEBA 2533	0.6	60	0.4	25	946	200	45	This work
28.6wt% ZIF-71/PEBA2533 MMMs	0.6	60	0.4	25	730	170	50	This work
<i>Aniline</i>								
PU	0.612	70	5	Unknown	488	29	10.1	[52]
PDMS composite membrane	1.86	80	30	1	8100	500	3.6	[51]
Polybutadiene (PB) composite membrane	1.1	80	30	Unknown	375	125	45	[51]
PEBA (GKSS, unknown grade)	1	80	30	70	430	185	75	[51]
PEBA 2533	0.6	60	0.4	25	1108	298	60	This work
28.6wt% ZIF-71/PEBA2533 MMMs	0.6	60	0.4	25	735	233	70	This work

7.4.1 Temperature Dependency of Membrane Performance

The temperature dependency of the permeation flux and the permeability follow an Arrhenius type of relation, as shown in Figure 7.13. It is shown that the permeation fluxes of all permeants increased significantly with an increase in temperature due to increased transmembrane driving force for mass transfer, whereas the permeability coefficients for all three permeants decreased. Compared to water, for which the permeation flux and permeability in the MMMs decreased with an increase in the content of ZIF-71, the effects of ZIF-71 loading on the permeation of phenol and aniline were less significant.

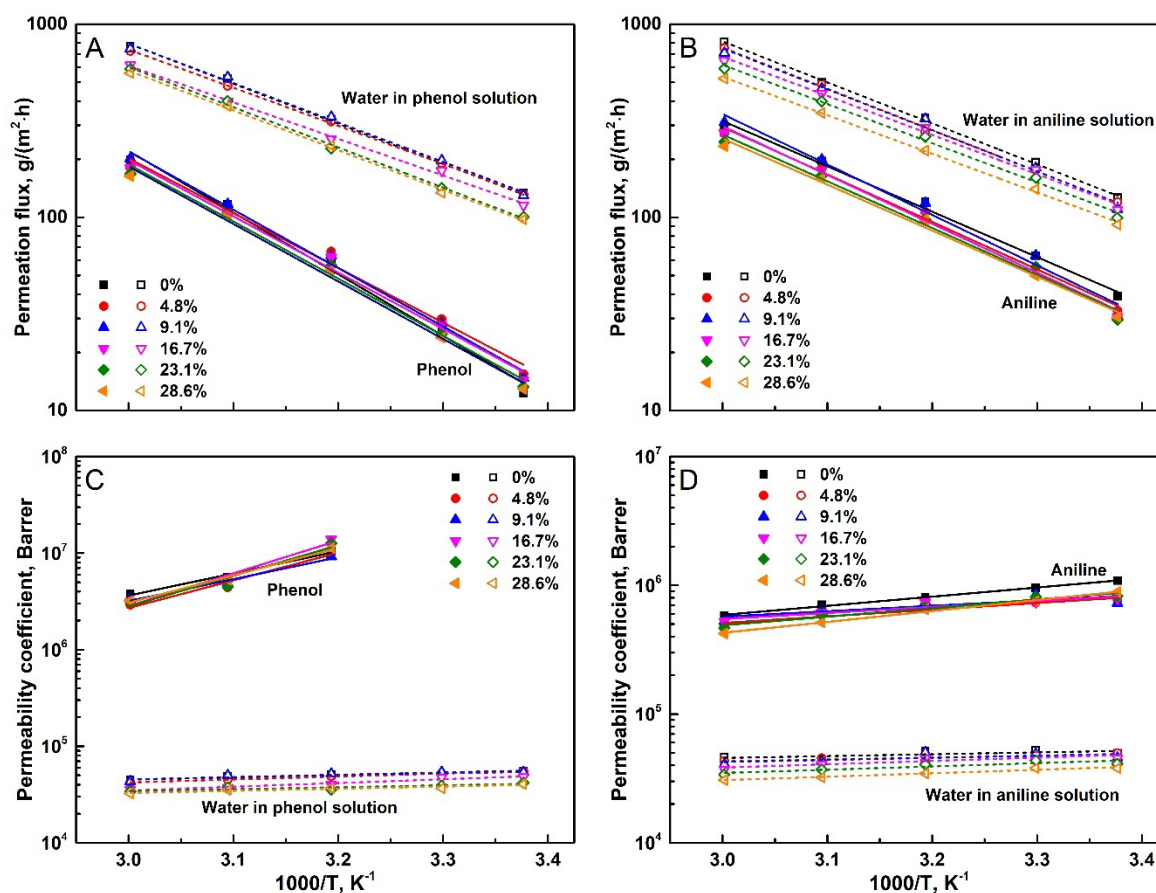


Figure 7.13 Temperature dependency of permeation flux for (A) phenol solution and (B) aniline solution, and temperature dependency of permeability coefficients for permeants in (C) phenol solution and (D) aniline solution. ZIF-71 loading (wt%) was shown in the Figure.

Figure 7.14 shows the effects of ZIF-71 loading in the MMMs on the apparent activation energy for permeation. The activation energy represents an energy barrier to be overcome by the permeating molecules for permeation to occur, and the apparent activation energy measures the overall temperature

effect on the permeation flux. It is shown that for the permeation of both aromatics (i.e., phenol and aniline) and water, the incorporation of ZIF-71 crystals in the membrane did not affect the activation energy significantly (the deviations of the activation energies for the three permeants were all within 5%).

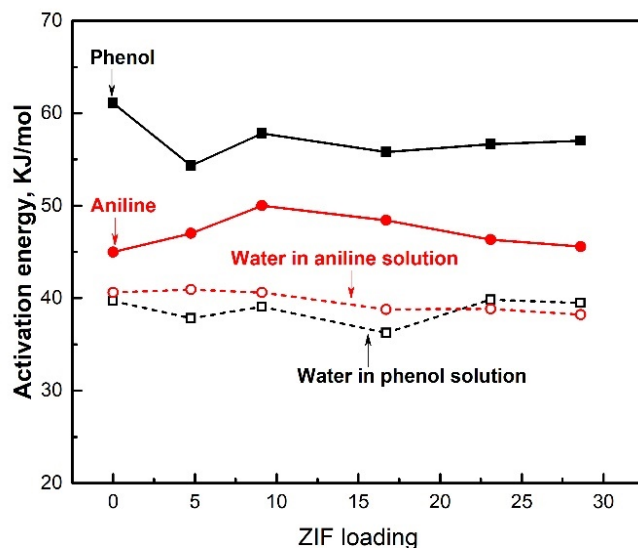


Figure 7.14 Effects of ZIF-71 loading in the MMMs on the apparent activation energy for permeation of phenol, aniline, and water.

Table 7.3 shows the apparent activation energy for permeation (E_J) based on temperature dependence of permeation flux and the intrinsic activation energy for permeation (E_P) based on temperature dependence of permeability. They can be obtained from the slopes of the straight lines in Figure 7.13. The difference between the two activation energies ($E_J - E_P$) was also presented in Table 7.3 for comparisons with the ΔH_V values. Similar to E_J , the E_P values for phenol, aniline and water showed no clear trend with ZIF-71 loading in the MMMs. Consistent with those obtained in Chapter 3 and Chapter 6, the relation $E_J - E_P = \Delta H_V$ did not work well for phenol which has very low volatility, but applied to aniline and water.

Table 7.3 Apparent activation energy and intrinsic activation energy for phenol, aniline, and water for MMMs with different ZIF-71 loadings.

ZIF-71 content, wt%	$E_{J-solute}$, kJ/mol	$E_{P-solute}$, kJ/mol	$(E_J - E_P)_{solute}$, kJ/mol	$E_{J-water}$, kJ/mol	$E_{P-water}$, kJ/mol	$(E_J - E_P)_{water}$, kJ/mol
Phenol solution	Phenol $\Delta H_V \approx 58$ kJ/mol			Water $\Delta H_V \approx (42-43.7)$ kJ/mol		
0	61.1	-44.1	105.2	39.7	-4.0	43.7
4.8	54.3	-54.8	109.1	37.8	-5.9	43.7
9.1	57.8	-43.5	101.3	39.1	-4.6	43.7
16.7	55.8	-64.9	120.7	36.2	-7.5	43.7
23.1	56.7	-60.4	117.1	39.8	-3.9	43.7
28.6	57.0	-54.3	111.3	39.5	-4.2	43.7
Aniline solution	Aniline $\Delta H_V \approx 54.8$ kJ/mol			Water $\Delta H_V \approx (42-43.7)$ kJ/mol		
0	45.0	-13.6	58.6	40.6	-2.8	43.4
4.8	47.0	-10.0	57.0	40.9	-2.8	43.8
9.1	50.0	-8.1	58.1	40.6	-3.1	43.8
16.7	48.4	-8.9	57.3	38.8	-5.0	43.8
23.1	46.3	-12.8	59.1	38.9	-4.9	43.8
28.6	45.6	-16.2	61.8	38.2	-5.1	43.4

7.4.2 Membrane Stability

To evaluate the stability of the so-prepared MMMs, a long-term test on MMM with 28.6wt% ZIF-71 for separating 6000 ppm aqueous phenol solution at 60°C was performed. Figure 7.15 shows the permeation flux and enrichment factor during 25 days' operation. Both the permeation flux and enrichment factor are stable, fluctuating slightly within allowable error range ($\leq 8\%$). The results demonstrate the good stability of the ZIF-71/PEBA 2533 MMM and the potential for application in practical water treatment. In view of the fact that polymeric membranes without the nanofillers became significantly swollen at high feed solute concentrations and the membrane stability was compromised especially at high operating temperatures, it is expected that the incorporation of ZIF-71 crystals in the

membrane will enhance the mechanical/thermal stability of the membranes, though there is no direct comparison of the stabilities for pure PEBA membrane and the MMMs.

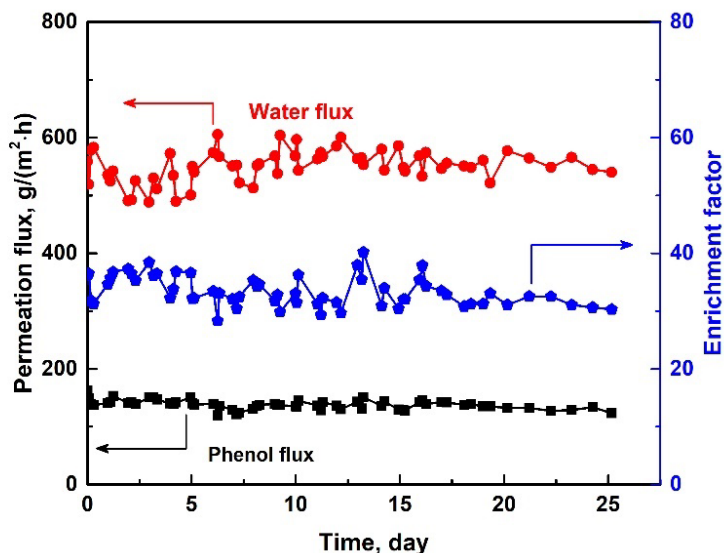


Figure 7.15 Stability of ZIF-71/PEBA MMM with a ZIF-71 loading of 28.6wt% for the separation of phenol solutions with concentration of 6000 ppm at 60°C.

7.5 Summary

ZIF-71/PEBA 2533 MMMs were successfully prepared for pervaporative separation of phenol and aniline from their aqueous solutions. ZIF-71 crystals showed good compatibility with PEBA polymer, making the MMMs defect-free at a ZIF loading up to 28.6wt%. ZIF-71 crystals favor the sorption and diffusion of the hydrophobic aromatic solutes, but the incorporation of ZIF-71 crystals into PEBA polymer affects the free volume and chain flexibility of the polymer, imposing an adverse effect on permeant mass transfer within the polymer matrix. The permeability of phenol was largely unaffected by the incorporation of ZIF-71 in the membrane, while aniline permeability was reduced slightly. Nonetheless, water permeability was reduced significantly by the incorporation of ZIF-71 due to lowered solubility and diffusivity, leading to increased enrichment factor. The permeability of phenol in the MMMs was higher than aniline due to the stronger polarity and smaller size of phenol molecules. However, at a given concentration, the permeation flux of aniline was higher than phenol flux primarily because of the higher transmembrane driving force. The ZIF-71/PEBA MMMs showed good stability, demonstrating its applicability in separation of phenol and/or aniline from their aqueous solutions.

Chapter 8

General Conclusions, Original Contributions and Future Prospects

8.1 General Conclusions and Original Contributions

Nonporous PEBA 2533 membranes and ZIF-71/PEBA 2533 MMMs were prepared in this work for separation of phenols and aniline from their aqueous solutions via pervaporation and perstraction. The mass transport fundamentals and permeation behavior of these aromatic compounds were investigated. The following general conclusions can be drawn from this research that are related to the original contributions:

- (1) Nonporous PEBA 2533 membrane was used to separate four representative phenolic compounds from aqueous solutions by pervaporation. In analogue with gas permeation, the permeability coefficient in pervaporation was evaluated. It was found the permeability coefficients of the phenolic compounds in PEBA 2533 were much higher than that of water. The phenolic compounds for which PEBA membrane had a high sorption uptake tended to be more prone to form clusters with neighboring phenolic molecules within membrane, blocking mass transfer passage and making permeation difficult. In separation of feed solutions containing multiple phenolic compounds, the coupling effects were found to be significant.
- (2) Nonporous PEBA membrane was used in a perstraction system to separate phenolic compounds from aqueous solutions, and sodium hydroxide was used as the stripping agent. The individual mass transfer resistances involved in various mass transfer steps of perstraction were evaluated. The good affinity between PEBA and phenols rendered perstraction particularly suitable for separation of phenols from their aqueous solutions. However, desorption of the phenols from the membrane would be difficult if the interactions between phenols and PEBA polymer were excessively strong. For the highly permeable membrane, the mass transfer resistance in the boundary layer was found to be nonnegligible, and vigorous turbulence should be provided to eliminate the boundary layer effect.
- (3) To further understand the mass transport and the permeation behavior of phenolic compounds in PEBA membranes, sorption and diffusion were evaluated. The solubility coefficient for phenolic compounds follows the order of $\text{PhOH} > \text{MePhOH} > \text{ClPhOH}$. The diffusivity coefficient is determined by the molecular size and mutual interactions between the polymer

and phenolic sorbates. The permeation behavior in the membrane depended strongly on the environment in which the membrane was equilibrated.

- (4) Phenol is the simplest phenolic compound and aniline is the simplest aromatic amine, both of which have the functional group connected to the benzene ring. The permeability, solubility, and diffusivity of aniline in PEBA membrane pertaining to aniline removal by pervaporation and sorption was investigated to see how the different functional groups attached to the benzene ring affect the mass transfer fundamentals. PEBA 2533 showed good performance for aniline separation, and the high permselectivity was derived exclusively from the solubility selectivity. At a given temperature and feed concentration, the sorption uptake of phenol was much higher than that of aniline. Membrane permeability for the different process modes was found to have the following order: permeability of a completely “wet” membrane (e.g., in liquid permeation) > permeability of a partially “wet” membrane (i.e., in pervaporation) > permeability of a “dry” membrane (e.g., in vapor permeation).
- (5) To further increase the permselectivity, ZIF-71 crystals were prepared and incorporated into PEBA membrane to form mixed matrix membranes, and the membranes were investigated for the separation of phenol and aniline from their aqueous solutions. The increased solute solubility and diffusivity within the ZIF-71 crystals were counterbalanced by the reduced free volume and chain flexibility of the polymer matrix, leading to a largely constant phenol permeability and slightly decreased aniline permeability. However, both the solubility and diffusivity of water within MMMs were reduced significantly due to the hydrophobic nature of ZIF-71, resulting in improved membrane selectivity. At a given temperature and feed concentration, though the permeability coefficient of aniline in PEBA was lower than phenol, the permeation flux of aniline was higher due to the higher driving force involved in aniline permeation as a result of its favorable thermodynamic properties.

8.2 Recommendations for Future Work

- (1) The majority of studies on the separation of phenolic compounds by pervaporation have been based on simple binary phenol/water model solutions, and complicated feed systems containing multiple phenolic compounds were investigated in this study to reveal the coupling effects. Based on the findings in this research, it is recommended that the pervaporative separation of phenolic compounds from real wastewater, where not only multiple phenolics but many other organic contaminants or non-volatiles may be present, be conducted. The presence of these

compounds/contaminants could affect the activity coefficients of the permeants, degree of membrane swelling, solubility of permeant in the membrane, the dissociation states of the solutes, and potential membrane fouling, which would ultimately affect the separation performance of the membrane. For example, in coking wastewater, in addition to phenol, ammonia, cyanide, thiocyanide, polycyclic aromatic hydrocarbons (PAHs) and some nitrogen-, oxygen- or sulfur-containing heterocyclic compounds often co-exist. The presence of these compounds will likely affect the overall separation performance. Investigations on real wastewater treatment will give an insight into practical aspects for treatment of phenolic wastewater.

- (2) All membranes used in the current study were dense flat-sheet membranes. To fully exploit the potential of the membranes for practical applications, the membrane thickness should be reduced effectively, as the permeation flux is inversely proportional to the effective membrane thickness. Nonetheless, the mechanical stability of thin films will be reduced. Therefore, composite membranes with a thin active layer supported on a porous substrate was recommended to increase the permeation flux and enhance the mechanical strength. It should be mentioned that the active layer of the composite membranes should not be too thin in order to prevent the formation of nonselective defects on an ultra-thin film. The properties of the substrate (e.g., polymeric materials, pore sizes, porosities, pore size distributions) would affect the formation of the composite membranes, thus influencing the membrane performance, and this also needs further investigations. Furthermore, asymmetric hollow fiber membranes, another membrane configuration widely used industrially due to its high membrane packing density and self-supporting design, may be prepared from PEBA 2533 to remove the aromatic contaminants from water. However, the permeate pressure build-up (which reduces the driving force for permeation) along the fiber length is significant when the permeate is drawn from the fiber bores. Based on the experimental data and modeling predictions, the extent of pressure build-up in permeate can be evaluated, and the membrane performance can be improved by optimizing the fiber dimensions or changing the permeate withdrawal locations.
- (3) A hybrid process in which pervaporation is combined with sorption can be developed to increase the overall separation efficiency. Due to the relatively low permeation rate in pervaporation, the concentration of the target components in the retentate stream from a single permeation stage can hardly meet the environmental regulation for discharge. A post-treatment is therefore needed for further water purification. PEBA 2533 shows excellent sorption capacity towards phenolic

compounds and aniline, thus can be used as a sorbent to remove them. In such a hybrid system, PEBA 2533 may be used to prepare both the pervaporation membrane and the sorbent. The permeate from pervaporation will be introduced to a decanter for phase separation, and the resulting water phase will be recycled to the pervaporation process, while the organic-rich phase can be further purified for recovery of organic compounds. The retentate from the pervaporation unit will be introduced to a sorption unit, and a final effluent that meets the environmental regulations can be discharged. The regeneration of PEBA sorbent is also important. PEBA sorbents can be regenerated via thermal regeneration or chemical regeneration using ethanol, methanol, acetone, as well as alkaline solutions (for sorbents exhausted with phenols) or acidic solutions (for sorbent exhausted with aniline). An economic study on such a hybrid system for the removal of phenols and aniline can also be performed as it is important for practical industrial applications.

- (4) To push up the trade-off between permeability and selectivity and thus to improve the separation performance of the membrane, proper fillers can be incorporated into the polymer membrane to form MMMs. To improve the separation performance, a high filler loading is critical [39]. At a high filler loading, fillers connect with each other within the polymer matrix, forming continuous channels, which can serve as “express-ways” for the permeation of the target component. Nonetheless, interfacial voids are likely to form easily when the filler loading is high. In this study, a maximum ZIF-71 loading of 28.6wt% was achieved, and a further increase in ZIF-71 loading will make the membrane defective. To further increase the filler loading, fillers can be modified using proper agents to alter the surface chemistry to increase the compatibility between the filler and the polymer, or synthesizing different ZIFs using different organic linkers with a better polymer compatibility. Perhaps decreasing the size of ZIF-71 crystals by controlling the reaction conditions (e.g., temperature, reactants ratios, reaction time) is a potential way to further increase the filler loading in the MMMs. It should be mentioned that the size of the fillers should not be too small as fillers with smaller sizes are easy to aggregate, which is detrimental to form non-defective MMMs. In addition, the membrane preparation process can also be modified. For example, a different solvent (e.g., butanol) can be used to dissolve the PEBA polymer and ZIF crystals as solvent evaporation rate may affect the formation of micro- or nano-voids at the polymer/filler interface. In a word, to achieve a desirable separation performance, MMMs should have a high filler loading without defects, and this merits further investigation.

Bibliography

- [1] S. Mohammadi, A. Kargaria, H. Sanaeepur, K. Abbassian, A. Najafi, E. Mofarrah, Phenol removal from industrial wastewaters: a short review, *Desalination Water Treat.*, 53 (2014) 2215-2234.
- [2] L.G.C. Villegas, N. Mashhadi, M. Chen, D. Mukherjee, K.E. Taylor, N. Biswas, A short review of techniques for phenol removal from wastewater, *Curr. Pollut. Rep.*, 2 (2016) 157-167.
- [3] W.W. Anku, M.A. Mamo, P.P. Govender, Phenolic compounds in water: sources, reactivity, toxicity and treatment methods, in: M. Soto-Hernandez, M. Palma-Tenango, M.d.R. Garcia-Mateos (Eds.) *Phenolic Compounds - Natural Sources, Importance and Applications*, 2017.
- [4] US Environmental Protection Agency, Health and environmental effects profile for aniline, Environmental Criteria and Assessment Office, Office of Health and Environmental Assessment, Office of Research and Development, Cincinnati, OH, 1985.
- [5] K. Yang, W. Wu, Q. Jing, L. Zhu, Aqueous adsorption of aniline, phenol, and their substitutes by multi-walled carbon nanotubes, *Environ. Sci. Technol.*, 42 (2008) 7931-7936.
- [6] J. Michałowicz, W. Duda, Phenols-sources and toxicity, *Pol. J. Environ. Stud.*, 16 (2007) 347-362.
- [7] D.C. Greminger, G.P. Burns, S. Lynn, D.H. Hanson, C.J. King, Solvent extraction of phenols from water, *Ind. Eng. Chem. Process Des. Dev.*, 21 (1982) 51-54.
- [8] Y. Fan, Y. Li, X. Dong, G. Hu, S. Hua, J. Miao, D. Zhou, Extraction of phenols from water with functionalized ionic liquids, *Ind. Eng. Chem. Res.*, 53 (2014) 20024-20031.
- [9] J.-K. Huh, D.-I. Song, Y.-W. Jeon, Sorption of phenol and alkylphenols from aqueous solution onto organically modified montmorillonite and applications of dual mode sorption model, *Sep. Sci. Technol.*, 35 (2000) 243-259.
- [10] M.H. El-Naas, S. Al-Zuhair, M.A. Alhajja, Removal of phenol from petroleum refinery wastewater through adsorption on date-pit activated carbon, *Chem. Eng. J.*, 162 (2010) 997-1005.
- [11] K. Zhang, Y. Liu, J. Deng, S. Xie, X. Zhao, J. Yang, Z. Han, H. Dai, Co-Pd/BiVO₄: High-performance photocatalysts for the degradation of phenol under visible light irradiation, *Appl. Catal., B*, 224 (2018) 350-359.
- [12] J. Li, Q. Liu, Q.q. Ji, B. Lai, Degradation of p-nitrophenol (PNP) in aqueous solution by Fe⁰-PM-PS system through response surface methodology (RSM), *Appl. Catal., B*, 200 (2017) 633-646.

- [13] M.M. Broholm, E. Arvin, Biodegradation of phenols in a sandstone aquifer under aerobic conditions and mixed nitrate and iron reducing conditions, *J. Contam. Hydrol.*, 44 (2000) 239-273.
- [14] N. Caza, J.K. Bewtra, N. Biswas, K.E. Taylor, Removal of phenolic compounds from synthetic wastewater using soybean peroxidase, *Water Res.*, 33 (1999) 3012-3018.
- [15] C. Yang, S. Yang, Y. Qian, J. Guo, Y. Chen, Simulation and operation cost estimate for phenol extraction and solvent recovery process of coal-gasification wastewater, *Ind. Eng. Chem. Res.*, 52 (2013) 12108-12115.
- [16] H. Jiang, Y. Fang, Y. Fu, Q.-X. Guo, Studies on the extraction of phenol in wastewater, *J. Hazard. Mater.*, 101 (2003) 179-190.
- [17] Q.-S. Liu, T. Zheng, P. Wang, J.-P. Jiang, N. Li, Adsorption isotherm, kinetic and mechanism studies of some substituted phenols on activated carbon fibers, *Chem. Eng. J.*, 157 (2010) 348-356.
- [18] D.P. Zagklis, A.I. Vavouraki, M.E. Kornaros, C.A. Paraskeva, Purification of olive mill wastewater phenols through membrane filtration and resin adsorption/desorption, *J. Hazard. Mater.*, 285 (2015) 69-76.
- [19] A. Kumar, H.M. Jena, Removal of methylene blue and phenol onto prepared activated carbon from Fox nutshell by chemical activation in batch and fixed-bed column, *J. Cleaner Prod.*, 137 (2016) 1246-1259.
- [20] G. Yang, L. Tang, G. Zeng, Y. Cai, J. Tang, Y. Pang, Y. Zhou, Y. Liu, J. Wang, S. Zhang, W. Xiong, Simultaneous removal of lead and phenol contamination from water by nitrogen-functionalized magnetic ordered mesoporous carbon, *Chem. Eng. J.*, 259 (2015) 854-864.
- [21] G. Busca, S. Berardinelli, C. Resini, L. Arrighi, Technologies for the removal of phenol from fluid streams: a short review of recent developments, *J. Hazard. Mater.*, 160 (2008) 265-288.
- [22] O. Gimeno, M.I. Carbajo, F.J. Beltran, F.J. Rivas, Phenol and substituted phenols AOPs remediation, *J. Hazard. Mater.*, 119 (2005) 99-108.
- [23] A. Tsioulpas, D. Dimou, D. Iconomou, G. Aggelis, Phenolic removal in olive oil mill wastewater by strains of *Pleurotus* spp. in respect to their phenol oxidase (laccase) activity, *Bioresour. Technol.*, 84 (2002) 251-257.
- [24] A. Robles, R. Lucas, G.A.d. Cienfuegos, A. Gálvez, Phenol-oxidase (laccase) activity in strains of the hyphomycete *Chalara paradoxa* isolated from olive mill wastewater disposal ponds, *Enzyme Microb. Technol.*, 26 (2000) 484-490.

- [25] M. Kissi, M. Mountadar, O. Assobhei, E. Gargiulo, G. Palmieri, P. Giardina, G. Sannia, Roles of two white-rot basidiomycete fungi in decolorisation and detoxification of olive mill waste water, *Appl. Microbiol. Biotechnol.*, 57 (2001) 221-226.
- [26] L.M. Vane, A review of pervaporation for product recovery from biomass fermentation processes, *J. Chem. Technol. Biotechnol.*, 80 (2005) 603-629.
- [27] W.J. Koros, Y.H. Ma, T. Shimidzu, Terminology for membranes and membrane processes (IUPAC Recommendations 1996), *Pure Appl. Chem.*, 68 (1996) 1479-1489.
- [28] Š. Schlosser, Pertraction through liquid and polymeric membranes, in: L. Gubicza, J. Mulder, K. Bélafi-Bakó (Eds.) *Integration Of Membrane Processes into Bioconversions*, Kluwer Academic/Plenum Publishers, New York, 2000.
- [29] S. Han, F.C. Ferreira, A. Livingston, Membrane aromatic recovery system (MARS) - a new membrane process for the recovery of phenols from wastewaters, *J. Membr. Sci.*, 188 (2001) 219-233.
- [30] F.C. Ferreira, S. Han, A. Boam, S. Zhang, A.G. Livingston, Membrane aromatic recovery system (MARS): lab bench to industrial pilot scale, *Desalination*, 148 (2002) 267-273.
- [31] J. Sawai, N. Ito, T. Minami, M. Kikuchi, Separation of low volatile organic compounds, phenol and aniline derivatives, from aqueous solution using silicone rubber membrane, *J. Membr. Sci.*, 252 (2005) 1-7.
- [32] J. Sawai, K. Higuchi, T. Minami, M. Kikuchi, Permeation characteristics of 4-substituted phenols and anilines in aqueous solution during removal by a silicone rubber membrane, *Chem. Eng. J.*, 152 (2009) 133-138.
- [33] P. Wu, R.W. Field, R. England, B.J. Brisdon, A fundamental study of organofunctionalised PDMS membranes for the pervaporative recovery of phenolic compounds from aqueous streams, *J. Membr. Sci.*, 190 (2001) 147-157.
- [34] D. Li, J. Yao, H. Sun, B. Liu, D. Li, S.v. Agtmaal, C. Feng, Preparation and characterization of SiO₂/PDMS/PVDF composite membrane for phenols recovery from coal gasification wastewater in pervaporation, *Chem. Eng. Res. Des.*, 132 (2018) 424-435.
- [35] W. Kujawski, A. Warszawski, W. Ratajczak, T. Porębski, W. Capała, I. Ostrowska, Removal of phenol from wastewater by different separation techniques, *Desalination*, 163 (2004) 287-296.
- [36] M.-Y. Jin, Y. Liao, C.-H. Tan, R. Wang, Development of high performance nanofibrous composite membranes by optimizing polydimethylsiloxane architectures for phenol transport, *J. Membr. Sci.*, 549 (2018) 638-648.

- [37] W. Kujawski, A. Warszawski, W. Ratajczak, T. Porębski, W. Capała, I. Ostrowska, Application of pervaporation and adsorption to the phenol removal from wastewater, *Sep. Purif. Technol.*, 40 (2004) 123-132.
- [38] X. Hao, M. Pritzker, X. Feng, Use of pervaporation for the separation of phenol from dilute aqueous solutions, *J. Membr. Sci.*, 335 (2009) 96-102.
- [39] R.W. Baker, *Membrane Technology and Applications*, 3rd ed., John Wiley & Sons Ltd, 2012.
- [40] K.W. Böddeker, Pervaporation of phenols, US Patent 4,806,245 (1989).
- [41] S. Lai, Sorptive separation of phenolic compounds from wastewater, Dissertation, University of Waterloo, 2017.
- [42] Y.K. Ong, G.M. Shi, N.L. Le, Y.P. Tang, J. Zuo, S.P. Nunes, T.-S. Chung, Recent membrane development for pervaporation processes, *Prog. Polym. Sci.*, 57 (2016) 1-31.
- [43] G. Liu, W. Wei, W. Jin, Pervaporation membranes for biobutanol production, *ACS Sustainable Chem. Eng.*, 2 (2013) 546-560.
- [44] A. Bakhshi, T. Mohammadi, A. Aroujalian, Pervaporation separation of binary and ternary mixtures with polydimethylsiloxane membranes, *J. Appl. Polym. Sci.*, 107 (2008) 1777-1782.
- [45] M. Hoshi, M. Kogure, T. Saitoh, T. Nakagawa, Separation of aqueous phenol through polyurethane membranes by pervaporation, *J. Appl. Polym. Sci.*, 65 (1997) 469-479.
- [46] T. Gupta, N.C. Pradhan, B. Adhikari, Separation of phenol from aqueous solution by pervaporation using HTPB-based polyurethaneurea membrane, *J. Membr. Sci.*, 217 (2003) 43-53.
- [47] H. Ye, X. Zhang, Z. Zhang, B. Song, W. Song, Application of polyurethane membrane with surface modified ZSM-5 for pervaporation of phenol/water mixture, *J. Polym. Eng.*, 37 (2017) 777-784.
- [48] K.W. Böddeker, G. Bengtson, E. Bode, Pervaporation of low volatility aromatics from water, *J. Membr. Sci.*, 53 (1990) 143-158.
- [49] C. Ding, X. Zhang, C. Li, X. Hao, Y. Wang, G. Guan, ZIF-8 incorporated polyether block amide membrane for phenol permselective pervaporation with high efficiency, *Sep. Purif. Technol.*, 166 (2016) 252-261.
- [50] S. Das, A.K. Banthia, B. Adhikari, Pervaporation separation of aqueous chlorophenols by a novel polyurethane urea-poly (methyl methacrylate) interpenetrating network membrane, *J. Membr. Sci.*, 280 (2006) 675-683.
- [51] K. Meckl, R.N. Lichtenthaler, Hybrid process using pervaporation for the removal of organics from process and wastewater, *J. Membr. Sci.*, 113 (1996) 81-86.

- [52] S.M. Byrne, The preparation and characterisation of hydrophobic polymeric membranes for use in the separation of liquid mixtures using pervaporation separation processes, Dissertation, Dublin City University, 1998.
- [53] P.D. Chapman, T. Oliveira, A.G. Livingston, K. Li, Membranes for the dehydration of solvents by pervaporation, *J. Membr. Sci.*, 318 (2008) 5-37.
- [54] H.O.E. Karlsson, GunTrägårdh, Pervaporation of dilute organic-waters mixtures. A literature review on modelling studies and applications to aroma compound recovery, *J. Membr. Sci.*, 76 (1993) 121-146.
- [55] I. Blume, J.G. Wijmans, R.W. Baker, The separation of dissolved organics from water by pervaporation, *J. Membr. Sci.*, 49 (1990) 253-286.
- [56] A. Jonquières, R. Clément, P. Lochon, J. Néel, M. Dresch, B. Chrétien, Industrial state-of-the-art of pervaporation and vapour permeation in the western countries, *J. Membr. Sci.*, 206 (2002) 87-117.
- [57] T. Kataoka, T. Tsuru, S.-I. Nakao, S. Kimura, Permeation equations developed for prediction of membrane performance in pervaporation, vapor permeation and reverse osmosis based on the solution-diffusion model, *J. Chem. Eng. Jpn.*, 24 (1991) 326-333.
- [58] J.G. Wijmans, R.W. Baker, A simple predictive treatment of the permeation process in pervaporation, *J. Membr. Sci.*, 79 (1993) 101-113.
- [59] X. Feng, R.Y.M. Huang, Estimation of activation energy for permeation in pervaporation, *J. Membr. Sci.*, 118 (1996) 127-131.
- [60] J. Neel, Q.T. Nguyen, R. Clement, D.J. Lin, Influence of downstream pressure on the pervaporation of water-tetrahydrofuran mixtures through a regenerated cellulose membrane (cuprophan), *J. Membr. Sci.*, 27 (1986) 217-232.
- [61] X. Feng, R.Y.M. Huang, Organic vapor gas mixture separation by membrane-a parametric study, *Sep. Sci. Technol.*, 27 (1992) 2109-2119.
- [62] J.G. Wijmans, A.L. Athayde, R. Daniels, J.H. Ly, H.D. Kamaruddin, I. Pinnau, The role of boundary layers in the removal of volatile organic compounds from water by pervaporation, *J. Membr. Sci.*, 109 (1996) 135-146.
- [63] L. Li, Z. Xiao, S. Tan, L. Pu, Z. Zhang, Composite PDMS membrane with high flux for the separation of organics from water by pervaporation, *J. Membr. Sci.*, 243 (2004) 177-187.
- [64] S. Li, F. Qin, P. Qin, M.N. Karim, T. Tan, Preparation of PDMS membrane using water as solvent for pervaporation separation of butanol–water mixture, *Green Chem.*, 15 (2013) 2180-2190.

- [65] T. Mohammadi, A. Aroujalian, A. Bakhshi, Pervaporation of dilute alcoholic mixtures using PDMS membrane, *Chem. Eng. Sci.*, 60 (2005) 1875-1880.
- [66] H.H. Nijhuis, M.H.V. Mulder, C.A. Smolders, Selection of elastomeric membranes for the removal of volatile organics from water, *J. Appl. Polym. Sci.*, 47 (1993) 2227-2243.
- [67] S.B. Harogopad, T.M. Aminabhavi, Diffusion and sorption of organic liquids through polymer membranes. II. Neoprene, SBR, EPDM, NBR, and natural rubber versus *n*-alkanes, *J. Appl. Polym. Sci.*, 42 (1991) 2329-2336.
- [68] S.B. Harogopad, T.M. Aminabhavi, Diffusion and sorption of organic liquids through polymer membranes. VIII. Elastomers versus monocyclic aromatic liquids, *J. Appl. Polym. Sci.*, 46 (1992) 725-732.
- [69] V.S. Cunha, M.L.L. Paredes, C.P. Borges, A.C. Habert, R. Nobrega, Removal of aromatics from multicomponent organic mixtures by pervaporation using polyurethane membranes: experimental and modeling, *J. Membr. Sci.*, 206 (2002) 277-290.
- [70] M.M. Cipriano, A. Diogo, M.N.d. Pinho, Polyurethane structure design for pervaporation membranes, *J. Membr. Sci.*, 61 (1991) 65-72.
- [71] A.V. Yakovlev, M.G. Shalygin, S.M. Matson, V.S. Khotimskiy, V.V. Teplyakov, Separation of diluted butanol–water solutions via vapor phase by organophilic membranes based on high permeable polyacetylenes, *J. Membr. Sci.*, 434 (2013) 99-105.
- [72] X.M. Wu, Q.G. Zhang, F. Soyekwo, Q.L. Liu, A.M. Zhu, Pervaporation removal of volatile organic compounds from aqueous solutions using the highly permeable PIM-1 membrane, *AIChE J.*, 62 (2016) 842-851.
- [73] M. Žák, M. Klepic, L.Č. Štastná, Z. Sedláková, H. Vychodilová, Š. Hovorka, K. Friess, A. Randová, L. Brožová, J.C. Jansen, M.R. Khdhayyer, P.M. Budd, P. Izák, Selective removal of butanol from aqueous solution by pervaporation with a PIM-1 membrane and membrane aging, *Sep. Purif. Technol.*, 151 (2015) 108-114.
- [74] I.L. Borisov, A.O. Malakhov, V.S. Khotimsky, E.G. Litvinova, E.S. Finkelshtein, N.V. Ushakov, V.V. Volkov, Novel PTMSP-based membranes containing elastomeric fillers: Enhanced 1-butanol/water pervaporation selectivity and permeability, *J. Membr. Sci.*, 466 (2014) 322-330.
- [75] S. Claes, P. Vandezande, S. Mullens, K. De Sitter, R. Peeters, M.K. Van Bael, Preparation and benchmarking of thin film supported PTMSP-silica pervaporation membranes, *J. Membr. Sci.*, 389 (2012) 265-271.

- [76] S. Claes, P. Vandezande, S. Mullens, P. Adriaensens, R. Peeters, F.H.J. Maurer, M.K.V. Bael, Crosslinked poly[1-(trimethylsilyl)-1-propyne] membranes: Characterization and pervaporation of aqueous tetrahydrofuran mixtures, *J. Membr. Sci.*, 389 (2012) 459-469.
- [77] P. Sukitpaneevit, T.-S. Chung, Molecular design of the morphology and pore size of PVDF hollow fiber membranes for ethanol–water separation employing the modified pore-flow concept, *J. Membr. Sci.*, 374 (2011) 67-82.
- [78] D.L. Vrana, M.M. Meagher, R.W. Hutkins, B. Duffield, Pervaporation of model acetone-butanol-ethanol fermentation product solutions using polytetrafluoroethylene membranes, *Sep. Sci. Technol.*, 28 (1993) 2167-2178.
- [79] K. Jian, P.N. Pintauro, R. Ponangi, Separation of dilute organic/water mixtures with asymmetric poly(vinylidene fluoride) membranes, *J. Membr. Sci.*, 117 (1996) 117-133.
- [80] K. Jian, P.N. Pintauro, Asymmetric PVDF hollow-fibre membranes for organic/water pervaporation separations, *J. Membr. Sci.*, 135 (1997) 41-53.
- [81] C. Shin, X.C. Chen, J.M. Prausnitz, N.P. Balsara, Effect of block copolymer morphology controlled by casting-solvent quality on pervaporation of butanol/water mixtures, *J. Membr. Sci.*, 523 (2017) 588-595.
- [82] C. Li, X. Zhang, X. Hao, X. Feng, X. Pang, H. Zhang, Thermodynamic and mechanistic studies on recovering phenol crystals from dilute aqueous solutions using pervaporation-crystallization coupling (PVCC) system, *Chem. Eng. Sci.*, 127 (2015) 106-114.
- [83] K.-i. Okamoto, A. Butsuen, S. Tsuru, S. Nishioka, K. Tanaka, H. Kita, S. Asakawa, Pervaporation of water-ethanol mixtures through poly-dimethylsiloxane block-copolymer membranes, *Polym. J.*, 19 (1987) 747-756.
- [84] C. Shin, Z.C. Baer, X.C. Chen, A.E. Ozcam, D.S. Clark, N.P. Balsara, Block copolymer pervaporation membrane for in situ product removal during acetone–butanol–ethanol fermentation, *J. Membr. Sci.*, 484 (2015) 57-63.
- [85] L. Liang, E. Ruckenstein, Pervaporation of ethanol-water mixtures through polydimethylsiloxane-polystyrene interpenetrating polymer network supported membranes, *J. Membr. Sci.*, 114 (1996) 227-234.
- [86] I. Ahmed, N.F.C. Pa, M.G.M. Nawawi, W.A.W.A. Rahman, Modified polydimethylsiloxane/polystyrene blended IPN pervaporation membrane for ethanol/water separation, *J. Appl. Polym. Sci.*, 122 (2011) 2666-2679.

- [87] J.P. Brun, C. Larchet, G. Bulvestre, B. Auclair, Sorption and pervaporation of dilute aqueous solutions of organic compounds through polymer membranes, *J. Membr. Sci.*, 25 (1985) 55-100.
- [88] A.E. Ozcam, N. Petzetakis, S. Silverman, A.K. Jha, N.P. Balsara, Relationship between segregation strength and permeability of ethanol/water mixtures through block copolymer membranes, *Macromolecules*, 46 (2013) 9652-9658.
- [89] N. Du, H.B. Park, M.M. Dal-Cin, M.D. Guiver, Advances in high permeability polymeric membrane materials for CO₂ separations, *Energy Environ. Sci.*, 5 (2012) 7306-7322.
- [90] H.B. Park, C.H. Jung, Y.M. Lee, A.J. Hill, S.J. Pas, S.T. Mudie, E.V. Wagner, B.D. Freeman, D.J. Cookson, Polymers with cavities tuned for fast selective transport of small molecules and ions, *Science*, 318 (2007) 254-258.
- [91] D. Korelskiy, T. Leppäjärvi, H. Zhou, M. Grahn, J. Tanskanen, J. Hedlund, High flux MFI membranes for pervaporation, *J. Membr. Sci.*, 427 (2013) 381-389.
- [92] I.F.J. Vankelecom, E. Scheppers, R. Heus, J.B. Uytterhoeven, Parameters influencing zeolite incorporation in PDMS membranes, *J. Phys. Chem.*, 98 (1994) 12390-12396.
- [93] L.M. Vane, V.V. Namboodiri, T.C. Bowen, Hydrophobic zeolite–silicone rubber mixed matrix membranes for ethanol–water separation: Effect of zeolite and silicone component selection on pervaporation performance, *J. Membr. Sci.*, 308 (2008) 230-241.
- [94] J. Gu, X. Shi, Y. Bai, H. Zhang, L. Zhang, H. Huang, Silicalite-filled PEBA membranes for recovering ethanol from aqueous solution by pervaporation, *Chem. Eng. Technol.*, 32 (2009) 155-160.
- [95] E.A. Fouad, X. Feng, Pervaporative separation of n-butanol from dilute aqueous solutions using silicalite-filled poly(dimethyl siloxane) membranes, *J. Membr. Sci.*, 339 (2009) 120-125.
- [96] X. Dong, Y.S. Lin, Synthesis of an organophilic ZIF-71 membrane for pervaporation solvent separation, *Chem. Commun.*, 49 (2013) 1196-1198.
- [97] M.-Y. Jin, Y. Lin, Y. Liao, C.-H. Tan, R. Wang, Development of highly-efficient ZIF-8@PDMS/PVDF nanofibrous composite membrane for phenol removal in aqueous-aqueous membrane extractive process, *J. Membr. Sci.*, 568 (2018) 121-133.
- [98] S. Li, P. Li, D. Cai, H. Shan, J. Zhao, Z. Wang, P. Qin, T. Tan, Boosting pervaporation performance by promoting organic permeability and simultaneously inhibiting water transport via blending PDMS with COF-300, *J. Membr. Sci.*, 579 (2019) 141-150.
- [99] S. Yuan, X. Li, J. Zhu, G. Zhang, P.V. Puyvelde, B.V.d. Bruggen, Covalent organic frameworks for membrane separation, *Chem. Soc. Rev.*, 48 (2019) 2665-2681.

- [100] H. Fan, Y. Xie, J. Li, L. Zhang, Q. Zheng, G. Zhang, Ultra-high selectivity COF-based membranes for biobutanol production, *J. Mater. Chem. A*, 6 (2018) 17602-17611.
- [101] Z. Si, G. Li, Z. Wang, D. Cai, S. Li, J. Baeyens, P. Qin, A particle-driven, ultrafast-cured strategy for tuning the network cavity size of membranes with outstanding pervaporation performance, *ACS Appl. Mater. Interfaces*, 12 (2020) 31887-31895.
- [102] R. Castro-Muñoz, F. Galiano, V. Fíla, E. Drioli, A. Figoli, Mixed matrix membranes (MMMs) for ethanol purification through pervaporation: current state of the art, *Rev. Chem. Eng.*, 35 (2019) 565-590.
- [103] T. Ma, E.A. Kapustin, S.X. Yin, L. Liang, Z. Zhou, J. Niu, L.-H. Li, Y. Wang, J. Su, J. Li, X. Wang, W.D. Wang, W. Wang, J. Sun, O.M. Yaghi, Single-crystal x-ray diffraction structures of covalent organic frameworks, *Science*, 361 (2018) 48-52.
- [104] R. Castaldo, V. Ambrogio, R. Avolio, M. Cocca, G. Gentile, M. Emanuela Errico, M. Avella, Functional hyper-crosslinked resins with tailored adsorption properties for environmental applications, *Chem. Eng. J.*, 362 (2019) 497-503.
- [105] E. Obotey Ezugbe, S. Rathilal, Membrane technologies in wastewater treatment: A review, *Membranes (Basel)*, 10 (2020) 89.
- [106] J.G. Wijmans, J. Kaschemekat, J.E. Davidson, R.W. Baker, Treatment of organic-contaminated wastewater streams by pervaporation, *Environ. Prog.*, 9 (1990) 262-268.
- [107] G. Liu, F. Xiangli, W. Wei, S. Liu, W. Jin, Improved performance of PDMS/ceramic composite pervaporation membranes by ZSM-5 homogeneously dispersed in PDMS via a surface graft/coating approach, *Chem. Eng. J.*, 174 (2011) 495-503.
- [108] X. Han, X. Zhang, X. Ma, J. Li, Modified ZSM-5/polydimethylsiloxane mixed matrix membranes for ethanol/water separation via pervaporation, *Polym. Compos.*, 37 (2016) 1282-1291.
- [109] X. Zhan, J. Lu, T. Tan, J. Li, Mixed matrix membranes with HF acid etched ZSM-5 for ethanol/water separation: Preparation and pervaporation performance, *Appl. Surf. Sci.*, 259 (2012) 547-556.
- [110] X. Zhuang, X. Chen, Y. Su, J. Luo, S. Feng, H. Zhou, Y. Wan, Surface modification of silicalite-1 with alkoxysilanes to improve the performance of PDMS/silicalite-1 pervaporation membranes: Preparation, characterization and modeling, *J. Membr. Sci.*, 499 (2016) 386-395.
- [111] P.V. Naik, S. Kerkhofs, J.A. Martens, I.F.J. Vankelecom, PDMS mixed matrix membranes containing hollow silicalite sphere for ethanol / water separation by pervaporation, *J. Membr. Sci.*, 502 (2016) 48-56.

- [112] H.-W. Yen, Z.-H. Chen, I.-K. Yang, Use of the composite membrane of poly(ether-block-amide) and carbon nanotubes (CNTs) in a pervaporation system incorporated with fermentation for butanol production by *Clostridium acetobutylicum*, *Bioresour. Technol.*, 109 (2012) 105-109.
- [113] Y. Wu, X. Fu, G. Tian, G. Xuehong, Z. Liu, Pervaporation of phenol wastewater with PEBA-PU blend membrane, *Desalination Water Treat.*, 102 (2018) 101-109.
- [114] Y. Li, L.H. Wee, J.A. Martens, I.F.J. Vankelecom, ZIF-71 as a potential filler to prepare pervaporation membranes for bio-alcohol recovery, *J. Mater. Chem. A*, 2 (2014) 10034-10040.
- [115] G. Wu, Y. Li, Y. Geng, Z. Jia, In situ preparation of COF-LZU1 in poly(ether-*block*-amide) membranes for efficient pervaporation of n-butanol/water mixture, *J. Membr. Sci.*, 581 (2019) 1-8.
- [116] H. Yin, C.Y. Lau, M. Rozowski, C. Howard, Y. Xu, T. Lai, M.E. Dose, R.P. Lively, M.L. Lind, Free-standing ZIF-71/PDMS nanocomposite membranes for the recovery of ethanol and 1-butanol from water through pervaporation, *J. Membr. Sci.*, 529 (2017) 286-292.
- [117] X. Zhan, J. Lu, H. Xu, J. Liu, X. Liu, X. Cao, J. Li, Enhanced pervaporation performance of PDMS membranes based on nano-sized Octa[(trimethoxysilyl)ethyl]-POSS as macro-crosslinker, *Appl. Surf. Sci.*, 473 (2019) 785-798.
- [118] S. Liu, G. Liu, X. Zhao, W. Jin, Hydrophobic-ZIF-71 filled PEBA mixed matrix membranes for recovery of biobutanol via pervaporation, *J. Membr. Sci.*, 446 (2013) 181-188.
- [119] L. Liu, Z. Jiang, F. Pan, F. Peng, H. Wu, The unusual change of permeation rate in PDMS membranes filled with crystalline calixarene and its derivative, *J. Membr. Sci.*, 279 (2006) 111-119.
- [120] R. Castro-Muñoz, Pervaporation: The emerging technique for extracting aroma compounds from food systems, *J. Food Eng.*, 253 (2019) 27-39.
- [121] E. Bengtsson, G. Trigrdrh, B. Hallstriim, Recovery and concentration of apple juice aroma compounds by pervaporation *J. Food Eng.*, 10 (1989) 65-71.
- [122] A. Raisi, A. Aroujalian, Aroma compound recovery by hydrophobic pervaporation: The effect of membrane thickness and coupling phenomena, *Sep. Purif. Technol.*, 82 (2011) 53-62.
- [123] M. She, S.-T. Hwang, Effects of concentration, temperature, and coupling on pervaporation of dilute flavor organics, *J. Membr. Sci.*, 271 (2006) 16-28.
- [124] N. Diban, A. Urriaga, I. Ortiz, Recovery of key components of bilberry aroma using a commercial pervaporation membrane, *Desalination*, 224 (2008) 34-39.

- [125] T.A. Weschenfelder, P. Lantin, M.C. Viegas, F.d. Castilhos, A.d. PaulaScheer, Concentration of aroma compounds from an industrial solution of soluble coffee by pervaporation process, *J. Food Eng.*, 159 (2015) 57-65.
- [126] D.M. Kanani, B.P. Nikhade, P. Balakrishnan, G. Singh, V.G. Pangarkar, Recovery of valuable tea aroma components by pervaporation, *Ind. Eng. Chem. Res.*, 42 (2003) 6924-6932.
- [127] J. Olsson, G. Trägårdh, Influence of temperature on membrane permeability during pervaporative aroma recovery, *Sep. Sci. Technol.*, 34 (1999) 1643-1659.
- [128] O. Trifunović, F. Lipnizki, G. Trägårdh, The influence of process parameters on aroma recovery by hydrophobic pervaporation, *Desalination*, 189 (2006) 1-12.
- [129] N. Rafia, A. Aroujalian, A. Raisi, Pervaporative aroma compounds recovery from lemon juice using poly(octyl methyl siloxane) membrane, *J. Chem. Technol. Biotechnol.*, 86 (2011) 534-540.
- [130] M. Mujiburohman, X. Feng, Permselectivity, solubility and diffusivity of propyl propionate/water mixtures in poly(ether block amide) membranes, *J. Membr. Sci.*, 300 (2007) 95-103.
- [131] C. Du, J.R. Du, X. Feng, J. Wang, Green extraction of perilla volatile organic compounds by pervaporation, *Sep. Purif. Technol.*, 261 (2021) 118281.
- [132] A. Baudot, M. Marin, Dairy aroma compounds recovery by pervaporation, *J. Membr. Sci.*, 120 (1996) 207-220.
- [133] G. Camera-Roda, V. Augugliaro, A. Cardillo, V. Loddo, G. Palmisano, L. Palmisano, A pervaporation photocatalytic reactor for the green synthesis of vanillin, *Chem. Eng. J.*, 224 (2013) 136-143.
- [134] A. Baudot, M. Marin, Pervaporation of aroma compounds: comparison of membrane performances with vapour-Liquid equilibria and engineering aspects of process improvement, *Food Bioprod. Process.*, 75 (1997) 117-142.
- [135] B. Zhang, Recovery of dairy aroma compounds and concentration of dairy solutions by membranes, Dissertation, University of Waterloo, 2018.
- [136] B. Van der Bruggen, P. Luis, Pervaporation as a tool in chemical engineering: a new era?, *Curr. Opin. Chem. Eng.*, 4 (2014) 47-53.
- [137] V. Outram, C.-A. Lalander, J.G.M. Lee, E.T. Davies, A.P. Harvey, Applied in situ product recovery in ABE fermentation, *Biotechnol. Prog.*, 33 (2017) 563-579.

- [138] H.-W. Yen, S.-F. Lin, I.-K. Yang, Use of poly(ether-block-amide) in pervaporation coupling with a fermentor to enhance butanol production in the cultivation of *Clostridium acetobutylicum*, *J. Biosci. Bioeng.*, 113 (2012) 372-377.
- [139] N. Qureshi, M.M. Meagher, J. Huang, R.W. Hutkins, Acetone butanol ethanol (ABE) recovery by pervaporation using silicalite–silicone composite membrane from fed-batch reactor of *Clostridium acetobutylicum*, *J. Membr. Sci.*, 187 (2001) 93-102.
- [140] W.V. Hecke, P. Vandezande, S. Claes, S. Vangeel, H. Beckers, L. Diels, H.D. Wever, Integrated bioprocess for long-term continuous cultivation of *Clostridium acetobutylicum* coupled to pervaporation with PDMS composite membranes, *Bioresour. Technol.*, 111 (2012) 368-377.
- [141] F. Lipnizki, S. Hausmanns, G. Laufenberg, R. Field, B. Kunz, Use of pervaporation-bioreactor hybrid processes in biotechnology, *Chem. Eng. Technol.*, 23 (2000) 569-577.
- [142] T. Lamer, H.E. Spinnler, I. Souchon, A. Voilley, Extraction of benzaldehyde from fermentation broth by pervaporation, *Process Biochem.*, 31 (1996) 533-542.
- [143] G. Bengtson, K.W. Bøddeker, H.-P. Hanssen, I. Urbasch, Recovery of 6-pentyl-alpha-pyrone from *Trichoderma viride* culture medium by pervaporation, *Biotechnol. Tech.*, 6 (1992) 23-26.
- [144] L.M. Vane, V.V. Namboodiri, R.G. Meier, Factors affecting alcohol–water pervaporation performance of hydrophobic zeolite–silicone rubber mixed matrix membranes, *J. Membr. Sci.*, 364 (2010) 102-110.
- [145] G. Liu, W. Wei, H. Wu, X. Dong, M. Jiang, W. Jin, Pervaporation performance of PDMS/ceramic composite membrane in acetone butanol ethanol (ABE) fermentation–PV coupled process, *J. Membr. Sci.*, 373 (2011) 121-129.
- [146] G. Camera-Roda, F. Santarelli, V. Augugliaro, V. Loddo, G. Palmisano, L. Palmisano, S. Yurdakal, Photocatalytic process intensification by coupling with pervaporation, *Catal. Today*, 161 (2011) 209-213.
- [147] G. Camera-Roda, F. Santarelli, Intensification of water detoxification by integrating photocatalysis and pervaporation, *J. Sol. Energy Eng.*, 129 (2007) 68-73.
- [148] G. Camera-Roda, V. Loddo, L. Palmisano, F. Parrino, F. Santarelli, Process intensification in a photocatalytic membrane reactor: Analysis of the techniques to integrate reaction and separation, *Chem. Eng. J.*, 310 (2017) 352-359.
- [149] G. Camera-Roda, A. Cardillo, V. Loddo, L. Palmisano, F. Parrino, Improvement of membrane performances to enhance the yield of vanillin in a pervaporation reactor, *Membranes (Basel)*, 4 (2014) 96-112.

- [150] F. Lipnizki, R.W. Field, Hydrophobic pervaporation for environmental applications: process optimization and integration, *Environ. Prog.*, 21 (2002) 265-272.
- [151] R.W. Field, V. Lobo, Hydrophobic pervaporation: toward a shortcut method for the pervaporation-decanter system, *Ann. N. Y. Acad. Sci.*, 984 (2003) 401-410.
- [152] F. Lipnizki, R.W. Field, Pervaporation-based hybrid processes in treating phenolic wastewater: technical aspects and cost engineering, *Sep. Sci. Technol.*, 36 (2001) 3311-3335.
- [153] R. Ray, R.W. Wytcherley, D. Newbold, S. McCray, D. Friesen, D. Brose, Synergistic, membrane-based hybrid separation systems, *J. Membr. Sci.*, 62 (1991) 347-369.
- [154] F. Lipnizki, R.W. Field, P.-K. Ten, Pervaporation based hybrid process: a review of process design, applications and economics, *J. Membr. Sci.*, 153 (1999) 183-210.
- [155] K.W. Böddeker, G. Bengtson, H. Pingel, S. Dozel, Pervaporation of high boilers using heated membranes, *Desalination*, 90 (1993) 249-257.
- [156] M. Kondo, S. Nagasawa, T. Nakagawa, Separation of phenol in aqueous solution by pervaporation using polyether-block-amides membranes incorporating polyester substrate, *Membrane*, 21 (1997) 343-350.
- [157] M. Kondo, H. Sato, Treatment of wastewater from phenolic resin process by pervaporation, *Desalination*, 98 (1994) 147-154.
- [158] G. Bengtson, H. Scheel, J. Theis, D. Fritsch, Catalytic membrane reactor to simultaneously concentrate and react organics, *Chem. Eng. J.*, 85 (2002) 303-311.
- [159] T. Asada, Future of pervaporation, in: R. Bakish (Ed.) *Proceedings of Sixth International Conference on Pervaporation Processes in the Chemical Industry*, Bakish Materials Corp, Englewood, Ottawa Canada, 1992, pp. 554-558.
- [160] L. Liu, A. Chakma, X. Feng, A novel method of preparing ultrathin poly(ether block amide) membranes, *J. Membr. Sci.*, 235 (2004) 43-52.
- [161] R.W. Baker, J.G. Wijmans, Y. Huang, Permeability, permeance and selectivity: A preferred way of reporting pervaporation performance data, *J. Membr. Sci.*, 348 (2010) 346-352.
- [162] W.M. Haynes, D.R. Lide, T.J. Bruno, *CRC Handbook of Chemistry and Physics 97th ed.*, CRC Press, 2016-2017.
- [163] X. Feng, *Studies on pervaporation membranes and pervaporation processes*, Dissertation, University of Waterloo, 1994.
- [164] M. Beneš, V. Dohnal, Limiting activity coefficients of some aromatic and aliphatic nitro compounds in water, *J. Chem. Eng. Data*, 44 (1999) 1097-1102.

- [165] R. Parthasarathi, V. Subramanian, N. Sathyamurthy, Hydrogen bonding in phenol, water, and phenol-water clusters, *J. Phys. Chem. A*, 109 (2005) 843-850.
- [166] S. Yan, L.H. Spangler, Intermolecular modes of S1 p-cresol dimer information concerning structure and dynamics, *J. Phys. Chem.*, 95 (1991) 3915-3918.
- [167] T.S. Zwier, The spectroscopy of solvation in hydrogen bonded aromatic clusters, *Annu. Rev. Phys. Chem.*, 47 (1996) 205-241.
- [168] A. Li, Q. Zhang, J. Chen, Z. Fei, C. Long, W. Li, Adsorption of phenolic compounds on Amberlite XAD-4 and its acetylated derivative MX-4, *React. Funct. Polym.*, 49 (2001) 225-233.
- [169] A. Heintz, S. Kapteina, S.P. Verevkin, Pairwise-substitution effects and intramolecular hydrogen bonds in nitrophenols and methylnitrophenols. Thermochemical measurements and ab initio calculations, *J. Phys. Chem. A*, 111 (2007) 6552-6562.
- [170] X. Zhang, C. Li, X. Hao, X. Feng, H. Zhang, H. Hou, G. Liang, Recovering phenol as high purity crystals from dilute aqueous solutions by pervaporation, *Chem. Eng. Sci.*, 108 (2014) 183-187.
- [171] G.V. Hartland, B.F. Henson, V.A. Ventura, P.M. Felker, Ionization-loss stimulated Raman spectroscopy of jet-cooled hydrogen-bonded complexes containing phenols, *J. Phys. Chem.*, 96 (1992) 1164-1173.
- [172] C.L. Yaws, *Chemical properties handbook: physical, thermodynamic, environmental, transport, safety and health related properties for organic and inorganic chemicals*, McGraw-Hill, New York, 1999.
- [173] O. Trifunovic, G. Trägårdh, The influence of permeant properties on the sorption step in hydrophobic pervaporation, *J. Membr. Sci.*, 216 (2003) 207-216.
- [174] B. Bettens, J. Degreève, B.V.d. Bruggen, C. Vandecasteele, Transport of binary mixtures in pervaporation through a microporous silica membrane: shortcomings of Fickian models, *Sep. Sci. Technol.*, 42 (2007) 1-23.
- [175] Š. Schlosser, E. Sabolová, Three-phase contactor with distributed U-shaped bundles of hollow-fibers for pertraction, *J. Membr. Sci.*, 210 (2002) 331-347.
- [176] X. Cao, H.-S. Lee, X. Feng, Extraction of dissolved methane from aqueous solutions by membranes: Modelling and parametric studies, *J. Membr. Sci.*, 596 (2020) 117594.
- [177] M. Xiao, J. Zhou, Y. Zhang, X. Hu, S. Li, Pertraction performance of phenol through PDMS/PVDF composite membrane in the membrane aromatic recovery system (MARS), *J. Membr. Sci.*, 428 (2013) 172-180.

- [178] E.A. Fouad, X. Feng, Use of pervaporation to separate butanol from dilute aqueous solutions: Effects of operating conditions and concentration polarization, *J. Membr. Sci.*, 323 (2008) 428-435.
- [179] G.D. Bella, D.D. Trapani, A brief review on the resistance-in-series model in membrane bioreactors (MBRs), *Membranes (Basel)*, 9 (2019) 24.
- [180] R.S. Brodkey, H.C. Hershey, Agitation, in: B.J. Clark (Ed.) *Transport Phenomena-A Unified Approach*, McGraw-Hill Book Company, New York, 1988, pp. 375.
- [181] R.B. Bird, W.E. Stewart, E.N. Lightfoot, *Transport Phenomenon*, 2nd ed., John Wiley & Sons, Inc., 2011.
- [182] C.R. Wilke, P. Chang, Correlation of diffusion coefficients in dilute solutions, *AIChE J.*, 1 (1955) 264-270.
- [183] Š. Schlosser, I. Rothova, H. Frianova, Hollow-fibre pertractor with bulk liquid membrane, *J. Membr. Sci.*, 80 (1993) 99-106.
- [184] Š. Schlosser, E. Sabolová, R. Kertész, L. Kubišová, Factors influencing transport through liquid membranes and membrane based solvent extraction, *J. Sep. Sci.*, 24 (2001) 509-518.
- [185] M. She, S.-T. Hwang, Concentration of dilute flavor compounds by pervaporation: permeate pressure effect and boundary layer resistance modeling, *J. Membr. Sci.*, 236 (2004) 193-202.
- [186] P.R. Brookes, A.G. Livingston, Aqueous-aqueous extraction of organic pollutants through tubular silicone rubber membranes, *J. Membr. Sci.*, 104 (1995) 119-137.
- [187] S.D. Doig, A.T. Boam, A.G. Livingston, D.C. Stuckey, Mass transfer of hydrophobic solutes in solvent swollen silicone rubber membranes, *J. Membr. Sci.*, 154 (1999) 127-140.
- [188] S. Yu, X. Wang, W. Yao, J. Wang, Y. Ji, Y. Ai, A. Alsaedi, T. Hayat, X. Wang, Macroscopic, spectroscopic, and theoretical investigation for the interaction of phenol and naphthol on reduced graphene oxide, *Environ. Sci. Technol.*, 51 (2017) 3278-3286.
- [189] R. Takagi, M. Tagawa, K. Gotoh, M. Nakagaki, Variation of membrane charge of nylon 6 with pH, *J. Membr. Sci.*, 92 (1994) 229-238.
- [190] S. Miyamoto, M. Tagawa, Kinetics of adsorption and desorption of sodium alkyl sulfates to and from nylon particles, *Colloid. Polym. Sci.*, 266 (1988) 1126-1132.
- [191] J. Crank, G.S. Park, *Diffusion in Polymers*, Academic Press, London, 1968.
- [192] J. Crank, *The Mathematics of Diffusion*, 2nd ed., Clarendon Press. Oxford, 1975.
- [193] R. Binning, R. Lee, J. Jennings, E. Martin, Separation of liquid mixtures by permeation, *Ind. Eng. Chem.*, 53 (1961) 45-50.

- [194] K. Okamoto, N. Tanihara, H. Watanabe, K. Tanaka, H. Kita, A. Nakamura, Y. Kusuki, K. Nakagawa, Vapor permeation and pervaporation separation of water-ethanol mixtures through polyimide membranes, *J. Membr. Sci.*, 68 (1992) 53-63.
- [195] M.-Y. Teng, K.-R. Lee, S.-C. Fan, D.-J. Liaw, J. Huang, J.-Y. Lai, Development of aromatic polyamide membranes for pervaporation and vapor permeation, *J. Membr. Sci.*, 164 (2000) 241-249.
- [196] J. Sarasa, S. Cortés, P. Ormad, R. Gracia, J.L. Ovelleiro, Study of the aromatic by-products formed from ozonation of anilines in aqueous solution, *Water Res.*, 36 (2002) 3035-3044.
- [197] L. Oliviero, J. Barbier, D. Duprez, Wet air oxidation of nitrogen-containing organic compounds and ammonia in aqueous media, *Appl. Catal., B*, 40 (2003) 163-184.
- [198] C. Li, X. Zhang, X. Hao, M. Wang, C. Ding, Z. Wang, Y. Wang, G. Guan, A. Abudula, Efficient recovery of high-purity aniline from aqueous solutions using pervaporation-fractional condensation system, *AIChE J.*, 61 (2015) 4445-4455.
- [199] Y. Chen, Y. Zhang, X. Feng, An improved approach for determining permeability and diffusivity relevant to controlled release, *Chem. Eng. Sci.*, 65 (2010) 5921-5928.
- [200] M. Bernauer, V. Dohnal, A.H. Roux, G. Roux-Desgranges, V. Majer, Temperature dependences of limiting activity coefficients and Henry's law constant for nitrobenzene, aniline, and cyclohexylamine in water, *J. Chem. Eng. Data*, 51 (2006) 1678-1685.
- [201] A. Dallos, I. Ország, F. Ratkovics, Liquid-liquid and vapour-liquid equilibrium data and calculations for the system aniline + water in the presence of NaCl, NaI, NH₄Cl and NH₄I, *Fluid Phase Equilib.*, 11 (1983) 91-102.
- [202] T. Lamer, M.S. Rohart, A. Voilley, H. Baussart, Influence of sorption and diffusion of aroma compounds in silicone rubber on their extraction by pervaporation, *J. Membr. Sci.*, 90 (1994) 251-263.
- [203] V.S. Praptowidodo, Influence of swelling on water transport through PVA-based membrane, *J. Mol. Struct.*, 739 (2005) 207-212.
- [204] X. Duthie, S. Kentish, C. Powell, K. Nagai, G. Qiao, G. Stevens, Operating temperature effects on the plasticization of polyimide gas separation membranes, *J. Membr. Sci.*, 294 (2007) 40-49.
- [205] L. Deng, M.-B. Hägg, Swelling behavior and gas permeation performance of PVAm/PVA blend FSC membrane, *J. Membr. Sci.*, 363 (2010) 295-301.
- [206] U. Spoerel, W. Stahl, The aniline-water complex rotational spectrum and molecular structure, *J. Mol. Spectrosc.*, 190 (1998) 278-289.

- [207] N.V. Sidgwick, P. Pickford, B.H. Wilsdon, CXX.—The solubility of aniline in aqueous solutions of its hydrochloride, *Journal of the Chemical Society, Transactions*, 99 (1911) 1122-1132.
- [208] D. Schemmel, M. Schütz, Molecular aniline clusters. I. The electronic ground state, *J. Chem. Phys.*, 132 (2010) 174303.
- [209] W.-M. Zhang, J.-L. Chen, B.-C. Pan, Q.-X. Zhang, Competitive and cooperative adsorption behaviors of phenol and aniline onto nonpolar macroreticular adsorbents, *J. Environ. Sci.*, 17 (2005) 529-534.
- [210] B. Will, R.N. Lichtenthaler, Comparison of the separation of mixtures by vapor permeation and by pervaporation using PVA composite membranes, *J. Membr. Sci.*, 68 (1992) 119-125.
- [211] K.S. Park, Z. Ni, A.P. Cote, J.Y. Choi, R. Huang, F.J. Uribe-Romo, H.K. Chae, M. O’Keeffe, O.M. Yaghi, Exceptional chemical and thermal stability of zeolitic imidazolate frameworks, *Proc. Natl. Acad. Sci. U.S.A.*, 103 (2006) 10186-10191.
- [212] H. Li, M. Eddaoudi, M. O’Keeffe, O.M. Yaghi, Design and synthesis of an exceptionally stable and highly porous metal-organic framework, *Nature*, 402 (1999) 276-279.
- [213] B.R. Pimentel, M.L. Jue, E.-K. Zhou, R.J. Verploegh, J. Leisen, D.S. Sholl, R.P. Lively, Sorption and transport of vapors in ZIF-11: adsorption, diffusion, and linker flexibility, *J. Phys. Chem. C*, 123 (2019) 12862-12870.
- [214] K. Zhang, R.P. Lively, M.E. Dose, A.J. Brown, C. Zhang, J. Chung, S. Nair, W.J. Koros, R.R. Chance, Alcohol and water adsorption in zeolitic imidazolate frameworks, *Chem. Commun.*, 49 (2013) 3245-3247.
- [215] R.P. Lively, M.E. Dose, J.A. Thompson, B.A. McCool, R.R. Chance, W.J. Koros, Ethanol and water adsorption in methanol-derived ZIF-71, *Chem. Commun.*, 47 (2011) 8667-8669.
- [216] G. Socrates, *Infrared and Raman Characteristic Group Frequencies: Tables and Charts*, Third ed., John Wiley & Sons, 2004.
- [217] A. Nalaparaju, X.S. Zhao, J.W. Jiang, Molecular understanding for the adsorption of water and alcohols in hydrophilic and hydrophobic zeolitic metal–organic frameworks, *J. Phys. Chem. C*, 114 (2010) 11542–11550.
- [218] F. Buss, J. Göcke, P. Scharfer, W. Schabel, From micro to nano thin polymer layers: thickness and concentration dependence of sorption and the solvent diffusion coefficient, *Macromolecules*, 48 (2015) 8285-8293.

- [219] S. Basu, M. Maes, A. Cano-Odena, L. Alaerts, D.E. De Vos, I.F.J. Vankelecom, Solvent resistant nanofiltration (SRNF) membranes based on metal-organic frameworks, *J. Membr. Sci.*, 344 (2009) 190-198.
- [220] D. Fairen-Jimenez, S.A. Moggach, M.T. Wharmby, P.A. Wright, S. Parsons, T. Duren, Opening the gate: framework flexibility in ZIF-8 explored by experiments and simulations, *J. Am. Chem. Soc.*, 133 (2011) 8900-8902.
- [221] C. Gücüyener, J.v.d. Bergh, J. Gascon, F. Kapteijn, Ethane/ethene separation turned on its head: selective ethane adsorption on the metal-organic framework ZIF-7 through a gate opening mechanism, *J. Am. Chem. Soc.*, 132 (2010) 17704-17706.
- [222] T. Gupta, N.C. Pradhan, B. Adhikari, Synthesis and performance of a novel polyurethaneurea as pervaporation membrane for the selective removal of phenol from industrial waste water, *Bull. Mater. Sci.*, 25 (2002) 533-536.

Appendix A

Estimation of Individual Resistances

To minimize the liquid boundary layer resistance in the stripping solution, sufficient mixing was provided in the stripping solution. Therefore, two additional propellers were used at high rotation speeds in the receiving compartment to enhance the turbulence (Figure A1†). The effect of Reynolds number on the overall mass transfer coefficient was investigated, as shown in Figure A2†. $Re (= \rho Nd^2/\mu)$ was calculated based on one agitation propeller in the stripping solution. It was expected that the overall mass transfer coefficient increased with an increase in Re in the stripping solution, and then levelled off when Re was higher than 43000. When Re in the stripping solution was high enough, a further increase in the mixing of the stripping solution did not show appreciable enhancement in mass transfer rate anymore. In view of the low phenol concentration and sufficient mixing of the stripping solution, the boundary layer resistance in the stripping liquid was thus negligible (i.e., $\frac{1}{K_O} = R_1 + R_2 + R_m + R_3$

). Therefore, the value of K_O' was estimated under such an agitation condition where Re in the stripping liquid (deionized water) was 52000 (which corresponded to an agitation speed of 1300 rpm).

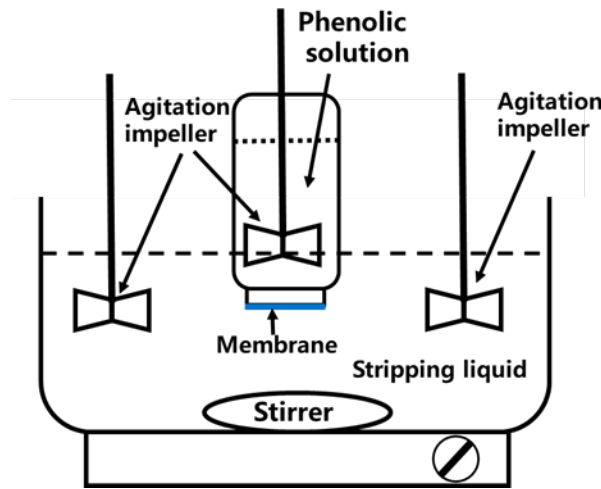


Figure A1†. Apparatus for determination of the liquid boundary layer resistance (R_4) in the stripping solution and the desorption resistance from the membrane (R_3) for perstration. The two agitation propellers in the stripping solution had a diameter of 4.4 cm.

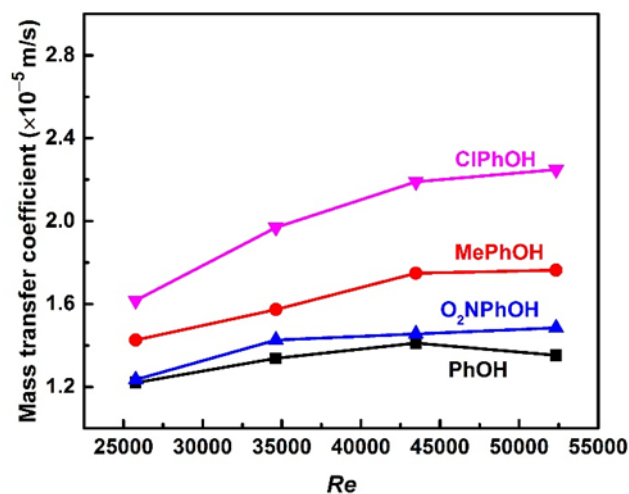


Figure A2†. Effects of the turbulent condition of the stripping solution on the overall mass transfer coefficient for perstraction. Membrane thickness, 25.4 μm . The operating conditions were the same as displayed in Table 4.1 in Chapter 4 except that two additional agitation propellers were used at high rotation speeds to enhance the turbulent condition in the stripping liquid (the stirring speed of the original stirrer in the stripping liquid was also increased accordingly). The value of Re represented the Reynolds number of one agitation propeller.

To minimize the boundary layer resistance and phenol desorption resistance from the membrane on the downstream side, the concentration of NaOH in the stripping solution should be high enough and the stripping liquid should be agitated sufficiently. This study showed that a NaOH concentration of 0.1 mol/L in the stripping solution was high enough for dissociation of the four phenolic compounds. Therefore, the overall mass transfer coefficient K_o'' was estimated under such conditions where the concentration of NaOH was 0.1 mol/L and Reynolds number was 52000 in the stripping solution. The desorption resistance from the membrane can be estimated from the difference between $(\frac{1}{K_o'} - \frac{1}{K_o''})$ and $(R_m - R_m'')$. The calculated results were shown in Table A1†.

Table A1†. Detailed calculation information of the individual resistances when membrane thickness was 25.4 μm .

	$1/K_O$	$1/K_O'$	$1/K_O''$	R_4	R_3
PhOH	105500	73200	50400	32300	16600
MePhOH	92600	56700	37400	35900	10800
O ₂ NPhOH	93900	67400	39100	31100	17800
ClPhOH	74600	44500	26900	30100	5400

For illustration purpose, consider perstraction of PhOH using the 25.4 μm -thick membrane as an example. The detailed calculations were as follows:

Under normal operating condition in this study, $\frac{1}{K_O} = 105500$ s/m.

When the stripping liquid (deionized water) was fully turbulent ($Re = 52000$), $\frac{1}{K_O'} = 73200$ s/m.

$$\text{Thus, } R_4 = \frac{1}{K_O} - \frac{1}{K_O'} = 105500 - 73200 = 32300 \text{ s/m.}$$

When the stripping liquid is an alkaline solution of 0.1 mol/L NaOH and at a Re of 52000, $\frac{1}{K_O''} = 50400$ s/m.

The membrane resistances with a NaOH concentration of 0 and 0.1 mol/L in the stripping solution were estimated to be $R_m = 50800$ s/m, and $R_m'' = 44600$ s/m, respectively.

Since $\frac{1}{K_O'} - \frac{1}{K_O''} = R_m + R_3 - R_m''$, then

$$R_3 = \left(\frac{1}{K_O'} - \frac{1}{K_O''} \right) - (R_m - R_m'') = (73200 - 50400) - (50800 - 44600) = 16600 \text{ s/m}$$

From the Sherwood correlation, R_1 was estimated to be 5600 s/m.

$$\text{Thus, } R_2 = \frac{1}{K_O} - R_1 - R_m - R_3 - R_4 = 105500 - 5600 - 50800 - 16600 - 32300 = 200 \text{ s/m.}$$